

ANALELE ȘTIINȚIFICE  
ALE  
UNIVERSITĂȚII „AL. I. CUZA“  
DIN IAȘI  
(SERIE NOUĂ)

# G E O L O G I E

Proceedings of the International Symposium  
**Geology of Natural Systems – Geo Iași 2010**  
September 1 – 4, 2010, Iași, Romania

---

Analele Științifice ale Universității "Al. I. Cuza" – a scientific journal since 1900  
Geologie Series – an international journal published in Iași since 1955  
ISSN 1223-5342

## **EDITOR**

**Dan Stumbea**

„Al. I. Cuza” University of Iași, Department of Geology, 20A Carol I Blv., 700505 Iași,  
Romania

## **SCIENTIFIC COMMITTEE**

Mircea Săndulescu (Romania), Radu Dimitrescu (Romania), Teodor Neagu (Romania), Gheorghe Udubașa (Romania), Nicolae Anastasiu (Romania), Sorin Filipescu (Romania), Mihai Brânzilă (Romania), Ovidiu Gabriel Iancu (Romania), Nicolae Buzgar (Romania), Mihai Șaramet (Romania), Dan Stumbea (Romania), Traian Gavriiloaiei (Romania), Dumitru Bulgariu (Romania), Paul Țibuleac (Romania), Laviniu Apostoae (Romania), Viorel Ionesi (Romania), Bogdan Hanu (Romania), Roberto Compagnoni (Italy), Yasunori Miura (Japan), Haino Uwe Kasper (Germany), Constantin Cocârță (France), Jean–Hughes Thomassin (France), Constantin Crânganu (USA), Octavian Cătuneanu (Canada), Mathias Harzhauser (Austria)

## CONTENTS

<b>Mineralogy and petrology</b>	<b>11</b>
<b>Geochemistry</b>	<b>45</b>
<b>Paleontology – Stratigraphy</b>	<b>85</b>
<b>Environmental Geology</b>	<b>151</b>
<b>Economic geology</b>	<b>185</b>
<b>Tectonics – Structural geology</b>	<b>215</b>

## DETAILED CONTENTS

### Mineralogy and petrology

---

<b>Nicolae BUZGAR, Andrei BUZATU, Andrei Ionut APOPEI, Vasile COTIUGA, Florin TOPOLEANU</b> MINERAL PIGMENTS OF GRECO-ROMAN AND BYZANTINE AGES FROM DOBROGEA.....	13
<b>Kocak KERIM, Veysel ZEDEF</b> MAFIC AND FELSIC MAGMA INTERACTION IN GRANITES: THE EOCENE HOROZ GRANITOID (NIGDE, TURKEY).....	14
<b>Yasunori MIURA, Takao TANOSAKI</b> THE FORMATION OF CONGO DIAMONDS WITH HALITE AND CARBON-BEARING MICRO-GRAINS.....	16
<b>Yasunori MIURA, Takao TANOSAKI, Ovidiu Gabriel IANCU</b> CONDITIONS INVOLVED IN THE FORMATION OF THE RIES CRATER, GERMANY, INFERRED FROM THE CARBON AND CHLORINE CONTENTS OF THE DRILLED SAMPLES.....	21
<b>Yasunori MIURA</b> FINE NANO-BACTERIA-LIKE TEXTURE WITH AN AKAGANEITE COMPOSITION.....	26
<b>Simona MOLDOVEANU, Ovidiu Gabriel IANCU, Gheorghe DAMIAN, Haino Uwe KASPER</b> MINERALOGY OF METAMORPHIC FORMATIONS FROM THE MĂNĂILA AREA (EASTERN CARPATHIANS).....	30
<b>Tamer RIZAOĞLU, Osman PARLAK, Fikret İŞLER, Volker HOECK</b> GEOCHEMISTRY AND TECTONIC SIGNIFICANCE OF THE CUMULATE ROCKS OF THE KÖMÜRHAN OPHIOLITE IN SOUTHEAST ANATOLIA (ELAZIĞ-TURKEY).....	35
<b>Reza Zarei SAHAMIEH, Amir PAZOKI, Peiman REZAEI, Ali SAKET</b> PETROLOGY, GEOCHEMISTRY AND TECTONIC SETTING OF MYRDEH AREA GRANITOID(S) (EAST OF BANEH CITY).....	38
<b>Ioan SEGHEDI, Mihai TATU</b> COMPARATIVE REMARKS ON THE PERMIAN VOLCANISM IN THE SIRINIA AND PRESACINA DOMAINS (SOUTH BANAT, ROMANIA).....	39
<b>Zdenka MARCINČÁKOVÁ, Marián KOŠUTH</b> CHARACTERISTICS OF XENOLITHS IN THE EAST SLOVAKIAN NEOGENE VULCANITES.....	43

### Geochemistry

---

<b>Dumitru BULGARIU, Nicolae BUZGAR, Feodor FILIPOV, Laura BULGARIU</b> SPECIATION OF SILICA AND ALUMINIUM IN HORTIC ANTHROSOILS – PEDOGEOCHEMICAL IMPLICATION.....	47
--	----

<b>Dumitru BULGARIU, Nicolae BUZGAR, Dan AȘTEFANEI</b> GENESIS OF PEDOGEOCHEMICAL SEGREGATION HORIZONS (FRAGIPANS) AND THEIR INFLUENCE ON THE GEOCHEMISTRY OF HORTIC ANTHROSOILS.....	49
<b>Valentin GRIGORAȘ, Ovidiu Gabriel IANCU, Nicolae BUZGAR, Meta DOBNIKAR, Mihael-Cristin ICHIM</b> THE DISTRIBUTION OF CERTAIN TRACE ELEMENTS IN ACTIVE STREAM SEDIMENTS OF THE BISTRIȚA RIVER (DOWNSTREAM IZVORUL MUNTELUI LAKE), ROMANIA.....	51
<b>Nurullah HANILÇI, Cemal ALTAYLI, Sinan ALTUNCU, Hüseyin ÖZTÜRK</b> WAS THE GÖL TEPE (NIĞDE, CENTRAL ANATOLIA, TURKEY) A TIN PROCESSING SITE DURING THE EARLY BRONZE AGE? PRELIMINARY FINDINGS FROM SOIL GEOCHEMISTRY.....	57
<b>Adriana ION, Șerban ANASTASE</b> NATURAL RADIOACTIVITY IN SOIL SAMPLES FROM THE AREA BETWEEN BISTRIȚA AND TROTUȘ VALLEYS.....	60
<b>Orhan KAVAK</b> ORGANIC GEOCHEMICAL COMPARISON BETWEEN THE ASPHALTITES FROM THE ŞIRNAK AREA AND THE OILS OF THE RAMAN AND DİNÇER FIELDS IN SOUTHEASTERN TURKEY.....	64
<b>Saheeb Ahmed KAYANI</b> ESTABLISHING THE ORIGINS OF A METEORITE DEBRIS BY USING CARBON ABUNDANCE.....	71
<b>Marián KOŠUTH, Zdenka MARCINČÁKOVÁ</b> CORDIERITE-BEARING XENOLITHS IN THE ANDESITES FROM VECHEC, SLOVAKIA: COMPOSITION AND ORIGIN.....	74
<b>Yasunori MIURA</b> MATERIAL INDICATORS IN THE CASE OF OCEAN IMPACT: HALITE AND CALCITE CARBONATES.....	76
<b>Yesim Bozkir OZEN, Fetullah ARIK, Ahmet AYHAN, Alican OZTURK</b> GEOCHEMICAL COMPARISON BETWEEN THE LATERITIC BAUXITES HOSTED BY THE BASIC VOLCANICS OF CARIKSARAYLAR AND KOZLUCA Y OCCURRENCES (ISPARTA, TURKEY).....	80
<b>Seyda PARLAR, Muhittin GORMUS</b> GEOCHEMICAL CHARACTERIZATION OF MARINE SEDIMENTS AND RECENT FORAMINIFERA IN SERIK, EAST ANTALYA, TURKIYE.....	82
<b>Asuman YILMAZ, Mustafa KUŞCU</b> GEOLOGY, GEOCHEMISTRY AND GENESIS OF MARGI MAGNESITE OCCURRENCES IN ESKISEHIR, NW TURKEY.....	83

## **Paleontology – Stratigraphy**

---

<b>Dorin Sorin BACIU</b> OLIGOCENE FISH FAUNA FROM THE PARATETHYS SEA – NATIONAL GEOGRAPHIC SOCIETY PROGRAMMES.....	87
---	----

<b>Ariana BEJLERI, Mensi PRELA, Flutura HAFIZI</b> THE DEVELOPMENT OF A DATABASE FOR RADIOLARIAN ASSEMBLAGES FROM THE JURASSIC CHERTS OF ALBANIA.....	93
<b>Gabriel CHIRILĂ, Daniel ȚABĂRĂ</b> PALYNOLOGICAL STUDY OF THE OUTCROP FROM THE CIOFOAIA BROOK (MOLDAVIAN PLATFORM) - PALAEOCLIMATIC AND PALAEOENVIRONMENTAL IMPLICATIONS.....	94
<b>Gabriel CHIRILĂ, Daniel ȚABĂRĂ</b> PALYNOFACIES AND TOTAL ORGANIC CARBON CONTENT FROM THE BAIJA BOREHOLE (MOLDAVIAN PLATFORM).....	100
<b>Ionuț V. CIOACĂ, Dan GRIGORE</b> NEW CRETACEOUS FOSSILS DISCOVERED IN THE CONGLOMERATES FROM CHEILE BICAZULUI – HĂȘMAȘ NATIONAL PARK (EASTERN CARPATHIANS).....	104
<b>Vlad CODREA, Laurențiu URSACHI, Daniel BEJAN</b> LATE MIOCENE VERTEBRATES FROM POGANA (SCYTHIAN PLATFORM).....	109
<b>Eugenia IAMANDEI, Stănilă IAMANDEI, Mihai BRÂNZILĂ, Daniel ȚABĂRĂ, Gabriel CHIRILĂ</b> FOSSIL WOODS IN THE COLLECTION OF THE AICU GEOLOGICAL MUSEUM.....	110
<b>Stănilă IAMANDEI, Eugenia IAMANDEI</b> NEW PETRIFIED WOODS FROM SOLEȘTI, ROMANIA.....	113
<b>Viorel IONESI, Florentina PASCARIU</b> THE RELATIONSHIP BETWEEN THE SARMATIAN AND QUATERNARY FORMATIONS FROM THE PĂCURARI AREA (IAȘI, ROMANIA).....	115
<b>Mihaela-Carmen MELINTE-DOBRINESCU, Marcos-Antonio LAMOLDA</b> CALCAREOUS NANNOFOSSIL FLUCTUATION RELATED TO THE OCEANIC ANOXIC EVENT 2 (OAE2).....	117
<b>Leonard OLARU, Daniel ȚABĂRĂ, Marina CHIHAIA</b> PALYNOLOGY, PALYNOFACIES AND TOTAL ORGANIC CARBON FROM SILURIAN DEPOSITS OF THE DNESTR BASIN (PODOLIA, UKRAINA).....	120
<b>Seyda PARLAR, Muhittin GORMUS</b> TAXONOMIC, QUANTITATIVE AND PALEOECOLOGICAL ANALYSES OF BENTHIC FORAMINIFERAL ASSEMBLAGES OF QUATERNARY MARINE SEDIMENTS IN SERIK, EAST ANTALYA, TURKEY.....	128
<b>Mensi PRELA</b> LITHO- AND BIO-STRATIGRAPHY OF THE PORAVA SECTION (NORTHERN ALBANIA).....	129
<b>Mensi PRELA</b> JURASSIC RADIOLARIAN CHERTS IN THE EASTERN PERIPHERAL UNITS OF THE ALBANIAN OPHIOLITES.....	131
<b>Mensi PRELA</b> RADIOLARIAN ASSEMBLAGES IN THE DERSTILA SECTION (ALBANIA).....	133
<b>Ilie TURCULEȚ, Paul ȚIBULEAC</b> RARĂU SYNCLINE (EASTERN CARPATHIANS, ROMANIA) – REGION TYPE FOR NEW MESOZOIC TAXA AND PARATAXA.....	135

<b>Camelia VĂRZARU, Mihaela C. MELINTE-DOBRINESCU, Titus BRUSTUR, Stefan-Andrei SZOBOTKA, Andrei BRICEAG</b> THE SIGNIFICANCE OF SEVERAL UPPER CRETACEOUS MARINE FOSSIL SITES FOR THE GEODIVERSITY OF THE HAȚEG COUNTRY .....	141
<b>Dan GRIGORE, Iuliana LAZĂR, Cosmin BUTNAR</b> GEOLOGICAL COLLECTION OF CHEILE BICAZULUI-HĂȘMAȘ NATIONAL PARK..	144

## **Environmental Geology**

---

<b>Laviniu APOSTOAE</b> INFORMATIONAL CHARACTERISTICS IN RATIONALIZATION OF SAMPLING NETWORKS OF SOIL IN ORDER TO ESTABLISH THE HEAVY METALS POLLUTION.....	153
<b>Sorin-Ionuț BALABAN, Ovidiu Gabriel IANCU, Dumitru BULGARIU</b> PRELIMINARY DATA REGARDING THE GEOCHEMICAL DISTRIBUTION OF MINOR ELEMENTS IN THE DEALU NEGRU MINE TAILINGS FROM THE FUNDU MOLDOVEI AREA, ROMANIA.....	157
<b>Ramona BALINT</b> EXPERIMENTAL STUDY OF NATURAL ZEOLITES FOR THEIR USAGE IN SOIL REMEDIATION.....	159
<b>Corneliu HORAICU</b> THE GEOLOGICAL ENVIRONMENT WITHIN SUSTAINABLE DEVELOPMENT .....	165
<b>Rodica MACALEȚ, Tudor MUNTEANU, Marian MINCIUNA</b> IMPLEMENTATION OF WATER FRAMEWORK DIRECTIVE 2000/60/EEC REGARDING GROUNDWATERS IN ROMANIA.....	168
<b>Sandro PRIVITERA</b> GEOMORPHOLOGICAL CHARACTERS OF THE ETNA COAST (EASTERN SICILY): EXAMPLES OF IRREVERSIBLE ENVIRONMENTAL DEGRADATION CAUSED BY ANTHROPIC ACTIVITIES.....	173
<b>Ionuț Mihai PRUNDEANU, Nicolae BUZGAR</b> THE DISTRIBUTION OF HEAVY METALS IN SOILS OF THE FĂLTICENI MUNICIPALITY AND ITS SURROUNDINGS.....	178
<b>Dan STUMBEA</b> MINERALOGY AND GEOCHEMISTRY OF SULFATES DEVELOPED ON SULFIDE-BEARING LOW-GRADE METAMORPHIC ROCKS OF SURFACE MINING WASTES....	179
<b>Dan STUMBEA</b> THE CLAY FRACTION FROM THE SOLID PRODUCTS OF ACID MINE DRAINAGE. A MINERALOGICAL APPROACH.....	182

## **Economic Geology**

---

<b>Fetullah ARIK, Umit AYDIN, Yesim Bozkir OZEN</b> GEOLOGICAL FEATURES AND ORE DEPOSITS OF ALADAG (EZINE/CANAKKALE).....	187
--	-----

<b>Gheorghe DAMIAN, Floarea DAMIAN, Vladimir A. KOVALENKER, Olga Yu. PLOTINSKAYA</b> NATIVE BISMUTH AND BISMUTH SULPHOSALTS IN CISMA POIANA BOTIZEI MINERALIZATIONS, BAIA MARE DISTRICT.....	189
<b>Mabrouk M. DJEDDI, Abdelkader A. KASSOURI</b> USING THE HODOGRAM AS AN AVO ATTRIBUTE TO IDENTIFY ANOMALIES OF GAS.....	191
<b>Nazan Yağın ERIK, Selin SANCAR</b> ORGANIC GEOCHEMICAL CHARACTERISTICS OF HAFİK COAL DEPOSITS (SİVAS BASIN, TURKEY).....	192
<b>Viorel IONESI, Mihaela Corina MERFEA, Ciprian APOPOEI</b> HYDROGEOLOGICAL STUDY FOR THE SUPPLY WITH WATER OF THE GLĂVĂNEȘTI AND GĂICEANA LOCALITIES (BACĂU COUNTY).....	199
<b>Marian MUNTEANU, Gordon CHUNNETT, Yong YAO, Allan WILSON, Yaonan LUO</b> THE PANXI REGION (SW CHINA) – STRUCTURE, MAGMATISM AND METALLOGENESIS.....	200
<b>Tudor MUNTEANU, Emilia MUNTEANU, Maria CĂLIN, Doina DRĂGUȘIN, Rodica MACALEȚ, George DUMITRAȘCU</b> HYDROGEOLOGICAL RESEARCH REGARDING THE BEȘTEPE-MAHMUDIA AREA, TULCEA COUNTY.....	204
<b>Zeynep ORU, Hasan EMRE</b> THE GEOCHEMICAL RELATIONSHIP BETWEEN THE COPPER MINERALIZATION AND REE PATTERNS: AN EXAMPLE FROM LYCIAN ALLOCHTHON, ÇAVDIR (BURDUR), SW TURKEY.....	205
<b>Alican OZTURK, Fetullah ARIK, M. Muzaffer KARADAG, Yesim Bozkir OZEN</b> REE CONTENTS AND BEHAVIORS OF PLACERS BELONGING TO THE BOZKIR OPHIOLITIC MELANGE IN BOZKIR COUNTY (KONYA-TURKEY).....	209
<b>Mihai Remus ȘARAMET, Constantin Cătălin CALU, Gabriel CHIRILĂ</b> THE ADVANTAGES OF USING THE MONTE CARLO SIMULATION METHOD IN ESTIMATING GEOLOGICAL GAS RESERVES.....	211
<b>Mihai Remus ȘARAMET, Răzvan RĂDUCANU, Iulian DIACONU, Iulia ZAHARIA</b> ON THE ESTIMATION OF THE HYDROGEOLOGICAL PARAMETERS IN THE CASE OF THE STATIONARY FLOW OF UNDERGROUND WATER.....	212
<b>Sorin Silviu UDUBAȘA, Gheorghe UDUBAȘA</b> THE DISTRIBUTION OF GOLD IN ROMANIA. ASSESSMENT OF ITS PRIMARY SOURCES.....	213

## **Tectonics - Structural Geology**

---

<b>Rahmi AKSOY</b> GEOLOGY AND DEFORMATION HISTORY OF MARMARA ISLAND AT THE NORTHERN EDGE OF THE SAKARYA ZONE NORTHWESTERN TURKEY.....	217
<b>Serafina CARBONE</b> THE APENNINIC-MAGHREBIAN OROGEN IN THE CENTRAL MEDITERRANEAN REGION: A REVIEW.....	221

<b>Fuat ÇÖMLEKCİLER, Hükmü ORHAN</b> SEDIMENTOLOGIC CHARACTERISTICS OF THE PLIOCENE-QUATERNARY ALLUVIAL FAN DEVELOPED SOUTHEAST OF SIZMA (KONYA-TURKEY).....	228
<b>Arif DELİ, Hükmü ORHAN</b> SYNSEDIMENTARY STRUCTURES IN JURASSIC ROCKS FOUND SOUTH-WEST OF ANKARA (TURKEY).....	229
<b>Diego PUGLISI</b> EARLY CRETACEOUS FLYSCH OF THE TETHYS REALM AND ITS EO- TO MESO- ALPINE DIACHRONOUS DEFORMATIONS.....	233
<b>George TUDOR</b> WEBGIS – A FRAMEWORK FOR THE WEB PRESENTATION OF THE 1:1 MILLION SCALE GEOLOGICAL MAP.....	240
<b>Mircea ȚICLEANU, Radu NICOLESCU, Adriana ION, Roxana CIUREAN, Rodica TIȚĂ, Ștefan GRIGORIU</b> THE TROVANTS OF THE CRETACEOUS AND NEOZOIC DEPOSITS IN THE CARPATHIAN AREA (ROMANIA).....	241



# **MINERALOGY AND PETROLOGY**



## **MINERAL PIGMENTS OF GRECO-ROMAN AND BYZANTINE AGES FROM DOBROGEA**

NICOLAE BUZGAR<sup>1</sup>, ANDREI BUZATU<sup>1</sup>, ANDREI IONUT APOPEI<sup>1</sup>, VASILE COTIUGA<sup>2</sup>, FLORIN TOPOLEANU<sup>3</sup>

<sup>1</sup>“Al. I. Cuza” University of Iași, Department of Geology, 20A Carol I Blvd., 700505 Iași, Romania; e-mail: nicolae.buzgar@uaic.ro

<sup>2</sup>“Al. I. Cuza” University of Iași, Department of History, 20A Carol I Blvd., 700505 Iași, Romania

<sup>3</sup> Institute of Eco-Museal Research Tulcea, 1 bis 14 Noiembrie Str., 820009, Tulcea, Romania

The purpose of the present paper is to identify the mineral pigments used in the painting of religious, military or administrative buildings from the Greco-Roman and Byzantine ages of Dobrogea through Raman spectroscopy. The buildings belong to the fortresses of Beroe, Argamum (Orgame) and Noviodunum, located on the right bank of the Danube river. Red ochre and hematite (red), black carbon ± siderite (black), lazurite (blue), verdigris (green) and natrojarosite (brownish yellow) have been identified. The black pigment does not contain black carbon only on a single fragment of a painted wall; instead, anglesite was identified, which leads us into believing that the pigment used was galena.

The building painted with natrojarosite certainly dates from the Greek age, as this pigment was mainly used during the maximum development period of Athens, being brought from the Pb mines of Attica.

### **Acknowledgements**

This work was supported by CNCSIS –UEFISCSU, project number PNII – IDEI code 2119/2008.

## MAFIC AND FELSIC MAGMA INTERACTION IN GRANITES: THE EOCENE HOROZ GRANITOID (NIGDE, TURKEY)

KERIM KOCAK<sup>1</sup>, VEYSEL ZEDEF<sup>1</sup>

<sup>1</sup> Selcuk University, Department of Geological Engineering, Konya, 42075, Turkey; e-mail: kkocak@yahoo.com; vzedef@selcuk.edu.tr

**Keywords:** Horoz, petrology, enclave, granitoid, Turkey.

The Eocene Horoz granitoid contains leucogranite and granodiorite, with mafic microgranular enclaves (MMEs). The leucogranite is relatively finer-grained than the granodiorite, which has relatively larger grains and more frequent MMEs. Generally, MMEs have very different sizes (from several cm up to several meters) and shapes (ellipse / round - cornered). The geometry of the MME – host contact varies from sharp to crenulate. MMEs usually exhibit a fine-grained margin against the host rock. Small blisters (1-10 cm in diameter) of the host rocks are incorporated into the MMEs.

The MMEs are characterized by the existence of resorbed, sieved-textured plagioclase, ocella quartz, poicilitic K-feldspar, magnesiohornblende with inverse chemical zoning, and acicular apatite, all of which are suggestive of a mingling between felsic and mafic magmas.

The granitoids and their enclaves contain low up to intermediate Nb (11-19), Zr (106-234 ppm), Y (10.2-33.7) ppm) and Zr/Nb (6.4-13.8), and low TiO<sub>2</sub> (0.15-0.48) contents, which are typical for calcalkaline associations. All samples display a K<sub>2</sub>O-rich composition, and, consequently, plot mostly on the fields of calcalkaline to high-K calcalkaline in composition. The felsic granites display, however, a considerably more potassic character by plotting high-K calcalkaline and shoshonite fields. Most of the samples have ASI values (Aluminium Saturation Index) < 1.1, limit between I and the S-type granitoid. MMEs and granitoids (granite and granodiorite) display distinct ranges of SiO<sub>2</sub> contents (56–63, 64–74 wt%, respectively); no overlap exists between the MMEs and their hosts. In Harker diagrams, SiO<sub>2</sub> increases with the decrease of Al<sub>2</sub>O<sub>3</sub>, CaO, MgO, FeO<sub>t</sub>, TiO<sub>2</sub>, Co and Eu, suggesting the fractionation of hornblende (pyroxene ± olivine), plagioclase, sphene and ilmenite. All samples generally display enrichment in large ion lithophile elements (LILEs), e.g. Cs, Rb and K, and depletion in high field strength elements (HFSEs), such as Y or Lu. MMEs and their host rocks have negative Nb, Ta and TiO<sub>2</sub> anomalies, which are characteristics of subduction-related magmas.

The REE patterns of granite and granodiorite are almost comparable, slightly concave-upward, and characterized by enrichment in Light REEs (LREEs) and depletion in Heavy

REEs (HREEs) contents, resulting in high  $(La/Lu)_N$  ratios (7.6-17.2). The existence of a slightly negative Eu anomaly ( $Eu/Eu^*$ : 0.67) suggests the fractionation of plagioclase crystals in the host magma. Compared with the host rocks, the enclaves have slightly lower  $(La/Lu)_N$  ratios (1.8-12) and a higher HREE content, with a more pronounced negative Eu anomaly ( $Eu/Eu^*$ : 0.53). Compared with granitoids, the enclaves are usually enriched in P, Ti, Y, Nb, and HREEs, probably due to the selective interdiffusion of these elements into the less polymerized magma.

Major, trace and REE data suggests that MMEs and their hosts may have derived from an enriched mantle, but more likely have also suffered crustal contamination. MMEs were possibly formed through injection of successive pulses of basic magma into upward mobile magma chambers containing cooler, crystalline granodiorite magma.

## THE FORMATION OF CONGO DIAMONDS WITH HALITE AND CARBON-BEARING MICRO-GRAINS

YASUNORI MIURA<sup>1</sup>, TAKAO TANOSAKI<sup>2</sup>

<sup>1</sup> Yamaguchi University, Yoshida 1677-1, Yamaguchi, 753-8512, Japan; e-mail: yasmiura@yamaguchi-u.ac.jp,

<sup>2</sup> Central Research Lab., Taiheiyo Cement Co. Ltd., Sakura, Japan

**Keywords:** Congo diamond, halite, limestone, carbon-bearing grains, sea-water effect.

### Introduction

Diamonds with large crystal planes, collected on the surface of the crust, are thought to have been formed within the deeper mantle, under high pressure, with xenolith grains of Fe and Mg and Si-rich grains, although such light elements of carbon or carbon dioxide gas were difficult to move deeper within the mantle after the formation of the planet Earth.

A detailed investigation carried out through ASEM (Analytical Scanning Electron Microscopy), however, revealed that micro-xenoliths of halite and calcite of carbonates mainly supplied from shallow origins (Miura et al., 2010; Miura and Iancu, 2009; Miura et al., 2009) have recently been found in DR (Democratic Republic) Congo diamonds by the senior author. As a result, the main purpose of the present paper is to elucidate the issue through in-situ ASEM analyses (Miura et al., 2010).

### Samples used in the present study, compared with the Kimberlite diamond

We collected several large pieces of Congo diamonds from central Africa, which display round or irregular shapes (fig. 1), and we compared the results obtained on them with those obtained on the Kimberlite diamond in South Africa, which displays clear shapes of diamond crystal planes. We noticed the following:

1) Congo diamonds from the Congo (Democratic Republic of Congo): (right in fig.1).

Xenoliths with fine grains and shallow places and with a round and irregular shape (left in fig. 2)

2) Kimberlite diamond (South Africa): Xenoliths with fine grains and deep place information (right diagram in fig.2).



Fig. 1 Sample location on the geographical map (left; Map of Africa, 2005) and Congo diamonds (right) dealt with in the present study.

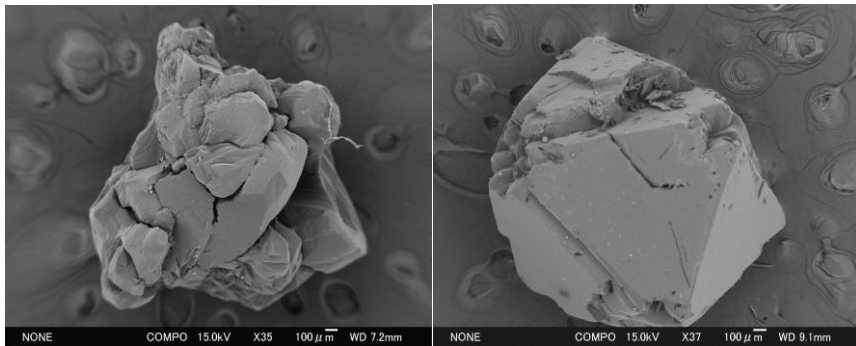


Fig. 2 SEM electron micrographs of diamonds of the DR of Congo with irregular shapes (left) and of the South African Kimberlite with sharp crystal planes (right). The scale bar is 0.1mm.

### In-situ analyses of the Kimberlite diamond

In-situ analyses using the FE-SEM with EDS analyzer indicate that Kimberlite diamonds from South Africa have foreign xenolith micro-grains of Fe, Mg-rich silicates and Ca, Fe and Mg carbonates (without any Na or Cl). It is believed that Kimberlite diamonds are direct remnants of deep mantle sources with Fe and Mg-rich micro-grains, although there are Ca-bearing micro-grains with carbon formed by metamorphic calcite-like grains, which are deficient of Al due to the little Ca from the anorthite component in the Earth's crust.

### Congo diamonds with halite crystals

According to in-situ FE-ASEM observation and analysis, the Congo diamonds contain the following micro-grains (fig. 3 and 4):

- 1) Nano-particles of calcite carbonates, carbon and gypsum in composition.
- 2) Halite (NaCl) crystals (fig.5) and Fe-silicate grains (without Mg).
- 3) Fine and irregular carbon-bearing grains (100nm in size), which are completely covered on the halite crystal plane formed after the formation of halite (fig. 5).

This indicates that there are dynamic explosions that destroy the original diamond crystals and mix them with the following quenched materials (Miura et al., 2010; 2009):

- 1) Carbon and carbonates (from limestone rocks) due to high Ca contents.
- 2) Halite (probably from salty water) due to high contents of both Na and Cl.
- 3) Carbon-bearing nano-particles due to high-temperature CO<sub>2</sub> explosions.

As, according to the ASEM data related to these samples, there is little akaganeite for chlorine sources, the explosion in the formation of the Congo diamond is not the normal type of meteoritic impact with fusion crust.

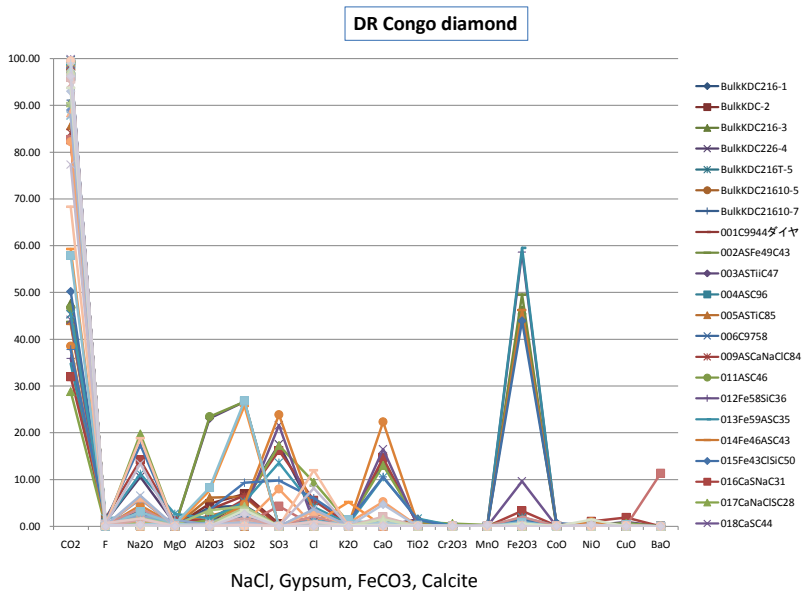


Fig. 3 In-situ analytical diagram with scanning electron micrograph (FE-ASEM) of the DR of Congo, Africa. There are diamonds with xenoliths of calcite, halite, gypsum and FeCO<sub>3</sub>.

### Processes involved in the formation of Congo diamonds

The present results indicate the following two steps in the formation of Congo diamonds:

1) Firstly, Congo diamonds are believed to have been formed at depth due to high pressure conditions. The first supply of carbon dioxide at depth is generated by massive impact processes during the primordial period in the history of the Earth (if there are any giant impacts).

2) The up-lift of Congo diamonds from the depth is triggered by a larger impact on the surface, meant to form a circular basin structure, where the crystalline surface of the original diamond is broken by dynamic high pressure and temperature. The second process through which present-day diamonds form at shallow depth is known through experimental results by a) the rounded and irregular surfaces of diamonds, b) shallow sedimentary rock remained as calcite carbonates with Ca, C and S elements, and c) the coating of irregular carbon-bearing micro-grains triggered by shallow explosion processes at the depth of the crust to halite crystal planes formed in the cavity and grains of Fe-silicates without Mg (probably caused by explosions in the presence of underground salty water).

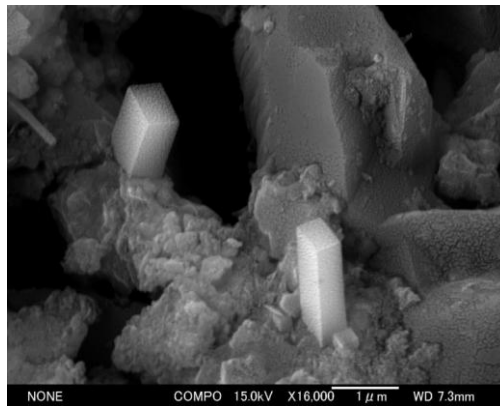


Fig. 4 Electron micrograph of the FE-ASEM data of the Congo diamond. The bar in the micrograph is 1 $\mu$ m in scale. The coated whitish grains are CO<sub>2</sub>-rich materials found on the halite and on other grain surfaces in the cavity of diamond grains.

### **Recent geological setting of the African continent**

The recent geological study of districts around the DR of Congo in Africa suggests the following:

1) The African continent is not a single geological unit, but several smaller continental units combined by continental drift. The DR of Congo consists of many geological units where there is impact signature at the end of the Permian (Fildani A. et al, 2009; fig. 1).

2) The districts around the DR of Congo display lower circulated basins, where the diamonds are mainly collected from the southern rim of the basin structure.

3) The relatively smaller circular structures found north-east of the DR of Congo are reported as impact craters ca.40km in diameter (Monegato G. et al., 2010); the DR of Congo also has relatively small impact craters.

### Summary

The results of the present study can be summarized as follows:

1) According to in-situ FE-ASEM investigation, Congo diamonds contain nanoparticles of calcite with halite crystals as remaining grains.

2) The Congo diamond is thought to be broken by explosions during up-lift process that occur at shallow depth, in the presence of salty liquid, and are probably accelerated by impact processes on the surface, which is estimated from the remaining circular basin.

### Acknowledgements

The authors wish to thank Professor Emeritus Dr. T. Kato of the Yamaguchi University for the discussion on diamond formation through electron microscopic study.

### References

- Fildani, A., Weislogel, A., Drinkwater, N.J., McHargue, T., Tankard, A., Wooden, J., Hodgson, D., Flint, S. , 2009. U-Pb zircon ages from the southwestern Karoo Basin, South Africa—Implications for the Permian-Triassic boundary. *Geology*, **37**, 719–722.
- Map of Africa , 2005. Africa relief and drainage. In: Institute for Civic Involvement. Fort Lauderdale, Florida. <http://teacherweb.ftl.pinecrest.edu/snyderd/APHG/projects/MUN-BC/maps/mapindex.htm>.
- Miura, Y., 2009. Lunar fluids from carbon and chlorine contents of the Apollo lunar samples. LPI Contribution No. 1515 (LEAG2009, USA), **45**, CD#2042 (p.2).
- Miura, Y., Iancu, O.G., 2009. Deposition of carbon, iron and nickel at geological boundaries of the ends of the Permian and Cretaceous Periods. *Geologie*, **55**, 105–112.
- Miura, Y., Tanosaki, T., Iancu, O.G., 2009. Mineral characteristics of carbonates with minor elements. Part 1. Calcites. *Geologie*, **55**, 97–104.
- Miura, Y., Tanosaki, T., Udagawa, M., 2010. Sea-Water Impact Materials: Carbon- and chlorine-bearing materials in impact glasses. *Shock Waves in Japan* (in Japanese with English abstract, Saitama Univ.), 117–118.
- Monegato, G. , Massironi, M., Martellato, E., 2010. The ring structure of Wembo-Nyama (Eastern Kasai, R.D. Congo): A possible impact crater in central Africa. 41<sup>st</sup> Lunar and Planetary Science Conference (LPI, NASA), CD#1601 (pp.2).

## **CONDITIONS INVOLVED IN THE FORMATION OF THE RIES CRATER, GERMANY, INFERRED FROM THE CARBON AND CHLORINE CONTENTS OF THE DRILLED SAMPLES**

YASUNORI MIURA<sup>1</sup>, TAKAO TANOSAKI<sup>2</sup>, OVIDIU GABRIEL IANCU<sup>3</sup>

<sup>1</sup> Yamaguchi University, Yoshida 1677-1, Yamaguchi, 753-8512, Japan; e-mail: yasmiura@yamaguchi-u.ac.jp,

<sup>2</sup> Central Research Lab., Taiheiyo Cement Co. Ltd., Sakura, Japan

<sup>3</sup> „Al. I. Cuza” University of Iași, Department of Geology, 20A Carol I Blv., 700505 Iași, Romania; e-mail: ogiancu@uaic.ro

**Keywords:** calcite, halite, carbon, chlorine, suevite, drilled core, limestone.

### **Introduction**

The impact processes and carbon sources of surface and underground rocks in the Ries crater, Germany, are not well known. This is mainly because there are few carbon sources on granitic target rocks at the surface, and carbon elements are considered extraterrestrial elements (rather than part of Earth's crust) in cosmic elemental abundances (Univ. Sheffield, 2006). The purpose of the present study is to show the carbon (C) contents and chlorine (Cl) distribution for surface samples and cores drilled from depths ranging between 300m and 1,000m (fig. 1), which have kindly been provided by the Ries Museum (Miura, 2007a).

### **Petrologic optical microscopy of surface suevite rocks**

In thin sections of suevite (impact breccias) on the surface (0 m in depth), there are the following dynamic flow textures caused by impact process (fig. 2):

- 1) Irregular and different-sized spherules formed through quenching from impact vapors and liquid states
- 2) Few matrix textures
- 3) Duplicated textures of breccias in breccias and the core-mantle.
- 4) Fine cavity and vacancy with spherules and matrix with iron and carbon formed by impact quenching of explosions.

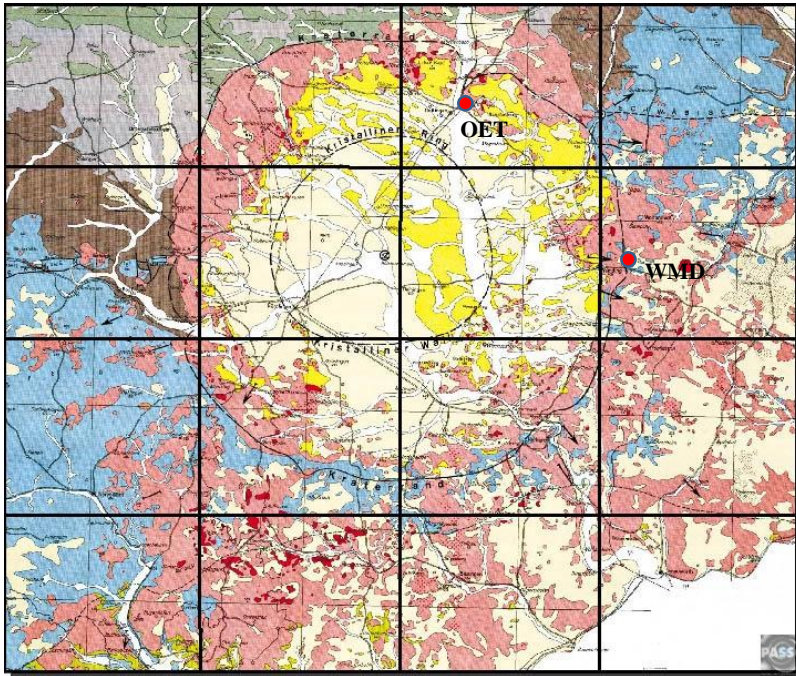


Fig. 1 Sample locations and core drilled at a depth of 500m within the Ries crater, Germany. On the geological map, the reddish (OET sample) and bluish (WMD sample) colors are granitic and limestone rocks, respectively.

### **X-ray fluorescence (XRF) analyses of suevite with carbon content**

In order to investigate the carbon contents of surface and drilled cores, the X-ray fluorescence (XRF) analyses of suevite using the Rigaku instrument are obtained through

the in-situ method as a whitish crystalline part and a black-matrix part of the sample found at a depth of 500m (right sample in fig. 1):

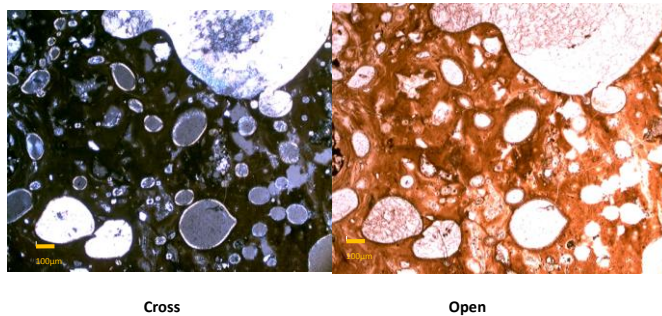


Fig. 2 Optical micrographs of surface suevite with dynamic flow and quenched textures in the Ries crater, Germany. The scale bar is 0.1mm. Cross and open Nichols.

1) Both the whitish (crystalline) part and the black (matrix) part contain carbon (7 to 11 wt.% CO<sub>2</sub>) as a plagioclase-like composition, as remnants of impact explosion products (fig. 3).

2) The whitish part formed by higher temperatures with a slower cooling history has a lower carbon content, whereas the black matrix part formed by quenched processes contains a relatively higher carbon content with many Ca ions (fig. 3).

### **Drilled core samples used in the present study**

The following five drilled cores with 6 samples (300m grey, 500m white, 500m black matrix, 700m reddish grey, 900m grey and 1000m grey) have been used for carbon distribution by comparing them with two grey surface samples (Wemding WMD, and OET Oettingen) obtained through carbon-detective XRF data, with the following results (fig. 3):

1) There are few regular changes of eight oxides (C, Ca, Na, Mg, Al, Si, S and K) from the surface to the depth (1000m), which is caused by the impact mixing of the samples even at depth.

2) The suevite composition of sample Oettingen QET (0m), with high Si and Al contents, is abundant in wide areas of the samples collected from 300m, 500m, 900m and 1000m, which are considered of mixed granitic composition. This indicates that suevite impact breccias are mainly impacted granite in composition.

3) High Ca and C contents with lower Si contents are obtained at the surface (WMD sample) and at a depth of 700m, which are considered a mixture of limestone with hot

carbon dioxide. This indicates that limestone-rich breccias are mixed with major limestone and minor granitic rock through impact mixing.

4) Based on the present XRF data with carbon analyses, both impacted rocks of suevite and limestone-rich breccias are impact mixing rocks, which cannot be explained by a relatively slow magmatic separation of magma.

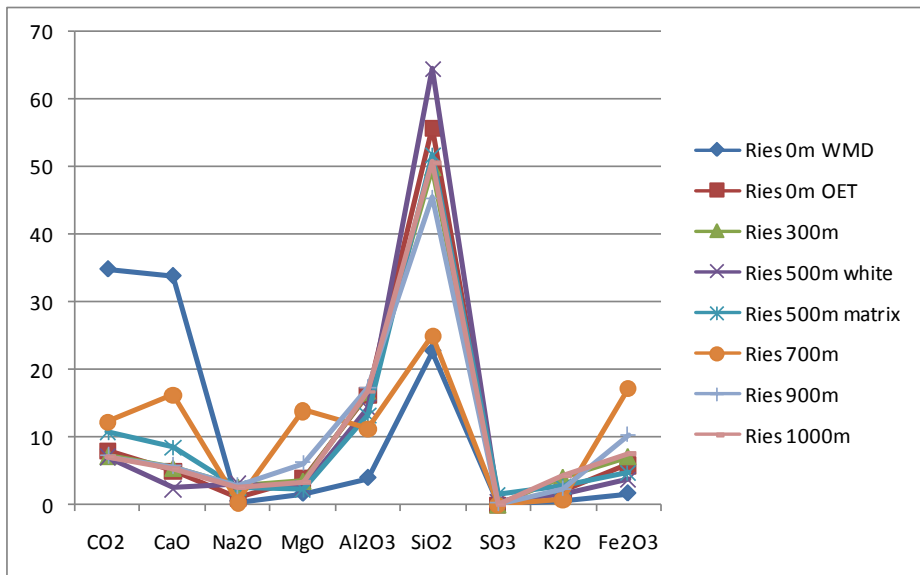


Fig.3. XRF compositional comparisons of 9 samples collected from the surface and depths of up to 1000m in the Ries crater, Germany. The samples are separated into granitic and limestone-rich breccias.

### Carbon abundances of the impacted matrix

Both the whitish crystalline part and the black matrix have different contents of Ca and C at surface level and in sample drilled at a depth of 500m (Miura, 2009; Miura et al., 2009; Miura, 2007a,b).

1) The suevite compositions of granitic rocks are a mixture of granitic (ca.70-85wt. %) and limestone (ca.11-17wt. %) during impact processes.

2) In the limestone-like composition of the suevite breccias, Ca combined with CO<sub>2</sub> remains, though almost all of the carbon dioxide escapes during impact processes.

### Chlorine contents of the drilled cores

The chlorine contents of bulk samples are obtained as follows (fig. 6; Miura, 2009; Miura and Iancu, 2009; Miura, 2007c):

1) The Na and Cl contents of surface samples are relatively lower (due to weathering processes), whereas the Na contents of the drilled cores are relatively higher in the granitic composition of suevite breccias, rather than those in limestone-like 700m samples.

2) The chlorine contents in the drilled cores are relatively lower due to few effects of sea-water impacts, whereas those in the black matrix (500m in depth) show relatively higher stored contents of gas states of C and Cl during impact quenching.

### **Elements Ni and Co of impact origin**

Refractory elements of Fe and Ni, Co and Cu are obtained at the bottom of the impact crater (Miura and Iancu, 2009; Miura, 2007c). In fact, there are sharp peaks of Fe and Ni contents at a depth of 700m, which is the crater bottom where impact materials are concentrated and where a similar increase of CO<sub>2</sub> contents is obtained.

### **Summary**

The results of the present study can be summarized as follows:

1) In-situ XRF analytical data from the surface and cores drilled at depths up to 1000m indicate that suevite and limestone breccias show impacted granite-rich and limestone-rich breccias, respectively.

2) The Ca and C contents are increased by limestone-rich target rock.

3) The Cl content is lower due to dry land impact, with little relation to Na.

4) Fe and Ni contents (as well as Co, Cu and C contents) are increased exclusively in cores drilled at a depth of 700m, which is considered the probable crater bottom for impact accumulation in the case of the present samples.

### **Acknowledgements**

The authors wish to thank the Director of the Ries Crater Museum for the samples provided and to Professor Emeritus Dr. T. Kato of the Yamaguchi University for the discussion on the topic.

### **References**

- Miura, Y., 2009. Lunar fluids from carbon and chlorine contents of the Apollo lunar samples. LPI Contribution No. 1515 (LEAG2009, USA), **45**, CD#2042 (p. 2).
- Miura, Y., 2007a. Analyses of drilled samples of Ries, Sierra Madera and Takamatsu craters. *Goldschmidt 2007 – Atoms to Planets* (Cologne, Germany), Cambridge Publications, 674–674.
- Miura, Y., 2007b. Shocked carbonate minerals formed by natural and artificial impact processes. In: *Frontiers in Mineral Sciences 2007* (Univ. of Cambridge, UK), 223–223.
- Miura, Y., 2007c. ASEM observation of impact spherules with carbon, Fe and Ni at the P/T and K/T geological boundaries. *Meteoritics and Planetary Science*, p. 109.
- Miura, Y., Iancu, O.G., 2009. Deposition of carbon, iron and nickel at geological boundaries of the ends of the Permian and Cretaceous Periods. *Geologie*, **55**, 105–112.
- Miura, Y., Tanosaki, T., Iancu, O.G., 2009. Mineral characteristics of carbonates with minor elements. Part 1. Calcites. *Geologie*, **55**, 97–104.
- Periodic table web-elements. Univ. Sheffield, 2006. <http://www.webelement.com>

## FINE NANO-BACTERIA-LIKE TEXTURE WITH AN AKAGANEITE COMPOSITION

YASUNORI MIURA<sup>1</sup>

<sup>1</sup> Yamaguchi University, Yoshida 1677-1, Yamaguchi, 753-8512, Japan; e-mail: yasmiura@yamaguchi-u.ac.jp

**Keywords:** fine nano-bacteria-like texture, akaganeite composition, iron meteorite, fusion crust.

### Introduction

A spherule texture can be formed in dynamic reaction during any meteoritic impact in the air of the Earth (Miura et al., 1995). However, there are few reports on nano-bacteria-like (i.e. spherule-chained) textures of akaganeite with iron (and nickel) oxides (with chlorine) in composition and micro-texture with 100nm in order in an iron meteorite (Miura, 2008, 2009).

The purpose of the present study is to elucidate the spherule-chained texture with micro-texture of 100nm in order found in the Kuga iron meteorite, in Iwakuni, Yamaguchi, Japan.

### Fine bacteria-like textures in the Kuga meteorite

The Kuga iron meteorite, found in Kuga, Iwakuni, Yamaguchi, Japan, reveals an irregular spherule-chained texture with a Fe and Ni-rich composition, 10 $\mu$ m in size, where each spherule contains a “long micro-texture 100nm in size” (fig. 1). The complex texture of flow and chained shapes can be found in the fusion crust of the iron meteorite formed by quenched and random processes with vapor-melting processes in the air of the Earth (Miura, 2008, 2009). The FE-ASEM with EDX analyses based on in-situ observation indicate that the matrix of the spherule-chained texture with Fe, Ni and O-rich (with minor Cl) composition is a carbon-rich composition formed through impact reactions in the air.

### Difference between textures with an akaganeite composition in the meteorite

Akaganeite is found in the fusion crusts of meteorites. In fact, it is obtained through in-situ FE-SEM investigations on the fusion crusts of Nio (fallen in Yamaguchi, Japan), Mihonoseki (Matsue, Japan) and Carancas (Peru) as rosette (flake) texture.

The main difference between the akaganeite found in meteorites is the micro-texture with carbon contents at nano-bacteria-like and rosette textures. The rosette texture is cause

by chlorine gas explosions while the meteorite is burning in the air, whereas the nano-bacteria-like texture can be found mainly in carbon-rich grains during the melting of the meteorite at high temperatures in the air.

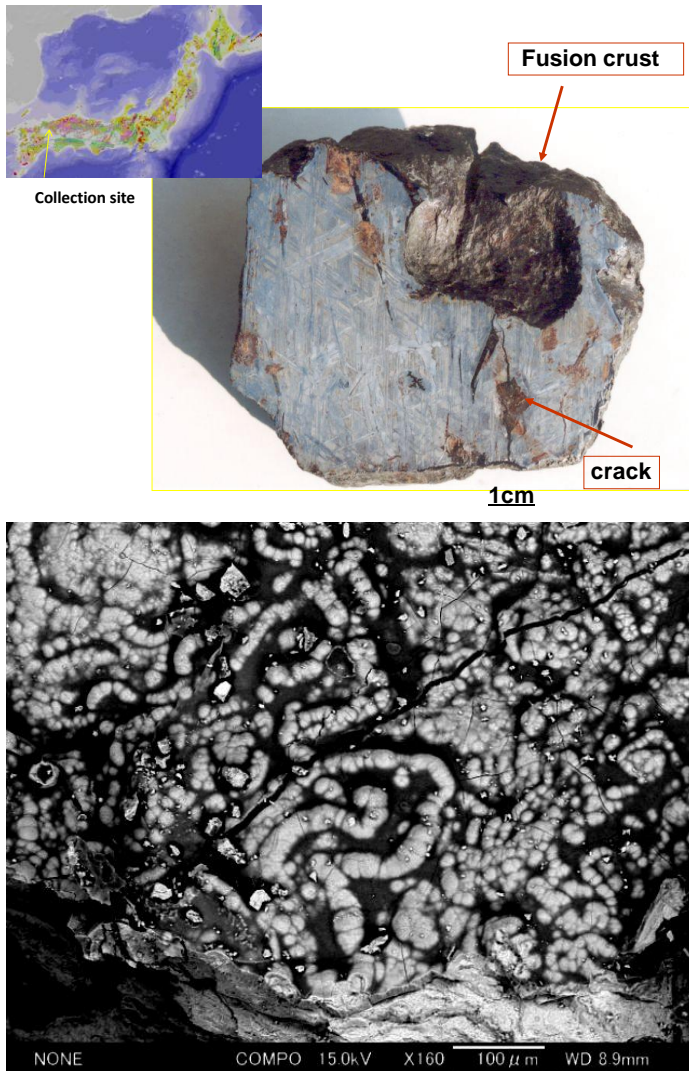


Fig. 1 Sample location of the Kuga iron meteorite found in Kuga, Yamaguchi, Japan (above), and electron micrograph (FE-SEM) of the Fe-Ni-Cl-rich texture of akaganeite with spherule-chained and long shapes in the Kuga iron meteorite (below).

## Comparison with the Martian meteorite

Remnants of life in the ocean are indicated by mineralized fossils, which can be found in the Martian meteorite ALH84001 as bacteria-like chained texture of magnetite in composition (100nm in order) around carbonate spherules (McKay et al., 1996). The similarity in the bacteria-like texture of the ALH84001, compared with that of the Kuga iron meteorites in the present study, is the Fe-rich, C-bearing composition and the small-sized chained texture being replaced by a Fe and O-rich composition in the air.

The major difference between these textures is the absence of carbonate minerals in the Kuga iron meteorite, compared with the Martian nano-bacteria texture, as listed in Table 1, although there are many carbon grains in Kuga iron meteorites. This indicates that the impact reaction of the iron meteorite and the atmosphere cannot form double-staged textures of Fe-O fossils and carbonate spherules of the Martian meteorite ALH84001 (Miura, 2009).

Tab. 1. Main characteristics of the fine-bacteria-like texture of Kuga iron meteorites (Miura, 2008, 2009).

Fine-spherule chained texture:	10 $\mu$ m in size
Nano-bacteria texture:	100nm in order
Fe, Ni-rich, C, Cl-bearing grains:	Akaganeite-like composition (grain) and C-rich (matrix)
No carbonates:	Few carbonate formations without a Ca or Mg source

## Summary

The results of the present study can be summarized as follows:

- 1) A spherule-chained texture of nano-bacteria-like grains with Fe, Ni, C and Cl can be found at the fusion crusts of the Kuga iron meteorite found in Japan, which are completely different from the double-stage textures of the Martian meteorite ALH84001.
- 2) The nano-bacteria-like texture of the Kuga iron meteorite is a significant example of how fine nano-particle coexisted with carbon-rich grains.

## Acknowledgements

The authors wish to thank Dr. T. Kato, Yamaguchi University, for the discussion on the topic.

## References

- McKay, D.S., Gibson Jr., E.K., Thomas-Keprta, K.L., Vali, H., Romanek, C.S., Clemett, S.J., Chillier, X.D.F., Maechling, C.R., Zare, R.Z., 1996. Search for past life on Mars: Possible relic biogenic activity in Martian meteorite ALH84001. *Science*, **273**, 924–930.
- Miura, Y., 2008. Formation of spherule-chained texture by shocked Kuga meteorite in air. *Meteoritics & Planetary Science*, 43–7, #5203.

- Miura, Y., 2009. Formations of bacteria-like textures by dynamic reactions in meteorite and syntheses. Eos Trans. AGU, **90**(22), Jt. Assem. Suppl., B73A16.
- Miura, Y., Iancu, O.G., Iancu, I., Yanai, K., Haramura, H., 1995. Reexamination of Mocs and Tauti chondritic meteorites: Classification with shock degree. Proc. NIPR Symp. Antarctic Meteorites (NIPR, Tokyo), **8**, 153–166.

## MINERALOGY OF METAMORPHIC FORMATIONS FROM THE MĂNĂILA AREA (EASTERN CARPATHIANS)

SIMONA MOLDOVEANU<sup>1</sup>, OVIDIU GABRIEL IANCU<sup>1</sup>, GHEORGHE DAMIAN<sup>2</sup>,  
HAINO UWE KASPER<sup>3</sup>

<sup>1</sup> „Al. I. Cuza” University of Iași, Department of Geology, 20A Carol I Blv., 700505 Iași, Romania; e-mail: iftode\_simona@yahoo.com; ogiancu@uaic.ro

<sup>2</sup> North University of Baia Mare, 62A Dr. Victor Babeș Street, 430083 Baia Mare, Romania; e-mail: gheorghe.damian@ubm.ro

<sup>3</sup> Institut für Geologie und Mineralogie der Universität zu Köln, Zùlpicher Str. 49a, D-50674 Köln, Deutschland

**Keywords:** Kuroko deposits, Mănăila area, pyrite, XRD.

### Geological setting

The Mănăila mineralization is located in the Crystalline-Mesozoic Zone of the Eastern Carpathians, in the Tulghes terrane. The geological formations from this area were formed during Precambrian to Upper Cretaceous. Most of the geological formations are composed of metamorphic rocks. Sedimentary rocks occur to a small extent, and igneous rocks occur only occasionally.

The Tulghes terrane displays a complex lithology (Balintoni et al., 2009). This Ordovician metamorphic unit was subdivided by Vodă (1993) into four formations, (from bottom to top): (1) the *Căboiaia sub-unit (Tg1)* – Quartzitic formation, (2) the *Holdița sub-unit (Tg2)* Quartzitic-graphitic formation, (3) the *Leșu Ursului sub-unit (Tg3)* – Volcano (rhyolitic)-sedimentary formation, and (4) the *Arșița Rea sub-unit (Tg4)* – Phyllitic-quartzitic formation. Only the third sub-unit occurs in the Mănăila area and consists of a metamorphosed sedimentary volcanogenic sequence, made up of two prevailing rock types – quartzites and quartz-feldspathic rocks (Iancu and Popa, 2010). They contain an important accumulation of a stratiform sulphide ore (Balintoni, 1997).

The carbonate rocks are poorly represented; they crop out especially in the *Holdița sub-unit*, where a characteristic association is found: black quartzite, white quartzite, carbonate rocks, chloritic and feldspar-rich green rocks, which represent sedimentary rocks whose origin was favored by the presence of iron. Metabasites are either scarce or absent (Balintoni, 1997).

## Samples and methods

Five metamorphic rock samples from the Mănăila area were analyzed by different methods (optical microscopy, XRD, XRF) in order to establish their nature and mineralogical composition.

Thin and polished sections were prepared at the North University of Baia Mare.

The analyses were performed in the laboratories of the Institute of Geology and Mineralogy at the University of Cologne, Germany.

A short description of the samples is provided below. Thus, sample no. 1 is a sericite-quartzite rock, gray-green in color, slightly brittle. Sample no. 2 is a quartzitic sericite-chlorite schist, white-gray to greenish-gray in color, slightly brittle. The third sample represents a quartzitic sericite-chlorite schist with feldspar, a rock with a clear schistosity, a greenish-gray color. Sample no. 4 is a compact pyrite ore, and sample no. 5 is represented by a quartzite sericite-chlorite schist, white-gray in color, weakly greenish, slightly brittle. All samples exhibit a lepidogranoblastic texture.

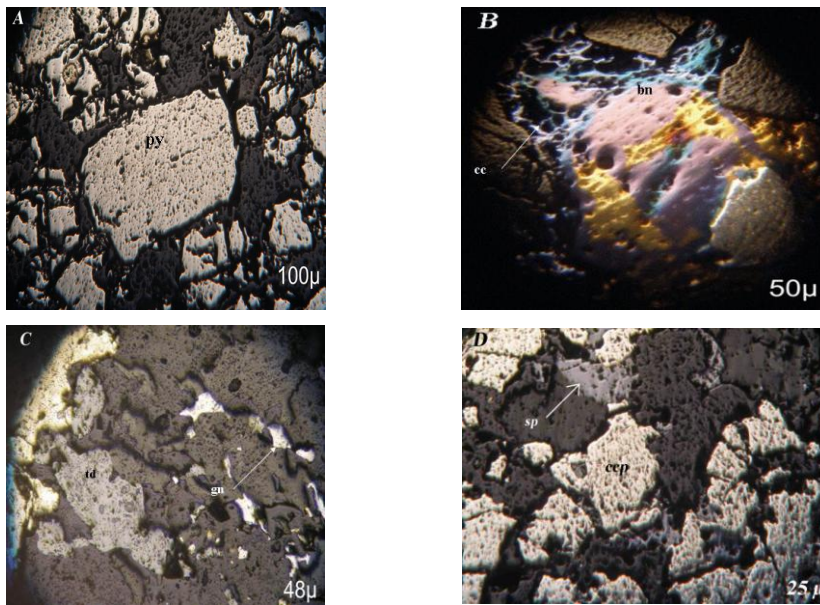


Fig. 1 Optical micrographs in reflected light of the main sulphides from the Mănăila area. **A** pyrite (py) crystals fissured by metamorphism; **B** bornite (bn) and chalcocite (cc); **C** tetrahedrite (td) crystal associated with chalcopyrite (ccp) and galena (gn); **D** sphalerite (sp) crystals associated with chalcopyrite. The lengths of figures are displayed in the bottom-right corner of the photos.

## Results and discussions

The association of ore minerals and their proportions compared to rock-forming minerals, allowed us to set up three economic important layered accumulations: (i) compact ore, (ii) semi-compact ore and (iii) disseminated ore altogether closely associated revealing gradual transitions from one texture to the other. The mineralogical composition common to all three types of ore is relatively simple: pyrite, chalcopyrite, sphalerite, galena and tetrahedrite, respectively (Fig. 1) in paragenesis with quartz, chlorite and muscovite. Pyrite is the major metallic ore which can be found as euhedral crystals (Fig. 1A). It contains small inclusions of bornite (Fig. 1B), commonly associated with covellite, sphalerite, chalcopyrite (Fig. 1D) and sometimes small grains of galena.

Tetrahedrite is represented by arsenic end member and intermediate arsenic-antimony member (Damian et al., 2005).

The main minerals pyrite, chalcopyrite, quartz and muscovite were identified by XRD analysis: (Fig. 2).

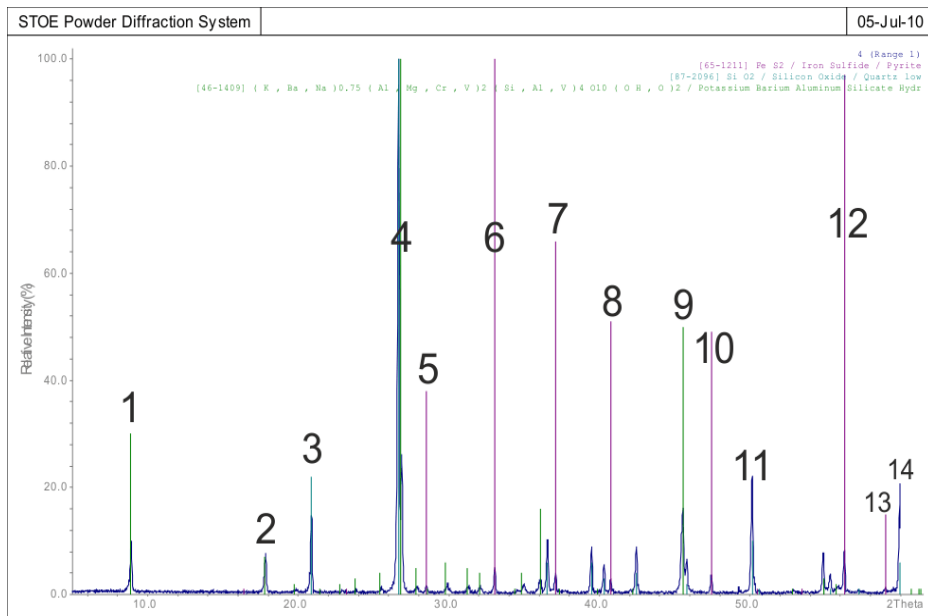


Fig. 2 Diffractometry of the main components of the Mănăila ore deposit (sample 4b: pyrite-peaks 4, 6, 12, chalcopyrite-peaks 7, 8, 9) (Radiation  $\text{CuK}\alpha_1$ ,  $\lambda = 15406 \text{ \AA}$ ) (By courtesy of Prof. Bohaty, Köln)

In order to determine the major elements, five rock samples were analyzed by using XRF.

The results contained in Table 1 highlight a wide range of variations of SiO<sub>2</sub> and Al<sub>2</sub>O<sub>3</sub> in the analyzed rocks.

Such high values can be found in quartzitic sericite schists (from 55.29 to 80.65%, samples 1a and 5a), while lower are found in sericite-chlorite schists.

Comparing the content of major elements of samples from the studied area with those of similar petrographic types, we notice that certain values are similar to the Kuroko-type deposits of Honshu, Japan. (SiO<sub>2</sub>: 0 to 82.0%, Fe<sub>2</sub>O<sub>3</sub>: 1.1 to 52.3) (Glasby *et al.*, 2008).

## Conclusions

According to microscopic studies the ore consists predominantly of pyrite and chalcopyrite. The XRD determinations of quartz, pyrite and chalcopyrite were performed with a reasonable accuracy.

Tab. 1 The chemical composition of the Mănăila schist

Oxides (%)	Samples				
	1a	2a	3a	4a	5a
SiO <sub>2</sub>	80.65	14.21	9.68	3.81	55.29
Fe <sub>2</sub> O <sub>3</sub>	8.94	57.05	68.25	75.93	30.96
Al <sub>2</sub> O <sub>3</sub>	7.29	9.17	7.36	1.45	7.57
TiO <sub>2</sub>	0.04	0.05	0.03	0.04	0.04
CaO	0.03	0.02	0.01	0.02	0.02
MgO	0.49	8.16	6.31	1.14	0.98
MnO	0.00	0.05	0.04	0.01	0.01
Na <sub>2</sub> O	0.31	0.34	0.10	0.32	0.30

1a – quartzitic-sericite schist; 2a – quartzitic sericite-chlorite schist; 3a – quartzitic sericite chlorite schist with feldspar; 4a – compact pyritic ore; 5a – quartzitic sericite-chlorite schist

The metamorphosed ore paragenesis is most likely of an initial vulcanogen Kuroko type and it consists of pyrite, chalcopyrite, some sphalerite, galena and tetrahedrite.

## Acknowledgments

The present work was supported by the European Social Fund in Romania, under the responsibility of the Managing Authority for the Sectoral Operational Programme for Human Resources Development 2007-2013 (grant POSDRU/88/1.5/S/47646).

## References

- Balintoni I., 1997. Geotectonics of metamorphic land from Romania, Carpathica Publishing House, Cluj Napoca, 177p. (In Romanian).
- Balintoni, I., Balica, C., Ducea, M.N., Fukun Chen, Hann, H.P., Şabliovschi, V., 2009. Late Cambrian- Early Ordovician Gondwanan terranes in the Romanian Carpathians: A zircon U-Pb provenance study. *Gondwana Research*, **16/1**, 119–133.

- Damian, Gh., Damian, F., Denuț, I., Iepure, Gh., Macovei, Gh., 2005. New data about tetrahedrite-group from metamorphosed ore deposits from Romania. *Buletin Stiințific Univ. de Nord Baia Mare, Seria D. Exploatare miniere, preparare metalurgie neferoasa, geologie si ingineria mediului*, **XIX**, 357–370.
- Glasby G.P., Iizasa K., Hannington M., Kubot H., Nots K., 2008. Mineralogy and composition of Kuroko deposits from northeastern Honshu and their possible modern analogues from the Izu-Ogasawara (Bonin) Arc south of Japan: Implications for mode of formation. *Ore Geology Reviews*, **34/4**, 547–560.
- Iancu, O.G., Popa, C., 2010. Mânăila quarry (metamorphosed base metal deposit), near the Valea Putnei village. In Iancu, O. G. & Kovacs, M. (eds.): *RO1 - Ore deposits and other classic localities in the Eastern Carpathians: From metamorphics to volcanics. Field trip guide. 20 General Meeting of the International Mineralogical Association, Budapest. Acta Mineralogica-Petrographica (Szeged), Field Guide Series*, **19**, 55p.
- Vodă, A., 1993. Tulgheș Series. Geologic report. Archive of S.C. "Prospectiuni" S.A., București. (In Romanian).

**GEOCHEMISTRY AND TECTONIC SIGNIFICANCE OF THE CUMULATE  
ROCKS OF THE KÖMÜRHAN OPHIOLITE IN SOUTHEAST ANATOLIA  
(ELAZIĞ-TURKEY)**

TAMER RIZAOĞLU<sup>1</sup>, OSMAN PARLAK<sup>2,3</sup>, FIKRET İŞLER<sup>2</sup>, VOLKER HOECK<sup>4</sup>

<sup>1</sup> K.S.U Department of Geological Engineering, TR46100 Kahramanmaraş, Turkey; e-mail: tamer@ksu.edu.tr

<sup>2</sup> Çukurova University, Department of Geological Engineering, TR01330 Adana, Turkey; e-mail: parlak@cukurova.edu.tr

<sup>3</sup> Adıyaman University, Faculty of Vocational and Technical Education, TR02040 Adıyaman, Turkey

<sup>4</sup> University of Salzburg, Department of Geography and Geology, Salzburg , A-5020, Austria; e-mail: volker.hoeck@sbg.ac.at

**Keywords:** Neotethys, ophiolite, cumulate, mineral chemistry, Kömürhan, Elazığ.

The southern Neotethyan oceanic basin was active during the Triassic-Miocene period, between the Tauride platform to the north, and the Arabian platform to the south (Şengör and Yılmaz, 1981). The remnants of Neotethys are characterized, in a descending structural order, by ophiolites, metamorphic soles and ophiolitic mélanges. The ophiolites and related subduction-accretion units were generated during the closing stages of Neotethyan oceanic basins since the Late Cretaceous (Pearce et al., 1984; Yalınız et al., 1996, 2000; Robertson, 2002, 2004; Parlak et al., 2004, 2009; Robertson et al., 2006, 2007). The late Cretaceous Kömürhan ophiolite is located west of the Hazar lake, in the Elazığ region. It is one of the best ophiolitic bodies, showing the characteristics of the emplaced Neotethyan oceanic crustal remnants from the eastern Taurides in southeastern Turkey. This ophiolitic body has a genetic link with the İspendere ophiolite to the west, and the Guleman ophiolite to the east (Yazgan, 1984; Yazgan and Chessex, 1991; Beyarslan and Bingöl, 1996, 2001; Rızaoğlu et al., 2006, 2009). In the north, the Kömürhan ophiolite is tectonically overlain by the Malatya-Keban platform, and is intruded by an Andean-type volcanic arc granitoid (Baskil granitoid), whereas in the south it thrusts over the Middle-Eocene Maden Complex (Rızaoğlu et al., 2006, 2009).

The Kömürhan ophiolite is characterized by a complete oceanic lithosphere succession and consists of mantle tectonites, ultramafic to mafic cumulates, isotropic gabbros, a sheeted dyke complex, plagiogranite, volcanics and associated volcano-sedimentary units. A thin slice of metamorphic sole rocks, showing inverted metamorphism (green-schist metamorphic facies at the bottom and amphibolite facies at the top), can be noticed at the

base of the tectonites. The cumulate rocks display cumulate structures such as igneous lamination and cross-and graded bedding. Petrographically, ultramafic cumulates are represented by wehrlite, whereas mafic cumulates are represented by olivine-gabbro, gabbro, gabbro-norite and amphibole-gabbro. The wehrlitic cumulates have an intrusive contact with the gabbroic cumulates. The wehrlitic rocks exhibit mesocumulate to poikilitic textures, and are represented by xenomorphic olivine (60-70 vol.%) and clinopyroxene (20-30 vol.%) as the main mineral phases. Limited amounts of chromites (1-2vol.%) are seen as dispersed crystals in the mass of variably serpentized olivines and pyroxenes. All mafic cumulate rock types display granular to poikilitic textures. The olivine-gabbro comprises olivine (Fo<sub>73-76</sub>; 20-30 vol.%), plagioclase (An<sub>92-94</sub>; 50-80 vol.%), clinopyroxene (En<sub>69-70</sub>Wo<sub>22-27</sub>Fs<sub>4-8</sub>; 5-30 vol.%), orthopyroxene (En<sub>76-77</sub>Wo<sub>0.6-0.7</sub>Fs<sub>22-23</sub>; <5 vol.%), chromite and Fe-Ti oxide minerals. Serpentine, chlorite, talc, epidote and amphibole appear as secondary phases. The gabbro-norite is characterized by clinopyroxene (En<sub>40-51</sub>Wo<sub>21-44</sub>Fs<sub>7-26</sub>; 20-30 vol.%), orthopyroxene (En<sub>57-61</sub>Wo<sub>1.3-2.2</sub>Fs<sub>37-40</sub>; 10-15 vol.%), plagioclase (An<sub>53-77</sub>; ~ 50 vol.%) and opaque minerals. The gabbro is characterized by plagioclase (60-80 vol.%), clinopyroxene (15-20 vol.%), orthopyroxene (1-2 vol.%) and amphibole (3-5 vol.%); secondary phases consist of kaolinite, sericite, chlorite and magnetite. The mineralogy of amphibole-gabbro is represented by plagioclase (An<sub>43-57</sub>; 80-85 vol.%), amphibole (10-15 vol.%), biotite (2-3 vol.%) and opaque minerals (1-2 vol.%).

The crystallization order of the cumulus and intercumulus phases is olivine ± chromian spinel, clinopyroxene, plagioclase and orthopyroxene. In the gabbroic cumulate rocks of the Kömürhan ophiolite, the crystallization of clinopyroxene before plagioclase, the presence of highly calcic plagioclase, as well as highly magnesian clinopyroxene and olivine are common characteristics of the rocks. All these data indicate that the Kömürhan ophiolite is compositionally similar to those observed in modern island arc tectonic settings. All data derived from the cumulate rocks of the Kömürhan ophiolite suggest that they formed in a tectonic setting of suprasubduction zone, during the Late Cretaceous, and display similar features to other ophiolites in the southern Neotethys (Parlak et al., 1996, 2000, 2004, 2009; Beyarslan and Bingöl, 2000; Bağcı et al., 2005, 2006, 2008; Dilek and Furnes, 2009; Robertson, 2002, Robertson et al., 2006, 2009; Yalınız et al., 1996, 2000).

## References

- Bağcı, U., Parlak, O., Höck, V., 2005. Whole-Rock Mineral Chemistry of Cumulates from the Kızıldağ (Hatay) Ophiolite (Turkey): Clues for Multiple Magma Generation During Crustal Accretion in the Southern Neotethyan Ocean. *Mineralogical Magazine*, **69**/1, 53–76.
- Bağcı, U., Parlak, O., Höck, V., 2006. Geochemical character and tectonic environment of ultramafic to mafic cumulates from the Tekirova (Antalya) ophiolite (southern Turkey). *Geological Journal*, **41**, 193–219.
- Bağcı, U., Parlak, O., Höck, V., 2008. Geochemistry and tectonic environment of diverse magma generations forming the crustal units of the Kızıldağ (Hatay) ophiolite southern Turkey. *Turkish Journal of Earth Sciences*, **17**, 43–71
- Beyarslan, M., Bingöl, A.F., 2000. Petrology of a Supra-Subduction Zone Ophiolite (Elazığ, Turkey). *Can. J. Earth Sci.*, **37**, 1411–1424.
- Beyarslan, M., Bingöl, A.F., 2001. Origin of Wehrlitic Intrusions in the İspendere (Malatya) and Kömürhan (Elazığ) Ophiolitic Complex (Eastern Taurus -Turkey). *Geosound*, **38**, 39–47.

- Dilek, Y., Furnes, H., 2009. Structure and geochemistry of Tethyan ophiolites and their petrogenesis in subduction rollback systems. *Lithos*, **113**, 1–20.
- Parlak, O., Delaloye, M., Bingöl, E., 1996. Mineral Chemistry of Ultramafic and Mafic Cumulates as an Indicator of the Arc-related Origin of the Mersin Ophiolite (Southern Turkey). *Geol. Rundsch*, **85/4**, 647–661.
- Parlak, O., Hoeck, V., Delaloye, M., 2000. Suprasubduction zone origin of the Pozanti-Karsanti ophiolite (Southern Turkey). Deduced from whole rock and mineral chemistry of the gabbroic cumulates. In Bozkurt, E., Winchester J.A., Piper, J.D.A. (Eds.), *Tectonics and magmatism in Turkey and the Surrounding area*. Geol. Soc. London, Spec. Publ., **173**, 219–234.
- Parlak, O., Höck, V., Kozlu, H., Delaloye, M., 2004. Oceanic Crust Generation in an Island Arc Tectonic Setting, SE Anatolian Orogenic Belt (Turkey). *Geological Magazine*, **141**, 583–603.
- Parlak, O., Rızaoğlu, T., Bağcı, U., Karaoğlu, F., Höck, V., 2009. Tectonic significance of the geochemistry and petrology of ophiolites in southeast Anatolia, Turkey. In Robertson, A.H.F., Parlak, O., Koller, F. (Eds.), *Tethyan Tectonics of the Mediterranean region: Some recent advances*. *Tectonophysics*, **473/1-2**, 173–187.
- Pearce, J.A., Lippard, S.J., Roberts, S., 1984. Characteristics and Tectonic Significance of Suprasubduction Zone Ophiolites. In Kokelaar, B.P., Howells, M.F. (Eds.), *Marginal Basin Geology*. Geological Society of London, Special Publication, **16**, 77–94.
- Rızaoğlu, T., Parlak, O., Höck, V., İşler, F., 2006. Nature and Significance of Late Cretaceous ophiolitic rocks and its relation to the Baskil granitoid in Elazığ region, SE Turkey. In Robertson, A.H.F., Mountrakis, D. (Eds.), *Tectonic Development of the Eastern Mediterranean Region*. Geological Society, London, Special Publications, **260**, 327–350.
- Rızaoğlu, T., Parlak, O., Höck, V., Koller, F., Hames, W.E., Billor, Z., 2009. Andean-type active margin formation in the eastern Taurides: Geochemical and geochronological evidence from the Baskil granitoid (Elazığ, SE Turkey). In Robertson, A.H.F., Parlak, O., Koller, F. (Eds.), *Tethyan Tectonics of the Mediterranean region: Some recent advances*. *Tectonophysics*, **473/1-2**, 188–207.
- Robertson, A.H.F., 2002. Overview of the Genesis and Emplacement of Mesozoic Ophiolites in the Eastern Mediterranean Tethyan Region. *Lithos*, **65**, 1–67.
- Robertson, A.H.F., 2004. Development of Concepts Concerning the Genesis and Emplacements of Tethyan Ophiolites in the Eastern Mediterranean and Oman Regions. *Earth Science Reviews*, **66**, 331–387.
- Robertson, A.H.F., Ustaömer, T., Parlak, O., Ünlügenç, U.C., Taşlı, K., İnan, N., 2006. The Berit transect of the Tauride thrust belt, S. Turkey: Late Cretaceous–Early Cenozoic accretionary/collisional processes related to closure of the southern Neotethys. *Journal of Asian Earth Sciences*, **27**, 108–145.
- Robertson, A.H.F., Parlak, O., Rızaoğlu, T., Ünlügenç, U.C., İnan, N., Taşlı, K., Ustaömer, T., 2007. Tectonic evolution of the South Tethyan ocean: evidence from the Eastern Taurus Mountains (Elazığ region, SE Turkey). In Ries, A.C., Butler, R.W.H., Graham, R.H. (Eds.), *Deformation of the Continental Crust: The Legacy of Mike Coward*. Geological Society, London, Special Publications, **272**, 233–272.
- Robertson, A.H.F., Parlak, O., Koller, F., 2009. Tethyan tectonics of the Mediterranean region: Some recent advances. *Tectonophysics*, **473**, 1–3.
- Şengör, A.M.C., Yılmaz, Y., 1981. Tethyan Evolution of Turkey: A Plate Tectonic Approach. *Tectonophysics*, **75**, 181–241.
- Yalınz, K.M., Floyd, P., Göncüoğlu, M.C., 1996. Supra-subduction Zone Ophiolites of Central Anatolia: Geochemical Evidence from the Sarıkaraman Ophiolite, Aksaray, Turkey. *Mineralogical Magazine*, **60**, 697–710.
- Yalınz, K.M., Floyd, K.M., Göncüoğlu, M.C., 2000. Geochemistry of Volcanic Rocks from the Çiçekdağ Ophiolite, Central Anatolia, Turkey, and their Inferred Tectonic Setting within the northern Branch of The Neotethyan Ocean. In Bozkurt, E., Winchester, J.A., Piper, J.D.A. (Eds.), *Tectonics and Magmatism in Turkey and Surrounding Area*. Geological Society Of London, Special Publication, **173**, 203–218.
- Yazgan, E., 1984. Geodynamic Evolution of the Eastern Taurus Region (Malatya- Elazığ area, Turkey). *Proceedings of International Symposium, Geology of Taurus Belt, MTA, Ankara*, 199–208.
- Yazgan, E., Chessex, R., 1991. Geology and Tectonic Evolution of the Southeastern Taurides in the Region of Malatya, Turk. Assoc. Petrol. Geol., **3**, 1–42.

## **PETROLOGY, GEOCHEMISTRY AND TECTONIC SETTING OF MYRDEH AREA GRANITOIDS (EAST OF BANEH CITY)**

REZA ZAREI SAHAMIEH<sup>1</sup>, AMIR PAZOKI<sup>1</sup>, PEIMAN REZAEI<sup>2</sup>, ALI SAKET<sup>3</sup>

<sup>1</sup> Lorestan University, Department of Geology, Faculty of Science, Khorram Abad, Iran; e-mail: zareisah@yahoo.com

<sup>2</sup> University of Hormozgan, Faculty of Science, Iran

<sup>3</sup> Natural Disaster Institute of Iran

**Keywords:** Astaneh, magmatic rocks, calc-alkaline, mineralization.

The granitoid complex of Astaneh is located in the west of Iran, next to Broujerd and within the frame of the 1:100000 scale of Broujerd's geological map. The lithostratigraphic units of the region essentially belong to the Sanandaj-Sirjan Zone (SSZ), and are almost as old as Eocene and Oligocene. Rocks including quartzdiorites, granodiorites, monzogranites and aciditic dikes (aplites and pegmatites) were observed in the area. Geochemical studies indicated that this complex is sub-alkaline and it displays features of I-type granites. Moreover, the studied showed that some mafic rocks contain Mg, Fe, Ca, Cu and Zn due to the separation of mafic minerals from the magma during the early stages of crystallization, and K, Na, W, Sn and Sb due to their intergration into felsic minerals at the end of the crystallization. The results also showed that the Astaneh granitoid complex has been enriched with elements such as Ba, Rb, K, and a Nb, Sr and Ti depletion could also be seen. In terms of magmatic series, the rocks of the region belong to the calc-alkaline category, which in turn confirms the occurrence of subduction in the continental margins (CAG). From the point of view of the economic potential, the mineralization of skarn, Fe, Cu, Pb, Zn and non-metallic minerals, such as kaolinite, is considerable.

## COMPARATIVE REMARKS ON THE PERMIAN VOLCANISM IN THE SIRINIA AND PRESACINA DOMAINS (SOUTH BANAT, ROMANIA)

IOAN SEGHEDI<sup>1</sup>, MIHAI TATU<sup>1</sup>

<sup>1</sup> Romanian Academy, Institute of Geodynamics, Bucharest, R-020032, Romania; e-mail: seghedi@geodin.ro

**Keywords:** Upper Paleozoic, Permian, rhyolite, effusive domes, phreatomagmatic deposits.

As in all Western and Central Europe, the complex Upper Paleozoic evolution of Eastern Europe was controlled by extensional tectonics. The continuous convergence between Laurasia and Gondwana generated a conjugate dextral – sinistral shear fault system adjacent to the Tornquist – Teisseyre Line (Ziegler, 1990), which induced the fragmentation of the Variscan fold belt. This resulted in the formation of many transtensional pull-apart continental-lacustrine sedimentary basins and intra-continental rift areas associated with widespread intrusive-extrusive magmatism along active deep crustal fractures. From climatic points of view, the main consequence of the continuous convergence between Laurasia and Gondwana is the transition from a relatively wet during the Pennsylvanian to an arid regime during the Lower Permian, especially for the periequatorial basins (Schneider et al., 2006).

The volcanic activity in the Sirinia and Presacina Upper Paleozoic domains belonging to the Danubian realm is rhyolitic and a direct consequence of post-Variscan extensional tectonic activity starting in the Upper Carboniferous and reaching up to Middle Permian times.

In the Sirinia basin, the Lower Permian is represented by lacustrine-fluviatile sedimentary deposits (red beds) with a basement provenance, which contain the rhyolitic volcanic clasts, associated with limnic carbonatic rocks, up to 200 m thick. The presence of rhyolitic clasts suggests the inception of volcanic activity. This entire assemblage was affected by the syn- and post-depositional tectonic events in transtensive-transpressive regime (fig. 1).

In spite of folding processes associated with the Alpine tectogenesis, the volcanic deposits in the Sirinia domain are rather well preserved and encompasses a mountain area which rises up to 600 m above the surroundings, has an estimated dimension of 6 x 10 km and a thickness of around 1000-2000 m. The Permian volcanic deposits represent ~ 90% of the all types of deposits, the others being terrestrial sedimentary. The main volume of

erupted magma has generated many subaqueous effusive domes surrounded by extensive hyaloclastic breccias as a result of the direct contact of magma with water (fig. 2).



Fig. 1 Large- to meso-scale dip-slip synthetic and antithetic normal faults showing a conjugate geometry, typical for the extensional evolution of the Early Permian basins (south of the emergence of Staristea river into the Danube – Sirinia Basin; the stick is 1 m long).



Fig. 2



Fig. 3

Fig. 2 Hyaloclastic breccia including cm-sized rhyolite clasts of various color (massive and flow banded); the smaller green clasts are chloritized – Danube River-Sirinia Basin;

Fig. 3 Succession of fine and coarse fallout tuffs variably rich in accretionary lapilli with impact sags generated by one centimeter-sized massive, angular juvenile clasts; the tuffs are covered by a microbreccia of angular massive rhyolite fragments – Danube River-Sirinia Basin.

The result of this activity is most impressive, draping the former morphology represented by terrigenous deposits as red beds. Plenty of secondary epiclastic deposits have also been formed, as turbidites or debris flow deposits (Cas et al., 1990).

The end of volcanic activity in the southern part of the basin was partially subaerial, partially subaqueous, represented by phreatomagmatic deposits or effusive domes, marking the final filling stage of the basin. Proximal pyroclastic flow (dominantly non-welded and

welded ignimbrites), pyroclastic surge and fallout (with rare impact ballistic structures), all rich in accretionary lapilli, are characteristic to the area (Kokelaar et al., 1985) (fig. 3).

Compared to the Sirinia basin, in the Presacina basin the terrigenous siliciclastic red-bed deposits are dominant. The sedimentary deposits are lacustrine-fluviatile, represented by polygenetic conglomerates (in the base), up to 300 m, which are covered by sandy – conglomerates and muddy – sandstone of variable thickness, up to 500 m (fig. 4).

In the Presacina domain, the Permian volcanism was also rhyolitic and subaqueous and generated effusive domes, however of much less volume, compared with Sirinia (~30%). The margins of the domes are bordered, as in Sirinia, by hyaloclastic breccias (fig. 5) and secondary epiclastic deposits. No subaerial volcanic deposits were found.



Fig. 4

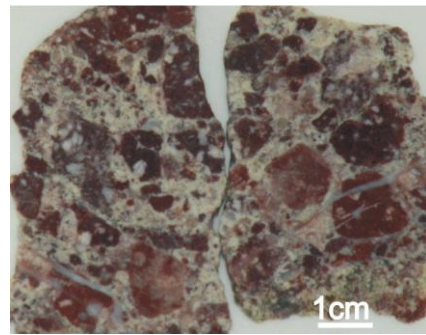


Fig. 5

Fig. 4 Successions of sandstone and conglomerate in terrigenous deposits, affected by NNE-SSW directed compression tectonics, illustrated by *en echelon* Riedel fractures filled with calcite – Iardașița valley-Presacina Basin;

Fig. 5 Hyaloclastic breccia including cm-sized glassy reddish rhyolite clasts (massive); – Iardașița valley-Presacina Basin.

Unlike Sirinia, where the end of volcanic activity in the southern part was partially subaerial, partially subaqueous, represented by phreatomagmatic deposits or effusive domes, marking the final filling stage of the basin, the Presacina basin most probably did not reach the filling stage during the Permian times. Late fluvial erosion and deposition dominated by rhyolitic clasts completed the evolution of the emerged part of the basin.

The similarities and differences in volcanic activity in the studied basins help and improve the geodynamic reconstruction linked to the generation of extensional basins during Paleozoic times, emphasizing the tectonic factors that allowed melting processes and magma generation.

The present work was funded through a PALEOCLIM project (grant ANCS – PN2, 31-063/2007), which is gratefully acknowledged.

## References

- Cas, R.A.F., Allen, R.L., Bull, S.W., Clifford, B.A., Wright, J.V., 1990. Subaqueous, rhyolitic dome-top tuff cones: a model based on the Devonian Bunga Beds, southeastern Australia and a modern analogue. *Bull Volcanol*, **52**, 159–172.
- Kokelaar, B.P., Bevins, R.E., Roach, R.A., 1985. Submarine silicic volcanism and associated sedimentary and tectonic processes, Ramsey Island, SW Wales. *J. Geol. Soc. London*, **142**, 591–613.
- Schneider, J.W., Körner, F., Roscher, M., Kroner, U., 2006. Permian climate development in the northern peri-Tethys area; the Lodève basin, French Massif Central, compared in a European and global context. *Palaeogeography, Palaeoclimatology, Palaeoecology*, **240**, 161–183.
- Ziegler, P.A., 1990. *Shell Int. Petrol. Mij. Dist. Geol. Soc. Publ. House, Bath*, 1–239.

## CHARACTERISTICS OF XENOLITHS IN THE EAST SLOVAKIAN NEOGENE VULCANITES

ZDENKA MARCINČÁKOVÁ<sup>1</sup>, MARIÁN KOŠUTH<sup>1</sup>

<sup>1</sup> Technical University in Košice, Institute of Geosciences, Faculty B.E.R.G. (Mining, Ecology, Process Control and Geotechnologies), 15, Park Komenskeho, 043 84 Košice, Slovak Republic; e-mail: marian.kosuth@tuke.sk

**Keywords:** Neogene vulcanites, magmatic enclave, xenoliths, andesites, Slanské vrchy Mts., Zemplinicum Unit

The East Slovakian Neogene volcanic bodies contain crustal xenoliths of various types. The chemical and mineral compositions of the xenoliths were studied through the use of several analytical methods. The xenoliths (enclaves) contain rare acid vulcanites, but are rich in intermediary and more basic volcanic rocks, such as andesites or basaltic andesites. Rhyodacites from the Zemplin tectonic Isle contain magmatic enclaves that display features of argillitization, silicification and K-metasomatism. The xenoliths from the andesites and their endogenous terms of the Slanské vrchy Mts. represent rocks of sedimentary and metamorphic origin, and some magmatic enclaves, as well. Interesting types of such enclaves are the pre-Tertiary Ca - skarn xenoliths with minerals such as wollastonite, danburite, datolite and hedenbergite.

### References

- Cox, K.G., Bell, J.D., Pankhurst, R.J., 1993. The interpretation of igneous rocks. Chapman & Hall, London, 450p.
- Deer, W.A., Howie, R.A., Zussman, J., 1992. An introduction to rock-forming minerals. 2<sup>nd</sup> edition, Longmans, London, 1696p.
- Kaličiak, M., Žec, B., 1995. Review of Neogene volcanism of Eastern Slovakia. *Acta Vulcanologica*, 7/2, 87– 5.
- Ludhová, L., Janák, M., 1999. Phase Relations and P-T path of Cordierite-bearing Migmatites, Western Tatra Mountains, Western Carpathians. *Geologica Carpathica*, 50/4, 283–293.
- Yang, W., Rosenberg, P.E., 1995. The free energy of formation of datolite. *American Mineralogist*, 80, 576–584.



# **Geochemistry**



## SPECIATION OF SILICA AND ALUMINIUM IN HORTIC ANTHROSOILS – PEDOGEOCHEMICAL IMPLICATION

DUMITRU BULGARIU<sup>1</sup>, NICOLAE BUZGAR<sup>1</sup>, FEODOR FILIPOV<sup>2</sup>, LAURA  
BULGARIU<sup>3</sup>

<sup>1</sup> „Al. I. Cuza” University of Iași, Department of Geology, 20A Carol I Blv., 700505 Iași, Romania; e-mail: dbulgariu@yahoo.com; nicolae.buzgar@uaic.ro

<sup>2</sup> „Ion Ionescu de la Brad” University of Agricultural Sciences and Veterinary Medicine Iași, Faculty of Agriculture, Romania; e-mail: ffilipov@uaiasi.ro

<sup>3</sup> Technical University „Gheorghe Asachi” of Iași, Faculty of Chemical Engineering and Environmental Protection, Department of Environmental Engineering and Management, Romania; e-mail: lbulg@tuiasi.ro

**Keywords:** speciation processes, hortic anthrosoils, silica.

The objectives of the present study were the following: (i) the determination of the total content and extractable fractions, the forms of speciation and the occurrence of silica (SiO<sub>2</sub>) and aluminium; (ii) the estimation of the potential risk of aluminium; (iii) the mechanisms involved in the speciation processes of silica (SiO<sub>2</sub>) and aluminium, and their influences on pedogenetical processes, under hortic anthrosoil conditions (soils from glass houses and solariums).

The studies were conducted on soil samples from the Copou-Iași glass house, and they included the following: (i) the determination of the total content and extractable fractions of silica and aluminium, through atomic absorption spectrometry and UV-VIS molecular spectrometry, after the extraction with: (a) 0.3 M ammonium citrate (sodium dithionite, bicarbonate buffer, pH = 7.3), (b) 0.2 M oxalic acid - ammonium oxalate (pH = 3.0), (c) sodium pyrophosphate 0.2 M (pH = 10), (d) 0.5 M NaOH, (e) 0.4 M oxalic acid – ammonium oxalate (pH = 3.2) (f) dissolution with HNO<sub>3</sub> and HClO<sub>4</sub> conc. (Borlan and Răuță, 1981; Quevauviller et al., 1994); (ii) the identification of the speciation and occurrence forms, of the parageneses and specific associations for silica and aluminium through chemical analyses, optical microscopy, X-ray diffraction, Raman spectrometry, IR and UV-VIS (Cady et al., 1986; White and Roth, 1986); (iii) the thermodynamic and kinetic modeling of the speciation processes of silica and aluminium (Bethke, 1996).

The results of the study indicated the following: (i) the contents of amorphous silica and aluminium are unexpectedly high (amorphous SiO<sub>2</sub> is 16.16-71.65% of free SiO<sub>2</sub>), and they present specific trends of accumulation in Aho2k(x) (content maximum) and lower

horizons; (ii) the predominant forms of occurrence are: aluminosilicious gels (upper horizons), silica-alumo-phosphates gels, and organic-mineral complexes (Aho2k(x) horizon),  $\text{SiO}_2 \cdot x\text{H}_2\text{O}$ ,  $\text{Al}_2\text{O}_3 \cdot x\text{H}_2\text{O}$ , and (S, Al)-organic complexes (lower horizons); (iii) some particular remarks, such as: (a) wide variety of speciation forms and occurrence of aluminium; (b) high contents of silica and aluminium from organic-mineral complexes (22.36–48.71% from amorphous silica, and 17.65–30.19% from extractable aluminium included in organic-mineral complexes); (c) presence of silica and aluminium in the Aho2k(x) horizon, as silica-alumo-phosphate solid solutions of the metastable type  $(\text{SiO}_2)_x(\text{Al}_2\text{O}_3)_y(\text{PO}_4)_z$  [ $x/z=(10-16)/1$ ;  $y/z=(3-5)/1$ ], with three-dimensional structures; (d) the risk potential of aluminium is significant, given the high weight of mobile fractions – as an average, 29.16% of the total amount of aluminium is directly accessible to plants (major risk potential), and 70.84% is indirectly accessible to plants (latent risk potential).

The financial support for the studies was provided by the Romanian Ministry of Education through grant PNCDI II, no. 51-045 / 2007.

## References

- Bethke, C., 1996. Geochemical reaction modelling. Concepts and applications. New York, Oxford University Press.
- Borlan, Z., Răuță, C., 1981. Metodologia de analiză agrochimică a solurilor în vederea stabilirii necesarului de amendamente și de îngrășăminte (vol. I-II). Academia de Științe Agricole și Silvice a României, ICPA, București.
- Cady, J.G., Wilding, L.P., Drees, L.R., 1986. Petrographic Microscope Techniques. In Klute A. (ed.) Methods of soil analysis. Part I – Physical and Mineralogical Methods (Second Edition), SSSA Book 5, Madison, 185–218.
- Quevauviller, P., Rauret, G., Muntau, H., 1994. Evaluation of sequential extraction procedures for the determination of extractable trace metal contents in sediments. Fresenius Journal of Analytical Chemistry, **349**, 808–814.
- White, J.L., Roth, C.B., 1986. Infrared spectrometry. In Klute A. (ed.) Methods of soil analysis. Part I – Physical and Mineralogical Methods (Second Edition), SSSA Book 5, Madison, 291–330.

## GENESIS OF PEDOGEOCHEMICAL SEGREGATION HORIZONS (FRAGIPANS) AND THEIR INFLUENCE ON THE GEOCHEMISTRY OF HORTIC ANTHROSOILS

DUMITRU BULGARIU<sup>1</sup>, NICOLAE BUZGAR<sup>1</sup>, DAN AȘTEFANEI<sup>1</sup>

<sup>1</sup> „Al. I. Cuza” University of Iași, Department of Geology, 20A Carol I Blv., 700505 Iași, Romania; e-mail: dbulgariu@yahoo.com; nicolae.buzgar@uaic.ro; astdan@yahoo.com

**Keywords:** hortic anthrosoils, pedogeochemical segregation, fragipan.

The objectives of the present study are the following: (i) describing the pedogeochemistry and mineralogy of pedogeochemical segregation horizons (fragipans), occurring in hortic anthrosoils; (ii) identifying the influence of pedogeochemical segregation horizons, on the physico-chemical properties of soils; (iii) identifying the conditions and mechanisms involved in the formation of fragipan horizons; (iv) establishing the relative indicators for diagnosing and differentiating fragipan horizons.

The studies were conducted on soil samples from glass houses in Iași-Copou, Bacău and Bârlad, and they included the following: (i) standard soil analyses - soil key indicators were measured (Borlan and Răuță, 1981); (ii) mineralogical analyses - minerals and organic components of soils, forms of occurrence, parageneses, and specific natural associations of these components were determined (Cady et al., 1986; Dean, 1995); (iii) geochemical analyses - the contents for the main macro- and micronutrients, the distribution of natural tendencies and the association with soil components were determined (Dean, 1995; Gill, 1997).

The results of the study indicated the following: (i) the hortic anthrosoils are characterized by high values of base saturation, available phosphorus and high ratios of huminic acids and fulvic acids; (ii) the specific hortic anthrosoils show: major changes through the profiles, wide variability of mineralogy and chemistry, salinization processes of the upper horizons, the formation of a horizon of pedogeochemical segregation (fragipan) at a depth of about 50 cm; (iii) the fragipan horizons determine the pedogeochemical segregation of soil profiles, as suggested by: (a) the discontinuity of the water movement in the soil profile; (b) the contrast between the physico-chemical conditions in the upper and lower horizons, as follows: upper horizons reveal slightly oxidizing conditions, neutral-slightly alkaline pH (7.61-8.04), high salinity (315.51-675.49 mg/100g of soil), and humidity; lower horizons display intense biological activity, slightly reducing conditions, weak acid pH (5.87-6.95), low salinity (152.95-288.38 mg/100g soils), and humidity; (c) a typical evolution of the organic matter, the distribution and speciation processes of trace

elements; (iv) a rapid degradation of physical and chemical properties of the soil; (v) as our experimental data revealed, some aspects have crucial roles in the formation of fragipan horizons: (a) the accumulation of fine particle fractions and of the amorphous mineral forms in these horizons; (b) the high amount of smectites, iron oxi-hydroxides, amorphous silica and organic matter in the composition of the soil aggregates; (c) high content of Si, Al, Fe, phosphorus, and organic-mineral complexes; (vi) the fragipan horizons display high contents of organic phosphate, as inositol-phosphoric esters, fulvic acids, and organic-mineral complexes.

The financial support for the present study was provided by the Romanian Ministry of Education through grant PNCDI II, no. 51-045/2007.

## References

- Borlan, Z., Răuță, C., 1981. Metodologia de analiză agrochimică a solurilor în vederea stabilirii necesarului de amendamente și de îngrășăminte (vol. I-II). Academia de Științe Agricole și Silvice a României, ICPA București.
- Cady, J. G., Wilding, L. P., Drees, L. R., 1986. Petrographic Microscope Techniques. In: Klute A. (ed.) Methods of soil analysis. Part 1 – Physical and Mineralogical Methods (Second Edition), p. 185-218. SSSA Book Ser. No. 5. SSSA and ASA, Madison, WI.
- Dean, J. A., 1995. Analytical Chemistry Handbook. McGraw-Hil, Inc., New York.
- Gill, R., 1997. Modern Analytical Geochemistry. An Introduction to Quantitative Analysis Techniques for Earth, Environmental and Material Scientists. Addison Wesley Longman Ltd., Essex, UK.

**THE DISTRIBUTION OF CERTAIN TRACE ELEMENTS IN ACTIVE STREAM  
SEDIMENTS OF THE BISTRIȚA RIVER (DOWNSTREAM IZVORUL  
MUNTELUI LAKE), ROMANIA**

VALENTIN GRIGORAȘ<sup>1</sup>, OVIDIU GABRIEL IANCU<sup>2</sup>, NICOLAE BUZGAR<sup>2</sup>,  
META DOBNIKAR<sup>3</sup>, MIHAEL-CRISTIN ICHIM<sup>1</sup>

<sup>1</sup> National Institute of Research and Development for Biological Sciences, “Stejarul”  
Research Center for Biological Sciences, Alexandru cel Bun, Piatra Neamț, 610004,  
Romania; e-mail: valygrigoras@yahoo.com; cichim@hotmail.com

<sup>2</sup> „Al. I. Cuza” University of Iași, Department of Geology, 20A Carol I Blv., 700505 Iași,  
Romania; e-mail: ogiancu@yahoo.com; nicolae.buzgar@uaic.ro

<sup>3</sup> University of Ljubljana, 012 Askerceva, Ljubljana, 1000, Slovenia; e-mail:  
meta.dobnikar@gmail.com

**Keywords.** Bistrița River, active stream sediment, XRF, trace elements.

**Description of Study Area**

The studied area is located in the central-northeastern part of Romania (fig. 1), in the Outer Eastern Carpathians. Downstream Izvorul Muntelui Lake, the Bistrița basin spreads over an area of approximately 2960 Km<sup>2</sup> (42% of the entire Bistrița basin). The geological background is represented exclusively by sedimentary formations with various degrees of consolidation, namely different types of limestone, sandstone, clay, sand, silt etc. (Grasu et al., 1988).

The river water in this sector is a mix of run-off water from Izvorul Muntelui Lake (Gassama et al., 2009; Apetroaei, 2003) and a number of tributaries with variables river flows. In this sector, some features of the Bistrița River (water and stream sediment) are induced by the existence of several dams.

**Sampling and preparation of sediment samples**

Sampling points were located along the river, at a distance of 5 km each, yielding a total of 18 initial samples. The sampling process was carried out according to Salminen et al. (1988) – the <0.5 mm fraction was retained for further analysis. In the laboratory, the initial samples were dried out at 105°C, then granulometrically separated for each location, resulting 5 fractions (500-250 μm, 250-125 μm, 125-63 μm, 63-45 μm and <45 μm); the analysis of the active stream sediment was performed on these samples.



Fig. 1 Location of study area

### Analysis of sediment samples

The mineralogy of the sediment samples was determined on the  $<45\ \mu\text{m}$  fractions of the samples within the Department of Geology in Ljubljana, Slovenia, through X-Ray powder Diffraction using a Philips PW 3710 diffractometer and  $\text{CuK}\alpha$  radiation. The results were analyzed using PC-Automatic Powder Diffraction (PC-APD) Philips software (Philips, Eindhoven, 1996). The diffraction patterns were identified using the data from the Joint Committee on Powder Diffraction Standard (JPDS standard-1977). Quantitative determinations of the trace metals were carried out within the Department of Geology of the “Al. I. Cuza” University of Iasi, using X-Ray Fluorescence Spectrometry (ED-XRF Epsylon 5).

### Results and Discussion

The granulometric spectrum of the active stream sediment in Bistrița is controlled by several dams located along the river. The coarser fractions are the main constituents, the particles larger than  $63\ \mu\text{m}$  always exceeding 96%. The  $<45\ \mu\text{m}$  fraction never exceeds 3%. Related to these values, the clay fraction appears to be totally subordinated within the granulometric composition of the sediment.

XRD analysis performed on the  $<45\ \mu\text{m}$  fraction showed a high homogeneity of the mineralogical composition (fig. 2). Quartz, albite, anorthite and calcite were identified as major components; minor components are dolomite, chlorite, illite and mica. Apart from a relative increase in the quartz content, there are no changes in mineralogical composition in the river profile.

Fe, Mn, Cr, Zn, Ni and Cu were determined as total content. The values of their distribution (tab. 1) have highlighted the following features:

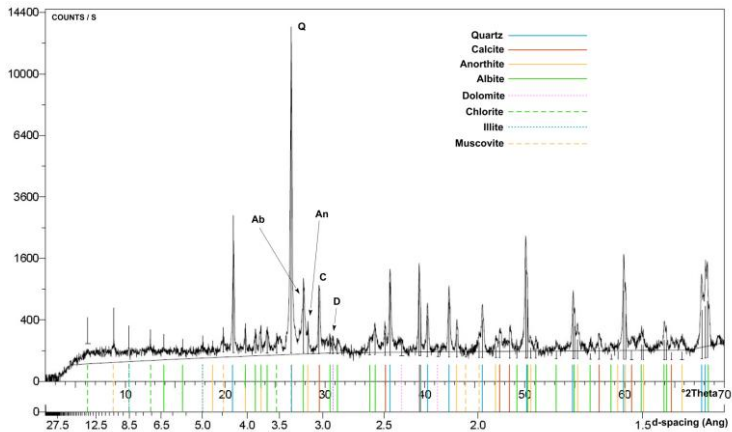


Fig. 2 Characteristic X-ray powder diffractogram of Bistrița active stream sediment

- along the river profile there is a slight increasing trend of the contents in each fraction, from upstream to downstream. The increase is higher in the finest fractions, although it is inferior to other values mentioned in the literature (Brekhovskikh et al., 2002, Saulwood et al., 2002, Sakan et al., 2007): in the case of the Bistrița sediment, the EF (enrichment factor) is 1.2-1.5 for Fe, Mn, Cr and Zn, while for Ni and Cr it is 2.0-2.1; in the case of the tributaries, the EF values are lower: 1.0-1.2 and 1.6-1.8, respectively.

$$EF = \text{Conc}(elem)_{<45\mu\text{m}} / \text{Conc}(elem)_{500-250\mu\text{m}}$$

- there is no significant correlation between trace elements and organic matter, most likely due to the existence of small plant fragments within the samples;

- with two exceptions (Fe-Zn, Fe-Ni), the correlation coefficient matrix (tab. 2) shows weak or no significant correlations. The main cause seems to be the low range of content variations and the relatively small length of the river in the studied area;

- in various studies (Robinson, 1981, Mielke, 1979 in Salminen, 2005), the sedimentary formations from the geological background have been characterized by low contents of Cr, Zn, Ni and Cu. In the Bistrița basin, Grasu et al. (1988) report high quantities of organic matter, which appear as intercalations within shales, limestones, sandstones etc., with higher contents of trace element (Ni up to 138 mg/kg, Cr-275 mg/kg, Cu-140 mg/kg, Zn-400 mg/kg). The lower stability of these compounds in the case of alteration processes (Reuter and Perdue, 1977) makes the stream sediment appear enriched in relation to “standard” sedimentary formations;

- compared to maximum values accepted by the Romanian legislation for river sediment quality, the contents determined on fractions < 63 μm are placed differently: zinc is under the limit (150 mg/kg), Cr and Cu are close to their respective limits (100 mg/kg and 40 mg/kg), and Ni exceeds the value of 35 mg/kg;

- the geochemical mobility of the trace elements is strongly reduced by the physico-chemical characteristics of surface water, especially its pH, which is slightly alkaline, and the close to zero values of the Eh (Grigoraş, 2009).

Tab. 1 Concentrations of trace elements: minimum, maximum and average values

		Bistrița tributaries					
		min	max	avg	min	Max	avg
Fe (%)	500-250 $\mu\text{m}$	1.84	4.93	3.20	3.03	4.99	4.02
	250-125 $\mu\text{m}$	1.76	5.02	3.49	3.39	4.98	4.09
	125-63 $\mu\text{m}$	1.83	4.83	3.80	3.36	4.84	3.86
	63-45 $\mu\text{m}$	2.95	5.27	4.29	3.69	5.03	4.38
	<45 $\mu\text{m}$	3.18	5.50	4.64	4.32	5.59	4.89
Mn (mg/kg)	500-250 $\mu\text{m}$	487	1316	763	840	1246	1026
	250-125 $\mu\text{m}$	565	1283	823	814	1259	989
	125-63 $\mu\text{m}$	585	1043	882	794	1092	890
	63-45 $\mu\text{m}$	718	1087	940	829	1083	922
	<45 $\mu\text{m}$	768	1168	1024	874	1071	989
Cr (mg/kg)	500-250 $\mu\text{m}$	51.15	129.85	89.10	77.00	133.25	107.84
	250-125 $\mu\text{m}$	44.20	168.55	98.45	63.80	156.90	108.71
	125-63 $\mu\text{m}$	73.95	166.35	113.35	84.90	142.80	114.64
	63-45 $\mu\text{m}$	83.00	143.65	112.53	79.80	186.95	117.79
	<45 $\mu\text{m}$	70.05	162.60	105.27	94.70	169.90	121.41
Zn (mg/kg)	500-250 $\mu\text{m}$	50.55	98.50	68.01	61.45	82.95	71.07
	250-125 $\mu\text{m}$	44.80	94.55	73.20	58.65	88.70	76.73
	125-63 $\mu\text{m}$	42.95	111.00	82.07	63.95	112.80	76.42
	63-45 $\mu\text{m}$	54.90	109.55	90.17	75.95	114.10	88.12
	<45 $\mu\text{m}$	63.85	123.70	101.79	90.60	113.45	100.04
Ni (mg/kg)	500-250 $\mu\text{m}$	5.25	64.25	22.50	18.65	31.00	25.68
	250-125 $\mu\text{m}$	9.35	75.75	28.49	19.70	43.95	33.15
	125-63 $\mu\text{m}$	4.10	50.45	30.07	17.10	52.55	33.18
	63-45 $\mu\text{m}$	3.25	67.55	38.46	20.05	60.55	41.42
	<45 $\mu\text{m}$	16.50	67.30	46.76	20.05	80.65	43.79
Cu (mg/kg)	500-250 $\mu\text{m}$	9.85	47.90	22.24	18.55	31.00	25.39
	250-125 $\mu\text{m}$	11.25	49.00	23.48	18.70	32.25	26.11
	125-63 $\mu\text{m}$	12.00	43.75	30.03	18.55	43.55	25.70
	63-45 $\mu\text{m}$	26.90	53.15	37.54	27.00	38.30	31.99
	<45 $\mu\text{m}$	29.00	81.40	44.35	32.30	49.25	39.81

## Conclusions

The total contents determined for Fe, Mn Cr, Zn, Ni, Cu and their variation within the basin does not suggest a significant anthropic contribution.

Although the rocks from the geological background are mentioned in the literature as having low concentrations of trace elements, the presence of numerous intercalations of organic matter leads to a significant increase of average contents.

Tab. 2 Correlation coefficient matrix for selected trace element in the active stream sediment of Bistrița and its tributaries

	Fe	Mn	Cr	Zn	Ni	Cu
Fe	1					
Mn	0.34	1				
Cr	0.52	-0.18	1			
Zn	<b>0.80</b>	0.31	0.39	1		
Ni	<b>0.90</b>	0.45	0.42	0.59	1	
Cu	0.38	0.50	0.17	0.58	0.33	1

Different partitioning processes of trace metals mentioned in the literature are barely visible or not visible at all: the only process which is highlighted is the influence of particle size. The organic matter is not mature enough for us to be able to determine its influence on the concentration levels.

The presence of some complex mineralisations in the upper sector of the Bistrița basin is not felt in the lower sector, Izvorul Muntelui Lake representing a geochemical barrier.

### Acknowledgments

The present research was partially funded by the Romanian Ministry of Education, Research, Youth and Sports, through the National University Research Council (BD-type fellowship).

### References

- Apetroaei, N., 2003. Sedimentele din lacul de baraj Izvorul Muntelui – Bicaz, Ed. Acad. Române, București.
- Brekhovskikh, V.F., Volkova, Z.V., Katunin, D.N., Kazmiruk, V.D., Kazmiruk, T.N., Ostrovskaya, E.V., 2002. Heavy Metals in Bottom Sediment in the Upper and Lower Volga. *Water Resources*, **29**/5, 539–547.
- Gassama, N., Cocîrță, C., Kasper, H.U., 2009. Hydrodynamics of the Bicaz Lake. Considerations Based on Selected Major and Trace Elements, *An. Șt. Univ. „Al. I. Cuza” Iași*, **LV**, 39–64.
- Grasu, C., Catana, C., Grinea, D., 1988. Flișul carpatic. Petrografie și considerații economice. Ed. Tehnică, București.
- Grigoraș, V., 2009. Caracteristici hidrogeochimice ale apelor din baz. Bistriței (aval de lacul de acumulare Izv. Muntelui): evoluție multianuală și variații sezoniere. Simpozionul Științific Național „Mircea Savul”, Iași, 24 octombrie 2009.
- Reuter, J.H., Perdue, E.M., 1977. Importance of heavy metal-organic matter interactions in natural waters. *Geochimica et Cosmochimica Acta*, **41**/2, 325–334.
- Robinson, G.E., 1981. Adsorption of Cu, Zn and Pb near sulfide deposits by hydrous manganese-iron oxide coatings on stream alluvium. *Chemical Geology*, **33**, 65–79.
- Sakan, S., Grzetic, I., Dordevic, D., 2007. Distribution and Fractionation of Heavy Metals in the Tisa (Tisza) River Sediments. *Env. Sci. Pollut. Res.*, **14**/4, 229–236.

- Salminen, R., Tarvainen, T., Demetriades, A., Duris, M., Fordyce, F.M., Gregorauskiene, V., Kahelin, H., Kivisilla, J., Klaver, G., Klein, H., Larson, J.O., Lis, J., Locutura, J., Marsina, K., Mjartanova, H., Mouvet, C., O'Connor, P., Odor, L., Ottonello, G., Paukola, T., Plant, J.A., Reimann, C., Schermann, O., Siewers, U., Steenfelt, A., Van der Sluys, J., Vivo, B. de, Williams, L., 1998. FOREGS Geochemical Mapping Field Manual. *Geologian tutkimuskeskus*, **47**, 36p.
- Salminen, R., Batista, M.J., Bidovec, M., Demetriades, A., De Vivo, B., De Vos, W., Duris, M., Gilucis, A., Gregorauskiene, V., Halamic, J., Heitzmann, P., Lima, A., Jordan, G., Klaver, G., Klein, P., Lis, J., Locutura, J., Marsina, K., Mazreku, A., O'Connor, P.J., Olsson, S.Å., Ottesen, R.-T., Petersell, V., Plant, J.A., Reeder, S., Salpeteur, I., Sandström, H., Siewers, U., Steenfelt, A., Tarvainen, T., 2005. *Geochemical Atlas of Europe. Part 1 – Background Information, Methodology and Maps*.
- Saulwood, L., Hsieh, I.J., Huang K.M., Wang C.H., 2002. Influence of the Yangtze River and grain size on the spatial variations of heavy metals and organic carbon in the East China Sea continental shelf sediments. *Chemical Geology*, **182**, 377–394.

## **WAS THE GÖL TEPE (NİĞDE, CENTRAL ANATOLIA, TURKEY) A TIN PROCESSING SITE DURING THE EARLY BRONZE AGE? PRELIMINARY FINDINGS FROM SOIL GEOCHEMISTRY**

NURULLAH HANİLÇİ<sup>1</sup>, CEMAL ALTAYLI<sup>2</sup>, SINAN ALTUNCU<sup>3</sup>, HÜSEYİN ÖZTÜRK<sup>1</sup>

<sup>1</sup> İstanbul University, Department of Geological Engineering, 34320, Avcılar – İstanbul, Turkey; e-mail: nurullah@istanbul.edu.tr; ozturkh@istanbul.edu.tr

<sup>2</sup> Kadir Has University, Department of International Trade, Selimpaşa - İstanbul, Turkey

<sup>3</sup> Niğde University, Department of Geological Engineering, Niğde, Turkey

### **Abstract**

Archeo-metallurgical investigations related to the tin smelting site in the Early Bronze Age have been focused on the Göl Tepe, located in the Niğde province, Central Anatolia, Turkey. The geology of the Göl Tepe consists of Paleocene-Eocene-aged sandstones and sandy limestones. Tin backgrounds lower than 1 ppm have been found in these rocks. On the other hand, the tin contents of the Göl Tepe soils range from 7 to 244 ppm (n= 48, average 95 ppm). These values are at least 95 times higher than the local sandstone and sandy limestone background (lower than 1 ppm). The enrichment factors of the Cu, Au, Pb, Zn, Ni, Co, As and Sb of the soils, compared to the local sandstone and sandy limestone background, are 3, 16.1, 5.2, 2.6, 3.11, 3.5, 20.4, and 28.3, respectively. The high enrichment factor of Sn, compared to that of the other elements (such as Cu, Au or Pb), along with the occurrence of tin values in the Göl Tepe soils and the gradual increase in tin content from the bottom to the top of the hill, clearly indicate the fact that the Göl Tepe was a tin processing site in the Early Bronze Age, rather than one for Cu, Au and Pb.

**Keywords:** tin, soil geochemistry, Early Bronze Age, Göl Tepe, Anatolia.

### **Introduction**

The Göl Tepe, located in the southeast of the Niğde province (fig. 1), elicited the interest of archeo-metallurgists, and excavations were carried out between 1987 and 1997 (e.g. Yener, 1989; Yener and Vandiver, 1993). After the excavations revealed ore processing materials (such as crucibles, crashing and grinding stones; fig.2) and tin-rich artifacts (such as rings, awls, pins and necklaces) (Yener 1989; Yener, 2009), the following questions arose: Was this location a processing centre for tin or other metals such as Au or

Cu? Where is the source of the tin? In order to answer the first question, we carried out a geochemical investigation of the soil and local rocks in the Göl Tepe site. For this purpose, 3 local rocks and 48 soils were sampled and analysed. The second question, on the other hand, has recently been discussed by several authors (e.g. Öztürk and Hanilçi, 2009; Yener, 2009).

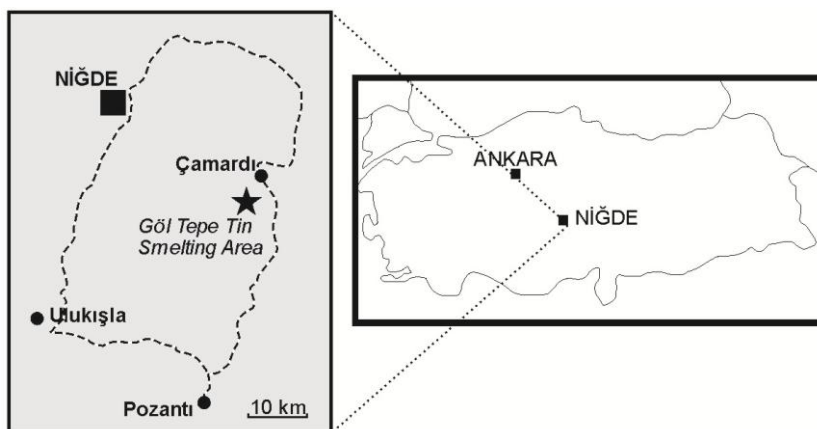


Fig. 1 Location map of the Göl Tepe (Niğde-Turkey) tin smelting area

### Preliminary Findings

Preliminary findings show that the Sn contents of 48 soil samples in the Göl Tepe range are between 7 and 244 ppm. However, the Sn contents of 3 sandstone (local rocks) samples in the same site are lower than 1 ppm. The average Sn content of the soil samples is 95 ppm (n=48), and the Sn enrichment is at least 95 times greater than that of the local rocks (sandstones). We accepted the Sn values of the local rocks (lower than 1 ppm) as a threshold and created a tin anomaly map of the Göl Tepe site. It is clear that the Sn values increase from the bottom to the top of the hill where archeo-metallurgical excavations were done.

The values of the Cu, Au, Pb, Zn, Ni, Co, As, and Sb of the soil samples are 34.4, 10.2, 18.7, 56.6, 75.3, 16.3, 146.5, and 2.8 ppm, and those of the sandstone (local rocks) samples are 11.4, 0.6, 3.6, 21.7, 24.2, 4.73, 7.2 and 0.1 ppm, respectively. The enrichment factors of these elements in the soil, compared to the local rocks, are 3, 16.1, 5.2, 2.6, 3.1, 3.5, 20.4, and 28.3, respectively. These data indicate that the ore material which processed in the Göl Tepe site should contain these metals. Yet, if we compare the enrichment factors of the examined elements, it is clear that the ore material processed especially for Sn, rather than Au, Cu or Pb.



Fig. 2 A grinding stone with central hollows on facet (a), grinding and crashing materials (b) in the Göl Tepe tin smelting site

### References

- Öztürk, H., Haniçlı, N., 2009. Metallogenic Evaluation of Turkey: Implications for Tin Sources of Bronze Age in Anatolia. *Turkish Academy of Sciences Journal of Archeology*, **12**/200, 105–116.
- Yener, K.A., 1989. Kestel: An Early Bronze Age Source of Tin Ore in the Taurus Mountains, Turkey. *Science*, **244**, 200–203.
- Yener, K.A., Vandiver, P.B., 1993. Tin processing at Göl Tepe, an Early Bronze Age site in Anatolia. *American Journal of Archeology*, **97**, 207–238.
- Yener, K.A., 2009. Strategic Industries and Tin In the Ancient Near East: Anatolia Updated. *Turkish Academy of Sciences Journal of Archeology*, **12**, 143–153.

## NATURAL RADIOACTIVITY IN SOIL SAMPLES FROM THE AREA BETWEEN BISTRIȚA AND TROTUȘ VALLEYS

ADRIANA ION<sup>1</sup>, ȘERBAN ANASTASE<sup>1</sup>

<sup>1</sup> Geological Institute of Romania-Bucharest, 1, Caransebeș Street, 012271 Bucharest, Romania; e-mail: adriana.ion@igr.ro

**Keywords:** natural radioactivity, soil, gamma-ray spectrometry, HPGe detector.

### Introduction

Natural radionuclides in soil generate a significant component of the background radiation exposure of the population. The terrestrial component of the natural background is dependent on the composition of the soils and rocks which contain the natural radionuclides. Natural and artificial radionuclides are retained by many environmental materials, including soil. The level of the uptake depends on the physical and chemical properties of radionuclides and also on the environmental matrix of interest (Shender, 1997). A significant contribution to total dose from natural sources comes from terrestrial radionuclides such as <sup>238</sup>U, <sup>232</sup>Th and <sup>40</sup>K.

The present preliminary study deals with the measurement of decay products of the uranium and thorium series, as well as of the primordial radionuclide <sup>40</sup>K, in soil samples collected at the surface from the area between Bistrița and Trotuș Valleys. (Andâr and Ion, 2002). The baseline data of this type will almost certainly be of importance in making estimations regarding the exposure of the population.

### Experimental

The surface soil samples were collected from representative areas during the summer of 2005. The sampling areas include urban sites close to highways and an industrial activity zone; 80 soil samples were collected from the central-eastern Eastern Carpathians. Soil sampling was carried out following a network of probation, so that a sample is representative for an area of approximately 100km<sup>2</sup>. The sampling stations are illustrated in figure 1. Grass and pieces of woods were manually eliminated and stored in plastic bags prior to the analyses. Because <sup>238</sup>U, <sup>232</sup>Th and <sup>40</sup>K are long-life isotopes, the soil samples were measured in 2009. All soil samples were dried at 110°C for 2 hours and kept in air-tight containers (Marinelli beakers) for about 40 days, so as to guarantee that the radionuclides <sup>227</sup>Ra and <sup>228</sup>Th attained radioactive equilibrium with their daughter products (IAEA, 2003).

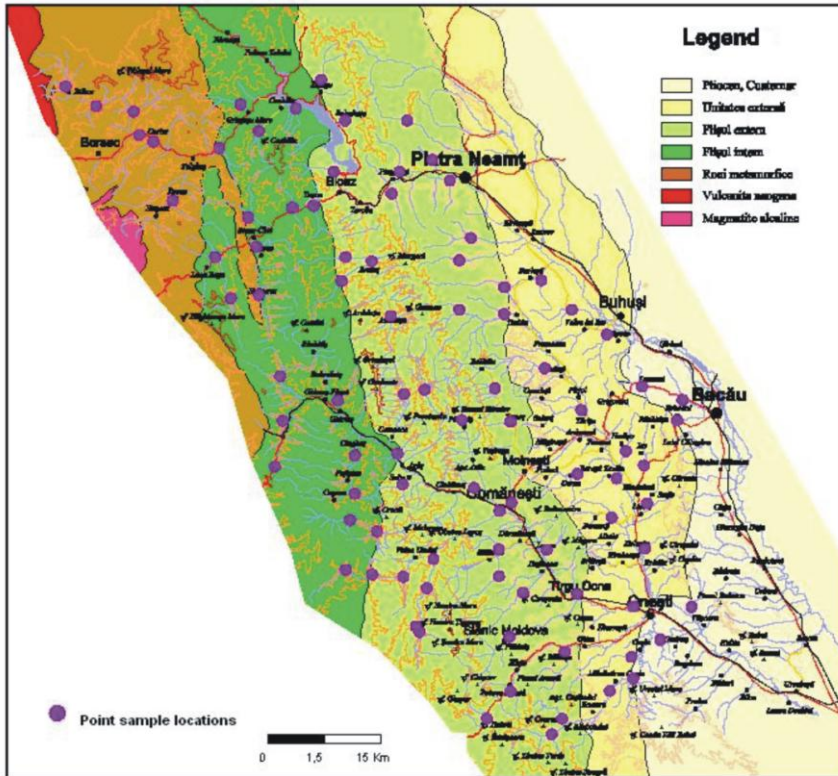


Fig. 1 The location map of the area under study and sample locations

The samples were analyzed non-destructively, using gamma-ray spectrometry with a high purity germanium (HPGe) detector. The detector has a relative efficiency of 27%, a resolution of 1.90keV and a peak/Compton ratio of 56:1 at 1.33MeV, and it is coupled to conventional electronics connected to a multichannel analyzer card (MCA- DSPEC jr.2.0 - ORTEC), installed in a PC computer. The detector was shielded from the background radiation using a 10cm-thick lead, which was internally lined with a 2mm copper foil. A software program called MAESTRO – 32 was used to accumulate and GAMMVISION – 32 for analyzing data. The analyses were carried out using a gamma library that includes over 300 nuclides and 4000 gamma lines. The system was calibrated for energy using radioactive standards of known energies, such as  $^{241}\text{Am}$ ,  $^{137}\text{Cs}$  and  $^{60}\text{Co}$ . For an efficient calibration, a multi-element standard, containing radionuclides with known activities was used. The standard has the same size and geometry as the sample under study. Each sample was counted for 80,000s. The background correction was accounted for by

measuring a distilled water sample spectrum in the same geometry, and was subtracted from each spectrum.

## Results and discussion

The activity concentrations of the uranium series were determined using gamma-ray emissions of  $^{238}\text{U}$  at 63.29 keV (3.9%),  $^{214}\text{Pb}$  at 351.921 keV (37.1%) and 295.213 keV (19.3%),  $^{214}\text{Bi}$  at 609.31 keV (46%) and 1120 keV (15.1%), for  $^{226}\text{Ra}$  186 keV (33%). In the  $^{232}\text{Th}$  series, the emissions of  $^{228}\text{Ac}$  at 338.4 keV (12.01%) and 911.2 keV (29%) were used as a measure for  $^{228}\text{Ra}$ , while  $^{226}\text{Ra}$  was determined from emissions of  $^{212}\text{Pb}$  at 238.6 keV (43.1%),  $^{212}\text{Bi}$  at 727 keV (6.65%), and  $^{208}\text{Tl}$  at 583 keV 86%). For the actinium series,  $^{223}\text{Ra}$  was determined from its emission at 154 keV (5.2%).  $^{40}\text{K}$  activity concentration was determined directly from its emission at 1460 KeV.

The results of measurements for 80 soil samples collected at different locations in the area under study were in the range of 7.54 to 57.25 Bq/kg for  $^{238}\text{U}$ , of 3.14 to 70.11 Bq/Kg for  $^{232}\text{Th}$ , and from 150.15 and 742.74 Bq/Kg for  $^{40}\text{K}$ .

Tab. 1 Concentrations of the natural radionuclides in soil samples (in Bq/kg) from different East European countries, compared with those of the present study

East Europe Country	Concentration in soil (Bq/Kg)		
	$^{238}\text{U}$ Range	$^{232}\text{Th}$ Range	$^{40}\text{K}$ Range
Bulgaria	8 - 190	7 - 160	40 - 800
Hungary	12 - 66	12 - 45	79 - 570
Poland	5 - 120	4 - 77	110 - 970
Russian Federation	0 - 67	2 - 79	100 - 1400
Slovakia	15 - 130	12 - 80	200 - 1380
<b>Present study</b>	<b>7.54 – 57.25</b>	<b>3.14 – 70.11</b>	<b>150.15 – 742.74</b>

Higher values of specific activity (for the  $^{232}\text{Th}$  series) were observed within the range measured in soil samples from Bistricioara (102 Bq/Kg), Grintieş (124 Bq/Kg), Tulgheş (111 Bq/Kg) and Bicazul Ardelean (116 Bq/Kg) points. The  $^{232}\text{Th}$  content of soils reflects the average  $^{232}\text{Th}$  content of the rocks from which they are derived (metamorphic rocks) (Dickson and Scott, 1997). Table 1 presents the average value of the specific activity regarding the natural radionuclides in soil samples from different East European countries, compared with those of the present study. The data of table 1 show a normal distribution. The measurements show that the values of specific activity in the soils from the investigated area are comparable with the limit recommended by the United Nation Scientific Committee on the Effect of Atomic Radiation (UNSCEAR, 2000).

## Conclusion

The measurement of the natural radioactivity in soil plays a crucial role in the assessment of the changes occurring in the natural background in time, as a result of radioactive release. Monitoring all releases of radioactivity into the environment is important for environmental protection. An important radiological concentration

consequence of the natural radioactivity in soil is the effect of  $\gamma$ - rays on the human body. The concentrations of  $^{238}\text{U}$ ,  $^{232}\text{Th}$  and  $^{40}\text{K}$  are comparable to the reported East European range. The activity of  $^{40}\text{K}$  is much higher than that of  $^{238}\text{U}$  and  $^{232}\text{Th}$ .

### **Acknowledgements**

The present investigation was supported by the Geological Institute of Romania and has benefited from a grant (Geochemical mapping of geological formations in Romania, 1:1.000.000 scale) awarded by the National Authority for Scientific Research (2005–2013).

### **References**

- Andâr, P., Ion, A., 2002. Geochemical mapping of geological formations in Romania, 1:1.000.000 scale. Report, Archives of the Geological Institute of Romania, Bucharest.
- Dickson, B.L., Scott, K.M., 1997. Interpretation of aerial gamma ray surveys-adding the geochemical factors. AGSO Journal of Australian Geology & Geophysics, **17/2**, 187–200.
- International Atomic Energy Agency, 2003. Guidelines for radioelement mapping using gamma ray spectrometry data. IAEA- TECDOC-1363, Vienna.
- Shender, M.A., 1997. Measurement of Natural Radioactivity Levels in Soil in Tripoli. Applied Radiation and Isotopes, **48/1**, 147–148.
- UNSCEAR, 2000. United Nations Scientific Committee on the Effects of Atomic Radiation. Report of UNSCEAR to the General Assembly, United Nations, New York, USA., Annex B: Exposures from Natural Radiation Source.

## **ORGANIC GEOCHEMICAL COMPARISON BETWEEN THE ASPHALTITES FROM THE ŞIRNAK AREA AND THE OILS OF THE RAMAN AND DİNÇER FIELDS IN SOUTHEASTERN TURKEY**

ORHAN KAVAK<sup>1</sup>

<sup>1</sup> Dicle University, Faculty of Engineering, Department of Mining Engineering, TR-21280 Diyarbakir, Turkey; e-mail: orkavak@dicle.edu.tr; kavakorhan@gmail.com

**Keywords:** asphaltite, Raman-Dinçer oil, southeastern Turkey, Şırnak area.

### **Abstract**

55 samples of asphaltites from 12 different veins in the Şırnak area and two oil samples from the Raman and Dinçer Oil fields in Southeast (SE) Turkey have been analyzed through a series of organic geochemical methods (TOC, rock-eval pyrolysis, gas chromatography of saturated fractions, gas chromatography-mass spectrometry and stable carbon isotope). The TOC contents in the asphaltites range from 12 to 65%. The Tmax values range between 428°C and 465°C. The hydrogen index (HI) values vary between 270 and 531 mg HC/g TOC. The levels of biodegradation of the asphaltites were studied through GC analyses of the saturated fractions and none to moderate biodegradation has been found. The maturity of the asphaltite samples was assessed using biomarker ratios provided by GC-MS analysis. Stable carbon isotope (<sup>13</sup>C) analyses of the Raman-Dinçer oils yielded values of about -27 per mil. and the asphaltene fractions of the asphaltite samples led to similar values, of about 26.8 per mil. It is presumed that the asphaltites are of oil origin and have solidified in veins close to the surface, and the geochemical correlation does suggest similarities between the Şırnak area asphaltites and Raman-Dinçer oils.

### **Introduction**

Asphaltite is a petroleum-origin rock. It is formed from liquid or semi-liquid asphalt material present at depth, which is placed in splits, cracks and empty spaces through transportation with effects such as pressure, gravitation and temperature. Due to the investigation of coal or petroleum-origin bitumen and pyrobitumen-containing formations found throughout the world as an alternative in the production of liquid/gas fuel and chemical raw material, this subject gained importance in Turkey, and the number of studies dedicated to the recognition and evaluation of asphaltite has increased (Bartle et al., 1981).

In the study area, the asphaltic veins are located at high angles in fractures of the bedding of the Campanian-Maestrihtian Germav Formation, the Paleocene-Lower Eocene Gerçüş Formation and the Jurassic-Triassic Cudi Group units. The asphaltic veins investigated were Segürük, Avgamasya, Seridahli, Nivekara, Milli, İspindoruk, Anılmış-Karatepe, Rutkekurat, Üçkardesler, Harbul, Silip, and Ortabağ-Ortasu, a total of 12 veins (fig. 1).



Fig. 1 Location map of investigated asphaltites

Given the varying descriptions of asphaltites, as well as of their origin and formation mechanisms, previous researchers have investigated the origin of avgamasya asphaltite through different methods, and have tried to compare asphaltites with nearby oil occurrences in order to discover whether asphaltite is petroleum-originated or not. For the comparison with petroleum, they have chosen very heavy and viscous Raman and Dinçer oils; API Gravity (13 and 15) Sulfur (wt.% 5.5 and 6.1). Other studies have noted chemical-compound similarities between asphaltite taken from only one vein of the Avgamasya region in Şırnak, and oils from the Raman and Dinçer fields, suggesting similar origins (Akrami et al., 1997; Erdem et al., 1991; Kavak and Yalçın., 2003; Kavak, 2007; Kavak, 2009). Furthermore, E. Muller et al. analyzed nine asphaltite sample from only one vein of SE Turkey, named the Seridahli vein, and five crude oils from 5 different reservoirs (Çelikli, Garzan, Raman, South Dinçer, West Raman Field) in the Southeast (SE) of Turkey, with the aim of relating the oils and asphaltites of SE Turkey (Muller et al., 1995). The samples collected from 12 different asphaltite veins of the Şırnak area have been described by using organic geochemical methods (Kavak et al., 2010).

The aim of the present study is to compare 12 asphaltite veins in the Şırnak area (including the Avgamasya area), two of which, namely the Kumçatı and Silip veins, possess oil seeps, with Raman and Dinçer petroleum, and to search for any clue that may indicate that asphaltite has any relation with these oils seeps found in the Kumçatı and Silip veins (Kavak et al., 2009; Kavak et al., 2010; Kavak and Connan, 2005) (fig. 2).

Tab. 1 Quantity, yield and gross composition of the CH<sub>2</sub>Cl<sub>2</sub> extract from asphaltites δ<sup>13</sup>C of asphaltenes and biomarker ratios

Location	%EO (weight%)	Leco TOC %/sample	% EO/TOC	Extract ppm	Saturates %	Aromatics %	Resins %	Asphal-tenes %	δ <sup>13</sup> C asphal (‰ PDB)	Ts/Tm	GA / C30 □ □ H
Seguruk	5.29	40.7	13.0	53	5.8	23.1	34.3	36.8	-26.8	0.04	0.007
Avgamasya	7.52	44.2	17.0	75	8.3	41.7	35.8	14.2	-26.8	0.05	0.007
Seridahli	2.08	38.7	5.4	20776	30.6	46.3	18.4	4.7	-	-	-
Nivekara	1.93	43.9	4.4	19348	26.3	49.2	21.1	3.4	-	-	-
Mili	3.40	34.1	10.0	34	8.3	38	33.9	19.8	-26.6	0.49	0.02
Karatepe	2.05	39.7	5.2	20535	41.1	38.7	18.1	2.1	-	-	-
Kartaltepe	11.39	47.5	24.0	114	3.3	27.4	31.8	37.5	-26.8	0.05	0.007
Harbul	21.67	49.6	43.6	217	4.1	27.2	36.2	32.5	-26.9	0.015	0.005
Kumcati	2.41	39.5	6.1	24086	6.9	32.4	26.5	34.2	-26.8	0.17	0.014

- not determined

Tab. 2 Biomarker ratios and isotope values of asphaltites

Vein Location	δ <sup>13</sup> C whole asphaltite (‰ /PDB)	Ts/Tm (surface area)	s/Tm peal height	Hopane / Hopane + C30Moretane (surface area)	Hopane / Hopane + C30Moretane (peak height)	22S / 22S + 22R (C31αβHopane ) surface area	22S / 22S + 22R (C31αβHopane ) peak height
Seguruk	-25.7	0.07	0.04	0.88	0.91	0.5	0.54
Seguruk	-23.6	0.47	0.3	0.89	0.94	0.6	0.6
Avgamasya	-23.6	0.21	0.18	0.84	0.92	0.52	0.55
Avgamasya	-24.8	0.15	0.14	0.72	0.88	0.55	0.57
Ciftciler	-23.3	-	0.06	0.87	0.9	0.54	0.55

- not determined



Fig. 2 Kumçatı-Silip Asphaltites Veins and Oil Seeps

## Methods

We carried out the organic geochemical evaluation of 55 asphaltite samples collected from 12 different veins of the Şırnak area, and petroleum samples taken from running oil-wells in the Raman and Dinçer fields in SE Turkey. In order to investigate the organic geochemistry of the asphaltite veins, TOC-Rock-Eval pyrolysis, GC, GC-MS and isotope analyses were performed on the selected samples.

## Results and Discussion

### TOC and Pyrolysis Analyses

As one would expect, the amount of TOC is high for asphaltites, varying between 12 and 65% (tab. 1). The average TOC value for the 55 samples collected from 12 different veins of the Şırnak area is 42.2%. Significant differences in TOC for asphaltites indicate that they were not extensively invaded with bitumen during the filling of the vein. Natural asphalt did not penetrate into the host rock due to its low porosity.

The interpretation of Rock-Eval data was based on parameters and experimental limits documented by Espitalie et al. (1985) and Peters (1986). For the samples studied, HI values are quite high, the average being 309 mg HC/g TOC, whereas Oxygen Index values are very low, contrary to expectations generated by the published papers (4 mg HC/g TOC on average).  $T_{max}$  values range between 440 and 479°C (446.2°C on average). A value of 609°C, recorded in a sample taken from the Segürük vein, belongs to a single sample that underwent high temperatures through natural burning. This value is, therefore, not representative for the asphaltite of this seam. In the  $T_{max}$ -HI diagram, the asphaltites are classified as Type-II kerogen. (fig. 3). The asphaltites were determined as mature to post mature according to the  $T_{max}$  values.

### Extraction and Group Analyses

The GC analyses showed that the saturated fractions were biodegraded in all asphaltites. For this reason, no evaluations related to the pristane-to-phytane (Pr/Ph) rate, carbon preference index (CPI), and n-alkan distribution were carried out. However, Bartle

et al. (1981) reported that asphaltite Pr/Ph rates were lower than 1, and that the source rock of the main asphaltite had settled in an anoxic area.

Nevertheless, parameters determined from hopane biomarker analysis, such as H/H+M, Ts/Tm, 20S/20S+20R, and 22S/22S+22R, which were detected at the end of the GC-MS analyses, and sterane biomarkers C<sub>27</sub>, C<sub>28</sub>, and C<sub>29</sub> –sterane abundances were used for the maturity and interpretation of the depositional environment. The resulting sterane isomerization (20S/20S+20R) and bishomohopane isomerization (22S/22S+22R) rates indicated that the isomerization was completed (fig. 4).

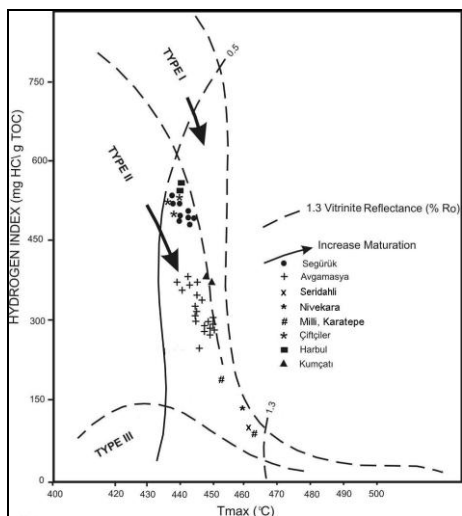


Fig. 3 HI-T<sub>max</sub> diagram of investigated asphaltites samples.

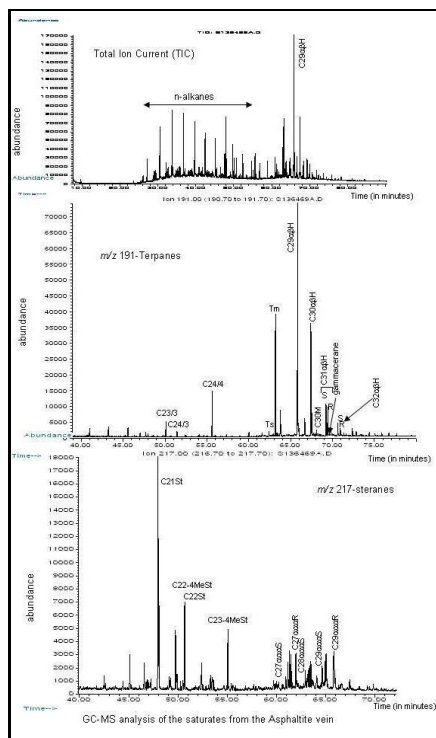


Fig. 4 GC-MS analysis of C15+ saturates: TIC, terpane (m/z191) and sterane (m/z 217) mass fragmentograms of an asphaltite (Kavak et al., 2010).

The above result is supported by the low ratio (<0.9) of Hopane/Hopane + Moretane. The Ts/Tm value of >1 showed that the probable main rock had a clay-rich lithology. The normal sterane percentages of C<sub>27</sub>, C<sub>28</sub>, and C<sub>29</sub> indicated a marine depositional environment. However, the average C<sub>29</sub> value of approximately 40% implied a land organic matter input (tab. 2). Regarding the maturity, a moderate one is indicated. Analyses of

Raman-Dinçer oils resulted in pr/ph rates  $<1$ , suggesting that the source rock of these oils was deposited in an anoxic environment (fig. 4).

Stable carbon isotope ( $^{13}\text{C}$ ) analyses of both oils of the Raman Dinçer and asphaltite samples revealed a value of  $-27$  per mil for the Raman Dinçer oils, and values between  $-23.5$  and  $-25.7$  for the asphaltites (tabs. 2, 3). Considering that the asphaltite was exposed to biodegradation, the asphaltite and Raman Dinçer petroleum can be said to have the same origin, in agreement with previous studies based on different methods (Akrami et al., 1997; Erdem et al., 1991; Kavak et al., 2007) (fig. 4).

## Conclusions

The asphaltite and Raman Dinçer petroleum can be said to have the same origin, in agreement with previous studies based on different methods. New studies at local and regional levels are needed, especially regarding the settlement mechanisms of asphaltites.

## Acknowledgements

The study was carried out with support from the Dicle University Research Fund Project No. DÜAP-2000-MF-403, DÜAPK-03-MF-85, DÜAPK-06-MF-01, DÜBAP 09-MF-54 and **TÜBİTAK-ÇAYDAĞ- Project No. 107Y201**. The author would also like to thank Prof. Dr. M. Namık YALÇIN (Istanbul University), Prof. Dr. Jacques CONNAN (France), Assoc. Prof. Dr. Sedat İNAN (TÜBİTAK-MAM), Assoc. Prof. Dr. Selami TOPRAK (MTA), and Assoc. Prof. Dr. M. Enver AYDIN (Dicle University) for their support. The entire staff of TKİ Şırnak, especially Adil TUNÇ, Meki AYDIN and all the colleagues who have contributed to the present study, are kindly acknowledged.

## References

- Akrami, H.A., Yardım, M.F., Akar, A., Ekinci, E., 1997. FTIR characterization of pitches derived from Avgamasya asphaltite and Raman-Dinçer heavy crude-oil. *Fuel*, **76**, 1389–1394.
- Bartle, K.D., Ekinci, E., Frere, B., Mulligan, M., Saraç, S., Snape, C.E., 1981. The nature and origin of harbolite and related asphaltite from southeastern Turkey. *Chem. Geol.*, **34**, 151–164.
- Erdem-Şenatalar, A., Ekinci, E., Keith, D., Bartle, K.D., Frere, B., 1991. Hydrocarbon minerals from South-Eastern Turkey-A Comparison of the chemical natures of the neighboring Raman-Dinçer crude-oil and Avgamasya asphaltite. *Erdol & Kohle Erdgas Petrochemie*, **44/7-8**, 298–300.
- Espitalie, J., Deroo, G., Marquis, F., 1985. Rock-Eval pyrolysis and its applications. Part 2. *Rev. Inst. Fr. Pet.*, **40/6**, 755–784.
- Kavak, O., 2007. Organic geochemical comparison of Avgamasya- Seguruk (Şırnak) Asphaltites and Raman-Dinçer Petroleum in Turkey. 23<sup>rd</sup> International Meeting on Organic Geochemistry (IMOG), 9-14 September, 2007, Torquay.
- Kavak, O., Yalçın, M.N., 2003. Organic geochemical properties of Şırnak asphaltites (In Turkish). Proceedings of 14<sup>th</sup> International Petroleum and Natural Gas Congress and Exhibition of Turkey, Ankara, 185–187.
- Kavak, O., Connan, J., 2005. Petrol/Bitumen seeps of South East Anatolian (In Turkish). Proceedings of 14<sup>th</sup> International Petroleum and Natural Gas Congress and Exhibition of Turkey, Ankara.
- Kavak, O., Erik, Y.N., Yalçın, N.M., Connan, J., 2009. Organic geochemical characteristics of Şırnak region asphaltites in Southeast Anatolia, Turkey. International Oil Shale Symposium, Oil Shale, 8-11 June, 2009, Tallinn.
- Kavak, O., Erik, Y.N., Yalçın, N.M., Connan, J., 2009. Geochemical evaluation of oil seeps in Turkey. The 24<sup>th</sup> International Meeting on Organic Geochemistry (IMOG), Bremen.

- Kavak, O., Connan, J., Erik, N.Y., Yalçın, M.N., 2010. Organic geochemical characteristics of Şırnak asphaltites in Southeast Anatolia, Turkey. *Oil Shale*, **27**/1, 58–83.
- Kavak, O., Connan, J., Yalçın, M.N., Jarvie, B., Jarvie, D., 2007. Geochemical characterization of the asphaltite veins from the Şırnak area, southeastern Turkey – their use as archaeological material. 23<sup>rd</sup> International Meeting on Organic Geochemistry (IMOG), 9-14 September, 2007, Torquay.
- Muller, E., Philp, R.P., Allen, J., 1995. Geochemical Characterization and Relationship of oils and solid bitumens from SE Turkey. *J. Petrol. Geol.*, **18**/3, 289-308.
- Peters, K.E., 1986. Guidelines for evaluating petroleum source rock using programmed pyrolysis. *Am. Assoc. Petr. Geol. Bull.*, **70**, 318–329.

## ESTABLISHING THE ORIGINS OF A METEORITE DEBRIS BY USING CARBON ABUNDANCE

SAHEEB AHMED KAYANI<sup>1</sup>

<sup>1</sup> National University of Sciences and Technology, Islamabad-44000, Pakistan; e-mail:  
saheebk@ceme.nust.edu.pk

**Keywords:** meteoritic carbon, combustion analysis, chondrites, asteroids.

### Abstract

In the present paper, the carbon content of meteorite debris located near the village of Lehri in the Jhelum district, Pakistan, has been determined through combustion analysis. This carbon abundance has been compared with the carbon weight % value of a certain type of meteorites, to establish the origins of the parent body of this particular meteorite debris.

### Background Information

Meteorite ablation debris has been identified near the village of Lehri (33°09'09"N; 73°33'35"E), in the Jhelum district, Pakistan (Kayani, 2009). The elemental and mineral composition of this meteorite debris have been determined using combined XRD-XRF analysis. Although X-ray fluorescence (XRF) spectrometry has become a fairly reliable method for elemental analysis, it can still miss on many lighter or trace elements like carbon and sulphur. As discussed in the next section, carbon abundance plays a significant role in the identification of the formation process and evolutionary stages that took place throughout the life span of a particular meteorite and its parent body.

In the present study, the total carbon content of the meteorite debris has been determined and this abundance has been compared with values reported in the literature in an attempt to identify the origins of the parent body of this meteorite debris.

### Testing and Analysis

Carbon is one of the most important elements in nature. It can exist in many stable forms and the chemical structure of carbonaceous matter depends upon available environmental conditions. The abundance, composition and structure of carbon can be analyzed to gather information about the initial formation process and the environmental changes undergone by the carbonaceous matter (Murae et al., 1993). In carbon rich chondrites (stony meteorites), carbonaceous matter has been identified as graphite, amorphous, kerogen-like, in some cases diamond, and mostly as a structurally unclear

insoluble high molecular organic compound. In iron and stony-iron meteorites, carbon is found as graphite or less ordered graphitic matter (Murae et al., 1993; Swart et al., 1983; Amari et al., 1990).

In light of the above, it seems that carbon abundance can serve as a useful clue in the identification of the nature and origin of a particular meteorite. Furthermore, it can be used to detect alterations in the structure of the original matter (of the meteorite) due to impacts, collisions etc. (In this regard, a very interesting study has been presented by Weller and Wegst (2009), in which the initial carbon abundance in a chondrite, detected using spectroscopic analysis, was further explored through Fe-C Snoek peak analysis, and it was determined that the structure of the chondrite has been altered because of local heating effects in a collision.)

For the meteorite debris under study, the XRD analysis has detected magnetite and wustite as predominant iron phases (Kayani, 2009). The presence of wustite shows a reducing environment which may have existed either due to the collision of the parent body with another celestial object, or to high pressure and temperature caused by resistance against the atmosphere of Earth. As the meteorite debris has been found lying over the site in the form of small stones, it seems that, upon its entrance into Earth's atmosphere, the parent meteoroid succumbed to increasingly high pressure and temperature, and, at a certain height, exploded into innumerable small pieces that came to rest on this particular site. This kind of behavior is typically observed with chondrites, as they are more vulnerable to high pressure and temperature effects due to their composition and structure.

Tab. 1 Carbon and Sulphur Abundance

Element	Abundance (wt%)
C	0.43
S	0.04

In order to determine the abundance of carbon and sulphur in the meteorite debris, a specimen was tested through combustion analysis using the facilities available at the Petroleum Geochemistry Laboratory of the Hydrocarbon Development Institute of Pakistan in Islamabad. In the combustion analysis of meteorites, carbon is released over three different heating ranges. Recent contaminants are detected below 500°C, while weathering products (i.e. carbonates) decompose around 1000°C. The spallogenic components (from metals and silicates) are identified during melting. Heating up to 1000°C is used to determine the weathering age, whereas the melt is analyzed to establish a terrestrial or residence age for the meteorite. The testing results are included in table 1.

The carbon abundance for this meteorite debris is in conformity with the median carbon abundance value for enstatite chondrites (i.e. 0.4 wt%), as reported by Moore and Lewis (1965). This carbon value, along with the elemental composition determined through XRF analysis by Kayani (2009), supports the idea that the parent meteoroid body of this debris may have been an enstatite chondrite. Enstatite chondrites have a high iron content (up to 30 wt%), and contain a magnesium-silicon mineral enstatite ( $Mg_2Si_2O_6$ ). The silicon

and magnesium abundance values detected through XRF analysis are 3.93 wt% and 0.342 wt%, respectively (Kayani, 2009). The increased relative abundance of iron (56.28 wt%) in the meteorite debris is attributed to ablation effects experienced by the parent meteoroid body upon its entry into Earth's atmosphere and its subsequent explosive disintegration into small meteorites. This meteoroid may be related to a primitive undifferentiated parent body or an asteroid. Such asteroids represent the earliest rocky bodies that originated within the solar system. Most of these asteroids float around the Sun within the orbits of Mars and Jupiter (the so-called "asteroid belt").

### **Conclusion**

Based on the analyses included in previous section, the meteorite debris is identified as enstatite chondrite in nature. The parent body of this meteorite debris may have originated from the "asteroid belt." It may have been hurled (as a result of a collision with a neighboring celestial object) into a trajectory that ultimately brought it into close proximity with Earth, and was finally pulled down by Earth's gravity, causing it to crash on this particular site. Because of technical limitations, attempts for radiocarbon analysis were not successful. As a result, a terrestrial age for the meteorite could not be established as of now. (the terrestrial age being the age or time elapsed since the meteorite landed on Earth and started absorbing  $^{14}\text{C}$ .) Further testing using the thermo-luminescence (TL) analysis is proposed for this purpose.

### **Acknowledgments**

The Radioisotope Hydrology Group at the Pakistan Institute of Nuclear Science and Technology was approached for the radiocarbon analysis of the meteorite specimens. Their interest and courtesy is gratefully acknowledged. I am also thankful to the technical staff of the Laboratory of Petroleum Geochemistry at the Hydrocarbon Development Institute of Pakistan for their assistance and expertise. The present work would not have been possible without the academic and research support received from the National University of Sciences and Technology in Pakistan.

### **References**

- Amari, S., Anders, E., Virag, A., Zinner, E., 1990. Interstellar graphite in meteorites. *Nature*, **345**, 238–240.
- Kayani, S.A., 2009. Using combined XRD-XRF analysis to identify meteorite ablation debris. In Proceedings of IEEE International Conference on Emerging Technologies, Islamabad, Pakistan, October 19-20, 219–220.
- Moore, C.B., Lewis, C., 1965. Carbon abundances in chondritic meteorites. *Science*, **149**, 317–317.
- Murae, T., Kagi, H., Masuda, A., 1993. Structure and chemistry of carbon in meteorites. In Oya, H. (ed.), *Primitive Solar Nebula and Origin of Planets*. Terra Scientific Publishing Company.
- Swart, P.K., Grady, M.M., Pillinger, C.T., Lewis, R.S., Anders, E., 1983. Interstellar carbon in meteorites. *Science*, **220**, 406–410.
- Weller, M., Wegst, U.G.K., 2009. Fe-C snook peak in iron and stony meteorites: metallurgical and cosmological aspects. *Materials Science and Engineering (A)*, **521/522**, 39–42.

## **CORDIERITE-BEARING XENOLITHS IN THE ANDESITES FROM VECHEC, SLOVAKIA: COMPOSITION AND ORIGIN**

MARIÁN KOŠUTH<sup>1</sup>, ZDENKA MARCINČÁKOVÁ<sup>1</sup>

<sup>1</sup> Technical University in Košice, Institute of Geosciences, Faculty B.E.R.G. (Mining, Ecology, Process Control and Geotechnologies), 15, Park Komenskeho, 043 84 Košice, Slovak Republic; e-mail: marian.kosuth@tuke.sk

**Keywords:** cordierite xenolith, phase composition, precursor rock.

The central neck of a parasitic andesite volcano, exposed at the eastern margin of the Slanske vrchy Mts., is found in the locality of Vechec; it belongs to a group of Neogene composite volcanoes developing in Eastern Slovakia. Pyroxene-bearing andesites (55.91÷57.51% SiO<sub>2</sub>, 3.81÷4.29% Na<sub>2</sub>O+K<sub>2</sub>O) are well-known for their content of tridymite and rare minerals, such as tobermorite, gyrolite, apophyllite etc., filling the cracks and cavities of the andesites; some carbonates (e.g. calcite, aragonite) and zeolites (e.g. stilbite, heulandite; Košuth, 1999) may also be identified in various enclosed xenoliths. The andesites were developed as a product of a relatively dry, Ca-alkaline, arc-type magma that enclosed a wide range of basement rock fragments.

Among the xenoliths from the studied andesites, the dark, cordierite-bearing ones, are the most interesting; the xenoliths of bluish-black, hornfels-like rock are mostly compact, homogeneous, without a distinct granular fabric. Using thin section microscopy and XRD (the powder technique), the petrographic features and the polymineral character of the xenoliths were studied. Selected cordierite and other mineral particles were identified through the WDS-EPMA technique. The samples consist mostly of  $\alpha$ -cordierite and plagioclase, associated with disseminated Fe-spinel. More detailed investigations have also revealed the presence of ilmenite, biotite, K-feldspar, apatite, ankerite, and andalusite; an amorphous glassy-phase was identified as well. Apart from this mineral composition, zeolitization processes or the magma caustic effect may also be assumed. The xenoliths belong to the CHA type and display a highly aluminous character, with just 45% SiO<sub>2</sub>. The Mg vs. Fe ratio indicates the prevalence of cordierite over the sekaninaite end-member. The analysis of anedral plagioclases shows the presence of the oligoclase term (Ab<sub>82.5-74.99</sub>); all K-feldspars are of the anortoclase type, with the albite/sandine mutual ratio close to 1:1. The mentioned spinels are either highly ferrous, with 0.65÷0.69 (Fe+Mn)/(Mg+Fe+Mn), or they belong to the hercynite term.

The low contents of some elements such as Ni and Cr (less than 0.06%), and some contamination with alkalis (Na<sub>2</sub>O up to 0.38%, and K<sub>2</sub>O up to 1.28 %), point to the origin

of its protolith from the upper crust. We assume that the sample VX7 is the only relevant protolith; it appears as a dark grey laminated xenolith with spinel and a MgO+Fe<sub>total</sub> content similar to that of the cordierite-bearing xenoliths. Based on its XRD patterns, the protolith is an An-plagioclase-bearing rock, with minor to accessory sanidine, ilmenite, titanite, clinopyroxene (Di-Hd with around 16.5 to 23.0% CaO), and fluorapatite. Medium Mg-Fe<sup>2+</sup> spinels differ from those from the cordierite xenoliths; an amount of around 12.5% MgO yield a (Fe+Mn)/(Mg+Fe+Mn) ratio within the 0.493÷0.508 range. The thin sections scanned showed calcite and younger feldspars crossing the cementing spinel.

Due to the magma caustic imprint and to additives, we assume the partial melting of such an An-plagioclase+spinel-bearing rock, which leads to an Al-Fe-Mg(Ti)-rich melt. We suggest that the compact fabric of the cordierite xenolith may be the consequence of a gradual crystallization from the dark Al-glassy phases (relics confirmed by EPMA). The appearance of cordierite through devitrification has already been proven (e.g. Grapes, 1985; Renzulli, 2003), and is often present in the fabrication process of industrial cordierite ceramics (Kobayashi, 2000; Shu et al., 2002). Thus, we assume that the  $\alpha$ -cordierite from the VX7 protolith was formed in the magma chamber through equations similar to those of the artificial sintering:



Fe-cordierite usually originates at about 850-900°C, through amorphous glassy stages or from intermediate silicate phases with spinel (McRae-Nesbitt, 1980). Associated with the hercynite end-member and with Cl+F fluid additives (relic contents confirmed), it may originate at temperatures of even 700°C.

### Acknowledgement

The present article was published with the significant support of the 1/0781/08 VEGA grant.

### References

- Grapes, R.H., 1985. Melting and Thermal Reconstruction of Pelitic xenoliths, Wehr Volcano, East Eifel, West Germany. *Journal of Petrology*, **27/2**, 343–396.
- Kobayashi, Y., Sumi, K., Kato, E., 2000. Preparation of dense cordierite ceramics from magnesium compounds and kaolinite without additives. *Ceramic International A.*, **26/7**, 739–743.
- Košuth, M., 1999. Xenoliths in Neogene vulcanites of the Slanske vrchy Mts (In Slovak). Manuscript, F-BERG TU, Košice, 171p.
- MacRae, N.D., Nesbitt, H.W., 1980. Partial melting of common metasedimentary rocks: A mass balance approach. *Contribution to Mineralogy and Petrology*, **75**, 21–26.
- Renzulli, A., Tribaudino, M., Salvioli-Mariani, E., Serri, G., Holm, P.M., 2003. Cordierite-anorthoclase hornfels xenoliths in Stromboli lavas (Aeolian Islands, Sicily): an example of a fast cooled contact aureole. *Eur. Journal of Mineralogy*, **15/4**, 665–679.
- Shu, C., Mingxia, X., Cailou, Z., Jiaqi, T., 2002. Fabrication of cordierite powder from Mg-Al hydroxide and Na silicate: its characteristics and sintering. *Material Research Bulletin*, **37/7**, 1333–1340.

## **MATERIAL INDICATORS IN THE CASE OF OCEAN IMPACT: HALITE AND CALCITE CARBONATES**

YASUNORI MIURA<sup>1</sup>

<sup>1</sup> Yamaguchi University, Yoshida 1677-1, Yamaguchi, 753-8512, Japan; e-mail: yasmiura@yamaguchi-u.ac.jp

**Keywords:** ocean impact, halite, calcite, micro-grains, carbon-bearing grain.

### **Introduction**

The main material indicators of impact-related mineral material are studied using optical microscopic observation on impacts on dry lands as remnants of Earth, the Moon, asteroids and Mars. Almost all ocean impact materials (including meteorites) are considered to be broken to melt away on the water-planet Earth. The main purpose of the present paper is to find any microscopic electron evidences of ocean impacts, which are solidified to other combined materials with supplied elements (a metamorphosis) during impact processes.

### **Samples of impacts on dry rocks and oceans**

The remnants of impact materials which have been studied extensively in previous papers are mainly metamorphic solids (after high pressure) of dry target-rocks as silica-rich rocks (silicates or oxides) and carbon-rich rocks (limestone or carbonates), together with meteoroid projectiles as iron-rich oxides etc., which have so far been found on Earth, the Moon, asteroids and Mars (Miura et al., 1995).

However, meteoroids (asteroids) which collide with oceans (ca.70 vol.% of the Earth's surface) are almost completely broken and melted away in the water after the impact, together with the target rocks. In this respect, previous material evidences on "ocean impact" are summarized as follows (Miura et al., 1995; Miura and Iancu, 2009; Miura et al., 2009):

- 1) "dark-brownish thin-layer of geological boundary" (the 65Ma KTB or 250Ma PTB) with iron-rich oxides or sulfides of heavy elements;
- 2) "bulk elemental concentration" of Pt-group elements (including Ir) after the impact, during the formation of geological boundaries;
- 3) remaining metamorphic materials of spherule glasses and minerals of graphite-diamond carbon, shocked quartz, shocked calcite or zircon, which are mainly based on target rocks from the bottom of the ocean if the impact is massive.

There is little direct information on the above-mentioned impact-related materials and ocean impact. This is mainly because these materials are based on re-formed materials of meteoritic or dry target rocks, except ocean or ocean-sedimentary rocks.

### Impact glasses and breccias that record information on ocean impact

After the ocean impact, in which almost all fragments are broken immediately in the water, the only materials remaining after the ocean impact are investigated by using data related to a) impact glasses and spherule quenched processes during impact, b) nano-grains (as 100nm aggregates composed of 10nm grains), and c) halite (solidified from the ocean) or calcite carbonates (from shallow ocean-bottom rocks) through quenching processes, as shown in Fig.1 (Miura, 2008, 2009b, c).

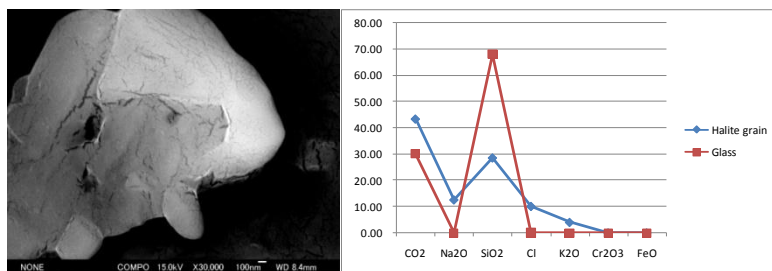


Fig. 1 The ASEM electron-micrograph (left) and compositional diagram (right) of the LDSG (Libyan Desert Silica Glass from Africa), with 100nm-sized fine grains of halite (NaCl) in cracks solidified from quenched water at impact. The scale bar is 100nm.

### Chlorine-bearing materials resulted from impacts

Significant amounts of chlorine are found in solidified materials of fine halite (NaCl) remained in the quenched glass from the salty ocean (Fig.1). This can be clearly distinguished from chlorine-bearing minerals resulted from the direct collision of meteoroids in the air, which show akaganeite with Fe, Ni and Cl (without Na) in composition, supplied directly from meteoritic projectiles (Miura, 2008, 2009a, b; Miura et al., 2010).

### Carbon-bearing materials resulted from impacts

Fine particles with carbon-bearing materials in LDSG impact glasses display the following characteristics: a) irregular shapes and nanometer sizes; b) various aggregates with sizes ranging from one micrometer to 100nm, which indicate metamorphosed limestone resulted through rapid cooling during the impact from target rocks of carbonates at shallow ocean-bottom sediments (Miura, 2009a; Miura et al., 2010).

In this respect, nano-sized carbon-bearing particles with irregular shapes are thought to be formed through ocean impact, together with chlorine-rich halite with fine nano-particles (without any Fe ions), by quenching in the ocean (Fig.2).

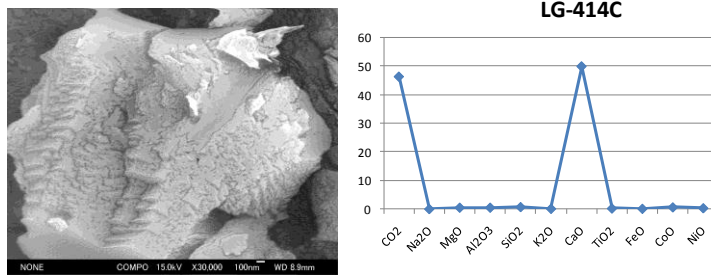


Fig. 2 The ASEM electron-micrograph (left) and compositional diagram (right) of the LDSG tektite sample of fine Ca-carbonate calcite, which represents aggregates of nano-particles (10nm in size) resulted from quenching in the ocean state. The scale bar is 100nm.

### Impact carbon- and chlorine-bearing particles in other impact sites

Fine carbon- and chlorine-bearing particles (without Fe) are found in samples of the ocean-impacts of the drilled core and glasses, as follows (Miura, 2008, 2009a,b; Miura et al., 2010; tab. 1):

- 1) Takamatsu (Kagawa, Japan) breccias in drilled grains near the crater bottom;
- 2) the Akiyoshi (Yamaguchi, Japan) Palaeozoic breccias in the drilled core;
- 3) Libyan desert silica glasses LDSG (Libya, Africa) in cavity or vein;
- 4) Congo diamond (DR of Congo, Africa) in vein and cavity;
- 5) the KT and PT geological boundary samples (Spain, and Meishan, China).

Tab. 1 Origins of carbon & chlorine in ocean-water impacts (Miura et al., 2010)

Carbon:	Shallow origin from carbonate rocks (calcite etc.) Deep origin from the ocean (carbonate ions etc.)
Chlorine:	Solidified halite ( <i>cf.</i> akaganeite from sources resulted from meteoritic collision)

### Summary

The present study is summarized as follows:

1) Material evidences of ocean impact are obtained as carbon-bearing fine-particles with irregular shapes supplied from carbonate rocks (with calcite) or the deep ocean, together with fine halite particles supplied by the chlorine-bearing ocean, although chlorine-bearing meteoritic sources are found as akaganeite phases with Fe ions.

2) Similar materials of fine carbon- and chlorine- bearing particles are found in the Takamatsu breccias(Japan), the Akiyoshi limestone breccias (Japan), the Libyan glasses

LDSG (Libya, Africa), Congo diamonds in cavity, and the KT and PT geological samples in spherule glasses (Europe, China etc.), which are related mainly to ocean impact.

### **Acknowledgements**

The authors wish to thank Professor Emeritus Dr. T. Kato of the Yamaguchi University and Dr. T. Tanosaki of Taiheiyo Cement Co. Ltd. for the discussion on the topic.

### **References**

- Miura Y., Takayama K., Kato T., Kawashima N., Imai M., Iancu G. and Okamoto M., 1995. Shocked quartz, silica and carbon materials in meteorites and impact craters. *Shock Waves* (Springer-Verlag), 19, 399-404.
- Miura Y., 2008. Impact origin of chlorine-bearing materials of salty sea-water of Early Earth. LPI Contribution No. 1439 (USA). CD#3001.
- Miura Y., 2009a. Carbon and chlorine contents of the Libyan desert glass compared with volcanic obsidian. *Antarctic Meteorites XXXII* (NIPR), 32, 39-40.
- Miura Y., 2009b. Impact-related indicators of grains with akaganeite composition found at Takamatsu, Nio, Kuga (Japan) and Carancas (Peru), LPI Contribution No. 1468 (LPSC40, USA), CD#2565 (p.2)
- Miura Y. and Iancu O.G., 2009. Deposition of carbon, iron and nickel at geological boundaries of the ends of the Permian and Cretaceous Periods. *Geologie*, 55, 105-112.
- Miura Y., Tanosaki T. and Iancu O.G., 2009. Mineral characteristics of carbonates with minor elements. Part 1. Calcites. *Geologie*, 55, 97-104.
- Miura Y., Tanosaki T. and Udagawa, 2010. Sea-Water Impact Materials: Carbon- and chlorine-bearing materials in impact glasses. *Shock Waves in Japan* (in Japanese with English abstract, Saitama Univ.), 117-118.

**GEOCHEMICAL COMPARISON BETWEEN THE LATERITIC BAUXITES  
HOSTED BY THE BASIC VOLCANICS OF CARIKSARAYLAR AND  
KOZLUCAY OCCURRENCES (ISPARTA, TURKEY)**

YESIM BOZKIR OZEN<sup>1</sup>, FETULLAH ARIK<sup>1</sup>, AHMET AYHAN<sup>1</sup>, ALICAN OZTURK<sup>1</sup>

<sup>1</sup> Selcuk University, Department of Geological Engineering, Konya, Turkey; e-mail:  
y\_bozkir@hotmail.com; ybozkir@selcuk.edu.tr

**Keywords:** bauxite, autochthonous, volcanic rocks, laterite, geochemistry.

Cambrian to Miocene magmatic, metamorphic and sedimentary rocks were observed in the area developed between Cariksaraylar and Kozlucay that is located about 50km northeast of Isparta; the perimeter covers an area of about 80km<sup>2</sup>. There are at least two autochthonous bauxite levels in the Islikayatepe volcanic rocks. These lateritic bauxite occurrences, generally aligned SE-NW, were observed around Kislatape, Muratbagi, Islikayatepe, Ortatas Hill, Uckardesler Hill, Hatibinagil Hill, and Kizil Hill. In the present study, three of them (Muratbagi, Uckardesler-Hatibinagil Hill and Kislatape) were investigated geochemically. All three lateritic bauxite levels occur at the top of the Islikayatepe volcanic rocks and show an autochthonous character. The three profiles are 103m, 167m and 120 m thick, and are represented by basic volcanic rocks, partly weathered volcanic rocks (saproilite) and bauxite levels, respectively. The bauxite levels occur between Mezardere formation (on the bottom), represented by dolomite and dolomitic limestone, and Aktassirti Limestone (on the top), represented by limestone and dolomitic limestone. The chemical composition of the three different bauxite occurrences is presented in table 1; the means of the major oxide composition of these lateritic bauxites are as follows: 42.01% Al<sub>2</sub>O<sub>3</sub>, 26.03% Fe<sub>2</sub>O<sub>3</sub>, 5.10% TiO<sub>2</sub>, 12.35% SiO<sub>2</sub>, 1.00% CaO, 0.78% MgO, 0.09% Na<sub>2</sub>O, and 0.46% K<sub>2</sub>O.

Tab. 1 The composition of the major oxides of Kislatape, Muratbagi and Uckardesler-Hatibinagil bauxite occurrences

Occurrence (location)	Chemical composition (wt %)							
	Al <sub>2</sub> O <sub>3</sub>	Fe <sub>2</sub> O <sub>3</sub>	TiO <sub>2</sub>	SiO <sub>2</sub>	CaO	MgO	Na <sub>2</sub> O	K <sub>2</sub> O
Kislatape	42.65	25.87	4.91	11.5	1.22	0.78	0.04	0.10
Muratbagi	39.98	25.22	5.61	14.19	1.31	0.76	0.12	0.26
Uckardesler - Hatibinagil	43.55	27.0	4.79	11.36	0.48	0.81	0.11	1.02

The mineralogical composition of the bauxite levels is represented by diaspore, hematite, boehmite, kaolinite, saponite, nontronite and anatase. The bauxites were classified as “autochthonous lateritic ferruginous bauxite”, according to their chemical composition and their geological settings.

## References

- Arik, F., Bozkir, Y., Ozturk, A., 2009. Geochemical Investigation of Basic Volcanite-Hosted Lateritic Bauxite Occurrence in Muratbagi (Isparta-Turkey) (In Russian). Mafic-ultramafic complexes of folded regions and related deposits Institute of Geology and Geochemistry UB RAS, Kachkanar-Ekaterinburg, Russia.
- Bozkir, Y., 2007. REE and formation conditions of bauxites between Cariksaraylar and Kozluçay (Sarkikaraagac-Isparta). MSc Thesis, Selcuk University, Konya, Turkey, 105p.
- Bozkir Y., Ayhan A., Arik F., 2008. Geological Investigation of the Çarıkisaraylar-Kozluçay area (Isparta-Türkiye). 8th International Scientific Conference, Bulgaria, **1**, 75–80.
- Bozkir, Y., Ayhan, A., Arik, F., 2009. Geologic and Geochemical Characteristics of Basic Volcanite-Hosted Lateritic Bauxite Occurrence in Uckardesler-Hatibinagil Hill (Isparta-Turkey). Mafic-ultramafic complexes of folded regions and related deposits Institute of Geology and Geochemistry UB RAS, Kachkanar-Ekaterinburg, Russia.

## **GEOCHEMICAL CHARACTERIZATION OF MARINE SEDIMENTS AND RECENT FORAMINIFERA IN SERIK, EAST ANTALYA, TURKIYE**

SEYDA PARLAR<sup>1</sup>, MUHİTTİN GORMUS<sup>2</sup>

<sup>1</sup> Selcuk University, Faculty of Engineering and Architecture, Department of Geological Engineering, 42075 Konya, Turkey; e-mail: sparlar@selcuk.edu.tr

<sup>2</sup> Suleyman Demirel University, Faculty of Engineering and Architecture, Department of Geological Engineering, 32260 Isparta, Turkey; e-mail: muhittin@mmf.sdu.edu.tr

**Keywords:** heavy metals, marine sediments, foraminiferal test, trace elements, Serik.

Geochemical analyses of sediments and foraminiferal tests could provide data for environmental interpretation. For this purpose, surface sediments collected from the shoreline area, along with sediments obtained by core drillings in Serik, were analyzed in order to determine their textural and compositional characteristics. Geochemically, the sediments have been compared in terms of the concentration of major and trace elements. The results indicate that the sediments have generally normal levels of heavy metals. However, a few samples display high Pb, Zn and Cu values, which suggest that the metals were transported away from the rock sources by rivers. Moreover, the results of compositional analysis reveal the relatively high amounts of organism remains. The semi-quantitative analysis of foraminiferal tests indicates that most of the tests have normal levels of heavy metals; just a few examples display relatively high values of Pb, Fe, Mn, Cr, Ni, Zn, Hg and Cu. The temperatures of seafloor water have been determined based on the Mg/Ca ratios of shells of foraminifera. Mg/Ca ratios vary between 2.123 and 129.74, and temperatures vary between 4.37 and 45.94°C. The values of  $\delta^{13}\text{C}$  -  $\delta^{18}\text{O}$  have provided information about the depositional environments of sediments. The results indicate that the sediments are of marine origin. The analyses of the grain size of these sediments have been performed in order to characterize the sediments and to acquire data about their depositional environment. All results of the present study provide useful information for ongoing scientific research.

## GEOLOGY, GEOCHEMISTRY AND GENESIS OF MARGI MAGNESITE OCCURRENCES IN ESKISEHIR, NW TURKEY

ASUMAN YILMAZ<sup>1</sup>, MUSTAFA KUŞCU<sup>2</sup>

<sup>1</sup> Disaster and Emergency Management Presidency, 06680 Ankara, Turkey; e-mail: asuman27@hotmail.com

<sup>2</sup> Suleyman Demirel University, Department of Geology, 32260 Isparta, Turkey

**Keywords:** isotopes, trace elements, geochemistry, magnesite, Margi, Turkey.

The magnesite mineralization is located in the Margi village of Eskisehir (NW Turkey). The magnesite deposits lie in serpentinized peridotite of Alpine-type ultramafic rocks, as individual veins and stockworks. The contacts between the magnesite veins and the host rocks are irregular and sharp. The veins display a NW-SE orientation. The thickness of the veins ranges from a few centimeters to 20 cm, and the length ranges between 3 and 9 m. Both types of magnesite are generally hard, have a conchoidal fracture and a white, porcelanous luster, and contain small amounts of Mn.

The analyses of the thin sections indicate that magnesite has a cryptocrystalline structure, as all ultramafic-related magnesite displays; it has a brecciate texture, which is not visible macroscopically. Thin section and XRD analyses reveal that some samples consist mostly of magnesite, some calcite and dolomite, and, only accidentally, serpentine.

The major, trace and rare earth element contents of magnesite were analyzed in the Canada ACME Analytical Laboratories Ltd. by means of the ICP-MS, Fire Assay, and ICP-ES methods. The major-oxide contents of magnesite are the following: MgO (46.04%), SiO<sub>2</sub> (1.41%), CaO (0.97%), Fe<sub>2</sub>O<sub>3</sub> (2.91%), Na<sub>2</sub>O (0.015%), Al<sub>2</sub>O<sub>3</sub> (0.048%); this chemistry is specific to magnesite that may be used as a sinter. In the study area, the amount of the minor elements is as follows: Ni (85-164ppm), Cr (123-6,844ppm); Co (0.5-13.3ppm); Cu (0.2-5.4ppm); Fe (419.58-9930.06ppm); Mn (77.45-1239.35ppm). The amount of Sr is 1.7-17.7ppm, and that of Ba ranges between 2.4 and 9.2ppm. The amounts of Hg and Ti are below the detection limit.

The Rare Earth Element (REE) amounts of magnesite show positive anomalies of La, Nd, Eu, Tb, Ho, Tm, and Lu, and negative anomalies of Pr, Ce, Sm, Gd, Dy, Er, and Yb, which indicate oxidizing conditions during deposition, and low temperature environments. Bau and Möller (1989) suggested that the positive Eu anomaly indicates a secondary mobilization of the mineral, at temperatures of 200-250°C. The magnesite in the study area displays Cr, Ni, Co, Cu, Fe, Ba, Ti and REE contents specific to magnesite from altered ultramafic rocks.

A  $^{13}\text{C}$  and  $^{18}\text{O}$  isotope study has been carried out on the magnesite samples at the Geoscience, Isotope Geochemistry Laboratory of Arizona University (USA), in order to explain the source of carbon and oxygen, and to estimate the temperature of magnesite. The magnesite of the study area displays  $\delta^{13}\text{C}$  (PDB) values ranging from -7.6 ‰, to -11.2 ‰, and  $\delta^{18}\text{O}$  (SMOW) values ranging between 27.8 ‰ and 30.8 ‰. Based on these isotopic data, the source of oxygen is the marine limestone and metamorphic rocks (Criss, 1999), while carbon originates from atmospheric  $\text{CO}_2$ ; the dissolved inorganic carbon is derived from the underground, i.e. freshwater carbonates or the carbonates of mantle origin (Clark and Fritz, 1997). According to these data, in the study area, the mineralization of the magnesite probably occurred after the serpentinization processes, near the earth surface, at low temperature; these conditions are rather similar to those which lead to the formation of other altered ultramafic-related magnesite deposits, in Turkey and Europe.

## References

- Bau, M., Möller, P., 1992. Rare Earth Element Fractionation in Metamorphogenic Hydrothermal Calcite, Magnesite and Siderite. *Mineralium Petrology*, **45**, 231–246.
- Clark, I., Fritz, P., 1997. *Environmental isotopes in Hydrogeology*. Lewis Publishers, New York.
- Criss, R.E., 1999. *Principles of Stable Isotope Distribution*. Oxford University Press, New York, 264p

# **Paleontology – Stratigraphy**



## OLIGOCENE FISH FAUNA FROM THE PARATETHYS SEA – NATIONAL GEOGRAPHIC SOCIETY PROGRAMMES

DORIN SORIN BACIU<sup>1</sup>

<sup>1</sup> „Al. I. Cuza” University of Iași, Department of Geology, 20A Carol I Blv., 700505 Iași, Romania; e-mail: dsbaci@clicknet.ro

**Keywords:** Oligocene, fish fossils, Paratethys Sea, anoxic sediments, paleobiogeographic, paleoecologic.

Fishes, as fossils, are almost exclusively autochthonous, and, thus, best suited as direct indicators of aquatic vertebrate life and vertebrate biodiversity in the past.

The main steps taken during the present project towards the establishment of extant Atlantic Ocean and Mediterranean Sea, as well as Indo-Pacific area fish fauna, shall rely on comparative investigations carried out on important fossil fish assemblages in the Eastern Carpathians (Romania), Northern Caucasus (Russia), Menilic Formation of the Outer Carpathians (Ždánice-Subsilesian Unit), Moravia (Czech Republic), and Frauenweiler, on the Rhine Valley (Germany) (fig. 1). The faunas and localities under consideration are well representative for different developmental stages of the Paratethys Sea, reaching from the Lower Oligocene to the Middle Miocene (34-16 M.a.). Many of the respective taxa have been described previously only on the basis of comparatively poor materials of synonymies, resulting from widespread scattering of type specimens over various collections. Therefore, critical revisions concerning the morphology, taxonomy and relationships of various fish groups are needed.

The effects of the African–Arabian–Eurasian collision, uplifting in the Alpine Foldbelt, along with the eustatic sea-level drop during the terminal Eocene, caused the separation of the northern basins from the Tethyan Realm. From the beginning of the Oligocene, these intercontinental domains with specific paleo- and biogeography, hydrological regime, and dynamics of sedimentation, were collectively named the Paratethys (Baldi et al., 1980). The Paratethys was subdivided into the Central European basin (Alpine-Carpathian) and the Euxinian-Caspian basin.

The isolation of the Paratethys, along with the cooling in the terminal Eocene, and the changes to mesophilic humid climatic conditions with intensive runoff, as well as the deepening of the basin bottom, led to thermohaline water stratification and to a primarily estuarine water circulation pattern, eventually resulting in recurrent episodes of stagnation and, consequently, to the accumulation of dysoxic to anoxic sediments. Such sediments



Paucă, 1931; Ciobanu, 1977; Baciú and Chanet, 2002). Unlike the Pietricica and Cozla fish faunas, in the Agârcia ichthyofauna the fishes of the genus *Bregmaceros* are rather abundant (these are absent in the other localities of the Piatra Neamț area); the species of the genera *Digoria*, *Zenopsis*, and *Seriola* are also recorded, as well as a number of new taxa belonging to the orders Gadiformes and Perciformes. The meso-batypelagic Sternoptychidae, Gonostomatidae and Myctophidae (characteristic for the Pietricica Mountain) have not yet been found in the Agârcia assemblage; neither has the pelagic predator *Palimphyes*, which is abundant in the Cozla Mountain.

The field excavations of 2002, carried out with the support of the National Geographic Society (project no. 7312-02), have yielded perfect results, published in two scientific papers, as follows: Baciú and Bannikov (2003), where a new genus and species of Bramidae were described, and Baciú and Bannikov (2004), that described two new genera and three new species of Ariommatidae and Centrolophidae. Specimens discovered in 2002 were also described in other two monographs on the revision of the Caproidae and Zeidae families (Baciú et al., 2005).

The Tethyan ichthyofauna of the second half of the Eocene is much less studied than that of the first half of the Eocene and the younger Oligocene fauna, and the Gorny Luch locality in the North Caucasus covers, to some extent, the gaps in the intervals in which the Tethyan fishes are poorly known. The excavations in the North Caucasus, carried out in July-September 2003 and 2007, and supported by the National Geographic Society, yielded more than 258 specimens of teleostean fishes, 2 shark teeth, a bird bone, and 7 imprints of bugs in the Gorny Luch locality. A number of specimens represent the first discoveries of the corresponding fishes in the Gorny Luch locality; apparently, all of them belong to new taxa, as follows: pipefish belonging to the Syngnathidae family; crestfish belonging to the Lophotidae family; two different rabbitfishes belonging to the Siganidae family; champsodontid fish representing a new species; juvenile specimens of leatherjacket belonging to the Balistidae family. Some new forms have not yet been identified. The bird femur bone also undoubtedly belongs to a new taxon.

In the West, outside the Carpathians and the Caucasus, fish facies have developed in the Rhine Graben. There are, among others, two important localities: Froidfontaine, on the French side, and the German locality of Frauenweiler (e.g., Micklich and Parin, 1996; Micklich, 1998; Pharisat and Micklich, 1998).

The field excavations of 2009, supported by the National Geographic Society, have yielded perfect results. The fossil site (official designation: "Grube Unterfeld") is the very last outcrop of a series of ancient clay pits and brick stone quarries in the Wiesloch and Rauenberg areas (Baden-Württemberg, S Germany), as well as in the Mayence Basin and complete Upper Rhine Valley. Here, the Oligocene "Rupelton"-deposits are still accessible for scientific excavations today. Only recently has it become famous for the world's oldest record of a fossil hummingbird. Aside nice plant, invertebrate and vertebrate fossils, it revealed a rather rich and well-preserved fossil fish fauna, which has been the subject of several publications since the beginning of the 20th century. Presently, apart from some "strange" taxa (e.g., Elopidae), the general composition of this fauna does not strikingly differ from contemporaneous fish associations of former outcrops in the Upper Rhine Valley, (e.g., Froidefontaine clay pit, Alsace, France). Nevertheless, many of the

Frauenweiler taxa are "waste paper" groups, which most likely consist of more than the actual nominal genus or species, and the ichthyofauna must, therefore, be expected to be much more diversified than is currently known.

According to the Frauenweiler fossil fish record, the scenario of Weiler (1966), who assumed a quiet, shallow and nutritious bay with some kind of shelter from the open sea, still seems to be a highly appropriate one. Although there are several fishes which must be considered demersal or deeper water inhabitants, some of their extant representatives are very flexible concerning their life-style; occasionally at least, they also occur in surface and/or inshore waters. In addition, there is a considerably large number of principally inshore, shallow water fishes, some of which clearly do not occur in depths greater than 20m (e.g., Hemiramphidae, Centriscidae, Synganthidae). Furthermore, there are several taxa which are reported to occur in brackish waters or even to enter river mouths and/or estuaries. It must also be taken into consideration (and is probably under-estimated in many correspondent publications, which mainly refer to the living habits of the adult) that most of the Frauenweiler fishes are either post-larval individuals, or at least early juveniles. Such developmental stages are not only distinctively smaller than the adults of the respective taxa, but their living habits may also strikingly differ from those of the latter. Coastal, shallow water sea grass meadows, estuaries, and mangrove swamps are well-known as nursery grounds for a large variety of different marine fish species (e.g., Laegdesgaard and Johnson, 2001; Cocheret de la Morinière et al., 2002). Therefore, they may be the favorite approximates for the reconstruction of the palaeoenvironment around the present-day fossil sites.

The list of the fish fauna for paleoecological analysis is based on published data (e.g., Gregorova, 1997) that summarize the distribution of fish taxa from the Moravian localities, Czech Republic, and on the unpublished material from the localities Litenčice and Bystřice/Olší.

The analysis of whole shark and fish assemblages from the Menilitic Formation of the Ždánice-Subsilesian Unit was used for subsequent larger paleoecological, biostratigraphical and paleogeographical interpretations. The assemblages were considered separately in the Subchert Member, Chert Member, Dynow Marlstone and Šitbořice Member.

In the Subchert and Chert Members, the fish fauna is sparse, but brings very important data about the fish assemblage evolution, and shows the necessity to focus future research on these horizons. The following taxa were recorded in the Subchert Member from the pteropod horizon (the Litenčice and Moutnice localities): *Cetorhinus parvus*, *Clupea*, *Vinciguerrria*, *Anachelum*, *Gadidae*, *Palimphyes*, and *Myctophidae*. Despite the sparse material, this assemblage represents a marine environment without brackish or freshwater components.

The fish assemblage of the Dynow Marlstone consists mainly of different quantities of representatives of bathy-mesopelagic photophore-bearing fishes of the families Myctophidae, Gonostomatidae and Photichthyidae, the bathybenthic trichiurid *Anachelum*, and the pelagic *Glossanodon* and *Paleogadus*; the remaining taxa are only represented by a low rate. The assemblage illustrates a bathy-mesopelagic, benthopelagic environment and no brackish fauna makes part of the assemblage of the Dynow Marlstone.

The assemblage of the Šitbořice Member, on the contrary, represents the onset of a new fish fauna, which reflects, on one hand, the open sea, and, on the other, the estuarine environment. The last one can be supported by the presence of the salinity tolerant *Alosa*, *Syngnathus*, *Oligolactoria*, *Hemiramphus*, and *Echeneidae*. All these taxa are absent in the Dynow Marlstone, which could suggest some environmental changes. Photophore-bearing mesopelagical fishes are represented by photichthyids (*Vinciguerria*), myctophids (*Eomyctophum*), and gonostomatids (*Kotlarczykia*), and by the first appearance of another mesopelagic family – Sternoptychidae (*Argyropelecus*). Clupeids also form a more significant part of the assemblage in the Šitbořice Member than in that of the Dynow Marlstone.

From a paleogeographical point of view, all teleostean genera and families from the Menilitic Formation of the Ždánice-Subsilesian Unit are present in the Pshikian horizon (NP 21 –NP 22 - 23) of the Caucasus and other parts of the Carpathian (Poland and Romania).

The study of fish fossils will help clarify the phylogenetic and biogeographic relationships of the Oligocene-Miocene ichthyofauna of the Paratethys Sea, and of the genera and families of marine fishes, now found in the Atlantic and Indo-Pacific oceans and in the Mediterranean Sea.

## References

- Baciu, D.S., Chanet, B., 2002. Les Poissons Plats Fossiles (Teleostei: Pleuronectiformes) de L'Oligocene de Piatra Neamt (Roumanie). *Oryctos*, **4**, 17–38.
- Baciu, D.S., Bannikov, A.F., 2003. Paucaichthys neamtensis gen. et sp. Nova - The first discovery of Sea Breems (Bramidae) in the Oligocene of Romania. *Journal of Ichthyology*, **43/8**, 598–602.
- Baciu, D.S., Bannikov, A.F., 2004. New stromateoid fishes (Perciformes, Stromateoidei) from the Lower Oligocene of Romania. *Journal of Ichthyology*, **44/3**, 199–207.
- Baciu, D.S., Bannikov, A.F., Tyler, C.J., 2005a. Revision of the fossil fishes of the family Caproidae (Acanthomorpha). *Miscellanea paleontologica*, 8. Studi e ricerche sui giacimenti terziari di Bolca, **XI**, 7–74.
- Baciu, D.S., Bannikov, A.F., Tyler, C.J., 2005b. Revision of the fossil fishes of the family Zeidae (Zeiformes). *Bollettino del Museo Civico di Storia Naturale di Verona*, **29**, 95–128.
- Baldi, T., 1980. O korai Paratethys tortenete. *Fold. Kozl.*, **110**, 456–472.
- Ciobanu, M., 1977. Fauna fosilă din Oligocenul de la Piatra Neamt. Editura Academiei R.S.R., București.
- Cocheret de la Morinière, E., Pollux, B.J.A., Negelkerken, I., Van der Velde, G., 2002. Post-settlement life cycle migration patterns and habitat preferences of coral reef fish that use seagrass and mangrove habitats as nurseries. *Estuarine, Coastal and Shelf Science*, **55**, 309–321.
- Constantin, P., 1999. Studiul ihtiifaunei oligocene dintre valea Troțușului și valea Ialomicioarei. Abstract of doctoral thesis.
- Cosmovici, L.C., 1887. Les cuches a Poissons des Monts Pietricica et Cozla, District de Neamtz, Ville de Peatra. *Buletinul Societatii medicilor naturalisti, Iași*.
- Gregorová, R., 1997. Les poissons lumineux fossiles des Carpathes. *Pour la Science*, **239**, 66–70.
- Laegdesgaard, P., Johnson, C., 2001. Why do juvenile fish utilise mangrove habitats?. *Journal of experimental Marine Biology and Ecology*, **257**, 229–253.
- Micklich, N., Parin, N.N., 1996. The fish fauna of Frauenweiler (Lower Oligocene, Rupelian; Germany): preliminary results of a revision. In Lobon-Cervia J., etc. (Eds.), *Fishes and their environment: proceeding of the 8<sup>th</sup> Congress of Societas Europaea Ichthyologorum* (Oviedo, Spain). *Publicaciones Especiales, Instituto Espanol de Oceanografia*, **21**, 308p.
- Micklich, N., 1998. New information on the fish fauna of the Frauenweiler fossil site. *Italian Journal of Zoology*, **65**, 169–184.

- Paucă, M., 1931. Neue Fische aus dem Oligozan von Piatra Neamț. Academie Roumanie, Bulletin de la Section Scientifique, **1/2**.
- Pharisat, A., Micklich, N., 1998. Oligocene fishes in the W Paratethys of the Rhine Valley Rift System. Ital. J. Zool., **65**, 163–168.
- Popov, S.V., Shcherba, I.G., Stolyarov, A.S., 2004. Map 2: Early Oligocene (Early Rupelian, Early Kiscellian - Pschekhian). In Popov, S.V., Rogl, F., Rozanov, A.Y., Steininger, F.F., Shcherba, I.G., Kovac, M. (Eds.). Lithological-Paleogeographic maps of Paratethys 10 maps Late Eocene to Pliocene. Courier Forsch.-Inst. Senckenberg, **250**, 1–46
- Simionescu, I.T., 1904. Asupra câtorva pesci fosili din terțiarul românesc. Academia Romana, Publicațiile Fondului Adamachi, **XII**, București.
- Weiler, W., 1966. Die Bedeutung der Fischfunde im Rupelton der Tongrube Frauenweiler bei Wiesloch südlich von Heidelberg. Zeitschrift der Rheinischen Naturforschenden Gesellschaft Mainz, **4**, 1–37.

## THE DEVELOPMENT OF A DATABASE FOR RADIOLARIAN ASSEMBLAGES FROM THE JURASSIC CHERTS OF ALBANIA

ARIANA BEJLERI<sup>1</sup>, MENSİ PRELA<sup>2</sup>, FLUTURA HAFIZI<sup>2</sup>

<sup>1</sup> Polytechnic University of Tirana, Faculty of Information Technology, Computer Engineering Department, Tiranë, Albania; e-mail: arianabejleri@yahoo.com.

<sup>2</sup> Polytechnic University of Tirana, Faculty of Geology and Mining, Earth Science Department, Tiranë, Albania; e-mail: mensiprela@yahoo.com; hflutura@yahoo.com

**Keywords:** Radiolarian assemblages, Jurassic, chert, MS-ACCESS, database, section, species, biozonation.

The present paper deals with the development of a database which allows the informatization of the data for the Radiolarian Assemblages from the Jurassic Cherts of Albania in order to facilitate the use of this data by different users. Radiolaria are protozoic organisms with siliceous shells, abundant in the sedimentary rocks lying above the ophiolites found throughout the Tethys realm. This data is collected from several chert sections. Some sections belong to the siliceous sedimentary cover of the ophiolites of the Mirdita Zone (Kalur Cherts), while other sections belong to the carbonate successions deposited on the continental margin of the ophiolites. This abundant information must be represented electronically in order to manage it simply and quickly. The database is developed through the application of the MS-ACCESS program and it allows us to perform many operations. One of them is entering the data for Radiolarian Assemblages from the Jurassic Cherts of Albania, for example entering all the data about different sections, the description for each of them, their location, their orientations, the graphics for each section, the general data for each sample, the section from which they are taken, the radiolarian assemblage in each sample, and the age of sections, samples and species. The database also allows us to edit all the data in a simple way. Furthermore, we can use different queries to search for the data needed by different users and print them according to the interests of the former. Moreover, the database will be used by geologists in order to better understand the timing of the beginning of the siliceous sedimentation in different parts of the Albanian Ophiolites, from north to south and from west to east. Apart from this, the database represents a basis for the development of the Jurassic radiolarian biozonation for the Albanian territory.

## **PALYNOLOGICAL STUDY OF THE OUTCROP FROM THE CIOFOAIA BROOK (MOLDAVIAN PLATFORM) - PALAEOCLIMATIC AND PALAEOENVIRONMENTAL IMPLICATIONS**

GABRIEL CHIRILĂ<sup>1</sup>, DANIEL ȚABĂRĂ<sup>1</sup>

<sup>1</sup>“Al. I. Cuza” University of Iași, Department of Geology, 20A Carol I Blvd., 700505 Iași, Romania; e-mail: gabiflogeoc@yahoo.com; tabara\_d@yahoo.com

**Keywords:** palynology, palaeoclimate, Volhynian, Moldavian Platform, dinoflagellate.

### **Geological settings**

The studied area belongs to Moldavian Platform, which represents the western part of the East European Platform. The Moldavian Platform is composed of a crystalline basement and a sedimentary cover. The deposits identified belong to the third stage of the Upper Badenian-Meotian sedimentation (Ionesi, 1994).

The studied outcrop is located near the city of Fălticeni, in the western part of the Moldavian Platform (fig. 1).

### **Fălticeni – Boroaia Formation**

According to Țibuleac (1998), the Ciofoaia brook represents the eastern limit of the Fălticeni-Boroaia Formation, which is of Volhynian age. For the Fălticeni – Sasca – Răucești area, the author divides the interval between Volhynian and Basarabian into 4 lithological units: the lithological unit of pelites, the lithological unit of pelites and psamites, the Fălticeni-Boroaia Formation, and the Valea Moldovei Formation. The present study is focused on deposits from the Fălticeni-Boroaia Formation. Lithologically, this formation consists of marls, clays, sands, sandstones and interbedded tuffs.

### **The outcrop from the Ciofoaia brook**

The geographical coordinates of the studied outcrop are: N 47°26'47.2", E 26°25'06.4". 12 samples have been collected from the outcrop, out of which 4 have been used for palynological investigations (Fig. 3). The geological succession is the following: at the base, between 297 and 299 m altitude, we have identified a succession of sands with layers of sandstone. In the geological column, between 299 m and 306 m, we have identified marls with *Cerithium* and thin layers of coal. 4 palynological samples collected from this interval have been analyzed: P 321 (300.5 m), P 322 (301.5 m), P 323 (302.5 m), P 324 (303.5 m).



### Palynological assemblage

Among the samples analyzed, we observed a higher taxonomic content in sample P321. The percentage of the organic matter in this sample is 15% (according to the diagram of Shvetsov, 1954).

Based on this study, we have divided the palynological content identified in the samples collected from the Ciofoaia brook into marine and continental assemblages.

**Marine assemblage (Marine domain).** In the samples from the Ciofoaia brook outcrop we have found many dinoflagellates: *Homotryblium* sp., *Tythyodiscus* sp., *Spiniferites ramosus*, *Operculodinium centrocarpum*, *Polysphaeridium* sp., *Lingulodinium machaerophorum*, *Systematophora* cf. *placacantha*, *Lingulodinium polyedrum*, *Botryococcus braunii*, *Wetzeliella* sp. (reworked).

The shelf zone is the source area for dinoflagellates, with a higher percentage in sample P 321 (300.5 m). As we can see, it is a proximal shelf area (inner neritic – outer neritic) with lower water depth, where we have found *Spiniferites* and *Operculodinium* taxa. In the inner neritic area, species such as *Homotryblium* are also present. Species such as *Homotryblium* have also been related to the area with reduced salinity conditions located near the shore (Dybkjær, 2004). In other studies (Sluijs et al., 2005), representatives of the latter genus have been interpreted as characteristic for high salinity or as lagoonal settings.

A similar dinoflagellate assemblage was presented by Chirilă and Țabără (2008) for the outcrop from the Țiganca brook. Both outcrops, from the Ciofoaia brook and from the Țiganca brook, belong to the same stratigraphic unit: the Fălticeni-Boroaia Formation (Țibuleac, 1998). The sedimentation environment is near the coast, a fact emphasized by a higher percentage of spores and pollen (continental organisms) and the predominance of terrigenous organic matter.

Paleoecological interpretation based on dinocysts association:

*Lingulodinium machaerophorum* (topical species) can be considered a temperate to tropical, coastal euryhaline species present in regions with summer sea-surface temperature (SST) exceeding 12°C (Marret and Zonneveld, 2003). It is distributed within a very broad salinity range and has been recorded in environments ranging from brackish to marine, with salinity between 16.9 – 36.7 ‰.

*Operculodinium centrocarpum* is generally reported as a cosmopolitan species that might have low relative abundances in the tropical area and high relative abundances in regions with cold/temperate waters, such as the North Atlantic (Wall et al., 1977; Marret and Zonneveld, 2003). This species is distributed within a very broad range: temperature (-2.1°C and 29.6°C) and salinity (16.1 – 36.8 ‰).

*Homotryblium* sp. is frequent in sample P321. This taxon is characteristic for marginal environment or lagoonal settings (Dale, 1966; Sluijs et al., 2005). *Homotryblium* have been cited in Denmark by Dybkjær (2004), being characteristic for the low salinity environment from Oligocene – Lower Miocene deposits.

*Spiniferites ramosus* is present in low percentage in the palynological assemblage identified in the samples from the Ciofoaia brook. This taxon is an indicator for outer neritic settings, together with *Lingulodinium* div. sp., *Operculodinium centrocarpum* and *Systematophora* cf. *placacantha*.

**Continental assemblage (Continental domain).** Based on the palynological assemblage, we have separated the following biocenosis for continental palynomorphs: swamp assemblage, mixed mesophytic forest, and terrestrial herbs (Fig. 4).

The swamp assemblage is represented by aquatic plants such as *Typha*, and green algae such as *Botryococcus*, which indicate the presence of freshwater in the depositional environment.

The mixed mesophytic forest is well represented by species of fossil pollen, such as *Carpinus*, *Quercus*, *Ulmus*, *Betula*, *Carya* or *Acer*. Pinaceae species are also very abundant in the mesophytic forest. The ground cover vegetation of the mixed forest is made up of herbaceous plants, and the presence of ferns indicates humidity (*Leiotriletes*, *Laevigatosporites*, *Polypodiaceosporites* a. o.).

The terrestrial herbs consist of seven taxa, mainly constituted of ground-cover vegetation in the mesophytic forest. *Chenopodiaceae* are the dominant groups in this assemblage.

### **Palynofacies analysis**

Quantitatively analyzed samples preserved in organic matter have values between 10 and 30%, according to the diagram of Shvetsov (1954). A higher percentage of organic matter was observed in P323 (approx. 30%). In this sample, the main components are small phytoclasts, black coal remains, yellow-brown fragments of tissue and cuticle. The Amorphous Organic Matter (AOM) represents maximum 5% of the total content of kerogen. The Thermal Alteration Index (TAI) established on the continental palynomorphs is between -2 and 2. The kerogen determined on optical criteria is type III. It can be concluded that the palynofacies analyzed from the Volhynian deposits of the Fălticeni-Boroaia Formation is in an immature stage of hydrocarbon generation.

### **Paleoclimatical interpretation**

In order to reconstruct the paleoclimate based on palynological records, the “Coexistence Approach” (CA) (Mosbrugger and Utescher, 1997) method was applied. This method was frequently used for the reconstruction of the European tertiary paleoclimate.

In the present study, we have calculated 4 paleoclimatic parameters: Mean annual temperature (MAT), Mean annual precipitation (MAP), Mean annual temperature of the warmest month (WMT), Mean annual temperature of the coldest month (CMT). Estimations of MAT and MAP have been obtained on 38 palynological taxa identified in 4 samples analysed from the Ciofoaia brook outcrop.

The values calculated by us, using the “Coexistence Approach” method are the following (Fig. 5): MAT 15.7 -16.7 °C, MAP 1300 – 1355 mm/yr, WMT 21.7 – 27.8 °C, and CMT -0.3 – 7°C. The lower limit for MAT (15.7°C) is given by *Araliaceoipollenites edmundi*, and the upper limit (16.7°C) is marked by *Sciadopityspollenites* sp. For MAP, the lower limit (1300 mm/yr) is also given by *Sciadopityspollenites* sp., and the upper limit (1355 mm/yr) belongs to *Carpinipites carpinoides*. The lower limit for WMT (21.7°C) is given by *Pterocaryapollenites stellatus*, while the upper limit (27.8°C) is attributed to *Sciadopityspollenites* sp. For the CMT, the lower limit (-0.3°C) belongs to *Cedripites* sp.,



The palaeoclimatic parameters calculated by us (Fig. 5) are similar to those calculated for the Țiganca brook outcrop by Chirilă and Țabără (2008): MAT between 15.3–16.6°C, and MAP between 1300–1355 mm/year. This is understandable, given the fact that the outcrop from the Ciofoaia brook is 20 km from the Țiganca brook outcrop, and both belong to the Fălticeni-Boroaia Formation. This type of assemblage present in the outcrops from the Țiganca and Ciofoaia brooks was not identified in any other outcrop from the Moldavian Platform that has been studied. Therefore, the outcrop from the Ciofoaia brook represents the most eastern part of the Fălticeni-Boroaia Formation.

### Acknowledgements

The present work has been supported by the Romanian Ministry of Education, Research and Innovation under a PN-II-IDEI No. 975/2008 research grant. The authors wish to thank the reviewers for their highly useful comments.

### References

- Chirilă, G., Țabără, D., 2008. Palaeofloristic study of the Volhynian from Râșca (Moldavian Platform) - Palaeoclimatic and palaeoenvironment implications. *Acta Palaeontologica Romaniae*, **VI**, 29–42.
- Dale, B., 1996. Dinoflagellate cyst ecology: modeling and geological applications. In Jansonius, J. and D.C. McGregor, editors. (eds.). *Palynology: Principles and Applications*. American Association of Stratigraphic Palynologists Foundation, Dallas, **3**, 1249–1275.
- Dybkjær, K., 2004. Morphological and abundance variation in *Homotryblium*-cyst assemblage related to depositional environments; uppermost Oligocene-Lower Miocene, Jylland, Denmark. *Paleogeography, Palaeoclimatology, Paleocology*, **206**, 41–58.
- Ionesi, L., 1994. The geology of platform units and North-Dobrogea orogeny. Ed. Tehnică, București, 279p. (In Romanian).
- Ionesi, L., Ionesi, B., Lungu, A., Roșca, V., Ionesi, V., 2005. Upper and Middle Sarmatian from Moldavian Platform. Ed. Academiei Române, 558p. (In Romanian).
- Marret, F., Zonneveld, K.A.F., 2003. Atlas of modern organic-walled dinoflagellate cyst distribution. Review of Palaeobotany and Palynology, **125**, 1–200.
- Mosbrugger, V., Utescher, T., 1997. The coexistence approach - a method for quantitative reconstructions of Tertiary terrestrial palaeoclimate data using plant fossils. *Paleogeography, Palaeoclimatology, Palaeoecology*, **134**, 61–86.
- Sluijs, A., Pross, J., Brinkhuis, H., 2005. From greenhouse to ice-house; organic walled dinoflagellate cysts as paleoenvironmental indicators in the Paleogene. *Earth Science Reviews*, **68**, 281–315.
- Țibuleac, P., 1998. Geological study of the Sarmatian deposits from Fălticeni - Sasca - Răucești area (Moldavian Platform), regarding coal layers. PhD. Thesis, Univ. „Al. I. Cuza” Iași. (In Romanian).
- Wall, D., Dale, B., Lohmann, G.P., Smith, W.K., 1977. The environmental and climatic distribution in modern marine sediments from regions in the North and South Atlantic oceans and adjacent seas. *Mar. Micropaleontol.*, **2**, 121–200.

**PALYNOFACIES AND TOTAL ORGANIC CARBON CONTENT FROM THE  
BAIA BOREHOLE (MOLDAVIAN PLATFORM)**GABRIEL CHIRILĂ<sup>1</sup>, DANIEL ȚABĂRĂ<sup>1</sup><sup>1</sup> “Al. I. Cuza” University of Iași, Department of Geology, 20A Carol I Blvd., 700505 Iași, Romania; e-mail: gabiflogeoc@yahoo.com; tabara\_d@yahoo.com**Keywords:** Baia borehole, TOC, kerogen, Sarmatian.**Geological settings**

The studied area is located in the Moldavian Platform, which represents the western part of the East European Platform. The Moldavian Platform is composed of a crystalline basement and a sedimentary cover. The deposits identified belong to the third stage of sedimentation ranging between Upper Badenian and Meotian (Ionesi, 1994). The samples analyzed in this study are from the Baia borehole, which is located near Fălticeni city, in the western part of the Moldavian Platform (fig. 1).

The lithology consist of sands/sandstone, claystone and shale. In this study, 16 samples from the 290-1050 m interval of the Baia borehole have been analyzed with the purpose of palynofacial interpretation.

Tab. 1 The results for TOC and H percentage of Baia borehole samples

Sample no.	Depth	(%) TOC	(%) H	Hydrocarbon potential
160	540 m	0.75	0.342	Fair
161	560 m	1.236	0.595	Good
162	580 m	0.778	-	Fair
163	710 m	0.998	0.722	Fair
164	720 m	0.593	0.265	Fair
165	810 m	0.82	0.301	Fair
166	930 m	0.873	-	Fair
167	940 m	0.756	-	Fair
168	960 m	1.156	-	Good
169	1010 m	0.708	-	Fair

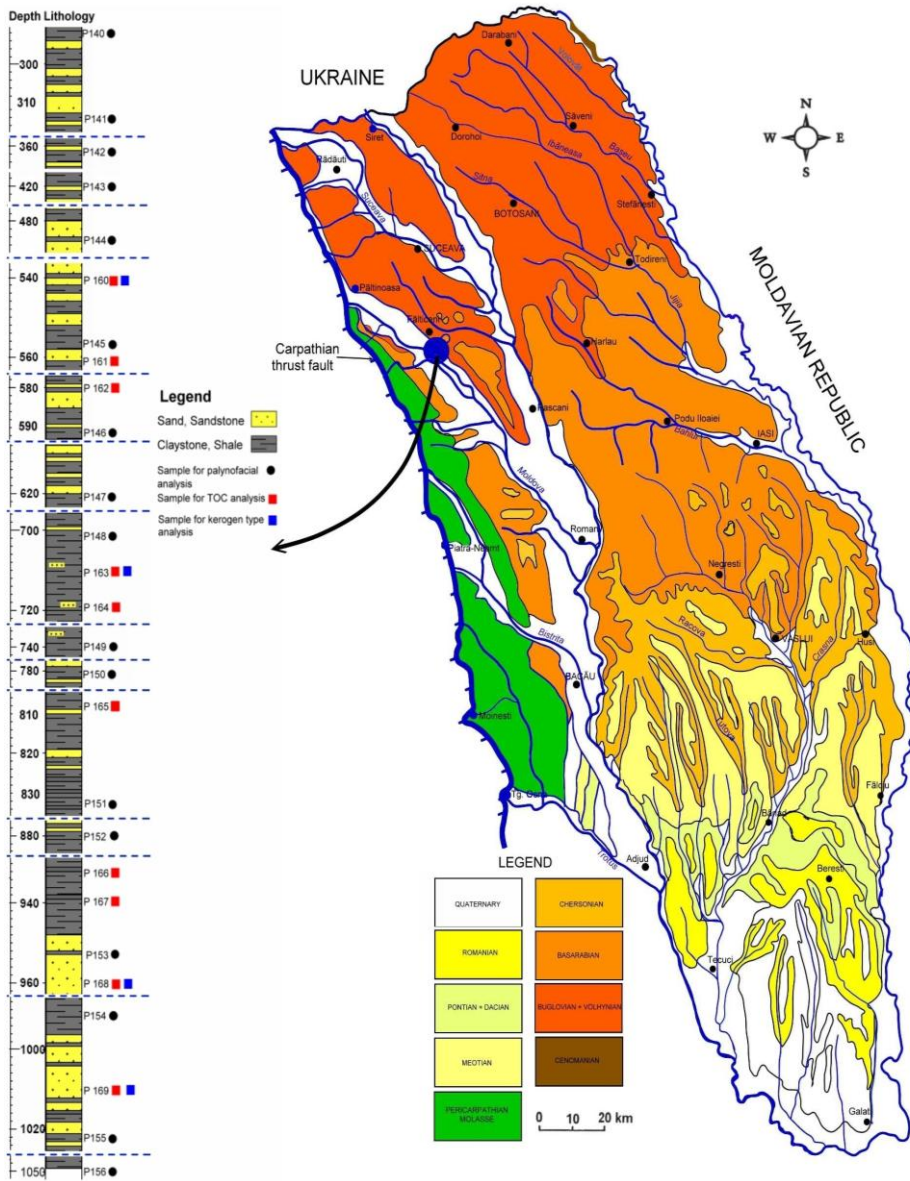


Fig. 1 Location and lithological column of the Baia borehole. The geological map is according to Ionesi (1994), with alterations.

**Results**

In the present study, 10 samples from the Baia borehole have been studied for TOC analysis. The results are presented in Table 1. The hydrocarbon potential has been established according to Tissot et Welte (1984) and Bordenave (1993). Samples 161 (560 m) and 168 (940 m) have a good hydrocarbon potential, while the other analyzed samples have a fair hydrocarbon potential.

In order to establish the type of kerogen for samples 160 (540 m), 163 (710 m), 168 (960 m) and 169 (1010 m), we have calculated the H/C and O/C ratios. The results are presented in Table 2. The values for the H/C ratio are between 0.8228 and 0.9272, the highest value having been calculated for sample 160. The values for the O/C ratio are relatively similar, being comprised between 0.2283 and 0.2758.

Tab. 2 The result for N, C, H, S, O percentages and H/C and O/C ratios

Sample no.	(%) N	(%) C	(%) H	(%) S	(%) O	H/C ratio	O/C ratio
160	2.804	54.059	4.177	-	19.880	0.9272	0.2758
163	2.743	56.106	4.192	-	17.155	0.8965	0.2293
168	2.199	51.131	3.506	-	16.840	0.8228	0.2470
169	-	65.263	4.554	1.45	19.871	0.8373	0.2283

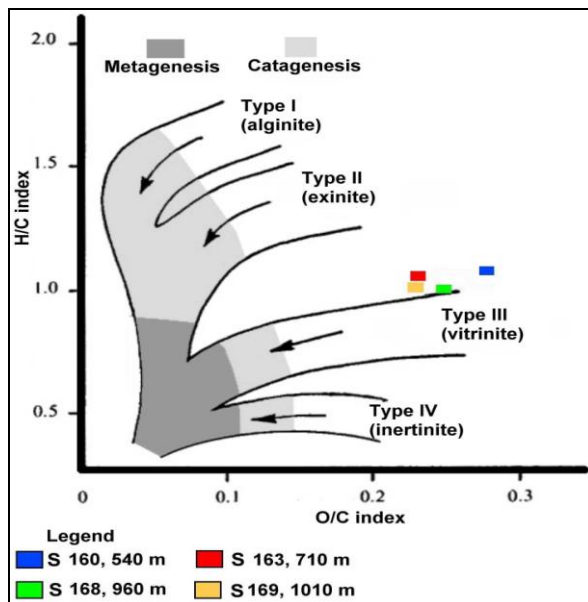


Fig. 2 The H/C and O/C ratios plotted in a van Krevelen diagram

The results obtained for kerogen analysis have been plotted in Figure 2. The kerogen type resulted on this diagram is type III. This type of kerogen has a low H/C ratio (<1.0) and a high O/C ration (up to ~0.3) (Peters and Moldowan, 1993). Such low hydrogen organic matter is polyaromatic and derived mostly from higher plants. Type III kerogen is the chemical equivalent of vitrinite, telinite, collinite, huminite, and so-called humic or woody kerogen. It produces natural gas and, occasionally, associated condensate if the thermal maturation is adequate.

## References

- Bordenave, M.L., 1993. The Sedimentation of Organic Matter. In Bordenave, M.L. (ed.), Applied Petroleum Geochemistry, Éditions Technip, Paris, 15–76.
- Ionesi, L., 1994. The geology of platform units and North-Dobrogea orogeny (In Romanian). Ed. Tehnică, București, 279p.
- Peters, K.E., Moldowan, J.M., 1993. The Biomarker Guide, Interpreting molecular fossils in petroleum and ancient sediments, Prentice Hall, 363p.
- Tissot, B.P., Welte, D.H., 1984. Petroleum formation and occurrence (2nd edition): Berlin, Springer-Verlag, 699p.
- Tyson, R.V., 1995. Sedimentary organic matter. Organic facies and palynofacies. Chapman and Hall, London, 615p.

**NEW CRETACEOUS FOSSILS DISCOVERED IN THE CONGLOMERATES  
FROM CHEILE BICAZULUI – HĂȘMAȘ NATIONAL PARK (EASTERN  
CARPATHIANS)**

IONUȚ V. CIOACĂ<sup>1</sup>, DAN GRIGORE<sup>1</sup>

<sup>1</sup> Geological Institute of Romania, Bucharest, RO-012721, Romania; e-mail:  
bonjuck@yahoo.com; dan1\_grigore@yahoo.com

**Keywords:** Cretaceous conglomerate, *Inoceramidae*, gastropods, Cheile Bicazului–Hășmaș National Park.

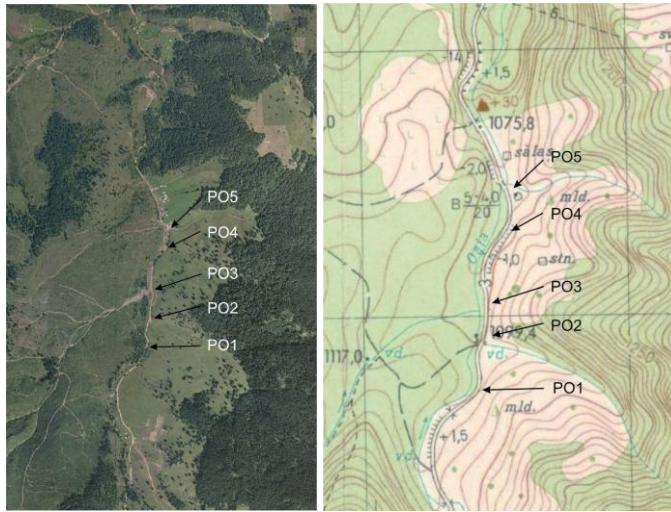
During the development of the Geobiohas Project (ANCS/CNMP CTR 31-059/2007), a new paleontological discovery was made in the conglomeratic deposits from Cheile Bicazului - Hășmaș National Park (CBHNP). The precise location is N 46° 45,456 E 25° 47,231 (GPS data), on the right slope of the Hăghimașului Valley (i.e. Oii Valley), near the confluence with the Ciofronca Valley. These conglomerates appear continuously throughout a large area in this median portion of the valley, and can be seen over a distance of almost 700 m in length, near the road. These deposits are stratified and an alternation of ruditic and psephitic layers can be noticed; all these deposits are slowly declined with 30 degrees to the NE.

These conglomeratic deposits were considered a part of the Barremian - Albian Wildflisch Formation by Săndulescu, 1975 (Fig. 3).

We analysed the fossil material through many points of observation and we summarized the analyses performed on the rock layers (Fig. 6). All biostratigraphic observations are synthesised in Table 1 and Fig. 4.

Here are some of the observations: the ruditic layers contain sorted elements as various as crystalline schists, Triassic dolomites, Jurassic limestones or sandstones, even Cretaceous marls or lime. The elements are no larger than 10 cm in diameter. Layers with small breccious elements, many sandy and, rarely, marl interbeds are also present. In the psephitic layers, fossils are very frequent: small gastropods and, rarely, bivalves, better preserved than the medium- or large-sized ones, which are many times more fragmentary. Very rare levels, such as that with *Bakevellia* and that at the top of this described succession, preserve big shells, corals or bio-casts (such as *Palaeodyction*). The differences in the preservation of some shells (gastropods and bivalves mostly) and a few corals reveal a marine shallow water range for these deposits.

The assemblage is characteristic for the Aptian – Albian interval.



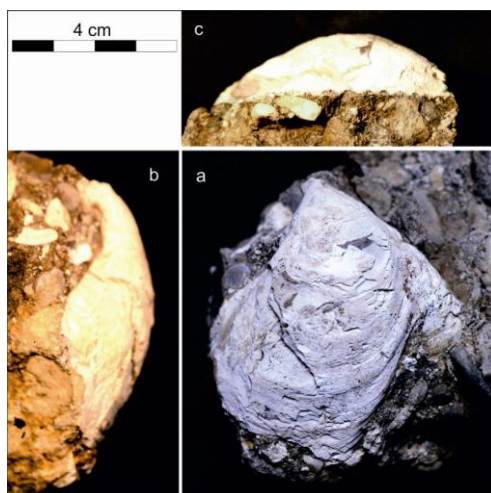


Fig. 5: *Bakevellia* cf. *ominensis*: a) lateral view; b) frontal view; c) dorsal view

Species	Age	Samples	Fig. 9
<i>Microschizia</i> ( <i>Cloughtonia</i> ) <i>scalaris</i> (Conrad, 1852)	Apt - Alb	O-15	e, f
<i>Gymnentome</i> ( <i>G.</i> ) cf. <i>zebra</i> Gabb, 1869	Apt - Alb	O-17	g
<i>Lunatia pedernalis</i> (Roemer, 1852)	Alb	O-25	c
<i>Trochocyathus conulus</i> (Miller, )	Apt - Alb	O-27	b
<i>Pyrazus</i> ( <i>Echinobathra</i> ) <i>valeriae</i> (Vemeuil and Lorie, 1868)	Apt - Alb	O-28	-
<i>Natica conradi</i> (Hill, 1888)	Apt - Alb	O-30	-
<i>Diptyxis alsusensis</i> Pcelintev	Apt - Alb	O-45	d
<i>Bakevellia</i> cf. <i>ominensis</i> Nakazawa and Murata, 1966	Apt - Alb	O-12	Fig. 5
Conglomerate with remains of conch	Apt - Alb	O-60	Fig. 6
Sandstone with <i>Bakevellia</i>	Apt - Alb	O-13	Fig. 7
Coral and <i>Diptyxis</i> sp.	Apt - Alb	O-48	Fig. 8

## Acknowledgements

The present study was financially supported by the National Centre for Project Management (CNMP), as part of the GEOBIOHAS Project (31-059 CTR/2007).

## References

- Săndulescu, M., 1975. Studiul geologic al părții centrale și nordice a sinclinalului Hăghimaș (Carpații Orientali). Anuarul Institutului de Geologie și Geofizică, București. 55/1, 200p.



Fig. 6

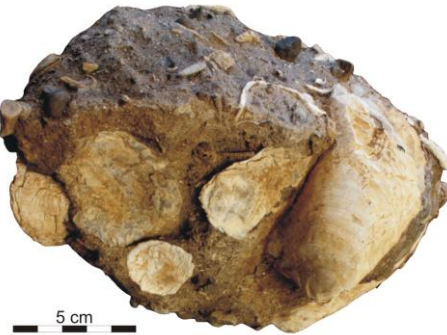


Fig. 7

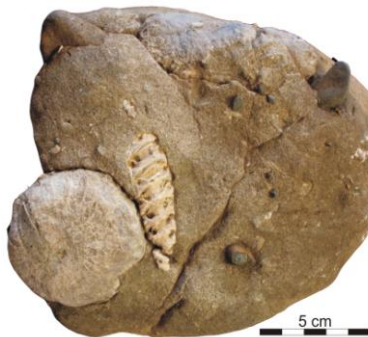


Fig. 8

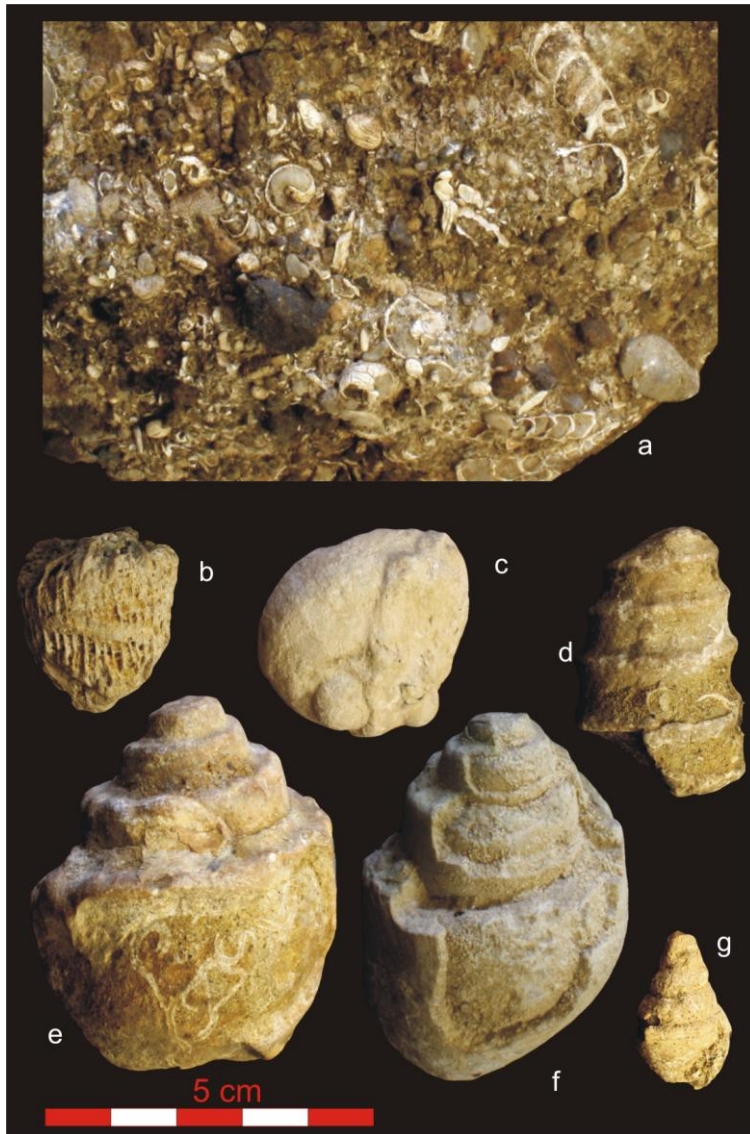


Fig. 9 (See the table)

## LATE MIOCENE VERTEBRATES FROM POGANA (SCYTHIAN PLATFORM)

VLAD CODREA<sup>1</sup>, LAURENȚIU URSACHI<sup>2</sup>, DANIEL BEJAN<sup>3</sup>

<sup>1</sup> “Babeș-Bolyai” University, Department of Geology-Paleontology, 400084 Cluj Napoca, Romania; e-mail: codrea\_vlad@yahoo.fr

<sup>2</sup> Bârlad Museum, Natural Science Branch, 731050 Bârlad, Romania; e-mail: ursachi\_laur@yahoo.com

<sup>3</sup> „Al. I. Cuza” University of Iași, Department of Geology, 20A Carol I Blv., 700505 Iași, Romania

**Keywords:** Meotian, rhinoceros, chilotherium, Scythian Platform.

In eastern Romania, illustrative Meotian (Middle Miocene) exposures can be followed on the Scythian Platform; they refer mainly to continental sequences. Sometimes, fossil vertebrates are present, like in Pogana (Vaslui district, Romania), on the left bank of Tutova River. There, grey clay, as well as cineritic sandstone documents fluvial environments, with ponds and, perhaps, even small lakes. Invertebrate fossils concern molluscs (various unionidae). The majority of fossil bones were roughly rolled before burial, being broken and exposing rounded margins. Among these fossils, the most relevant are some lower and upper rhinoceros teeth, belonging to *Chilotherium*. In Moldova, this genus is known from Bacău (Early Meotian), in association with *Aceratherium incisivum*, *Choerolophodon pentelici*, *Hipparion* sp., Palaeotraginae cf. *Samotherium* sp. The species *C. cf. sarmaticum*, is reported from Reghiu-Scruntar (Late Kersonian/Early Meotian; Rădulescu et al., 1995; Știucă, 2003), in a mammalian assemblage very similar to the one of Bacău. The presence of *Chilotherium* around the Sarmatian/Meotian boundary in Moldova reveals an intrusion of these rhinoceros, as newcomer immigrants of eastern origin.

### References

- Codrea, V.A., 2000. Tertiary Rhinoceroses and Tapirs in Romania (In Romanian, with abstract in French). Presa Universitară Clujeană, Cluj-Napoca, 174p.
- Lungu, A.N., 1984. The Middle Sarmatian Hipparion Fauna from Moldavia (Hoofed mammals) (In Russian). Izd-vo “Shtiintsa”, Kishinev, 158p.
- Rădulescu, C., Știuca, E., Brustur, T., Zaharia, S., 1995. Neogene mammalian fauna from the bend zone of the east Carpathians. Romanian Journal of Stratigraphy, **76** /6, 13–25.
- Știuca, E., 2003. Preliminary note on mammalian fauna from Reghiu Miocene (Vrancea county, Romania) (In French). Advances in Vertebrate Paleontology "Hen to Panta", București, 113–116.

## FOSSIL WOODS IN THE COLLECTION OF THE AICU GEOLOGICAL MUSEUM

EUGENIA IAMANDEI<sup>1</sup>, STĂNILĂ IAMANDEI<sup>2</sup>, MIHAI BRÂNZILĂ<sup>3</sup>, DANIEL  
ȚABĂRĂ<sup>3</sup>, GABRIEL CHIRILĂ<sup>3</sup>

<sup>1</sup> Geological Institute of Romania-Bucharest, 1, Caransebeș Street, 012271 Bucharest, Romania; e-mail: iamandei@gmail.com

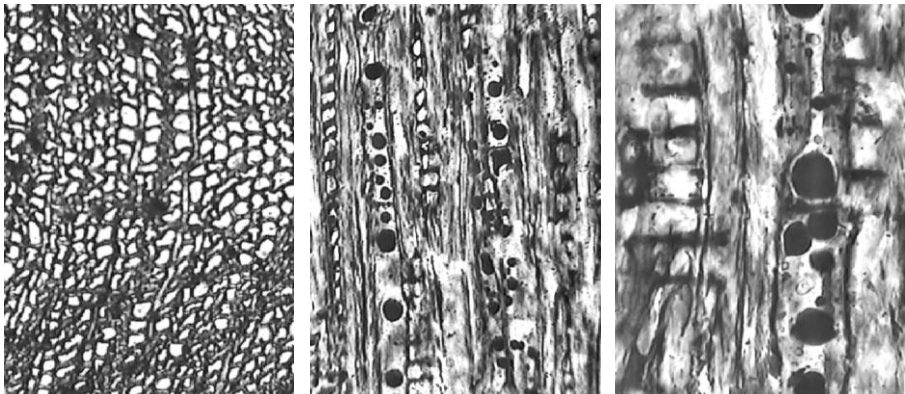
<sup>2</sup> National Geological Museum (IGR), 2, Kiseleff Ave., 011345 Bucharest, Romania

<sup>3</sup> „Al. I. Cuza” University of Iași, Department of Geology, 20A Carol I Blv., 700505 Iași, Romania; e-mail: mib@uaic.ro; tabara\_d@yahoo.com; gabriel.chirila@uaic.ro

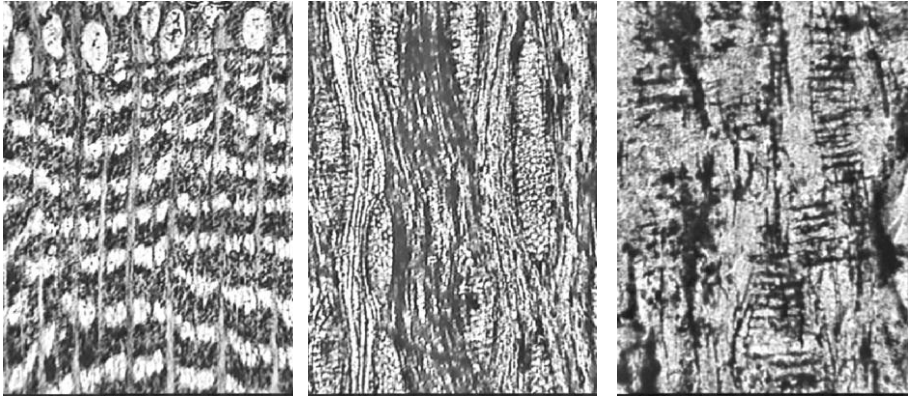
**Keywords:** fossil wood, petrified forest, palaeoenvironment, palaeoclimate.

The studied material, presented as petrified trunks, is part of the Collection of the Geological Museum of the “A.I. Cuza” University (AICU) of Iași. Some small samples were either kindly offered by our colleagues, interested to know more about those samples, or collected over the previous years, during field trips carried out in the Moldavian Area. Standard-oriented polished sections were prepared and studied under a reflecting-light microscope, in order to observe special structural details and to identify the original tree.

*Taxodioxyton sp.*



*Ulmoxylon* sp.



Previous studies on Tertiary fossil wood from the Moldavian Area (between the Eastern Carpathians and Dniester) have been carried out by Cantuniari (1935), Starostin and Trelea (1969, 1984), Lupu et al. (1984, 1985, 1987, 1993), and Iamandei et al. (2001, 2005, 2006, 2007, 2008). All the taxa identified contributed to the reconstruction of the fossil vegetation; more information was added through the results of the studies on fossil plant parts, i.e. leaf or fruit imprints, pollen and spores. Such studies also contributed to the interpretation of the palaeoenvironment and the palaeoclimate.

As a result of the present study, the taxonomic identification of two new specimens of Conifers and Dicots has been carried out; the figures of the present paper include microphotographs of the two new identified species: *Taxodioxylon* and *Ulmoxylon*.

## References

- Cantuniari, St., 1935. Étude d'un fragment de bois silicifié de Lipcani (Bessarabie). *Compte Rendus des séances de l'Institut Géologique de Roumanie*, **XX**, 83–96.
- Iamandei, S., Iamandei, E., Ionesi, V., 2001. Sarmatian fossil wood from Fălticeni-Suceava region. *Analele Științifice ale Universității "Al. I. Cuza" Iași, Geologie*, **XLVII**, 235–240.
- Iamandei, S., Iamandei, E., Lupu, A.I., 2001. Some fossil woods in the Iași Botanical Garden Collection. *Analele Științifice ale Universității "Al. I. Cuza" din Iași, Geologie*, **XLVII**, 267–274.
- Iamandei, S., Iamandei, E., Lupu, A.I., 2008. Late Miocene oak trees from Solești - Vaslui. (Fossil woods from Iași Botanical Garden Collection). *Rev. Roum. de Géologie*, **44**, 57–61.
- Iamandei, S., Iamandei, E., Obadă, T., 2006. Sarmatian Petrified wood within "Bursuc Flora" (Moldova Rep.) *Acta Paleontologica Romaniaae*, **V**, 223–229.
- Iamandei, S., Iamandei, E., Obadă, T., Lungu, A., Postolachi, V., 2006. New Sarmatian Petrified Woods from Moldova Rep. *Acta Paleontologica Romaniaae*, **VI**.
- Iamandei, S., Iamandei, E., Țibuleac, P., 2001. Fossil Wood from Coal-layer "B" of Volhinian Formation in Leucuşești - Fălticeni area. *Analele Științifice ale Universității "Al. I. Cuza" din Iași, Geologie*, **XLVII**, 211–218.
- Lupu, I. A., 1984. Étude d'un bois de chêne fossile provenant de l'interfleuve Siret-Moldova (Roumanie). *Bul. Grad. Bot. Iași, (Special Issue "150 ani de la înființarea Muzeului de Istorie Naturală")*, 369–372.
- Lupu, I.A., 1993. Datarea unor lemne subfosile din aluviunile râului Moldova. *Bul. Grăd. Bot. Iași*, **4**, 369–372.

- Lupu, I.A., Roman, F., 1985. *Cercis siliquastrum* L., specie lemnoasă termofilă prezentă în flora postglaciară din bazinul Siretului inferior. *Analele științifice ale Universității "A.I. Cuza", Biologie*, **XXXI**, 79–82.
- Lupu, I.A., Roman, F., 1987a. La datation approximative de certain bois sous-fossiles de *Quercus*, *Faxinus* et *Alnus* des alluvions du cours inférieur du Siret. *Culeg. Studii & Art. Biol.*, **3**, 175–185.
- Lupu, I.A., Roman, F., 1987b. Espèces ligneuses thermophiles de la flore tardiglaciaire et postglaciaire du cours inférieur de la Rivière Putna, dans le dép. de Vrancea. *Culeg. Studii & Art. Biol.*, **3**, 186–193.
- Lupu, I.A., Roman, F., Agherghinei, I., 1984. Încercare de datare pentru arbori subfosili de *Ulmus* L., extrași de sub aluviunile văii Siretului inferior. *Bul. Grad. Bot. Iași, (Special Issue "150 ani de la înființarea Muzeului de Istorie Naturală")*, 373–378.
- Starostin, G., Trelea, N., 1969. Paleoxylologic study of flora from the Pliocene of Moldova (In Romanian). *Analele științifice ale Univ. "Al. I. Cuza" Iași, Biologie*, **XV/2**, 447–451.
- Starostin, G., Trelea, N., 1984. Contributions à l'étude du genre *Quercus* du Sarmatien de Moldavie (Roumanie). *Bul. Grad. Bot. Iași, (Special Issue "150 ani de la înființarea Muzeului de Istorie Naturală")*, 317–322.

## NEW PETRIFIED WOODS FROM SOLEȘTI, ROMANIA

STĂNILĂ IAMANDEI<sup>1</sup>, EUGENIA IAMANDEI<sup>2</sup>

<sup>1</sup> National Geological Museum (IGR), 2, Kiseleff Ave., 011345 Bucharest, Romania;  
e-mail: iamandei@gmail.com

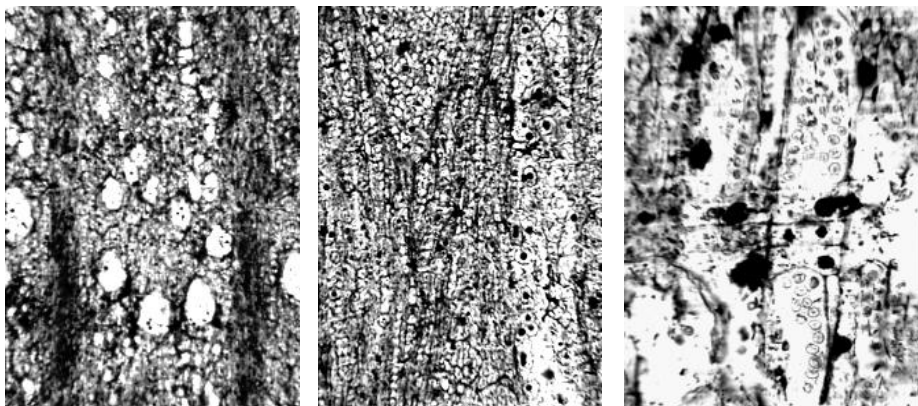
<sup>2</sup> Geological Institute of Romania, 1, Caransebeș Street, 012271 Bucharest, Romania

**Keywords:** Sarmatian, oak-forest, petrified wood, paleoenvironment, paleoclimate.

Over the last years, a collection of petrified woods coming from Solești, Vaslui County, housed by the “A. Fătu” Botanical Garden in Iași, was studied (Iamandei et al., 2001, 2008). Seven large trunks were properly exhibited close to the administrative building; recently, we found them moved to another location, without any protection. All of them represent morphospecies of fossil *Quercus* (oak).

During a recent field trip in the Solești area, we identified the place of their origin and we also found new samples; by extending the research to other perimeters, we discovered new specimens, which were studied and identified as species of Dicots and Conifers. This fact increases the initial number of taxa considered within the Sarmatian oak forest of the Solești area, and shows its mixed mesophytic character. Nevertheless, *Quercus* remains the dominant taxon in numerous other points where Sarmatian plant remains have been described (Starostin and Trelea, 1969, 1984; Givulescu, 2001).

*Quercoxylon* sp.



## References

- Givulescu, R., 2001. Contributions to the knowledge of flora and vegetation of the Tertiary in the extracarpathian area of Romania. *Studia Universitatis Babeş-Bolyai, Geologia*, **XLVI**/2, 5–21.
- Iamandei, S., Iamandei, E., Lupu, A.I., 2001. Some fossil woods in the Iaşi Botanical Garden Collection. *Analele Ştiinţifice ale Universităţii "Al. I. Cuza" din Iaşi, Geologie*, **XLVII**, 267–274.
- Iamandei, S., Iamandei, E., Lupu, A.I., 2008. Late Miocene oak trees from Soleşti - Vaslui. (Fossil woods from Iasi Botanical Garden Collection). *Rev. Roum. de Géologie, Acad. Rom.*, **44**, 57–61.
- Starostin, G., Trelea, N., 1969. Paleoxylologic study of flora from the Pliocene of Moldova (In Romanian). *Analele ştiinţifice ale Univ. "Al. I. Cuza" Iaşi, Biologie*, **XV**/2, 447–451.
- Starostin, G., Trelea, N., 1984. Contributions to the study of *Quercus* genera from the Sarmatian of Moldova (Romania) (In French). *Bul. Grăd. Bot. Iaşi (Issue "150 ani de la înfiinţarea Muzeului de Istorie Naturală")*, 317–322.

## THE RELATIONSHIP BETWEEN THE SARMATIAN AND QUATERNARY FORMATIONS FROM THE PĂCURARI AREA (IAȘI, ROMANIA)

VIOREL IONESI<sup>1</sup>, FLORENTINA PASCARIU<sup>1</sup>

<sup>3</sup> „Al. I. Cuza” University of Iași, Department of Geology, 20A Carol I Blv., 700505 Iași, Romania; e-mail: vioion@uaic.ro

**Keywords:** *Foraminifera*, *Mollusca*, Sarmatian, Quaternary, Formation with *Cryptomacra*, Iași, Păcurari.

During the execution of a foundation for a six-floor building in the Păcurari area (Iași), we took micropaleontological and lithological samples, and we collected fauna from the artificial outcrops or from the soils taken from the drilling operations carried out with this occasion.

From a lithological point of view, the material found in the artificial outcrops (over 8m high) and in the drillings (5m deep) consists mostly of clay deposits with a sand-gravel layer (20 – 30cm thick), and other millimeter-sized interlayers of sand. Generally, the colour of these deposits ranges from yellow to grey.

The main criterion used in separating Sarmatian formations from the Quaternary formations was the presence of the *Cryptomacra pesansensis* Mayer-Eymar taxon. The first occurrence of this taxon was noticed at a depth of over 6m from the soil surface.

In the Sarmatian deposits, apart from *Cryptomacra pesansensis* (Mayer-Eymar), we identified foraminifera (*Porosonion subgranosus subgranosus* (Egger), *Porosonion subgranosus umboelata* (Gerke), *Porosonion martkobi* (Bogdanowicz), *Elphidium macellum* (Fichtel et Moll), *Nonion bogdanowiczi* Voloschinova, *Quinqueloculina akneriana* (d’Orbigny), Mysid statoliths, ostracods etc. The fossils were found both in yellow and grey clays.

Generally, the Quaternary deposits are barren or very poor from a faunistic point of view. Nevertheless, we identified some Quaternary samples with rich microfaunistic content, like those from the Sarmatian; this can be explained by a resuming of microfauna sedimentation during the Quaternary landslides. We presume that during these landslides, the fragile valves of *Cryptomacra pesansensis* (Mayer-Eymar) did not resist, and, as a result, their presence was not reported.

The occurrence of the landslides is also confirmed by the sliding surface that we identified in the artificial outcrop.

In addition to the sliding planes from the outcrop, a discordant surface, which is overlain by a gravel-sand level, has been identified. Given that this level is approximately

1m above the first occurrence of the *Cryptomactra pesanseris* taxon, we believe that it can represent the boundary between the Sarmatian and the Quaternary formations.

## CALCAREOUS NANNOFOSSIL FLUCTUATION RELATED TO THE OCEANIC ANOXIC EVENT 2 (OAE2)

MIHAELA-CARMEN MELINTE-DOBRINESCU<sup>1</sup>, MARCOS-ANTONIO LAMOLDA<sup>2</sup>

<sup>1</sup> National Institute of Marine Geology and Geo-ecology, 23-25 Dimitrie Onciul Street, RO-024053, Bucharest, Romania; e-mail: melinte@geoecomar.ro

<sup>2</sup> Universidad de Granada, Facultad de Ciencias, Departamento de Estratigrafía y Paleontología, Avda. de Fuentenueva s/n18002 Granada, Spain; e-mail: mlamolda@ugr.es

**Keywords:** calcareous nannoplankton, diversity and abundance, Cenomanian-Turonian boundary anoxic event, Tethys.

A significant biotical turnover accompanied the deposition of the Oceanic Anoxic Events (OAE2), mirrored in the diversity and composition of the marine planktonic faunas and floras, especially of calcareous nannofossils. This group of organisms is very sensitive to palaeoenvironmental changes, being affected both by oceanic and atmospheric modifications.

We have studied the fluctuation pattern of calcareous nannofossils in sections from the European Tethys Realm (Southern Carpathians, Romania, and NE Spain), during the OAE2, anoxic event that is placed within the Cenomanian-Turonian boundary interval. The above-mentioned interval is known as one of the major Cretaceous carbon-cycle perturbations that included warming, sea-level rise and extinction.

In the studied sections, below the OAE2 interval, the calcareous nannoplankton assemblages contain a diversified and abundant nannoflora, dominated by two taxa, namely *Watznaueria barnesiae* and *Eprolithus floralis*, both known to be solution-resistant forms. In fact, these two nannofossils represent around 50 % of the encountered nannofloras.

An increase in the abundance of *Biscutum constans* was noticed just below the interval that contains the positive excursion of the  $\delta^{13}\text{C}$  isotope, which marks the beginning of the OAE2. This nannofossil is known as a fertility proxy, blooming under mesotrophic conditions of surface waters.

At the beginning of the OAE2, in both studied sections, peaks of *Zeugrhabdotus erectus* reflect changes in the primary productivity of the surface waters, from a mesotrophic setting (prior to the OAE2) towards an eutrophic setting (at the debut of the OAE2), preceding the instauration of an anoxic regime.

The bloom of *Zeugrhabdotus erectus* is followed by another bloom, of *Biscutum constans*, towards the lower part of OAE2. This trend presumably indicates high fertility

episodes, but also cooling intervals, as the nannofossil *Biscutum constans* seems to be more related to cooler-surface waters.

Above the interval that contains blooms of nannofossil high fertility proxies, a significant increase of the dinoflagellate genus *Thoracosphaera* was recorded within the middle part of the OAE2. This nannofossil event, synchronous with the occurrence of scarce nannofossil assemblages, of low abundance and diversity, is linked to the establishment of stressful marine conditions, together with a high nutrient supply in surface waters.

Blooms of *Thoracosphaera*, often called the “disaster” taxon, were identified during several critical intervals of our planet’s history, i.e. from the base of the Danian, just above the Cretaceous/Paleogene boundary event, or across the Paleocene/Eocene boundary interval. The *Thoracosphaera* bloom is coincident, in the studied sections, with the temporary disappearance of the two high fertility proxies – *Biscutum constans* and *Zeugrhabdotus erectus*. Upwards, within the upper part of the OAE2 intervals, three successive blooms of the nannofossil *Eprolithus floralis* were remarked, possibly related to the instauration of an oligotrophic palaeoenvironment.

Hence, the critical interval of the turnover is characterised by the successive blooms of *Cyclagelosphaera margerelii*, *Biscutum constans*, *Eiffellithus turriseiffelii*, *Zeugrhabdotus erectus*, *Thoracosphaera* spp., *Erolithus floralis*, and *Prediscosphaera* spp., followed by secondary peaks of *Biscutum constans* and *Thoracosphaera* spp. No record of high-productivity nannofossils such as *Zeugrhabdotus erectus*, *Cyclagelosphaera margerelii* or *Biscutum constans* was made towards the top of the interval containing the OAE2.

Above the OAE2 interval, a first step of ecosystem recovery was noticed. Thus, the nannofloral abundance and diversity increased, but it did not reach the record of the interval placed below the instauration of the OAE2.

As elsewhere, the Cenomanian/Turonian boundary interval, where the OAE2 is placed, is characterized by a significant nannofloral turnover. As a result, five last occurrences (LO) and four first occurrences (FO) were noticed. The recorded nannofossil events are the successive LOs of *Corollithion kennedyi*, *Axopodorhabdus albianus*, *Lithraphidites acutus* and *Rhagodiscus asper*, followed by the FOs of *Quadrum intermedium*, *Eprolithus octopetalus*, *Quadrum gatneri* and *Eiffellithus eximius*.

Concerning the productivity of surface-waters, this seems to be increased through a short period preceding the critical turnover episode, but quickly the ecosystem becomes starved as blooms are less relevant, and mesotrophic or eutrophic components, e.g. *B. constans* and *Z. erectus*, disappear from the record. These nannofloral events indicated the fact that the calcareous nannofloral ecosystems show evident signs of instability.

To sum up, the record of nannofossils shows a turnover coeval with the OAE2, with a stressed environment whose critical scenario is coincident with anoxic and disoxic facies, synchronous with the minimum of the absolute abundance and diversity of nannofossils, and blooms of the disaster dinoflagellate genus *Thoracosphaera*. The floral turnover was extended during the entire OAE2, with 5 extinctions and 3 taxon appearances. Even within a reduced time scale, it is still possible to distinguish short periods of relative high productivity linked to the temporary instauration of mesotrophic and eutrophic environments. Therefore, the surface-water productivity seems to be increased during a

short period preceding the critical turnover episode, but quickly the ecosystem becomes starved, as blooms are less relevant, and mesotrophic or eutrophic components, e.g. *B. constans* and *Z. erectus*, disappear from the record. The relative high percentages of *Thoracosphaera* spp. could indicate restricted or somehow critical environmental conditions prior to the development of the OAE2, leading to the occurrence of calcareous nanofloral ecosystems with evident signs of instability.

## **PALYNOLOGY, PALYNOFACIES AND TOTAL ORGANIC CARBON FROM SILURIAN DEPOSITS OF THE DNESTR BASIN (PODOLIA, UKRAINA)**

LEONARD OLARU<sup>1</sup>, DANIEL ȚABĂRĂ<sup>1</sup>, MARINA CHIHAIA<sup>1</sup>

<sup>1</sup>“Al. I. Cuza” University of Iași, Department of Geology, 20A Carol I Blvd., 700505 Iași, Romania; e-mail: tabara\_d@yahoo.com

**Keywords:** palynology, palynofacies, TOC, Silurian, Podolia.

Silurian deposits characterized by different facies features are present in the Podolia region, located in the W-SW of the East European Platform. The Silurian sedimentary basin is located in the vicinity of the Teisseyre-Tornquist (TTZ) mobile area. The Dnestr River and its tributaries flow across the sedimentary paleobasin, outcrops showing the sequence of Silurian deposits.

Our studies were made on two important areas where the Silurian deposits have been identified:

- the Zhvanets locality area, located on the left side of the Dnestr River (N 48° 32' 47,9''; E 26° 29' 13,3'').

- the Smotrich brook (a left-side tributary of the Dnestr River) area, near the Kamenets Podolsky locality (N 48° 40' 26,5''; E 26° 34' 10,4'')

The lithostratigraphic log of the Silurian from the studied region is represented by two formations:

1. the Malynivtsy Formation, of Middle-Upper Ludlowian age.

2. the Skala Formation, of Upper Ludlowian age (Kaljo et al., 2007; Fig. 1).

The **Malynivtsy Formation** from the Podolia region covers the entire development area of a sedimentary paleobasin from the eastern part of the Teisseyre – Tornquist area (Skompski et al. 2008).

An outcrop in which we identified this formation is the Smotrich brook (near the medieval fortress of Kamenets Podolsky), where we intercepted nodular limestones which gradually pass into dolomites and dolomitic marl (Fig. 2). These rocks are attributed to the Sokol Members of the Malynivtsy Formation, which has a thickness of approximately 50 m. The fauna contained by this formation consists of tabulate and rugose corals, stromatoporoids and brachiopods characteristic for a Ludlowian age (Tsegelnjuk et al., 1983).

From the studied outcrop we collected samples PS112 and PS114 from nodular limestones with stromatoporoids and corals, and sample PS111 from the basis limestone of

the outcrop. Sample PS113 comes from dolomitic marl interbedded between the limestones (Fig. 2).

The palynological analysis of these rocks emphasized specific Ludlowian chitinozoan species, such as: *Eisenackitina bohémica* Eis., *E. lagenomorpha* Eis., *Urnochitina urna* Eis., *Angochitina echinata* Eis., *Eisenackitina barrandei* Paris & Kříž, *Belonechitina latifrons* Eis., *Angochitina* cf. *tsegelnjuki* Paris & Grahn or *A. elongata* Eis. (Table 1). The frequency of these species is high enough, the former being present in all the samples analyzed.

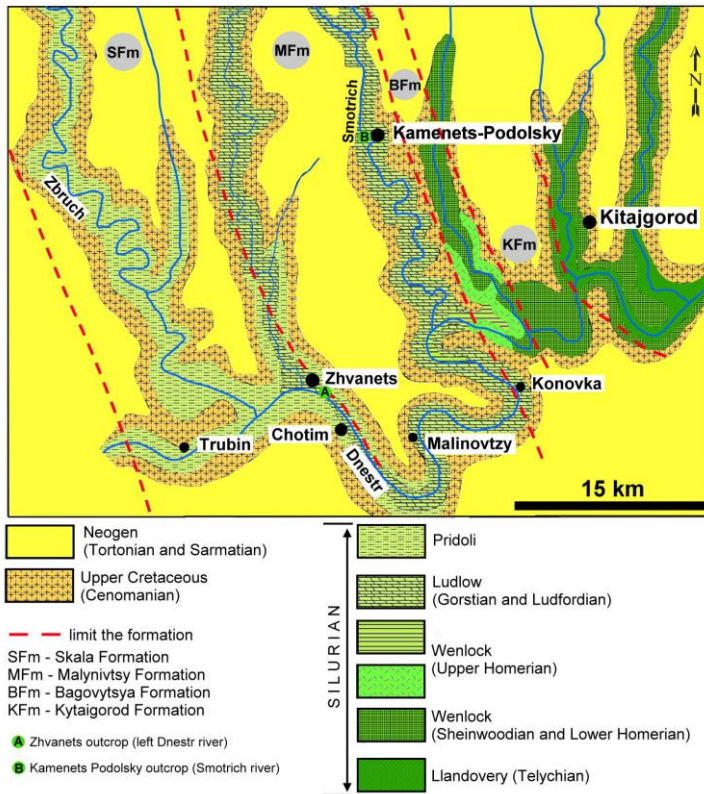


Fig. 1 Silurian geological sketch map of Podolia outcrop along the Dnestr tributaries (after Teller, 1997; Skompski et al., 2008; modified).

Among acritarchs, only the *Dictyotidium* cf. *dictyotum* Eis. species is present (PS114). Miospores are represented by a few species, such as *Ambitisporites avitus* Hoffmeister and *Archaeosporites chlus* (Cramer) Rich & Lister, which were noticed only in sample PS112.

The **Skala Formation**. The boundary between the Skala and Malynivtsy Formations was established in the location of the samples taken from Zhvanets, on the left side of the Dnestr River (Fig. 1). The samples collected by us (RN103 - RN109) come from the location "at pillbox" (about 300 m downstream the Dnestr River, from the bridge at Chotin). They are attributed to the Isakivtsi Member (RN105, RN106) from the basis of the Skala Formation, and the Prygorodok Upper Member (RN103 - RN109) (Fig. 3).

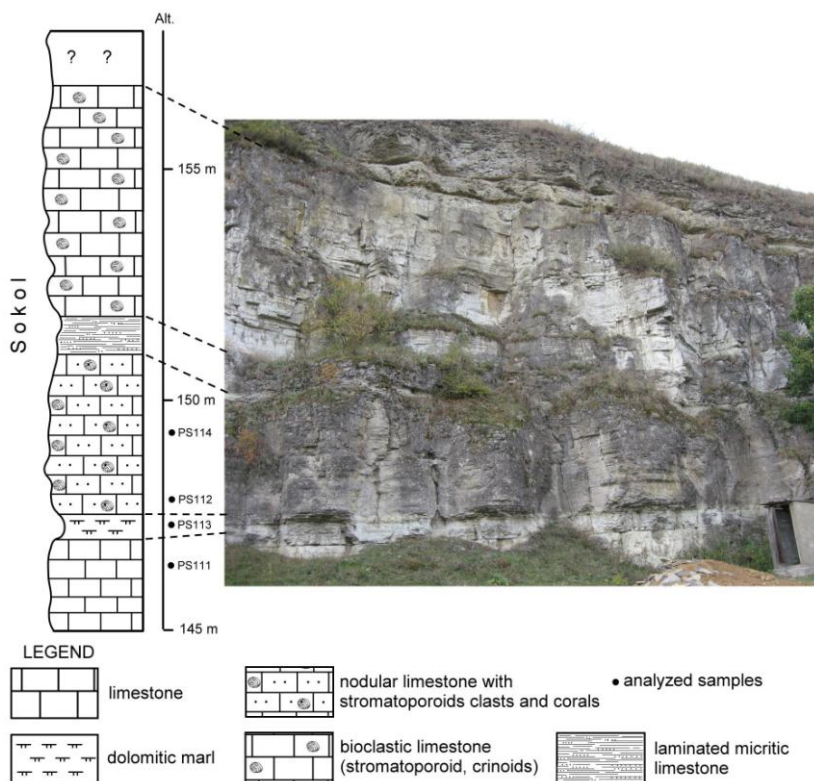


Fig. 2 Lithological log of a Sokol Member, Smotrich brook outcrop, near the Kamenets Podolsky locality.

The Isakivtsi Member (from the base) outcrops on a thickness of 10-15 m, consisting of hard gray dolomite.

The Prygorodok Member is represented by gray dolomite, which is hard and arranged in 10 - 15 cm - thick plates with polygonal dry traces on the contact surfaces. These rocks alternate with blackish dolomitic marl, with a schistuos aspect. Towards the top of this lithological member, the thickness of dolomite interbedded in the plates decreases. The thickness of this member is of about 20-23 m.

Table 1 Taxonomical list with the palynomorphs from analyzed samples.

Age of lithological formations and members analyzed	Middle Ludlow					Upper Ludlow					
	Malynivtsy Form.					Skala Formation					
	Sokol Member			Isakivtsi Memb.		Prygorodok Memb.					
	Smotrich brook					Dnestr river left side					
Location and number of collected samples and name of identified species	Kamenets Podolsky					Zhvanets					
	PS 111	PS 112	PS 113	PS 114	RN 105	RN 106	RN 104	RN 109	RN 107	RN 108	RN 103
<b>Chitinozoans</b>											
<i>Belonichitina latifrons</i> Eisenack	x	x									
<i>Conochitina turis</i> Taugourdeau	x										
<i>Eisenackitina lagenomorpha</i> Eisenack	x		X	x	x	x		x	x	x	x
<i>Eisenackitina bohémica</i> Eisenack	x	x	X	x		x		x			
<i>Eisenackitina</i> aff. <i>Elongata</i> Eisenack	x										
<i>Urnochitina urna</i> Eisenack	x	x	X					x		x	
<i>Angochitina echinata</i> Eisenack	x	x	X								
<i>Eisenackitina barrandei</i> Paris & Kříž	x	x		x					x	x	
<i>Eisenackitina philipi</i> Laufeld	x					x					
<i>Angochitina</i> cf. <i>tzegehnjuki</i> Paris & Grahn	x	x									
<i>Angochitina elongata</i> Eisenack	x		x								
<i>Conochitina</i> cf. <i>parvicola</i> Taugourdeau		x									
<i>Angochitina</i> cf. <i>echinata</i> Eisenack		x									
<i>Rhabdochitina magna</i> Eisenack			x								
<i>Linochitina klonkensis</i> Paris & Laufeld			x			x		x			x
<i>Eisenackitina</i> cf. <i>barrandei</i> Paris & Kříž			x								
<i>Eisenackitina elongata</i> Eisenack						x			x	x	
<i>Eisenackitina</i> cf. <i>lagenomorpha</i> Eisenack						x					
<i>Eisenackitina</i> cf. <i>philipi</i> Laufeld						x					
<i>Clathrochitina aquitanica</i> Taugourdeau						x					
<i>Sphaerochitina</i> cf. <i>sphaerocephala</i> Eisenack							x				
<i>Fungochitina kosoviensis</i> Paris & Kříž								x			
<i>Vinnalochitina suchomastensis</i> Paris & Laufeld								x			
<i>Angochitina</i> cf. <i>capillata</i> Eisenack								x			
<i>Conochitina</i> cf. <i>decepiens</i> Taug. et De Jekhowski								x			
<i>Eisenackitina intermedia</i> Eisenack											x
<b>Acritarchs</b>											
<i>Dictyotidium</i> cf. <i>dictyotum</i> (Eis.) Eisenack				x							
<i>Clypeolus tortugaides</i> (Cramer) Miller et al.					x						
<i>Pterospermella onondagensis</i> Deunff							x				
<i>Pterospermella hermosita</i> Cramer							x				
<i>Eupoikilofusa</i> cf. <i>striatifera</i> (Cramer)								x			x
Cramer											
<i>Moyeria</i> cf. <i>cabottii</i> (Cramer) Miller & Eames								x	x		
<i>Leiofusa striatifera</i> Cramer											x
<b>Miospores</b>											
<i>Ambitisporites avitus</i> Hoffmeister		x			x	x	x		x		
<i>Archaeozonotriteles chlus</i> (Cramer)		x			x	x			x		
Richardson & Lister											
<i>Cymbosporites cattilus</i> Allen						x					x

The age of the lower part of the Skala Formation is Upper Ludlowian.

As in analyzed samples from the Smotrich Brook, chitinozoans such as *Eisenackitina lagenomorpha* Eis. prevail (Table 1). In addition to this species, *Linochitina klonkensis* Paris & Laufeld, *Eisenackitina barrandei* Paris & Kříž, *E. elongata* Eis., *E. bohémica* Eis., and *Urnochitina urna* Eis. have also been identified.

Between the two formations analyzed, Malynivtsy and Skala, no important differences have been noticed between the chitinozoan assemblages identified, both formations being of Ludlowian age. The frequency of species from the Skala Formation is much lower than that of those identified in samples from the Malynivtsy Formation. The richest sample is

PS111, with 10 species, followed by samples PS112 and PS113, all of the Ludlowian from the Smotrich Brook. Some samples from the left side of the Dnestr River (RN106, RN109) contain 8 species of chitinozoans, the rest being poor in fossil content, but the acritarch microflora is more abundant in all the samples from the Dnestr River. We determined the following acritarch species: *Pterospermella onondagensis* Deunff, *P. hermosita* Cramer, *Eupoikilofusa* cf. *striatifera* Cramer, *Moyeria* cf. *cabottii* (Cramer) Miller & Eames, and *Leiofusa striatifera* Cramer (Table 1).

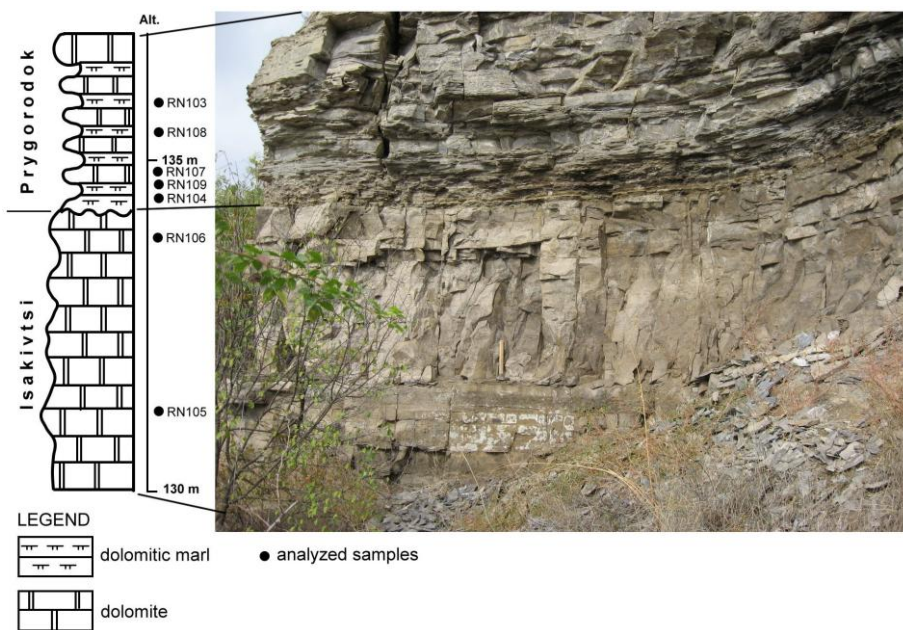


Fig. 3. Lithological section of Isakivtsi and Prygorodok Members (Skala Formation), left Dnestr River, south of the Zhvanets locality.

Miospores, like acritarchs, are more frequent in the samples from the Dnestr River, with the following species: *Ambitisporites avitus* Hoffmeister, *Archaeozonotriletes chlus* (Cramer) Rich & Lister, and *Cymbosporites cattilus* Allen (Table 1). Generally, it can be noticed that miospores and acritarchs are less represented than chitinozoans, in both locations of the two formations analyzed.

### Interpretation of paleofacies and paleoenvironment

The biostrome complex with stromatoporoids, corals and crinoids that appears on the Smotrich brook indicates a shallow water marine environment with sandbanks, barrier coral reefs and a flat bottom. Moreover, the presence of ostracods in limestone deposits indicates

an environment between intra- and supratidal zones, characteristic for the Silurian from marginal marine areas (Skompski et al., 2008).

The limestone lithological complex was formed directly from reef biostromes, or through the accumulation of reworked limestone particles resulting from erosion.

Near the shore, through changes in the marine level, lagoon and swamp deposits with shallow water were formed, where a mixed vegetation, of both marine and continental types, has developed.

Benthic organisms (chitinozoans) and planktonic ones (acritarchs) developed under these paleofacies and paleoenvironment conditions.

Chitinozoans, which prevail in the samples analyzed, prefer open marine or lagoon areas with fine sands, limestone or marl clay on the bottom, and shallow, clear and transparent water, where they receive light and food. Acritarchs, as planktonic organisms, prefer marine photic zones, near the shore, where they can obtain their food. Miospores prove the presence of swamp facies, where the primitive plants which accepted such environment conditions lived.

Dolomitic marl and limestone deposits indicate, through their thickness, long periods of open sea or lagoon, in which these lithological formations were deposited. The presence of interbedded dolomitic marl, sometimes sandstone, indicates fluctuations in water depth, through a phenomenon of subsidence.

The analysis at depth of the marine bottom development (Kaljo et al., 2007) indicated that, predominantly in limestone and dolomite rocks, a Sokol Member of a Malynivtsy Formation (Ludlowian) was formed under environmental conditions of relatively deep marine waters, with a marine bottom composed of fine sediments, where chitinozoans were predominant. Our analysis of the Smotrich brook confirmed this hypothesis.

During the sedimentation of the Isakivtsi and Prygorodok Members from the Skala Formation (Upper Ludlowian), the environmental conditions changed. The marine waters were shallow, with episodes of change in sedimentary facies, from a limestone-reef facies to a lagoon and swamp facies. Therefore, thinner limestone deposits alternate with marl deposits (Prygorodok Member). In this case, the organisms have diversified: apart from chitinozoans, less abundant acritarchs, miospores, along with a larger amount of Amorphous Organic Matter, have also developed.

## **Conclusion**

Our palynological and palynostratigraphical studies were focused on geological formations of Middle-Upper Ludlowian age from the Dnestr River basin (Zhvanets locality area) and the Smotrich Brook (Kamenets Podolsky locality).

The rocks analyzed are generally limestone with dark dolomitic marl interbedded. These rocks belong to the Sokol Member of the Malynivtsy Formation, and the Skala Formation with the Isakivtsi and Prygorodok Members.

Calcareous rocks of the Smotrich Brook contain a rich fauna, with stromatoporoids, tabulate and rugose corals, and brachiopods, which give them a knotty aspect. Limestones on the left side of the Dnestr River contain fauna consisting of brachiopods, ostracods and dasycladaceae algae, typical for a lagoon facies. The Prygorodok Member found in this

outcrop contains a sequence of limestones and dolomitic marls, indicating an alternation of a lagoon with a swamp facies. This member lacks fauna.

The chitinozoan assemblage is typical for the Middle and Upper Ludlowian, with species such as *Eisenackitina lagenomorpha*, *E. barrandei*, *E. bohémica*, *Linokitina klonkensis*, *Urnochitina urna* etc. (Table 1). Acritarchs, less represented in the palynological assemblage, are identified only through a few species of the genera *Pterospermella*, *Eupoikilofusa*, *Dictyotidium*, and *Leiofusa*. Miospores are also less represented, being identifiable through the genera *Ambitisporites* and *Archaeozonotrites*, which are characteristic of the late Silurian. They come from the first land plants that evolved in a marsh environment.

The end of the Silurian is a significant step towards the reduction of acritarch and chitinozoan species across all the regions of the globe, therefore their number in the samples analyzed by us is not very high.

The palynofacies of the rocks analyzed consist of an Amorphous Organic Matter (AOM) that sometimes constitutes the majority, in association with black and brown phytoclasts (in small amounts). Optically, the largest amount of organic matter could be observed in samples PS113 and PS114, taken from the outcrop of the Smotrich Brook. In sample PS113, the content of AOM (approximately 90-95%) shows a brown color, being grouped in agglomerations, while in sample PS114 black and brown phytoclasts, probably coming from a continental source, prevail. These phytoclasts have small sizes. The samples of the Dnestr River are low in organic matter, with the exception of samples RN106 and RN108, in which light-colored particles of AOM could be observed in association with black phytoclasts.

The present paper contains analyses of Total Organic Carbon (TOC), an index for the possible hydrocarbon potential from Silurian rocks. Of the two outcrops studied, the only rocks in which a TOC content was established are dolomitic marls arranged in plates from the Dnestr River outcrop (Skala Formation, Prygorodok Member) (Fig. 3). The TOC content varies between 1,108 to 1,224, indicating a fair/good hydrocarbon potential.

## References

- Kaljo, D., Grytsenko, V., Martma, T., Mõtus, M.A., 2007. Three global carbon isotope shifts in the Silurian of Podolia (Ukraine): stratigraphical implications. *Estonian Journal of Earth Sciences*, **56/4**, 205–220.
- Laufeld, S., 1974. Silurian chitinozoa from Gotland. *Fossils and Strata*, **5**, Universitetsforlaget, Oslo, p.130.
- Nikiforova, O.I., Predtechensky, N.N., Abushik, A.F., Ignatovitch, M.M., Modzalevskaya, T.L., Berger, A.Y., Novoselova, L.S., Burkov, Y.K., 1972. Opornyj razrez silura i nizhnego devona Podolii. *Nauka, Leningrad*, 1–262.
- Olaru, L., Brânzilă, M., Țabără, D., 2006. Geological and palynological contribution to the Silurian from the north of Moldavian Platform. *Analele Științifice ale Universității „Al. I. Cuza” Iași, Geologie*, **LII**, 67–84.
- Paris, F., Grahn, Y., 1996. Chitinozoa of the Silurian-Devonian boundary sections in Podolia, Ukraine. *Palaeontology*, **39/3**, 629–649.
- Skompski, S., Łuczyński, P., Drygant, D., Kozłowski, W., 2008. High-energy sedimentary events in lagoonal successions of the Upper Silurian of Podolia, Ukraine. *Facies*, **54**, 277–296.
- Teller, L., 1997. The subsurface Silurian in the East European Platform. In: A. Urbanek and L. Teller (eds), *Silurian Graptolite Faunas in the East European Platform: Stratigraphy and Evolution*. *Palaeontologia Polonica*, **56**, 7–21.

Tsegelnjuk, P.D., Gritsenko, V.P., Konstantinenko, L.I., Ishchenko, A.A., Abushik, A.F., Bogoyavlenskaya, O.V., Drygant, D.M., Zaika-Novatsky, V.S., Kadlets, N.M., Kiselev, G.N., Sytova, V.A., 1983. The Silurian of Podolia. The guide to excursion. Naukova Dumka, Kiev, 1–224.

**TAXONOMIC, QUANTITATIVE AND PALEOECOLOGICAL ANALYSES OF BENTHIC FORAMINIFERAL ASSEMBLAGES OF QUATERNARY MARINE SEDIMENTS IN SERIK, EAST ANTALYA, TURKEY**

SEYDA PARLAR<sup>1</sup>, MUHİTTİN GORMUS<sup>2</sup>

<sup>1</sup> Selcuk University, Faculty of Engineering and Architecture, Department of Geological Engineering, 42075, Konya, Turkey; e-mail: sparl@selcuk.edu.tr

<sup>2</sup> Suleyman Demirel University, Faculty of Engineering and Architecture, Department of Geological Engineering, 32260, Isparta, Turkey; e-mail: muhittin@mmf.sdu.edu.tr

**Keywords:** fossil assemblages, quantitative, environment, foraminifera, Serik, taxonomic.

In the present study, foraminiferal fossil assemblages of marine sediments were analyzed in detail and taxonomic, quantitative and paleoecological analyses were made in order to obtain environmental information. For this purpose, a total of 144 drilling samples and 76 surface samples were used. The fossil contents, dominant species and assemblages were determined for all samples. A total of 56 species and 109 genera were determined from these samples. According to grain-size analysis, the average grain size of the sediments was determined. The marine sediments are generally characterized by unchoosive coarse to thin sands of sediments. Three types of shell-wall composition were observed; porcellanaceous and hyaline foraminifera were widely recorded, whereas *agglutinated* foraminifera were recorded only rarely. The AMS dating (radiocarbon analysis) method was carried out on marine sediments. Planktic and benthic foraminifer contents were compared. Apart from this, the relationship of ground grain sizes with the organisms was discussed. Consequently, all the data obtained was used for environmental interpretation.

## LITHO- AND BIO-STRATIGRAPHY OF THE PORAVA SECTION (NORTHERN ALBANIA)

MENSI PRELA<sup>1</sup>

<sup>1</sup> Polytechnic University of Tirana, Faculty of Geology and Mining, Earth Sciences Department, Tirana, Albania; e-mail: mensiprela@yahoo.com

**Keywords:** biostratigraphy, radiolarian chert, Jurassic, continental margin.

The Porava section belongs to the western continental margin of the Mirdita ocean. This section is located in Northern Albania, about 1 km south-southwest from the Porava village (Puka town). From bottom to top, the lithostratigraphic column of the Porava section consists of the following:

- A terrigenous detritic sequence (Verrucano type) probably of P-?Tr<sub>1</sub> age (thickness of about 10 meters);
- Grey yellow thickly bedded dolomitic limestones (about 30-40m thick);
- Reddish nodular limestone, related to the Anisian age, with ammonites (thickness of about 3-4 meters); in some rare areas, these limestones are accompanied by rift related volcanics;
- Reddish radiolarian cherts belonging to the Anisian/Ladinian boundary (thickness of 3-4 meters);
- Pelagic cherty limestones (about 150m thick). These deposits are related to the Middle Triassic-Lower Jurassic age, based on conodonts and *Involutina liassica* (Xhomo et al., 2008). At this level, inserted layers of turbiditic limestone are also present.
- This succession is topped by radiolarian cherts (about 12 meters thick) and conformably overlaid by a mélange of the block-in-matrix type.

In this section, the samples collected for the analyses of radiolaria belong to the level of radiolarian cherts, situated on the top of the section. The samples PM1 (10 cm from the mélange of the block-in-matrix type) and PM4 (6 meters from the mélange) yielded the following radiolarian assemblages:

Sample PM1: *Eucyrtidellum unumaense* s.l. YAO, *Parvicingula* sp., *Stichocapsa japonica* YAO, *Theocapsomma cordis* KOCHER, *Tricolocapsa plicarum* YAO, *Tricolocapsa* sp. M. (Baumgartner et al., 1995), *Unuma* sp. A. (Baumgartner et al., 1995), *Williriedellum* sp. A. sensu Matsuoka. The age of PM1 is related to 5-6 U.A.Z. (Late Bajocian-Early Bathonian to Middle Bathonian) due to the coexistence of *Theocapsomma cordis* and *Unuma* sp. A. (Baumgartner et al., 1995).

Sample PM4: *Eucyrtidiellum semifactum* NAGAI & MIZUTANI, *Eucyrtidiellum unumaense* s.l. (YAO), *Parvicingula dhimenaensis* s.l. BAUMGARTNER, *Theocapsomma cordis* KOCHER, *Tricolocapsa conexa* MATSUOKA. The age of PM4 is related to 5-7 U.A.Z. (Late Bajocian-Early Bathonian to Late Bathonian-Early Callovian) due to the presence of *Theocapsomma cordis* and *Eucyrtidiellum semifactum*.

In conclusion, the age of radiolarian cherts situated on the top of this section can be related to ages ranging from the Late Bajocian-Early Bathonian to the Middle Bathonian.

## References

- Baumgartner, P.O., Bartolini, A.C., Carter, E.S., Conti, M., Cortese, G., Danelian, T., De Wever, P., Dumitrica, Jud, R., Gorican, S., Guex, G., Hull, D., Kito, N., Marcucci, M., Matsuoka, A., Murchez, B., O., Dogherty, L., Savarz, L., Vishnevskaja, V., Widz, D., Yao, A., 1995. Middle Jurassic to Early Cretaceous radiolarian of Tethys: occurrences, systematics, biochronology. *Mém. Géol., Lausanne*, **23**, 1013–104.
- Xhomo, A., Kodra, A., Shallo, M., 2008. Harta Gjeologjike e Shqiperise (shkalle 1: 200 000). Studim monografik.

## JURASSIC RADIOLARIAN CHERTS IN THE EASTERN PERIPHERAL UNITS OF THE ALBANIAN OPHIOLITES

MENSI PRELA<sup>1</sup>

<sup>1</sup> Polytechnic University of Tirana, Faculty of Geology and Mining, Earth Sciences  
Department, Tirana, Albania; e-mail: mensiprela@yahoo.com

**Keywords:** biostratigraphy, radiolarian chert, Jurassic, Pelagonian microplate.

Albanian tectono-stratigraphic terranes include continental margin sequences, rift assemblages and ophiolites. The eastern peripheral units belong to the Korabi zone, which represents the western part of the Pelagonian microplate (Kodra and Gjata, 1989; Shallo, 1992). From west to east, 3 tectonic units can be distinguished on the Albanian territory, namely the Mbasdeja unit, the Gjallica unit, and the Korabi unit; they belong to the Korabi-Pelagonian microplate. The relationships between the ophiolites and the western flank of the Korabi-Pelagonian microplate (Mbasdeja unit) are characterized by mainly subvertical tectonic contacts.

In the Mbasdeja unit, radiolarian cherts lie above the Middle Triassic-Lower Jurassic pelagic cherty limestones (the Hallstat facies) and are topped by an olistostrome formation (mélange of the block-in-matrix type). This mélange shows a fabric that includes blocks ranging from several centimeters to several hundred of meters in size set in a well foliated shaly matrix. The lithology of the blocks includes rocks derived from both continental and oceanic environments.

The formations of the Gjallica unit are well-spread over the Albanian territory, from north to south. In these formations, radiolarian cherts lie over the Upper Triassic-Lower Jurassic, platformal, thick-bedded, massive limestones. In some places, condensed Lower/Middle Jurassic, nodular limestones are also present at the bottom of the radiolarian cherts. Radiolarian cherts are topped by ophiolitic breccias.

In the Korabi unit, the radiolarian cherts have a limited exposure. They lie above the cherty, pelagic limestones, and are covered by a mélange of the block-in-matrix type.

The age of radiolarian chert formations in the above-mentioned tectonic units can be related to the Middle Jurassic.

### References

- Kodra, A., Gjata, K., 1989. Evolucioni mesozoi i Albanideve te brendshme, fazat e riftezimit dhe zgjerimi oceanik Mirditor. *Bul. Shkencave Gjeologjike*, 45–65.

Shallo, M., 1992. Geological evolution of the Albanian ophiolite and their platform periphery. *Geologische Rundschau*, **81**/3, 681–694.

## RADIOLARIAN ASSEMBLAGES IN THE DERSTILA SECTION (ALBANIA)

MENSI PRELA<sup>1</sup>

<sup>1</sup> Polytechnic University of Tirana, Faculty of Geology and Mining, Earth Sciences  
Department, Tirana, Albania; e-mail: mensiprela@yahoo.com

**Keywords:** biostratigraphy, radiolarian assemblages, Jurassic, limestone.

The radiolarian assemblages described in the present paper come from the Derstila section, which belongs to the continental formations located at the western periphery of the Shpati ophiolitic unit. This perimeter is situated at about 30-40 meters north of the Derstila village (near the Elbasani town, Albania). The section consists of the following:

1. Platformic Upper Triassic-Lower Jurassic limestones;
2. Red, nodular, Lower-Middle Jurassic limestones (with *Involutina liassica*);
3. Red radiolarian cherts (about 1.5 meters thick)
4. "Blocks in matrix" mélange.

Samples D 0.44 and D 0.44/1 are taken from level (3), at 0.2m and 0.9m from the contact with the nodular limestones. The samples have been etched with hydrofluoric acid at different concentrations. In the present paper we adopted the radiolarian zonation based on Unitary Association Zones (U.A.Z) proposed by Baumgartner et al. (1995). The complete faunal assemblages from the examined samples are as follows:

Sample D 0.44: *Tricolocapsa plicarum* ssp. A. (Baumgartner et al., 1995); *Transhssum maxwelli* gr. (PESSAGNO); *Tricolocapsa plicarum* s. l. YAO; *Zhamoidellum ventricosum* DUMITRICA; *Sethocapsa* sp. cf. *S. funatoensis* AITA; *Protunuma* (?) *ochiensis* MATSUOKA; *Unuma* sp. A. (Baumgartner et al., 1995); *Eucyrtidiellum unumaense pustulatum* BAUMGARTNER.

Sample D 0.44/1: *Parvicingula cappa* DUMITRICA; *Transhssum maxwelli* gr. (PESSAGNO); *Unuma* sp. A. (Baumgartner et al., 1995); *Zhamoidellum ventricosum* DUMITRICA; *Tricolocapsa plicarum* s. l. YAO; *Protunuma* (?) *ochiensis* MATSUOKA; *Sethocapsa* sp. cf. *S. funatoensis* AITA.

The age of Sample D 0.44 is 5 U.A.Z. or Late Bajocian-Early Bathonian due to the coexistence of *Protunuma* (?) *ochiensis*, *Eucyrtidiellum unumaense pustulatum* and *Tricolocapsa plicarum* ssp. A.

The age of Sample D 0.44/1 is 5-6 U.A.Z. or Late Bajocian-Early Bathonian to Middle Bathonian due to the presence of *Protunuma* (?) *ochiensis* and *Unuma* sp. A. (Baumgartner et al., 1995).

The age of the Derstila section can be related to the Late Bajocian-Early Bathonian to Middle Bathonian.

## References

- Baumgartner, P.O, Bartolini, A.C., Carter, E.S., Conti, M., Cortese, G., Danelian, T., De Wever, P., Dumitrica, Jud R., Gorican, S., Guex, G., Hull, D., Kito, N., Marcucci, M., Matsuoka, A., Murchez, B.O, Dogherty, L., Savarz, L., Vishnevskaja, V., Widz, D., Yao, A., 1995. Middle Jurassic to Early Cretaceous radiolarian of Tethys: occurrences, systematics, biochronology. *Mém. Géol., Lausanne*, **23**, 1013–1043.

## RARĂU SYNCLINE (EASTERN CARPATHIANS, ROMANIA) – REGION TYPE FOR NEW MESOZOIC TAXA AND PARATAXA

ILIE TURCULEȚ<sup>1</sup>, PAUL ȚIBULEAC<sup>1</sup>

<sup>1</sup> „Al. I. Cuza” University of Iași, Department of Geology, 20A Carol I Blv., 700505 Iași, Romania; e-mail: paul.tibuleac@uaic.ro

### Abstract

Throughout the decades of research, the Mesozoic fauna of both par-autochthonous and allochthonous rocks which build the sedimentary infill of the Rarău Syncline has provided holotypes for new taxa/parataxa. These will all be recorded in the present paper, followed by several critical annotations.

**Keywords:** Rarău Syncline, Mesozoic new taxa and parataxa, inventory.

### Introduction

The Rarău Syncline represents a structural unit of the so-called Median Dacides (*sensu* Săndulescu, 1984) developed in the northern part of the Eastern Carpathians.

It has of a crystalline basement, a Mesozoic sedimentary infill (topped by the Early Cretaceous wildflysch), and magmatic rocks (known only as allochthonous blocks). Only Bucovinian Nappes (par-autochthonous rocks) and Transylvanian Nappes (allochthonous rocks) occur here.

### Historical overview of the paleontological research

Beginning with the second half of the XIX<sup>th</sup> century, the paleontological valencies of the Mesozoic rocks from the Rarău Syncline were emphasized by the geologists from the famous “geological school of Vienna.” Mojsisovics (1874, 1882, and 1893), Uhlig (1900), Volz (1903), Kittl (1912) have added valuable data on new fossil taxa. Furthermore, Romanian researchers have outlined the outstanding paleontological heritage of the Rarău Syncline, new taxa being described by Patrușiu (1965) and Turculeț (a series of papers from 1964 until today); the Polish researcher Elżbieta Morycowa (1971) has also brought new data about the corals.

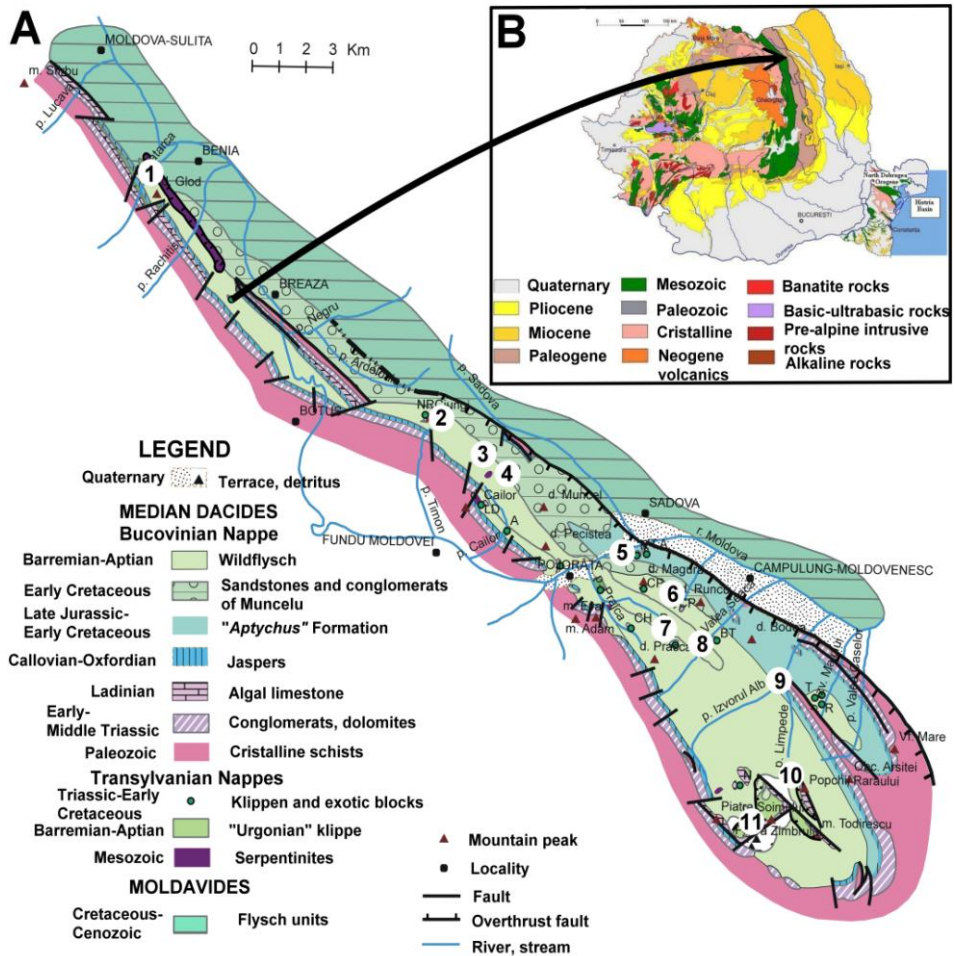


Fig. 1 Geological setting of the Rarău Syncline. A Geological map of the Rarău Syncline (after Turculeț, 1971) and the main fossiliferous outcrops: 1. Tătarca stream; 2. Timon klippe - Ciungi, Fundu Moldovei; 3. Măceș hill - Sadova; 4. Pârâul Cailor klippe; 5. „Aptychus” Formation - Pojorâta; 6. Runc hill; 7. Prașca klippe; 8. Valea Seaca stream; 9. Izvorul Alb stream; 10. Rarău Plateau. 11. Piatra Zimbrului. B. Geological map of Romania (after Gheucă, internet).

### New taxa and parataxa described

Specimens of algae, foraminifera, poriferans, cnidarians, cephalopods, aptychi, gastropods, bivalves and brachiopods have been selected as holotypes for the description of

new species/para-species and subspecies/para-subspecies. Moreover, after the studies performed on several fossil taxa from the Rarău Syncline, new genera–para-genera/subgenera – para-subgenera were established. By summarizing the data, tens of new genera/subgenera and species/subspecies were described throughout the decades of research. The most important groups will be summarized further on.

Fossil cnidarians (colonial corals) are common records in the Mesozoic klippen and exotic blocks of the Early Cretaceous wildflysch, but they cannot be observed in properly exposed patch reefs. Several authors, such as Volz (1903) and Morycowa (1971) have emphasized the taxonomical importance of the coral fauna from the Rarău Syncline. The corals belong to *Zoantharia* – *Scleractinia* and *Octocoralia* – *Alcyonida*. Volz (1903) described 9 new species, Early Cretaceous in age, from the Izvorul Alb, Valea Seacă and Izvorul Malului streams, and also from the Rarău Plateau. Morycowa (1971) also published an important paper on the coral records collected by Patrulius from the Early Cretaceous rocks of the Rarău Syncline. The author encountered several of Volz's species, but also described four new genera (*Pseudomyriophyllia*, *Hidnophoromeandraraea*, *Trochoidomeandra*, and *Pseudopolytremacis*) and 22 new species/subspecies from the Izvorul Alb and Valea Seacă streams, the Rarău Plateau, and Pietrele Albe. Generally, the taxa were largely adopted by paleontologists, being cited in many parts of the world (Poland, Serbia, Spain, Mexico, Afghanistan etc.).

Ammonoids have been studied extensively throughout the years, but only one new genus and subgenus have been described from the Rarău Syncline rocks.

Firstly, Mojsisovics (1893) proposed the *Eremites* genus, having as type species *Trachyceras orientale*, also a new species signaled by Mojsisovics (1882) from the Transylvanian Triassic of the Pârâul Cailor Klippe. The genus was included in Moore's Treatise (1957), and has been cited in different part of the world (e.g. Laws, 1982; Hallam and Wignall, 2000).

The new subgenus of *Harpophylloceras* and *Bucoviniceras*, respectively, was proposed by Turculeț (1970 a), who noticed the fact that the species *Harpophylloceras bucovinicus* (UHLIG, 1900) shows features that are intermediary between those of the *Harpophylloceras*, *Meneghiniceras*, and *Juraphyllites* genera. Uhlig's species being quite strange and rare, the validity of the subgenus was not disputed until now.

The new described ammonoid species, of Triassic and Early Jurassic ages, are more numerous.

From the Triassic, Mojsisovics (1882) described several new prolecanitids and ceratitids (all of them from the Pârâul Cailor Klippe), more frequently cited in the papers being *Sageceras walteri*, (e. g. Tatzreiter, 1986; Cataloi-Dobrudja – Turculeț, 2009). Several authors adopted the Simionescu's point of view, who considered *S. walteri* synonymous with the relative *S. haindingeri* HAUER.

Subsequently, Turculeț (2000) selected specimens for two new species – *Paratibetites carpathicus* and *Halorites excentricus* – from the Timon/Timen Klippe (Tabel 2), which are stored in the Museum of Paleontology and Stratigraphy of the Department of Geology of the “Alexandru Ioan Cuza” University of Iași. *Paratibetites carpathicus* is of a special interest because it shows an evidence for the connection between Carpathian and Himalayan areas at this stratigraphic level – the Norian.

Uhlig (1900) described five new ammonite species, from the Sinemurian of the Prașca Klippe (Transylvanian Nappes). As was mentioned above, „*Rhacophyllites*” (= *Harpophylloceras* or *Juraphyllites*) *bucovinicus* requires special attention as regards its morphological convergences with *Harpophylloceras eximius*, *Meneghiniceras lariense*, and *Juraphyllites mimatensis*. The other four species belong to the *Paltechioceras* genus, the most widely quoted being *Paltechioceras romanicus*. Several authors (e.g. Blau, 1998) considered the other *Paltechioceras* species (*P. waechneri*, *P. boesei*, and *P. herbichi*) synonymous of *P. romanicus*. The main part of Uhlig’s collection from the Prașca Klippe is stored in the Museum of Geological Survey of Austria (Vienna).

A new species of *Leioceras* (*L. giganteum*) was described by Turculeț (1982) from the Aalenian blocks which are to be found near the Pojorâta village (Transylvanian Nappes). It was described based on a single specimen of big dimensions which preserves only the body chamber, and consequently the validity of the taxon is not very precise. The specimen is hosted in the Museum of Paleontology and Stratigraphy, Geological Department, „Alexandru Ioan Cuza” University of Iași.

New sub-paragenera, para-species and para-subspecies of *aptychi* were described by Turculeț along last four decades in a series of papers. Several syntheses of his papers were published in the last part of that period (Turculeț, 1994; Turculeț, 2000). Thus, Turculeț (1994) proposed four new sub-paragenera for *Lamellaptychus*, following the basic arrangements of the ribs as in the types of Trauth and Gasiorowsky: *Beyrichilamellaptychus*, *Lamellosulamellaptychus*, *Thorolamellaptychus*, *Didayilamellaptychus*; moreover, Turculeț and Avram (1995) used the name *Beyrichipunctaptychus* for several species of punctaptychi with trajectories of the ribs similar to those in *Beyrichilamellaptychus*. This proposal represents “a new stage in the classification of aptychi” (Méchová et al., 2010), and several authors assumed it (with several additions and changes), trying to adopt and improve a new systematics of aptychi (Méchová et al., 2010).

Turculeț (1964, 1971, 1973, 1989, 1992-1993, and 2000) described as well twelve new para-species and para-subspecies from the so-called “*Aptychus*” Formation of the Rarău Syncline, which are the valid para-taxa encountered in the different regions of the Alpine chain.

*Bivalves* are, likewise, common mollusks in the Mesozoic rocks of the Rarău Syncline. A highly important contribution was Turculeț’s proposal for the five new subgenera of *Daonella* (*Mousonella*, *Grabella*, *Arzelella*, *Loemelella*, *Pichlerella*), which was largely adopted by researchers. This proposal (Turculeț, 1972) emerged as a result of the studies performed on the daonellid from the klippen of Pârâul Cailor, Pietra Șoimului, Pietra Zimbrului, and Izvorul Malului stream.

Using the same reasoning as in the *Daonella* case, and based on the fossil records from Rarău Syncline, Turculeț adopted the same sub-genera separation for the halobiids and monotids: *Dispersehalobia*, *Styrihalobia*, *Austrihalobia*, *Carlyhalobia*, *Halorihalobia*, *Norihalobia*, *Salihalobia*, *Radihalobia*, and *Rugohalobia* (Turculeț, 2002), respectively *Scutimonotis*, *Ochotimonotis*, *Zabaikalimonotis*, and *Salimonotis* (Turculeț, 2005). The bivalve collected during the time by Turculeț are stored in the same museum of University „Al. I. Cuza” Iași.

Furthermore, several new bivalve species/subspecies were proposed by Mojsisovics (1874; Kittl 1912; and Turculeț (1990, 1998, 2002, 2004 a, b, 2005) from the Triassic of the Pârâul Cailor Klippe, Izvorul Malului stream, Runc hill Klippe, and from the Middle Jurassic autochthonous rocks of the Tâtarca stream. In addition to the new described bivalve taxa, it should be mentioned that there were not made ontogenetic observations on the morphological changes, the specimens being sometimes incomplete or not well preserved; consequently, the new named taxa could be affected by a future taxonomical revision in this dynamic process which is the systematics of fossil fauna.

## Conclusions

The Mesozoic sedimentary rocks of the Rarău Syncline provided a rich and attractive Mesozoic fauna. Throughout the decades of research, foreign and Romanian paleontologists have selected specimens as holotypes for tens of new species-subspecies/para-species, and, consequently, as type species for over twenty-five genera/para-genera. Given their importance, several outcrops were protected by law (Pârâul Cailor, the “Aptychus” Formation at Pojorâta), and many others were proposed for protection (Timon Klippe–Fundu Moldovei), Runc hill, Piatra Zimbrului and Prașca klippen, Tâtarca stream etc).

Future taxonomical revisions could affect the new taxa and para-taxa from the Mesozoic sedimentary rocks of the Rarău Syncline, as well future researches could enlarge the amount of the new described taxa. This inventory represents different stages in the knowledge of the fossil fauna and in the paleontological researches, in general.

## References

- Blau, J., 1998. Monographie der Ammoniten des Obersinemurium (Lotharingium, Lias) der Lienzer Dolomiten  
Blau, J., 1998. Monographie der Ammoniten des Obersinemurium (Lotharingium, Lias) der Lienzer Dolomiten (Österreich): Biostratigraphie, Systematik und Paläobiographie. *Revue de Paléobiologie*, **17** (1), 177–283.
- Hallam, A., Wignall, P.B., 2000. Facies changes across the Triassic–Jurassic boundary in Nevada, USA. *Journal of the Geological Society*, **157**/1, 49–54.
- Kittl, E., 1912. Materialien zu einer Monographie der Halobiidae und Monotidae der Trias. *Res. Wiss. Erf. Balatonsees*, Bd. II, Wien.
- Laws, A.R., 1982. Late Triassic depositional environments and molluscan associations from west-central Nevada. *Palaeogeography, Palaeoclimatology, Palaeoecology*, **37**/2-4, 131–148.
- Méchová, L., Vašíček, Z., Houša, V., 2010. Early Cretaceous ribbed aptychi – a proposal for a new systematic classification. *Bulletin of Geosciences, Czech Geological Survey*, **85**/2.
- Mojsisovics, E., 1874. Über die Triadischen Pelecypoden-Gattungen Daonella und Halobia. *Abhandlungen der K. K. Geologischen Reichsanstalt*, **7**, 1–35.
- Mojsisovics, E., 1882. Die Cephalopoden der Mediterranean Provinz. *Abhandlungen der K. K. Geologischen Reichsanstalt, Wien*.
- Mojsisovics, E., 1893. Die Cephalopoden der Hallstatter Kalke. *Abhandlungen der K. K. Geologischen Reichsanstalt*, **6**/2, 835p.
- Moore, R., (ed.), 1957. *Treatise on Invertebrate Paleontology, Part L. Mollusca 4, Cephalopoda, Ammonoidea*. University of Kansas Press, 490p.
- Morycova, E., 1971. Hexacorallia et Octocorallia du Crétacé inférieur de Rarău (Carpathes Orientales Roumaines). *Acta Palaeontologica Polonica*, **XVI**/1-2, 149p.
- Patruluius, D., 1965. Note sur deux espèces des Chaetetopsis des calcaires urgoniens: Chaetetopsis zonata Patruluius et Chaetetopsis favrei (Deninger). *Dări de seama ale ședințelor*, 25–29.

- Săndulescu, M., 1984. Geotectonica României. Editura Tehnică, București, 336p.
- Tatzreiter, F.v., 1886. Katalog der typen und Abbildungsoriginale Geologischen Bundesanstalt. 4. Teil: Typen Abbildungsoriginale und Belegstücke zu Mojsisovics E. v. (1882): Die Cephalopoden der mediterranen Traisprovinz. Jahrbuch der Geologischen Bundesanstalt, **129/1**, 129–140.
- Turculeț, I., 1964. Stratele cu *Aptychus* din Chiuveta Rarău. Analele științifice ale Universității „Al. I. Cuza“, Geologie, **X**, 47–70.
- Turculeț, I., 1968. Observations sur l'Algue *Globochaete alpina* Lomb. des depots liassiques de la Cuvette de Rarău. Rivista Italiana di Paleontologia e Stratigrafia, **74/4**, 1155–1174.
- Turculeț, I., 1970a. *Bucovinicerias* - un nou subgen de *Phylloceratidae* liasice din Cuveta Rarău. Buletinul Societății de Științe Geologice din R. S. România, **XII**, 149–152.
- Turculeț, I., 1971. Cercetări geologice asupra depozitelor jurasice și eocretacee din Cuveta Rarău-Breaza. Studii tehnice și economice, seria J, **10**, 140p.
- Turculeț, I., 1972. Contribuții la studiul genului *Daonella*, cu privire specială asupra faunei de halobiide ladiniene din regiunea Rarăului. Analele științifice ale Universității „Al. I. Cuza“ Iași, Geologie, **XVIII**, 115–123.
- Turculeț, I., 1973. *Lamellaptychus beyrichi pseudoundocosta* - o nouă subspecie de aptihi din Malmul Cuvetei Rarău-Breaza. Muzeul de Științe Naturale Piatra Neamț, Studii și cercetări, Geologie-Geografie, **II**, 155–157.
- Turculeț, I., 1982. *Leioceras giganteum* - une nouvelle espèce de *Leioceratinae* de l'Aalenien inférieur du Synclinal de Rarău. Analele științifice ale Universității „Al. I. Cuza“. Iași, Geologie, **XXVIII**, 25–27.
- Turculeț, I., 1989. *Punctaptychus monsalvensis divergens* et *Punctaptychus monsalvensis fracto-divergens*, deux sous-espèces nouvelles d'*Aptychus* du Malm du Synclinal de Rarău. Analele științifice ale Universității „Al. I. Cuza“ Iași, Geologie, **XXXV**, 21–23.
- Turculeț, I., 1990. *Leptochondria bucovinensis* - une nouvelle espèce de *Pectinides* neotriasiques du Synclinal de Rarău-Breaza. Analele științifice ale Universității „Al. I. Cuza“. Iași, Geologie, **XXXVI**, 21–28.
- Turculeț, I., 1992-1993. *Punctaptychus punctatus carpathicus*-une nouvelle para-sous-espèce d'*Aptychi* du Malm des Carpates Romaines. Analele științifice ale Universității „Al. I. Cuza“. Iași, Geologie, **XXXVIII-XXXIX**, 259–262.
- Turculeț, I., 1994. Asupra oportunității separării de parasubgenuri în cadrul paragenului *Lamellaptychus* (Cephalopoda, Ammonoidea). Studii și cercetări de Geologie, Geofizică și Geografie, seria Geologie, **39**, 119–126.
- Turculeț, I., Avram, E., 1995. Lower Cretaceous *Aptychus* assemblages in Romania. 1) Svința region (SW Romania). Analele științifice ale Universității „Al. I. Cuza“. Iași, Geologie, **XL-XLI**, 87–112.
- Turculeț, I., 1998. Sur des *Pectinacees* du Jurassique bucovinique de la zone Târnița-Rarău-Breaza (Carpates Orientales). I. ENTOLIIDAE. Studii și cercetări de Geologie, Geofizică și Geografie, seria Geologie, **42**, 91–100.
- Turculeț, I., 2000. *Aptychi* din România. Editura Academiei Române, București, 178p.
- Turculeț, I., 2000a. Date noi privind fauna de amoniți norieni de la Ciungi (Rarău) și valențele ei himalaiene. Studii și cercetări de Geologie, Geofizică, Geologie, seria Geologie, **45**, 127–148.
- Turculeț, I., 2002. Des quelques nouveaux sous-genre appartenants au genre *Halobia* (*Bivalvia*, Triasic). Analele științifice ale Universității „Al. I. Cuza“. Geologie, **XLVIII**, 187–192.
- Turculeț, I., 2004. Paleontologia Triasicului transilvan din Rarău. Editura Arvin-Press, București, 170p.
- Turculeț, I., 2004a. Paleontologia Jurasicului și Cretacicului din Rarău. Editura Junimea, Iași, 221p.
- Turculeț, I., 2004b. La faune norienne de la klippe de Ciungi (Rarău). IV. *Monotidae* (*Bivalvia*). Analele științifice ale Universității „Al. I. Cuza“. Geologie, **XLIX**, 161–166.
- Turculeț, I., 2005. Considérations concernant la structure taxonomique du genre *Monotis* BRONN, 1830 (*Bivalvia*, Triasic). *Acta Palaeontologica Romaniae*, **5**, 477–481.
- Turculeț, I., 2009. New data about the ammonite fauna from the Triassic developed in the Wengen facies at Cataloi (North Dobrudja Orogen). Analele științifice ale Universității „Al. I. Cuza“. Geologie, **LV/2**, 45–49.
- Uhlig, V., 1900. Ueber eine unterliassische Fauna aus der Bukowina. Abhandlungen des deutschen naturwissenschaftlich-medizinischen Vereines für Böhmen „Lotos“, **II/1**, 5–31.
- Volz, W., 1903. Über eine Korallenfauna aus dem Neocom der Bukowina. Beiträge zur Paläontology und Geologie, Österreich-Ungarns und des Orients, **15/1**, 9–30.

## THE SIGNIFICANCE OF SEVERAL UPPER CRETACEOUS MARINE FOSSIL SITES FOR THE GEODIVERSITY OF THE HAȚEG COUNTRY

CAMELIA VĂRZARU<sup>1</sup>, MIHAELA C. MELINTE-DOBRINESCU<sup>1</sup>, TITUS BRUSTUR<sup>1</sup>,  
STEFAN-ANDREI SZOBOTKA, ANDREI BRICEAG<sup>1</sup>

<sup>1</sup> National Institute of Marine Geology and Geo-ecology, 23-25, Dimitrie Onciul Street,  
RO-024053 Bucharest, Romania; e-mail: camelia.cazacu@geoecomar.ro;  
melinte@geoecomar.ro; tbrustur@geoecomar.ro; szobi@usa.net;  
andrei.briceag@geoecomar.ro

**Keywords:** Upper Cretaceous, marine sediments, marine macrofaunas, Hațeg Basin.

The Hațeg Country is a region famous worldwide for the Dinosaur Geopark, which contains many sites of continental macrofaunal assemblages. In particular, it includes one of the latest assemblages of dinosaurs in the world, Late Campanian-Maastrichtian in age, enclosing endemic species (Grigorescu, 1983, 2010; Csiki et al., 2010), known as the "dwarf dinosaurs of Transylvania". Apart from the above-mentioned continental sites, the region exposed Upper Cretaceous marine sites, yielding significant fossil assemblages of fauna and flora (Pop et al., 1973; Stilla, 1985; Grigorescu and Melinte, 2001; Neagu, 2006; Melinte and Bojar, 2008).

In the NW part of the Hațeg Basin, the Upper Cretaceous marine deposits are characteristic for an outer shelf developed up to a deep-water palaeosetting, while in the SE part, the palaeoenvironment of Late Cretaceous age was infralittoral, occurring up to an inner shelf (Melinte-Dobrinescu, 2010). Due to this setting, the Late Cretaceous marine macrofauna-rich assemblages are present only in the SW region of the Hațeg Country.

Our studies revealed that two particular Upper Cretaceous marine exposures in the SE of the Hațeg Basin contain significant macrofaunal assemblages, and could be included as protected palaeontological sites of the Hațeg Country Geopark. These sites are Ohaba-Ponor and Strei.

The Ohaba-Ponor site studied (known also as the Dealul cu Melci from Ohaba-Ponor) is placed aside from the road towards the Ohaba-Ponor village, along a path that follows the right (western) bank of the Ohaba-Ponor brook. The base of the outcrop is composed of the lacustrine-deltaic sandstones of the Federi Formation. This unit is overlain by the Valea Dreptului Formation, which is divided into the following three members: Slatina, Ohaba-Ponor and Coroi.

The oldest deposits of the Slatina Member consist of calcarenites, with rudists and gastropods. The latter macrofaunal group is mainly represented by the taxa of the

*Actaeonella* and *Itruvia* genera (Lupu, 1966), found in a large number, and displaying a good preservation. Other encountered gastropods are *Nerinea incavata* and *Nerinea caucasica*. Rudist taxa, such as *Durania conectens* LUPU 1966, *Eoradiolites triangularis* d'ORBIGNY 1842, *Neocaprina gigantea* GEMMELLARO 1865, *Sauvagesia praesharpei* TOUCAS 1909, *Praeradiolites fleuriau* d'ORBIGNY 1842, *Sphaerulites foliaceus* LAMARCK 1815 and *Sphaerulites astrei* LUPU 1966, are commonly present.

The Slatina Member is overlain by the Ohaba-Ponor Member, which consists of fossiliferous marls, including ammonites, bivalves (mainly inoceramids) and gastropods. Notably, the macrofaunal assemblages contain significant biostratigraphical ammonites, such as *Acanthoceras rhotomagense*, *Acanthoceras jukes-brownei* and *Eucalycoceras pentagonum* (Szasz, 1976), which are index species of the Middle Cenomanian ammonite zones.

The youngest deposits that crop out in the Ohaba-Ponor Site belong to the upper Coroi Member of the Valea Dreptului Formation, being composed of grey-yellowish clays, alternating with thin calcareous sandstones and grey marls. The features of the exposed sequence indicate significant palaeoenvironmental changes that occurred within the Late Albian-Coniacian interval, from a lacustrine setting to an infralittoral-littoral, eventually passing to an outer shelf towards the top.

The site with Rudists from Strei is placed on the right bank of the Strei Valley, upstream its confluence with the Ohaba Valley. This is the single place in the Hațeg Country where marine (infralittoral to littoral) deposits, probably placed in the Campanian-Maastrichtian boundary interval (according to Melinte-Dobrinescu, 2009), occur. Hence, the site contains the youngest Cretaceous marine sediments of the region, overlaying the turbidites of the Pui Formation. The site contains a macrofaunal assemblage unique in the Hațeg basin, mainly enclosing the species *Hippurites gosaviensis* and *Actaeonella gigantea*.

The two above-described sites are representative for the geodiversity of the Upper Cretaceous marine deposits of the Hațeg Country. They are important for the palaeontological heritage of this region, and improve the knowledge on the geological evolution of the Southern Carpathian area.

## References

- Csiki, Z., Grigorescu, D., Codrea, V., Therrien, F., 2010. Taphonomic modes in the Maastrichtian continental deposits of the Hațeg Basin, Romania - Palaeoecological and palaeobiological inferences. *Palaeogeography, Palaeoclimatology, Palaeoecology*, **293**, 375–390.
- Grigorescu, D., 1983. A stratigraphic, taphonomic and palaeoecological approach to a “forgotten land”: the dinosaurs bearing deposits from the Hațeg basin (Transylvania-Romania). *Acta Palaeontologica Polonica*, **28**, 103–121.
- Grigorescu, D., 2010. The Latest Cretaceous fauna with dinosaurs and mammals from the Hațeg Basin - A historical overview. *Palaeogeography, Palaeoclimatology, Palaeoecology*, **293**, 271–282.
- Grigorescu, D., Melinte, M.C., 2001. The stratigraphy of the Upper Cretaceous marine sediments from the NW Hațeg area (South Carpathians, Romania). *Acta Palaeontologica Romaniaae*, **3**, 153–160.
- Lupu, D., 1966. Rudiștii cenomanieni de la Ohaba-Ponor (Bazinul Hațeg). *Studii și Cercetări de Geologie*, **11/1**, 29–38.

- Melinte-Dobrinescu, M.C., 2010. Lithology and biostratigraphy of Upper Cretaceous marine deposits the Hateg region (Romania): Palaeoenvironmental implications. *Palaeogeography, Palaeoclimatology, Palaeoecology*, **293**, 283–294.
- Melinte-Dobrinescu, M.C., Bojar. A-V., 2008. Biostratigraphic and isotopic record of the Cenomanian-Turonian deposits in the Ohaba-Ponor section (SW Hațeg, Romania). *Cretaceous Research*, **29**, 1024–1034.
- Neagu, Th., 2006. Turonian-Lower Senonian planktonic foraminifera from Ohaba-Pui-Ponor area, Hațeg, Romania. In Csiki, Z. (Ed.), *Mesozoic and Cenozoic Vertebrates and Palaeoenvironments, Tributes to the career of Dan Grigorescu*. Editura Ars Docenti, 175–195.
- Pop, G., Neagu, T., Szasz, L., 1973. Senonianul din regiunea Hațegului. *Dări de Seama ale Institutului Geologic*, **VLIII/4**, 95–118.
- Stilla, A., 1985. Géologie de la région de Hațeg-Cioclovina-Bănița (Carpatés Méridionales). *Anuarul Institutului de Geologie și Geofizică*, **66**, 91–179.
- Szasz, L., 1976. Nouvelles espèces d'ammonites dans le Cénomanien de la région de Hațeg (Carpatés Meridionales). *Dări de seamă ale Institutului de Geologie și Geofizică București*, **LXII**, 169–174.

## GEOLOGICAL COLLECTION OF CHEILE BICAZULUI – HĂȘMAȘ NATIONAL PARK

DAN GRIGORE<sup>1</sup>, IULIANA LAZĂR<sup>2</sup>, COSMIN BUTNAR<sup>3</sup>

<sup>1</sup> Geological Institute of Romania, Bucharest, RO-012721, Romania; e-mail: dan1\_grigore@yahoo.com

<sup>2</sup> University of Bucharest, Faculty of Geology and Geophysics, Bucharest RO-010041, Romania; e-mail: iul\_lazar@yahoo.com

<sup>3</sup> Cheile Bicazului-Hășmaș National Park Administration, 537346 Izvorul Mureșului, Romania; e-mail: cosminbutnar@yahoo.com

**Keywords:** geological collection, Cheile Bicazului–Hășmaș, National Park.

In the Geobiohas Project a new geological collection was founded in Cheile Bicazului - Hășmaș National Park (CBHNP) Administrative Headquarters from Izvorul Mureșului locality. These collections comprise 400 samples of rocks and fossils and separately inventoried (45 of rocks and 355 fossils). Many of this were already studied and described in scientific paper or are in work at this moment. All are representing petrographic and palaeontologic heritage of the CBHNP. Are represented different type of rocks and a part of paleontological heritage, from the most important paleontological sites of this Park.

The aim of this collection was that of a well founded patrimony of this area.

The petrographic collection comprises: Hăghimaș Granite, Bârnadu Conglomerate, different limestones from the region and other types of rocks, of different age which are registrated as in the following table.

Inv.	Rock	Age	Location	Observation
G1	Dolerit	-	Piatra Singuratică	Olistolite from wildflysh
G2	Hăghimaș Granite	Palaeozoic	Vereșcheu Valley	From an pit
G3	Sandstone with belemnites	Dogger	Ghilcoș Valley	F5 Site
G4	Quartzite conglomerate	Seisian	Suhardului Valley	(the oldest sedimentary rock from CBHNP)
G5	Carbonaceous sandstone with ammonites	Early Kimmeridgian	Ghilcoș (north)	F2 Site
G6	Limestone with <i>Lacunosella</i>	Early Kimmeridgian	Fagu Oltului Valley	F12 Site

G7	Limestone with crinoids	Kimmeridgian - Tithonian	Suhardul Mic	F26 Site
G8	Limestone with <i>Nerinea</i>	Berriasian	Ghilcoş (northern route)	F29 Site
G9	Limestone with algal nodules	Early Cretaceous	Ghilcoş (northern route)	F28 Site
G10	Jasper (red)	Oxfordian	Piatra Siguratică	F17 Site
G11	Green nodular limestone with ammonites	Early Kimmeridgian	Ghilcoş (north)	F2 Site
G12	Red nodular limestone with ammonites	Early Kimmeridgian	Ghilcoş (west)	F1 Site
G13	Glauconitic sandstone with ammonites and plant remains	Early Tithonian	Ghilcoş (west)	F1 Site
G14	Breccias	Early Liassic	Oii Valley	F Site
G15	Oolith limestone with belemnites	Liassic	Oii Valley	F Site
G16	Dolomite	Anisian	Oii Valley	F Site
G17	Serpentine		Piatra Altarului	G Site
G18	Jasper (green – grey)	?Callovian - Oxfordian	Oii Valley	G Site
G19	Ocular Gneiss		Balan	G Site
G20	Quartzite		Balan	G Site
G21	Limonite (“Klauss Beds”)	Bathonian	Suhard Valley	-
G22	Marls (brawn)	Early Cretaceous	Bicajel Valley	-
G23	Micro-conglomerate	?Cenomanian	Cherec Valley	F Site
G24	Reccifal limestone	Barremian - Aptian	Ghilcoş (north)	F28 Site
G25	Bio-accumulate limestone	Tithonian - Berriasian	Bicaz Gorges	
G26	Marls with <i>Myophoria</i> <i>costata</i>	Werffanian (Triassic)	Lazar resurgence	F Site

The paleontologic specimens from this Collection are representing some of the studied sites, presented in a recent paper (Grigore et Al, 2009); they proceeds from:

- Ghilcoş kimmeridgian ammonites from northern site (F2)
- Ghilcoş kimmeridgian ammonites from western (walls) site (F1)
- Ghilcoş cretaceous reef (F28)
- Liassic from Ghilcoş Valley (F5-6)
- Liassic from Oii Valley (F10)
- Kimmeridgian with *Lacunosella* from Fagu Oltului Valley (F13)
- Berriasian with *Nerinea* from Ghilcoş northern site (F27)
- Aptian from Cherecului Valley (F7)
- Liassic from Licaş Valley (F29)
- Kimmeridgian ammonites from Cheia Valley (“Ciofranca”) (F17)
- Lower Cretaceous (Berriasian – Valanginian) *Nerinea* beds from Cherec.

In the following table are exemplified some of the specimen inventoried here:

Inv.	Species	Max. size	Age	Site
P1	<i>Sowerbicerias tortisulcatum</i> (d'Orbigny, 1840)	60	km	
P2	<i>Calliphyloceras manfredi</i> (Oppel, 1865)	30	km <sub>1</sub>	
P3	<i>Aspidoceras</i> cf. <i>acanthicum</i> (Oppel, 1863)	75	km	
P4	<i>Calliphyloceras manfredi</i> (Oppel, 1865)	34	km	
P5	<i>Lythoceras polycyclum polycyclum</i> Neumayr, 1871	70	km	
P6	<i>Taramelliceras</i> ( <i>T.</i> ) <i>pseudoflexuosum</i> (Favre, 1877)	29	km	
P7	<i>Aspidoceras binodum</i> (Oppel, 1863)	18	km	
P8	<i>Calliphyloceras manfredi</i> (Oppel, 1865)	14	km	
P9	<i>Nebroditis heimi</i> (Favre, 1877)	40	km	
P10	<i>Aspidoceras</i> sp.	12	km	
P11	<i>Taramelliceras</i> cf. <i>pseudoflexuosum</i> (Favre, 1877)	124	km	
P12	<i>Taramelliceras</i> cf. <i>trachinotum</i> (Oppel, 1863)	16	km	
P13	<i>Phylloceras</i> sp.	-	km	
P14	<i>Orthaspidoceras lallerianum</i> (d'Orbigny, 1848)	-	km	F2
P15	<i>Laevaptychus</i> sp.	-	km	
P16	<i>Ardescia</i> sp.	-	km	
P17	<i>Lythoceras montanum</i> (Oppel, 1865)	41	km	
P18	<i>Taramelliceras</i> ( <i>Taramelliceras</i> ) <i>compsum</i> (Oppel, 1863)	151	km	
P19	<i>Orthosphinctes</i> ( <i>Progeronia</i> ) <i>triplex</i> (Quenstedt, 1888)	46	km	
P20	<i>Lythoceras polycyclum polycyclum</i> Neumayr, 1871	106	km	
P21	<i>Nebroditis favaraensis</i> (Gemmellaro, 1872)	34	km	
P22	<i>Calliphyloceras benacense</i> (Catullo, 1847)	60	km	
P23	<i>Sowerbyceras silenum</i> (Fontannes, 1876)	59	km	
P24	<i>Taramelliceras</i> cf. <i>pseudoflexuosum</i> (Favre, 1877)	83	km	
P25	<i>Aspidoceras binodum</i> (Oppel, 1863)	135	km	
P26	<i>Taramelliceras</i> ( <i>T.</i> ) <i>compsum kochi</i> (Herbich, 1878)	96	km	
P27	<i>Taramelliceras</i> cf. <i>platyconcha</i> (Gemmellaro, 1872)	135	km	
P28	<i>Aspidoceras</i> cf. <i>acanthicum</i> (Oppel, 1863)	131	km	
P29	<i>Sowerbyceras silenum</i> (Fontannes, 1876)	40	km <sub>1</sub>	F17
P30-36	<i>Cyclothyris lata</i> (d'Orbigny)	-	br-ap	
P37-40	<i>Cyrtothyris moutoniana</i> (d'Orbigny)	-	br-ap	
P41-56	<i>Trochocyathus conulus</i> (Michelin, 1840)	-	br-ap	
P57	<i>Microphyllia</i> cf. <i>undans</i> (Koby, 1887)	-	br-ap	
P58	<i>Flexigyra patrulei</i> Morycowa, 1971	-	br-ap	F28
P59-60	<i>Actinastrea pseudominima</i> (Koby, 1896)	-	br-ap	
P61-62	<i>Diplogyra lamellosa</i> Eguchi, 1936	-	br-ap	
P63-66	<i>Heliocoenia</i> cf. <i>carpathica</i> Morycowa, 1971	-	br-ap	
P67	<i>Pseudomelania</i> cf. <i>jaccardi</i> Pictet & Campiche,	-	br-ap	
P68-80	<i>Nerinea silesiaca</i> (Ziittel, 1873)	-	be	
P81-94	<i>Lacunosella arolica</i> (Oppel, )	-	km <sub>1</sub>	F13
P95-100	<i>Septaliphoria moravica</i> (Uhlig, )	-	km <sub>1</sub>	
P101-104	<i>Sutneria eumela</i> (d'Orbigny, 1847)	-	km <sub>1</sub>	
P105	<i>Presimoceras</i> sp.	-	km <sub>1</sub>	
P106	<i>Nebroditis</i> cf. <i>agrigeninus</i> (Gemmellaro, 1872)	-	km <sub>1</sub>	F2
P107	<i>Aspidoceras acanthicum</i> (Oppel, 1863)	-	km <sub>1</sub>	
P108	<i>Laevaptychus latus</i> (Parker)	-	km <sub>2</sub>	
P109-110	<i>Lamellaptychus sparsilamellosus</i> Guembel	-	km <sub>2</sub>	
P111	<i>Phylloceras saxonicum</i> Neumayr, 1871	-	km <sub>1</sub>	
P112	<i>Phylloceras consanguineum</i> Gemmellaro, 1872	-	km <sub>1</sub>	
P113	<i>Pygope janitor</i> (Pictet)	-	km <sub>2</sub>	
P114	<i>Phylloceras ptychoicum</i> (Quenstedt, 1845)	-	th <sub>1</sub>	F1

P115	<i>Taramelliceras (T.) cf. trachinotum</i> (Oppel, 1863)	122	km <sub>1</sub>	
P116	<i>Taramelliceras (T.) cf. compsum</i> (Oppel, 1863)	75	km <sub>1</sub>	
P117	<i>Taramelliceras (T.) cf. compsum</i> (Oppel, 1863)	119	km <sub>1</sub>	F1
P118	<i>Taramelliceras (T.) compsum kochi</i> (Herbich, 1878)	54	km <sub>1</sub>	
P119	<i>Calliphylloceras benacense</i> (Catullo, 1847)	75	km <sub>1</sub>	

Many of the paleontologic specimens were already analysed in Geological Institute of Romania and Geological Faculty of Bucharest University laboratories. At this moment in the inventoried CBHNP Collection are included: Upper Jurassic ammonites (studied – Grigore, 2002, 2009a, b), Liassic belemnites, Kimmeridgian and Barremian - Aptian brachiopods (Lazar et al. 2009 and other in work), Barremian - Aptian corals (in work), Jurassic and Cretaceous gastropods (in work), Oxfordian - Tithonian crinoids and Mesozoic bivalves.

Some of the specimens are special for its preservation or other qualities (as dimension, rarity...): specimens of *Sutneria* - only here abundant from all Romanian sites; a huge specimen of *Aspidoceras acanthicum* (Oppel) – over 300 mm in diameter; rare specimens of *Lacunosella*; well preserved specimen of cretaceous corals and others.

This collection serves for future studies and as a public museum, for the area of CBHNP.

### Acknowledgements

This study was financially supported by National Centre for Projects Management (CNMP) in the GEOBIOHAS Project (31-059 CTR/2007).

### References

- Grigore, D., 2002. Formațiunea cu *Acanthicum* din regiunea Lacu Roșu (Msv. Hăghimaș-Carpații Orientali) - posibil hipostratotip al limitei Kimmeridgian – Tithonic. Stratigrafie. Paleontologie. Teză Doctorat, Univ. „Al.I.Cuza” Iași, 347p.
- Grigore, D., 2009. Aulacostephanids species (*Sutneria* genus) from “*Acanthicum* Beds” of Ghilcoș Massif (The Eastern Carpathians – Romania). *Oltenia. Studii și Comunicări, Șt. Naturii, Craiova*, **25**, 366–374.
- Grigore, D., in press. Kimmeridgian – Lower Tithonian Ammonite Assemblages from Ghilcos – Haghimas Massif (Eastern Carpathians – Romania). *Acta Palaeontologica Romaniae, Cluj Napoca*, **7**.
- Grigore, D., Marcu, I., 2009. Aulacostephanids species (*Aulacostephanus*, *Ringstedia*, *Simocosmoceras* and *Gravesia* genera) from “*Acanthicum* Beds” of Ghilcoș Massif (The Eastern Carpathians – Romania). *Oltenia. Studii și Comunicări, Șt. Naturii, Craiova*, **25**, 351–354.
- Grigore D., Lazăr, I., Grasu, C., Gheuca, I., Ciobanete, D., Constantinescu, A., Marcu, I., 2009. Paleontological sites from Cheile Bicazului – Hășmaș National Park. *Oltenia. Studii și Comunicări, Șt. Naturii, Craiova*, **25**, 355–365.
- Lazăr, I., Grigore, D., Sandy, M.R., 2009. Upper Jurassic Brahiopod Assemblages from the Haghimas Montains (Eastern Carpathians, Romania) – Taxonomy, Paleoecology and Palobiogeographical Significance. 9<sup>th</sup> North American Paleontological Convention Abstracts, Cincinnati, **3**, 206.







# **Environmental Geology**



## INFORMATIONAL CHARACTERISTICS IN RATIONALIZATION OF SAMPLING NETWORKS OF SOIL IN ORDER TO ESTABLISH THE HEAVY METALS POLLUTION

LAVINIU APOSTOAE<sup>1</sup>

<sup>1</sup> „Al. I. Cuza” University of Iași, Department of Geology, 20A Carol I Blv., 700505 Iași, Romania; e-mail: laviniu.apostoae@clicknet.ro

**Keywords:** Iași, heavy metals, soil, informational energy, informational entropy, optimal sampling equidistance.

### Introduction

Concentration of heavy metals due to human activities and their impact on the biosphere represent extremely studied processes of the geochemical cycle. Implicitly, the optimization of sampling networks must provide the necessary information with maximum economic efficiency within the limits of acceptable errors (Zorilescu, 1986; de Fouquet, 1997; van Groenigen et al., 2000; Hengl et al., 2003; Lamé et al., 2005; Webster and Oliver, 2007).

### Materials and Methods

#### Investigated area

Being located in northeastern part of Romania, Iași City, which is the second largest city of Romania, was highly industrialized until 1989 due to its metallurgic and heavy equipment industry, chemical industry, pharmaceuticals, textile industry, food industry, energetic industry and furniture industry. Iași City has shown a permanent decrease of the industrial activity during 1991-2010.

Geologically, Iași City belongs to the Moldavian Platform, which, according to Ionesi (1994), is made of a basement and a sedimentary cover (deposits belonging to the Upper Vendian, Palaeozoic, Cretacic, Palaeocene, Eocene, Upper Badenian, Sarmatian and Meotian periods), at which the quaternary deposits are added.

In the studied perimeter, that occupies an area of 25,576 km<sup>2</sup>, protisols (39%), cernisols (38%), anthrisols (9%) and soil complexes (14%) represent the soil type.

#### Sampling and Analysis

In the examined perimeter it was harvested a total of 1,030 soil samples from a depth of 0.00 – 0.30 meters of a quadratic network nodes, whose side has been established empirically to 500 m.

The weight of one sample varies between 1.5 and 2.5 kg.

Once the samples were air-dried and crumbled into fragments < 0.2 mm, there were determined the total heavy metal content through the atomic absorption spectroscopy (AAS Solar type), in air-acetylene flame, in the hydrochloric solution obtained after digestion with a concentrated nitric and perchloric acid mixture (ICPA-Bucharest methodology).

**Statistical treatment**

In order to establish the main characteristics of the populations of heavy metals, we determined the main statistical perimeters, the Pearson correlation coefficients and the rank correlation coefficients.

**Informational characteristics**

In order to optimize the sampling equidistance there were calculated the information entropy, the information energy, the informational center of gravity and relative errors for different sampling equidistances (500 m, 1,000 m, 1,500 m, 2,000 m, 2,500 m, 3,000 m, 3,500 m).

**Informational entropy**

Considering a finite probability field consisting in a complete system of elementary events

$A_1, A_2, \dots, A_n$  with the probabilities  $P_1, P_2, \dots, P_n$  ( $P_i \geq 0, i = 1, 2, \dots, n$  și  $\sum_{i=1}^n P_i = 1$ ),

then the informational entropy (Shannon, 1948; Zorilescu, 1986; Lee, 1998; Baltrunas, Gaigalas, 2004; Mogheir et al., 2004), defined as a measurement of the degree of indeterminacy of a field of probability or as a measurement of the amount of information contained by a finite probability field can be defined as:

$$H = H(P_1, P_2, \dots, P_n) = -\sum_{i=1}^n \log_2 P_i$$

In practice, instead of  $P_i$  probabilities, relative frequencies  $f_i = \frac{n_i}{N}$  will be used, where

$n_i$  are empirical absolute frequencies and  $N$  is the total volume of empirical selection (Zorilescu, 1986).

**Informational energy**

The informational energy (Onicescu, Ștefănescu, 1979; Zorilescu, 1986, Pardo, Menéndez, 1992) of a finite states system (elementary events)  $A_1, A_2, \dots, A_n$ , which are produced with the probabilities  $P_1, P_2, \dots, P_n$  and which verify the conditions  $P_i \geq 0$  și  $\sum_{i=1}^n P_i = 1$  is given by the relation:

$$E = E(P_1, P_2, \dots, P_n) = \sum_{i=1}^n P_i^2$$

In practice, instead of  $P_i$  probabilities, relative frequencies  $f_i = \frac{n_i}{N}$  will be used, where

$n_i$  are empirical absolute frequencies and  $N$  is the total volume of empirical selection (Zorilescu, 1986).

### Informational center of gravity

It characterizes a states system or a system of elementary events that occur with certain probabilities, by coupling the average value of the random variable attached to the system with its informational energy.

### Relative errors

Two sampling networks can be considered equivalent if, within the limit of some acceptable errors, they lead to similar values of informational characteristics.

In order to determine the rational sampling network (Zorilescu, 1986), there are calculated the relative errors  $\delta_z(h_i)$  between the values  $Z(h_i)$  determined for the equidistance  $h_i$  and the value  $Z(h_1)$  corresponding to the initial equidistance  $h_1$  with the relation:

$$\delta_z(h_i) = \frac{|Z(h_i) - Z(h_1)|}{Z(h_1)}$$

and they are compared to an accepted  $\delta_0$  error. If  $\delta_z(h_i) \leq \delta_0$  then the sampling network of  $h_i$  equidistance can be considered equivalent to the initial network of equidistance  $h_1$ .

## Results

### Statistical results

The statistical parameters determined for heavy metal contents from soils of Iași City indicated wide variation fields, the mean values of Zn, Cu, Pb, Ni and Cr contents exceeding the normal values from soils. The variation coefficients had high values, especially for Zn, Pb and Cd. The skewness values especially in case of Zn, Pb, Cd, Ni and Co, indicated the high weight of small contents compared with the total number of studied samples. The evaluation of correlation coefficients has shown very weak links for most of pairs of elements, except Ni and Cr, where a weak positive correlation was found. The correlation coefficient of ranks, which is much less influenced by exceptional samples, indicates significant positive link between Zn-Cu, Zn-Pb and Ni-Cr.

### Informational characteristics results

By determining the values of  $Z(h)$ :

$$Z(h) = \begin{cases} H(h) = -\sum p_i \log p_i \\ E(h) = \sum p_i^2 \\ \bar{x} = \sum p_i f(x_i) \\ V = \frac{\sum p_i [f(x_i) - \bar{x}]^2}{\sum p_i f(x_i)} \end{cases}$$

for different sampling equidistances (500 m, 1,000 m, 1,500 m, 2,000 m, 2,500 m, 3,000 m, 3500 m), the relative errors  $\delta_z(h_i)$  indicated, in the case  $\delta_H(h_i)$  and  $\delta_E(h_i)$  optimal sampling equidistances that range between 500 m (Mn) and 1,500 m (Zn, Cu, Pb, Co, Ni,

Cr) for an accepted error  $\delta_0 = 10\%$ . In the case besides  $\delta_H(h_i)$  and  $\delta_E(h_i)$  there are also used  $\delta_x(h_i)$  and  $\delta_V(h_i)$  as optimization criteria of sampling equidistance, its values record pronounced variations, and this aspect can be confirmed with the presence of exceptional samples.

The criterion of the gravity informational center suggests values around 1,500 m as the optimal sampling equidistances for chemical elements in the soils studied in Iași City.

## Conclusions

Although there were not used the traditional methods of sampling networks optimization, informational characteristics have proved an opportunity to establish reasonable equidistance of soil sampling in order to determine the contents of heavy metals. Thus, it can be considered that the sampling equidistance of 1,500 m is equivalent to the sampling equidistance of 500 m, providing the necessary information with a maximum economic efficiency within the limit of an acceptable error.

## References

- Baltrūnas, V., Gaigalas, A., 2004. Entropy of Pleistocene till composition as an indicator of sedimentation conditions in Southern Lithuania. *Geological Quarterly*, **48** (2), 115-122.
- de Fouquet, C., 1997. Influence of the Estimation Method and Reconnaissance Network on Pollution Quantification. Methodological Study in 2D. In Nicolas (ed.), *Echantillonnage et environnement*. Liège :Cebedoc, 39-63. (in French).
- van Groenigen, J. W., Pieters, G., Stein, A., 2000. Optimizing spatial sampling for multivariate contamination in urban areas. *Environmetrics*, **11**, 227-244.
- Hengl, T., Rossiter, D.G., Stein, A., 2003. Soil sampling strategies for spatial prediction by correlation with auxiliary maps. *Australian Journal of Soil Research*, **41**, 1403-1422.
- Iancu, O.G., Buzgar, N. (main eds.), 2008. *The Geochemical Atlas of Heavy Metals in the Soils of the Municipality of Iasi and the Surrounding Areas*. Editura Universității „Alexandru Ioan Cuza” Iași.
- International Atomic Agency, 2004. *Soil sampling for environmental contaminants*. IAEA-TECDOC-1415.
- Ionesi, L., 1994. *The Geology of the Platform Units and of the North Dobrogean Orogen*. Ed. Tehnică. (in Romanian).
- Lamé, F., Honders, T., Derksen, G., Gadella, M., 2005. Validated sampling strategy for assessing contaminants in soil stockpiles. *Environmental Pollution*, **134**, 5-11.
- Laperche, V., Mossmann, J.R., 2004. *Protocol of sampling of the urban grounds polluted by lead*. BRGM/RP-52928-FR. Mars. (in French).
- Lee, Y.M., 1998. A Methodological Study of the Application of the Maximum Entropy Estimator to Spatial Interpolator. *Journal of Geographic Information and Decision Analysis*, **2**, 2, 243-251.
- Shannon, C.E., 1948. A Mathematical Theory of Communication. *The Bell System Technical Journal*, **27**, 379-423 & 623-656.
- Mogheir, Y., de Lima, M.P., Singh, V.P., 2004. Characterizing the spatial variability of groundwater quality using the entropy theory: I. Synthetic data. *Hydrological Processes*, **18**, 2165-2179.
- Onicescu, O., Ștefănescu, V., 1979. *Elements of Informational Statistics with Applications*. Ed. Tehnică. (in Romanian).
- Pardo, L., Menéndez, M.L., 1992. Informational energy in the sequential design of experiments in a Bayesian context. *Information Sciences*, **64**, 3, 271-283.
- Zorilescu, D., 1986. *Introduction to information geostatistics*. Editura Academiei Republicii Socialiste România. (in Romanian).
- Webster, R., Oliver, M.A., 2007. *Geostatistics for Environmental Scientists*, 2nd Edition. Wiley.

**PRELIMINARY DATA REGARDING THE GEOCHEMICAL DISTRIBUTION OF  
MINOR ELEMENTS IN THE DEALU NEGRU MINE TAILINGS FROM THE  
FUNDU MOLDOVEI AREA, ROMANIA**

SORIN-IONUȚ BALABAN<sup>1</sup>, OVIDIU GABRIEL IANCU<sup>1</sup>, DUMITRU BULGARIU<sup>1</sup>

<sup>1</sup>“Al. I. Cuza” University of Iași, Department of Geology, 20A Carol I Blvd., 700505 Iași, Romania; e-mail: steelkarma@yahoo.com; ogiancu@uaic.ro; dbulgariu@yahoo.com

**Keywords:** mine tailings, minor elements, spatial distribution, pH, Eh.

The objectives of the present study were the following: **(i)** to determine the total contents of minor elements (Cr, Cu, Mn, Zn, Cd, Pb, Co, As, Ni and Fe) in samples of tailings dissolved using HNO<sub>3</sub> and concentrated HClO<sub>4</sub>, **(ii)** to determine the pH of the samples in both aqueous and saline suspensions, **(iii)** to determine the Eh of the samples and **(iv)** to calculate the correlation factors between the minor elements, the pH and Eh.

The studies were conducted on a series of 22 samples collected from the surface of the Dealu Negru mine tailings, Fundu Moldovei area, Romania. The total concentration of minor elements was determined by using Atomic Absorbtion Spectrometry after treating the samples with HNO<sub>3</sub> and concentrated HClO<sub>4</sub> (Borlan and Răuță, 1981). The pH was determined by using the potentiometric method in both aqueous and saline suspensions, while the Eh was determined directly in aqueous solution (Florea et al., 1986; Bloom, 2000). The data obtained up to that point was summed up and projected onto concentration maps and spatial distribution diagrams for each minor element, as well as for the pH and Eh. The concentration maps and 3D-diagrams were built by using Golden Software's Surfer 9.7.543 and Visual Basic scripts applied to it. The 3D surface of the mine tailings was approximated by using the same software. The correlation matrices between the minor elements and the values of the pH and Eh were obtained by using StatSoft's Statistica 8.0.

The results of the study have indicated that, while the concentrations of Zn, Cu, Fe, Pb, Co, Cr, Cd and As tend to increase in the proximity of the top of the mine tailings, the higher concentrations for Ni and Mn correspond to the samples collected from the bottom of the tailings. The highest pH values were also determined for the samples collected from the top of the mine tailings. A possible explanation for this phenomenon would be the presence of a draining pool that dried out some 5 years ago.

The work on which the present paper is based was supported by the European Social Fund in Romania, under the responsibility of the Managing Authority for the Sectoral Operational Programme for Human Resources Development 2007-2013 [grant POSDRU/88/1.5/S/47646].

## References

- Bloom P. R., 2000. Soil pH and the pH buffering. In Sumner, M. (ed.): Handbook of soil science, p. B333-B352. CRC Press, Boca Raton.
- Borlan Z., Răuță C., 1981. Metodologia de analiză agrochimică a solurilor în vederea stabilirii necesarului de amendamente și de îngrășăminte (vol. I și II). Academia de Științe Agricole și Silviculturale a României, ICPA București, Romania
- Florea N., Bălăceanu V., Răuță C., Canarache A. (coord.), 1986. Metodologia elaborării studiilor pedologice (vol. I-III). Academia de Științe Agricole și Silviculturale, I.C.P.A. București, Romania

## EXPERIMENTAL STUDY OF NATURAL ZEOLITES FOR THEIR USAGE IN SOIL REMEDIATION

RAMONA BALINT<sup>1</sup>

<sup>1</sup> Geological Survey of Romania, 012271 Bucharest, Romania; e-mail: balint.ramona@yahoo.com

**Keywords:** zeolites, heavy metals, pollution, ion exchange, pH, molecular sieves.

### Introduction

The aim of the present work is to establish the efficiency of natural zeolites in soil remediation, and is based on an experimental approach under laboratory conditions. In order to achieve it, soil collected from the mining perimeter of Bălan and zeolites from the Dej tuffs, which occur over large areas in the Transilvanian Basin, were used.

The reliability of the study is sustained by: (i) the structural features of zeolites, which enable ion exchanges with the environment and, thus, the extraction of polluting elements from soils and/or waters; (ii) the high regeneration capacity of zeolites after being used in decontamination activities; and (iii) the use of zeolites on a relatively long period of time in various fields, for example in reestablishing the geoecological balance in areas with environmental issues.

### Chemical and structural features of zeolites

Zeolites are tectosilicates with tridimensional structures, constituted of (Si,Al)<sub>4</sub> tetrahedra, every oxygen atom belonging to two adjacent tetrahedra. This structure leads to the formation of a lattice with internal cavities, often called “supercages,” allowing intakes of large radius cations, such as Na<sup>+</sup>, Ca<sup>2+</sup>, K<sup>+</sup>, Ba<sup>2+</sup>, and, rarely, Li<sup>+</sup>, Rb<sup>+</sup> and Cs<sup>+</sup>.

Such channels are usually larger than the size of ions that can penetrate them, allowing the accumulation of organic molecules or inorganic compounds (e.g. SO<sub>2</sub>), and giving zeolites the possibility of acting as ionic filters or as molecular sieves (Bedelean and Stoici, 1984).

The tetrahedral Si:(Si+Al) ratio has a major effect on the properties of zeolites. Thus, the Al-Si substitution (or Fe<sup>3+</sup>-Si) alters the chemistry and the charge of the framework structure and, therefore, changes of the chemistry of the extra-framework cations occur (Bish and Guthrie, 1993).

### Research methodology and techniques

The experiment was carried out in the laboratory, under environmental conditions (T=23±3 °C), on a zeolite sample collected from the Vultureni occurrence (Transilvanian

Basin) and on a soil sample taken from an area of the mining perimeter of Bălan, where a large number of mine shafts were reported; the zeolite and soil samples were prepared in the laboratory and were subjected to analytical investigations.

The preparation of the zeolite sample included two stages: (i) a mechanical preparation, consisting of grinding, mixing, reducing, milling, sieving, by using sieves in the range of 0.43-0.80mm; and (ii) a separation under a strong magnetic field, in order to extract minerals with magnetic properties. For a more efficient extraction, the process was repeated, in order to obtain a non-magnetic fraction that would be pure as possible. The soil sample was submitted to a mechanical preparation only, the class with a diameter smaller than 0.315 mm being used.

The chemical composition of the zeolites used in the experiment (tab. 1) is similar to the theoretical one, where elements such as Al, Si, Na and Ca, as well as Fe<sup>3+</sup>, Mg, and K, are present, pointing out possible substitutions, such as Al–Fe<sup>3+</sup>, Ca–Mg, and Na–K, in the sites of the structural framework.

Tab. 1 Major chemical composition of the zeolite sample (wt.%)

Oxide	SiO <sub>2</sub>	Al <sub>2</sub> O <sub>3</sub>	Fe <sub>2</sub> O <sub>3</sub>	CaO	MgO	K <sub>2</sub> O	Na <sub>2</sub> O
Concentration	66.43	11.36	0.74	6.55	0.47	1.27	1.47

The physical methods of investigation consisted of X-ray diffraction, for the identification of zeolite mineral species that occur in the sample. The analysis revealed a high purity and crystallinity degree, and the presence of a mineral association consisting of thomsonite–mesolite–clinoptilolite (tab. 2).

Tab. 2 Crystallochemical formulas and X-ray diffraction patterns [d(Å)] of the zeolite sample

Mineral	Theoretical formula*	Calculated formula	d(Å)
Thomsonite	NaCa <sub>2</sub> [Al <sub>5</sub> Si <sub>5</sub> O <sub>20</sub> ]·6H <sub>2</sub> O	(Na <sub>0.12</sub> K <sub>0.25</sub> Ca <sub>0.95</sub> Mg <sub>0.27</sub> ) [Al <sub>2.80</sub> Fe <sub>0.17</sub> Si <sub>7.07</sub> O <sub>20</sub> ]·nH <sub>2</sub> O	3.27/3.18/2.86/ 2.79/2.43/2.25/ 2.09/1.95/1.75/ 1.67/1.65
Mesolite	Na <sub>16</sub> Ca <sub>16</sub> [Al <sub>48</sub> Si <sub>72</sub> O <sub>240</sub> ] 64H <sub>2</sub> O	(Na <sub>1.83</sub> K <sub>3.68</sub> Ca <sub>7.03</sub> Mg <sub>1.98</sub> ) [Al <sub>24.87</sub> Fe <sub>1.55</sub> Si <sub>94.31</sub> O <sub>240</sub> ]·nH <sub>2</sub> O	3.08/2.87/2.5/ 2.41/2.34/2.27/ 2.05/1.95/1.75/ 1.68/1.64/1.59/ 1.52
Clinoptilolite	(Na,K,Ca <sub>0.5</sub> ,Sr <sub>0.5</sub> ,Ba <sub>0.5</sub> ,Mg <sub>0.5</sub> ) <sub>6</sub> [Al <sub>6</sub> Si <sub>30</sub> O <sub>72</sub> ] ~20H <sub>2</sub> O	(Na <sub>0.56</sub> K <sub>1.13</sub> Ca <sub>2.16</sub> Mg <sub>0.61</sub> ) [Al <sub>2.55</sub> Fe <sub>0.16</sub> Si <sub>32.17</sub> O <sub>72</sub> ]·nH <sub>2</sub> O	7.9/3.12/3.07/ 2.87/2.73/2.44/ 2.42/2.29

\* after The Canadian Mineralogist (1997)

The experiment consisted of: (i) weighing of soil and zeolite samples and mixing with

doubly distilled water and acid water, in well-determined proportions (tab. 3); (ii) stirring of the mixtures with the stirrer of a pH-meter, 540 GLP, WTW Co. type, 2 hours daily, for 11 days; and (iii) monitoring the ionic exchange between: zeolites and distilled water, zeolites and acid water, soil and distilled water, soil and acid water, soil-zeolites-distilled water, soil-zeolites-acid water; the procedure was carried out by measuring certain parameters (pH, conductivity, total dissolved solids) and highlighting the concentration of heavy metals (Cu, Pb, Zn, Ni) in the above-mentioned solutions.

Tab. 3 Experimental methodology

Solution	Soil (g)	Zeolite (g)	Water (ml)	pH
A	-	0.5	40	5.7
B	-	0.5	40	3.2
C	5	-	40	5.7
D	5	-	40	3.2
E	5	0.5	40	5.7
F	5	0.5	40	3.2

Mixing the samples with doubly distilled water and acid water, respectively, had the purpose of monitoring the changes of the soil sample under simulated common rain (by mixing with distilled water) and acid rain (by mixing with acid water) conditions, and to compare its behaviour in the presence or absence of zeolites. The acid water was prepared by adding a very small volume of 96% H<sub>2</sub>SO<sub>4</sub> to the distilled water; the soil/zeolites ratio was 10:1.

The soil sample has been analysed during previous research regarding the heavy metal pollution in the mining area of Bălan (Balint, 2010). For the considered sample (number 49), analyses of Cu, Pb, Zn and Ni were carried out, and the values are presented in table 4.

Tab. 4 Heavy metal ion concentrations in the analysed soil (Balint, 2010)

Heavy metal	Cu (mg/kg)	Pb (mg/kg)	Zn (mg/kg)	Ni(mg/kg)
Concentration	844.8	252.5	258.2	49.1

The soil sample was analysed using a X-ray fluorescence spectrometer (MINIPAL 4 - PANalytical), and the solutions resulted by mixing the soil and zeolites with distilled water and acid water, respectively, were investigated with an atomic absorption spectrometer, through the graphite furnace technique (ZEE nit-700 - AnalyticJena). The pH of these solutions was determined using an Orion 210A+ (Thermo) pH-meter, while the conductivity and the total dissolved solids were measured with an Orion 130A (Thermo) conductivity

meter .

The data were processed using specific software (EXCEL).

**Results and discussions**

The first phase of the experiment consisted of: (i) blending 0.5g of zeolites with 40mL of distilled water (pH 5.7) and 40mL of acid water (pH 3.2), respectively; and (ii) mixing 5g of soil with the same volume of distilled and acid water. The resulted mixtures were stirred 2h/day, for 11 days, and the heavy metal content that the zeolites and the soil can release into aqueous solutions was measured. The variation of pH, TDS and conductivity were also determined. Finally, the interpretation of the results (tab. 5) pointed out the high purity and alkalinity of the zeolite species, as well as the solubility of the studied metals and the acidity of the soil.

Tab. 5 Heavy metal ion concentrations, pH, TDS and conductivity of solutions: zeolites-distilled water (A), zeolites-acid water (B), soil-distilled water (C), and soil-acid water (D)

Sol.	Cu(µg/L)	Pb(µg/L)	Zn(µg/L)	Ni(µg/L)	pH	TDS(mg/L)	C(mS/m)
A	0	3.4	0	4.4	7.04	47	0.114
B	0	3	0	4.4	6.82	56	0.131
C	2335.3	129	146.9	662.3	2.89	1844	4.31
D	2414	110.6	101	720.2	2.89	1801	4.22

The same parameters were determined in similar conditions for the soil-zeolites-distilled water and soil-zeolites-acid water solutions, in order to establish the effect of the zeolites on a polluted soil, during the event of common and acid rains; the measurements were made on certain days during the experiment and the values are indicated in table 6.

Tab. 6 Heavy metal ion concentrations, pH, TDS and conductivity of solutions: soil-zeolites-distilled water (E) and soil-zeolites-acid water (F)

Sol.	Day	Cu(µg/L)	Pb(µg/L)	Zn(µg/L)	Ni(µg/L)	pH	TDS(mg/L)	C(mS/m)
E	3	2056.7	103.1	135.6	554.4	3.30	1411	3.20
	5	1957.2	104.0	104.8	434.2	3.36	1441	3.17
	7	1895.1	100.0	85.2	443.3	3.43	1476	3.30
	10	1617.5	90.4	83.6	448.1	3.41	1525	3.44
	11	1411.3	74.3	72.6	403.3	3.38	1565	3.60
F	3	2325.8	96.2	99.4	629.7	3.24	1447	3.22
	5	2128.3	96.8	96.9	442.2	3.31	1474	3.23
	7	2057.4	93.7	82.5	456.8	3.37	1510	3.37
	10	1775.0	86.6	78.5	544.9	3.38	1535	3.47
	11	1665.1	78.3	77.9	561.7	3.38	1576	3.60

A correlation of the analytical data (fig. 1) suggestively presents the variation in time of copper, lead, zinc and nickel ions in the mixtures of soil, zeolites and distilled water, and soil, zeolites and acid water. The concentrations specified for the first day of the experiment resulted by investigating the soil-distilled water and soil-acid water solutions.

A descendant trend for Cu, Pb and Zn concentrations is highlighted, due to a gradual sorption of these heavy metals by zeolites; Ni has a more peculiar behaviour, as a desorption phase is well emphasized, much more obvious in the acid solution. Mentioned also other authors as well (Sprynskyy et al., 2006; Wang and Peng, 2010), this aspect can be considered normal for Ni and may accounted for by the selectivity of zeolites for H<sup>+</sup> and other heavy metal ions.

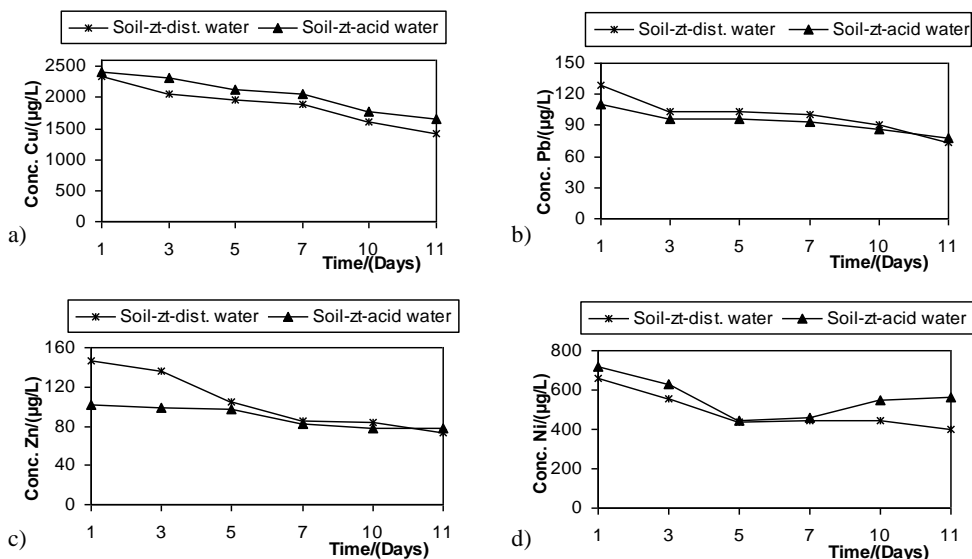


Fig.1 The variation of heavy metal amounts in solutions resulted by mixing soil with zeolites and distilled or acid water

The pH of the solutions is more variable and the trend is different from one mixture to another. The pH of acid solutions slightly increases with the addition of zeolites, but this tendency is less obvious than in the case when only zeolites and acid water were mixed; the pH of soil, zeolites and distilled water drastically decreases, from 5.7 to 3.30, although not as much as when no zeolite was used. These variations could be caused by pollution, as well as by humic acids.

Initial and final concentrations of heavy metals are summarized in table 7, the following formulae being used to determine the sorption capacity of zeolites:

$$(\%)adsorption = \frac{C_i - C_f}{C_i} \times 100 \quad (1)$$

where  $C_i$  – initial concentration, and  $C_f$  – final concentration (Erdem et al., 2004).

Tab. 7 Initial and final concentrations of heavy metals and the amount of sorption (%) by the zeolites

Sol.	Cu (µg/L)			Pb (µg/L)			Zn (µg/L)			Ni (µg/L)		
	Initial	Final	Sorbed (%)	Initial	Final	Sorbed (%)	Initial	Final	Sorbed (%)	Initial	Final	Sorbed (%)
E	2335.3	1411.3	39.6	129	74.3	42.4	146.9	72.6	50.6	662.3	403.3	39.1
F	2414	1665.1	31	110.6	78.3	29.2	101	77.9	22.9	720.2	561.7	22

## Conclusions

Natural zeolites are low cost and efficient materials in the retention of heavy metals from polluted soils. The experimental study has emphasized the high reliability of zeolites for soil remediation, as they decrease the heavy metal concentrations, both in distilled and acid solutions, even when used in a multi-component system.

The process is influenced by the cation exchange capacity (CEC) of the zeolites and by the pH of the solution, as there is an obvious ion selectivity and competitive adsorption between heavy metals and  $H^+$  ions, as well as between  $Cu^{2+}$ ,  $Pb^{2+}$ ,  $Zn^{2+}$ , and  $Ni^{2+}$ ; the sorption efficiency is the following:  $Zn^{2+} > Pb^{2+} > Cu^{2+} > Ni^{2+}$ .

## References

- Balint, R., 2010. Heavy metal variation in the soils associated with the Bălan mining perimeter. Proceedings of 10<sup>th</sup> International Multidisciplinary Scientific GeoConference, SGEM 2010, **II**, 617–624.
- Bedelean, I., Stoici, S.D., 1984. Zeolites (In Romanian). Editura Tehnică, Bucureşti.
- Bish, D.L., Guthrie, Jr.G.D., 1993. Mineralogy of clay and zeolite dusts (exclusive of 1:1 layer silicates). In Health effects of mineral dusts. Reviews in Mineralogy, **28**, 139–184.
- Coombs, D.S., Alberti, A., Armbruster, T., Artioli, G., Colella, C., Galli, E., Grice, J.D., Liebau, F., Mandarino, J.A., Minato, H., Nickel, E.H., Passaglia, E., Peacor, D.R., Quartieri, S., Rinaldi, R., Ross, M., Sheppard, R.A., Tillmanns, E., Vezzalini, G., 1997. Recommended nomenclature for zeolite minerals: Report of the subcommittee on zeolites of the International Mineralogical Association, commission on new minerals and mineral names. Canadian Mineralogist, **35**, 1571–1606.
- Erdem, E., Karapinar, N., Donat, R., 2004. The removal of heavy metal cations by natural zeolites. Journal of Colloid and Interface Science, **280**, 309–314.
- Sprynskyy, M., Buszewski, B., Terzyk, A.P., Namiesnik, J., 2006. Study of the selection mechanism of heavy metal ( $Pb^{2+}$ ,  $Cu^{2+}$ ,  $Ni^{2+}$  and  $Cd^{2+}$ ) adsorption on clinoptilolite. Journal of Colloid and Interface Science, **304**, 21–28.
- Wang, S., Peng, Y., 2010. Natural zeolites as effective adsorbents in water and wastewater treatment. Chemical Engineering Journal, **156**, 11–24.

## THE GEOLOGICAL ENVIRONMENT WITHIN SUSTAINABLE DEVELOPMENT

CORNELIU HORAICU<sup>1</sup>

<sup>1</sup> „Al. I. Cuza” University of Iași, Department of Geology, 20A Carol I Blv., 700505 Iași, Romania; e-mail: choraicu@yahoo.com

**Keywords:** environment, geology, development, sustainability.

### Introduction

The current paper suggests and tries to answer, through a very brief analysis, several questions, such as:

- What is the geological environment?
- How does the geological environment generally interfere with the surrounding environment and especially with the socio-economic development?
- When did the geological environment start to be viewed as a well-outlined entity of the environment in general?
- Who are the managers of the activity of geological environment preservation and what are their responsibilities?

Why is eco-economy a “must”? (Barbier, 1987; Brown and Merideth, 1988).

### Geological environment

The geological environment clearly represents a part of the natural environment. Therefore, it could be considered a part of the lithosphere, with which the living creatures, particularly the human beings, and their activities come into contact, in order to provide the necessary substances and energy supplies.

Considering the limits of the geological environment, we can define the upper limit as being represented by the relief forms, ranging from the maximal altitude (8,849.86 km – Everest, Himalaya Mountains) to the minimal altitude (minus 11,034 m, Mariana Trench, Pacific Ocean) of the relief from the lithosphere. The lower limit of the geological environment is determined by the technico-scientific development of the human society (nowadays, about 15 km in one drilling from the Kola Peninsula).

The geological environment can be clearly outlined by specifying its evolution conditions, namely the geologico-tectonical, hydrogeological, geomorphological, geophysical, geochemical, biological systemic conditions, and even climatic conditions.

Relating the technogenic activity to the above-mentioned conditions, one discovers that it has influenced the evolution of the geological environment in effective time up to the present level, when the human activity surpasses, several times in some cases, the natural historical activity of the geological processes (Capcelea et al., 2000).

### **Exploitation in the geological environment**

Geological research, along with the exploitation of deposits in all its stages, from *exploration* to *exploitation*, imposes a more accurate knowledge of the physico-mechanical properties of the rocks and of the useful mineral substances (Băncilă et al., 1980).

### **Geological environment modeling**

The problematic of geological environment modeling, with all its particularities, which sometimes have a difficult-to-make-out complexity, starts with the detailed differentiation of the geological environment.

This differentiation is based on the analysis of the researched technico-natural systems, from the litho-stratigraphic spatial homogeneity to the structural one, or even a natural climatic one, within the diversity of the technogenic activity. The geological environment has several heterogeneities, compared to the biological or the geographical environment. Therefore, the uncertainties (either natural, spatiotemporal or conceptual) determine the imperfection of each model of the geological environment.

Nevertheless, in order to have an analysis lead to a proper geological model, an evaluation of the possibilities for evolution within the limits of the geological and technogenic processes that are dangerous for biodiversity must be performed.

Moreover, we must consider the socio-economic and the socio-ecologic aspects (environmental preservation and protection), as well as the organizing, monitoring and methodic aspects (Rojanschi et al., 1997).

### **Systems of the geological environment**

The systemic organization of the geological environment represents its abstract formulation and is a preoccupation which derives from the general theory of the systems (Ionescu, 2000).

### **Monitoring the geological environment**

The monitoring process is defined as an integrate evaluation activity of the physical, chemical and biological characteristics (geological environment) related to human activity.

The integrated approach in the management of the monitoring activity is imposed by the construction of a system of active control, prediction and intervention (Horaicu, 2004).

### **References**

- Băncilă, I., Florea, M.N., Fota, D., Georgescu, M., Lazar, L.F., Mocanu, Gh., Moldoveanu, T., Munteanu, A., Privighetorita, C., Văduva, C., Zamfirescu, F., 1980. Engineering geology, I (In Romanian). Editura Tehnică, București, 594p.

- Barbier, E., 1987. The Concept of Sustainable Economic Development. *Environmental Conservation* **14/2**, 101–111.
- Brown, B.J., Merideth, R.W., 1988. Global Sustainability: Towards Measurement. *Environmental Management* **12/2**, 133–143.
- Capcelea, A., Osiuk, V., Rudko, G., 2000. Fundamentals on ecological geology in Republic of Moldova (In Romanian). Editura Știință, Chișinău, 256p.
- Horaicu, C., 2004. Integrate monitoring of the environment (In Romanian). Editura TipoMoldova, Iași, 140p.
- Ionescu, C., 2000. How to build up and to apply a system of environment management according with ISO 14100 (In Romanian). Editura Economică, București, 304p.
- Rojanschi V., Bran F., Diaconu G., 1997. Preservation and engineering issues on the environment (In Romanian). Editura Economică, București, 368p.

## **IMPLEMENTATION OF WATER FRAMEWORK DIRECTIVE 2000/60/EEC REGARDING GROUNDWATERS IN ROMANIA**

RODICA MACALEȚ<sup>1</sup>, TUDOR MUNTEANU<sup>1</sup>, MARIAN MINCIUNA<sup>1</sup>

<sup>1</sup> National Institute of Hydrology and Water Management, 97, București – Ploiești Road, 013686 Bucharest, Romania; e-mail: rmacalet@yahoo.fr; tudor.munteanu@hidro.ro

**Keywords:** groundwater bodies, monitoring programme, management plan.

### **Abstract**

In order to implement the Water Framework Directive 2000/60/EEC, Romania has delineated, based on geological and hydrogeological criteria (fig. 1), 142 groundwater bodies, out of which 17 are transboundary.

The delineation of groundwater bodies was made only for the areas in which there are significant aquifers for water supply (yielding more than 10 cubic meters).

In Romania, porous-permeable, karstic, fissural and mixed groundwater bodies were delimited. The most part of the groundwater bodies are of the porous-permeable type.

The groundwater dynamics and storage potential depend on the local/regional hydrogeological conditions, such as lithology, aquifer spatial disposition and recharge. These characteristics generally determine the hydraulic conditions, phreatic, middle-depth or depth groundwater bodies being, thus, separated.

Phreatic groundwater bodies occur up to a depth of 30-50 meters, are generally unconfined, directly influenced by meteorological factors, and in connection with surface water. The middle-depth and depth groundwater bodies, which occur below the depth of 30-50m, are confined and isolated from the surface waters and the phreatic ones by impermeable layers.

The National Institute of Hydrology and Water Management has undertaken the following activities, concerning groundwaters in Romania:

- identification, delineation and characterization of the groundwater bodies based on geological and hydrogeological criteria, and criteria related to the potential anthropogenic influences on the quantitative and qualitative status of groundwater bodies, and to sustainable water management;
- evaluation of anthropogenic impact on groundwater and establishment of the groundwater bodies at risk;

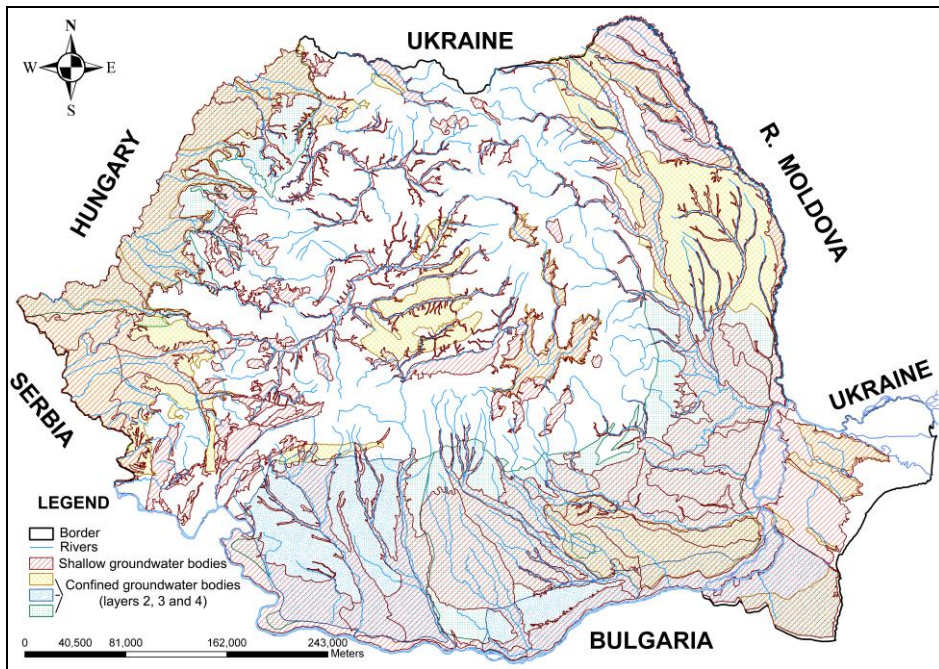


Fig.1 Groundwater bodies which were delineated in Romania

- establishment of the transboundary groundwater bodies, considered those with areas exceeding 4,000km<sup>2</sup> and/or important for water supplying, and harmonization of the characterization of important transboundary groundwater bodies between neighboring countries;

- identification of protection areas for groundwater catchments.

In Romania, 17 transboundary groundwater bodies (Bretotean et al., 2006) shared with the neighboring countries have been identified; through bilateral agreements, a number of 8 bodies were established as being important for a integrated management, as follows (fig. 2):

- 4 transboundary groundwater bodies with Hungary;
- 1 transboundary groundwater body with Serbia;
- 2 transboundary groundwater bodies with Bulgaria;
- 1 transboundary groundwater body with the Republic of Moldova.

The main characteristics of these transboundary groundwater bodies are presented in the table 1.

According to Water Framework Directive 2000/60/EC, the groundwater monitoring programmes must provide the information necessary to assess whether relevant environmental objectives are performed, in particular the groundwater quantitative status, the chemical status and significant long-term trends of the groundwater bodies resulting from human activity.

In our country, the monitoring of groundwaters is carried out through the following networks:

**National Hydrogeological Network**, which follows:

- the knowledge of the spatial development of the shallow and deep aquifer structures, and of their aquifer potential;
- the knowledge of groundwater level regime;
- the knowledge of groundwater physico – chemical properties.

This network is based on the monitoring of wells for shallow aquiferous strata (depths of 20 –50m), and for deep aquiferous strata (depths of 50 – 400m).

**Local Monitoring Network**, which monitors the evolution of the water quality (local pollution) in the case of certain pollutant objectives – factories, wastelands etc. (through wells for shallow aquiferous strata), as well as the evolution of piezometric levels, in areas of some important groundwater catchments (through wells with depths depending on the caught aquifer).

The local monitoring networks and measurement programmes are accessed by the owners of potential polluting objectives or the owners of the important catchments.

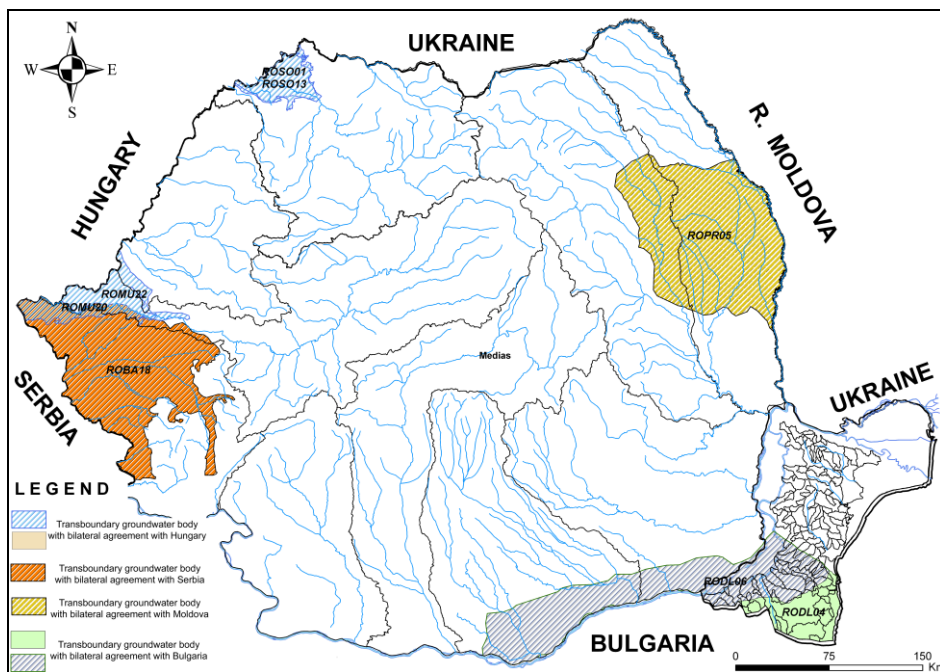


Fig.2 Transboundary groundwater bodies from Romania

Tab. 1 General characteristics of the transboundary groundwater bodies

River basin	Aquifer	Predominant lithology or lithologies	Stratigraphy and age	Thickness (m)		Areal extent (km <sup>2</sup> )	Dominant groundwater flow direction
				mean	max		
Somes/ Szamos	Holocene-Lower Pleistocene Somes/Szamos alluvial fan	Holocene-Lower Pleistocene alluvial sediments of sands, clayey sands, gravels and even boulders	Upper Pleistocen – Lower Holocene unconfined upper part and the confined Lower Pleistocene	40	130	1390	from East (Romania) to West (Hungary)
Mures/ Maros	Pleistocene-Holocene Mures/Maros alluvial fan	Alluvial sediments, predominantly pebbles, sands and locally boulders	Upper Pleistocen – Lower Holocene unconfined upper part and the confined Lower Pleistocene	65	75	1690	from Romania to Hungary
Banat	Pleistocene-Pannonian	Sarmatian deposits, clay, marl, sand intercalations of calcareous sandstones and limestones oolythics inches	Porous-permeable	30	350	11408	from Romania to Serbia
Prut	Middle Sarmantian Pontian	Pontian sediments from the Central Moldovian Plateau, predominantly sands, sandstones and limestones	Porous-permeable	20	50	22194	from Moldova (N – NW) to Romania (S - SE)
Dobrogea - Litoral	Sarmatian	Sarmatian deposits from South Dobrodja, predominantly sandstones	Oolitic sandstones fissured	75	250	2178	from Bulgaria (SW-NE) to Romania
	Barremian-Jurassic	Upper Jurassic – Lower Cretaceous from south Dobrodja,	Karstic-fissured	140	600	11320	from Bulgaria (SW-NE) to Romania

Since 2006, two new monitoring programmes have been developing in agreement with the Water Framework Directive 2000/60/EC and Guide 15 (Monitoring guide. Monitoring programs that apply in Romania (Bretotean et al., 2008)), as follows:

- Surveillance programme (S). This programme is applied to all groundwater bodies, once every six years.
- Operational programme (O). This programme is applied to all groundwater bodies, in areas with quantitative and qualitative risk.

In 2009, all groundwater bodies were monitored through wells or springs, as follows (tab. 2):

Tab. 2 Monitoring programmes

Monitoring points	Wells	Springs	Total
Quantitative programme	2880	24	2904
Chemical programme	1431	43	1474

An estimation of the qualitative status of the groundwater bodies in Romania was made in 2008 (Bretotean et al., 2009). The chemical data obtained through the monitoring programs in the 2006 and 2007 were compared with the threshold values (established for NO<sub>3</sub>, NO<sub>2</sub>, NH<sub>4</sub>, PO<sub>4</sub>, chlorides, sulfates, lead, cadmium, mercury, arsenic etc.).

During 2009, a Management Plan was developed for each river basin in Romania, which was sent to the European Commission (General Direction of Environment) and to the International Commission for the Protection of the Danube River in Vienna. This management plan includes both surface waters and groundwaters, in each hydrographic basin.

The National Management Plan of the waters in Romania is a component part of the Management Plan of the Danube River Basin (MPDRB).

The objectives of the Management Plan are the following:

- the achievement of a good status of waters by 2015;
- the uniform protection of waters, from spring to river mouths;
- the insurance of the same living conditions, from the point of view of water resources, for all Romanian citizens.

## References

- Bretotean, M., Macaleț, R., Munteanu, M., 2008. Monitoring Programmes for the Groundwaters in Romania. Unesco Bresce, Thessaloniki.
- Bretotean, M., Macaleț, R., Radu, E., Radu, C., 2009. Quantitative and qualitative assessment of the groundwater bodies from Romania (In Romania). Univ. Tehnică de Construcții, București, in press.
- Bretotean, M., Macaleț, R., Țenu, A., Tomescu, G., Munteanu, M.T., Radu, E., Drăgușin, D., Radu, C., 2006. The transboundary groundwater bodies from Romania (In Romania). Hidrogeologia, 7/1, 6–21.

## **GEOMORPHOLOGICAL CHARACTERS OF THE ETNA COAST (EASTERN SICILY): EXAMPLES OF IRREVERSIBLE ENVIRONMENTAL DEGRADATION CAUSED BY ANTHROPIC ACTIVITIES**

SANDRO PRIVITERA<sup>1</sup>

<sup>1</sup> University of Catania, C.U.T.G.A.N.A. (Centro Universitario per la Tutela e Gestione degli Ambienti Naturali e degli Agrosistemi), 81, Via Androne, 95124 Catania, Italy;  
e-mail: sandroprivitera@unict.it

**Keywords:** Mount Etna, Sicily, coastal geomorphology, geomorphosites, anthropic impact.

### **Abstract**

The present paper describes the geological and geomorphological outlines of the Etna coast (fig. 1), together with a list of the main natural problems, which strongly affect its stability.

Furthermore, the effects of a locally severe anthropic impact will be analyzed in order to emphasize the risk of the possible permanent loss and/or irreversible degradation of outcrops or of several beautiful sectors along the eastern coast of Sicily.

### **Introduction and objectives**

Peculiar volcanological aspects (pillow-lavas, columnar basalts, spectacular abrasion marine caves, cliffs etc.) and local sites of cultural/historical heritages allow us to recognize, throughout the entire Etna coast, several geomorphosites, according to the definition of Panizza (2001) and Reynard and Panizza (2005).

These volcanic landscapes are strongly affected locally by natural and/or anthropic actions, which caused their environmental degradation. Several examples along this unique coast will be described and analyzed.

### **The Castle Rock of Acicastello coast**

This coastal sector is very important, due to the presence of pillow-lava, hyaloclastite, columnar basalt and subaerial lava flow outcrops, located in a very urbanized area of northern Catania.

In the Acicastello area, one can see the outcrops of the most ancient volcanic products of Etna (Romano et al., 1979), intruded and/or overlying the most recent sediments of the Etna basement, represented by the Early Pleistocene Blue Marly Clays (fig. 2).

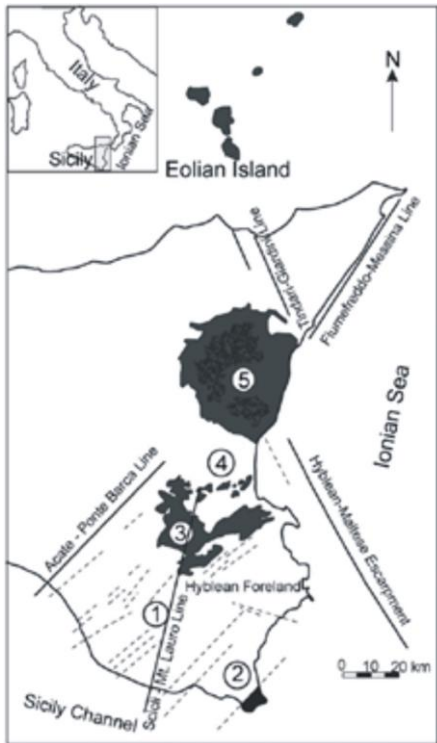


Fig. 1

Fig. 1 Tectonic setting of eastern Sicily with the main volcanic areas. 1-buried Triassic volcanics near Ragusa; 2-Cretaceous lavas and dykes; 3-volcanics of the Upper Cretaceous–Pleistocene in the northern sector of the Hyblean Mountains and in the Catania Plain; 4-Quaternary volcanics of Etna; 5-Etna volcanic cone (modified from Rittmann, 1963).

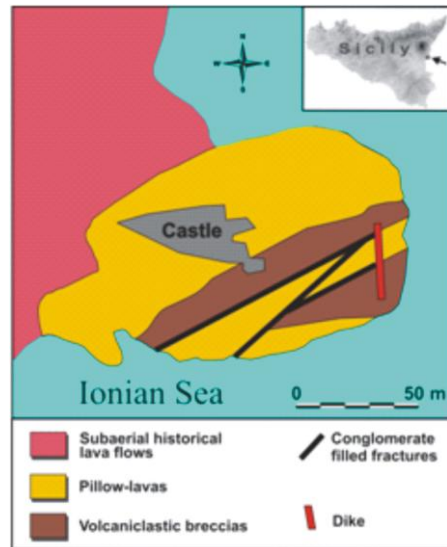


Fig. 2

Fig. 2 Geological sketch of the Castle Rock outcrop

The Castle rock of Acicastello, which holds the remnants of the medieval castle (fig. 3a), displays nearly vertical slopes, made up by volcaniclastic breccias and pillow-lavas (Corsaro and Cristofolini, 2000) that belong to the so-called “Basal Sub-alkaline Lava Flows” (Romano et al., 1979).

The changes induced by the anthropic activity in this area started at the beginning of the seventies (Privitera, 2006; Trimarchi and Privitera, 2007) and increased yearly, as a consequence of the development of the town of Catania, which is now in the very proximity of the small town of Acicastello. Figure 4 displays the changes mentioned above.

In fact, the construction of the new harbour caused the near destruction of a wide outcrop of columnar basalts, buried under the cement of the dock and under the adjacent parking lot (fig. 4, right side).

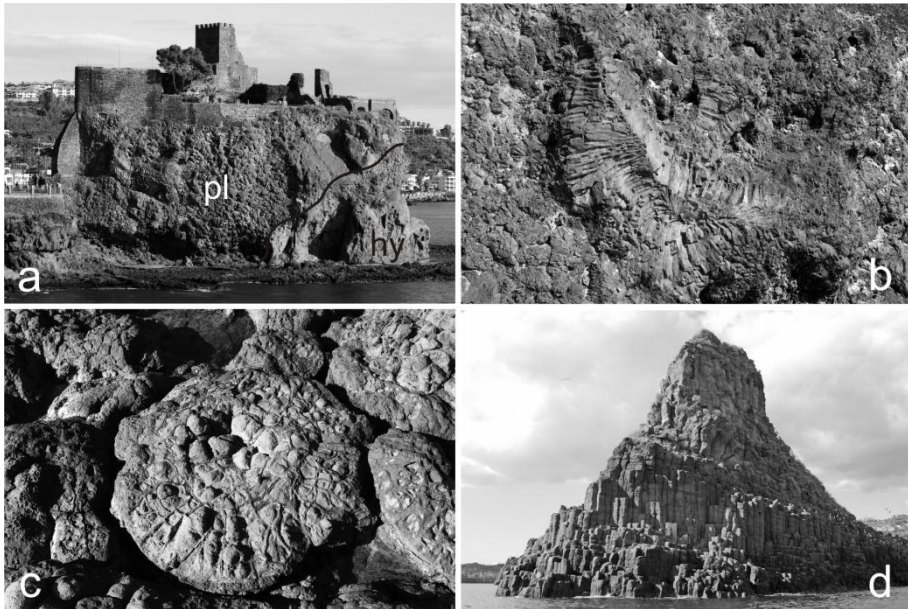


Fig. 3 The Acicastello Castle Rock and related abrasion platforms (southern view, a), showing pillow-lavas (**pl**) (a, b and c) associated with hyaloclastites (**hy** in photo a). Columnar basalts of the Cyclops's stack, cropping out in the very vicinity of the Acicastello Castle Rock, are shown in d.

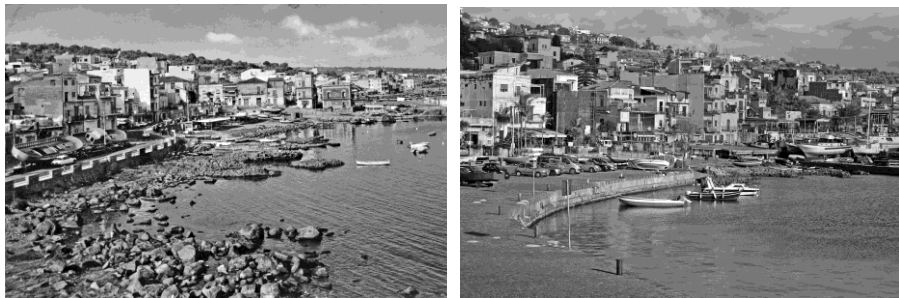


Fig. 4 Old and new harbour of Acicastello (left and right, respectively) showing the effect of the anthropic activity.

Remnants of the causeways made of columnar basalts, once extending along the entire shoreline, are shown in figure 5.



Fig. 5 Columnar basalt, with details in the right side photo, showing the interstices filled by silty and organic sediments.

Another example of the careless and unnecessary use of the coastal territory in the study area is represented by the destruction of subaerial lava flows that, initially, were showing rare pahoehoe morphology and many other very interesting Hawaiian-like structures (fig. 6, left).

The construction of small barracks and of a stairway necessary in order to reach them, used only in the summer season, strongly changed the original shape of a peculiar pressure ridge, without taking into account the enormous importance of these rare volcanic morphologies (fig. 6, right).



Fig. 6 Big cement platform, obliterating the original pahoehoe morphology (left) and an anthropized pressure ridge (right).

## Conclusions

The examples of wasting and environmental degradation along the Etna coast of eastern Sicily described above represent irreversible processes of “anthropic erosion,” which progressively destroy important, rare and very special outcrops.

At the moment, a rigorous count of the coastal geomorphosites, which represent very attractive natural monuments, is still missing in Sicily. Such an approach is required by the necessity to preserve the original landscapes within the framework of a sustainable development of the territory, as an important natural and economic resource.

## References

- Corsaro, R.A., Cristofolini, R., 2000. Subaqueous volcanism in the Etnean area: evidences for hydromagmatic activity and regional uplift inferred from the Castle Rock of accastello. *J. Volc. Geoth. Res.*, **95**, 209–225.
- Panizza, M., 2001. Geomorphosites: concepts, methods and example of geomorphological survey. *Chinese Science Bulletin*, **46**, 4–6.
- Privitera, S., 2006. Siti di interesse ambientale: conflittualità rilevate, in «I Quaderni dell'Interreg». La valutazione ambientale. Materiali per un progetto transfrontaliero. Un Sistema informativo per la valutazione delle attività sulla costa (SIVAC) Quaderno 3. Progetto GES.S.TER. Gestione sostenibile delle aree costiere. Interreg III A Transfrontaliero Adriatico, cap. 3, 123–151.
- Reynard, E., Panizza, M., 2005. Geomorphosites: définition, évaluation et cartographie. Une introduction. *Géomorphologie. Relief, Processus, Environnement*, **3**, 177–180.
- Rittmann, A., 1963. Vulkanismus und Tektonik des Aetna. *Geol. Rundsch.*, **53/2**, 788–800.
- Romano, R., Lentini, F., Sturiale, C., Amore, C., Attori, P., Carter, S.R., Cristofolini, R., Di Geronimo, I., Di Grande, A., Duncan, A.M., Ferrara, V., Ghisetti, F., Guest, J.E., Hamill, H., Patanè, G., Pezzino, A., Puglisi, D., Schilirò, F., Torre, G., Mezzani, L., 1979. Carta geologica del Monte Etna, scala 1:50.000. Litogr. Art. Cartogr., Firenze.
- Trimarchi, R., Privitera, S., 2007. Pressione antropica e degrado ambientale nelle aree costiere siciliane; la dispersione del patrimonio paesaggistico della Riviera dei Ciclopi. *Annali della Facoltà di Scienze della Formazione, Università degli Studi di Catania*, 187–247.

## **THE DISTRIBUTION OF HEAVY METALS IN SOILS OF THE FĂLTICENI MUNICIPALITY AND ITS SURROUNDINGS**

IONUȚ MIHAI PRUNDEANU<sup>1</sup>, NICOLAE BUZGAR<sup>1</sup>

<sup>1</sup> „Al. I. Cuza” University of Iași, Department of Geology, 20A Carol I Blv., 700505 Iași, Romania; e-mail: prundeanu.ionut@geology.uaic.ro; nicolae.buzgar@uaic.ro

**Keywords:** urban soils, heavy metals, GIS, pH.

The study of heavy metals (Cd, Co, Cr, Cu, Fe, Mn, Ni, Pb, Zn) in the topsoil (0-25 cm) of the Fălticeni municipality and some of its surroundings generally indicated the presence of contents specific to the natural geochemical background; some interferences were observed, associated with urban soils and areas covered with orchards or other crops, on which fertilizers and pesticides are used intensively. The maximum values for Co do not exceed the maximum accepted threshold (MAT) in Romania. For Cd and Cr, in small areas, there are contents over the MAT in Romanian soils. Some of the concentrations obtained for Cu, Ni, and Zn are above the alert threshold, but they are still far from the intervention threshold for sensitive terrains. Pb is the only heavy metal with the maximum content higher than the intervention threshold for a sensitive terrain; only one sample from the total of 63 analyzed is over this threshold. Obviously, that is the case of a punctual contamination with Pb. Along with the analysis of the chemical amounts of heavy metals, the pH of the soil samples was also determined.

## MINERALOGY AND GEOCHEMISTRY OF SULFATES DEVELOPED ON SULFIDE-BEARING LOW-GRADE METAMORPHIC ROCKS OF SURFACE MINING WASTES

DAN STUMBEA<sup>1</sup>

<sup>1</sup> „Al. I. Cuza” University of Iași, Department of Geology, 20A Carol I Blv., 700505 Iași, Romania; e-mail: dan.stumbea@uaic.ro

**Keywords:** efflorescent sulfates, acid mine drainage, sulfate geochemistry, XRD, SEM(EDS), Eastern Carpathians, Romania.

Mine wastes are lasting sources of environmental contamination, mostly in the form of acid mine drainage (AMD); as many scientific papers state (e.g. Lefebvre et al., 2001; Sracek et al., 2004; Cánovas et al., 2010), there are three general types of acid release from mine wastes, namely iron sulfide oxidation, the dissolution of soluble iron sulfate minerals, and the dissolution of less soluble sulfate minerals (i.e. the alunite/jarosite series). On the other hand, there are two types of mine waste: (a) mine tailings, which are the final product of ore processing and are composed of sand and silt-size particles; (b) waste rock, which is the non-economic material removed from a mine in order to access the ore body (blocks and fragments of disseminated sulfide-bearing rocks).

The present study deals with a mineralogical and geochemical approach undertaken on excavation wastes (sulfide-bearing blocks and fragments of low-grade metamorphic rocks) from the Eastern Carpathians, Romania (the Bălan district), in order to determine the mineralogical composition and the geochemical features of efflorescent aggregates developed on the surface of rock debris through weathering processes; an attempt to assess their role in the generation of acidity and the release of pollutants during acid mine drainage (AMD) was made as well.

The study relies on the macroscopical and microscopical description of efflorescent products, as well as on XRD analyses, chemical composition obtained through the SEM-EDS technique and pH/Eh data on leachates evolved through the dissolution of efflorescent materials.

The mineralogical and chemical composition of efflorescent products shows two successive processes: (1) the alteration of in-situ sulfide-bearing schists that lead to the development of an oxidation zone affecting the mineralization; (2) the weathering of already oxidized fragments of sulfide-bearing rocks brought to the surface by mine works; the minerals developed through the first processes are considered secondary, while mineral associations developed through weathering (efflorescent sulfate aggregates) are tertiary.

XRD analyses display the patterns of three groups of minerals with different origins: (1) primary minerals (chlorite, sericite) which originate from the primary groundmass minerals of schists; (2) secondary minerals, evolved from the oxidation processes affecting the sulfides: limonite and lepidocrocite that appear on the account of pyrite, and/or malachite and azurite, developed through the alteration of chalcopyrite; (3) tertiary minerals (efflorescent Al-Fe-Mg sulfates) evolved from the weathering of sulfide-bearing schist debris: alunogen, pickeringite, ferri- and magnesiocopiapite, halotrichite, apjohnite, butlerite, römerite, hexahydrite, rhomboclase. Patterns of jarosite, coquimbite, gypsum, epsomite, brochantite, and chalcantite were identified as well.

The efflorescent aggregates appear as yellow-brownish, yellow-greenish or yellow-bluish materials, they are highly soluble in water, produce acid leachates (pH lower than 5.0) and consist mostly of sulfates; the high susceptibility to solubilization of the sulfates results from their sizes of only tens of microns, which implies large surface areas.

According to the three-stage model of mineral formation under subaerial conditions proposed by Velasco et al. (2005), most sulfates have formed during stage II. Stage II is controlled by oxidation conditions and by moderate to low dehydration processes; the XRD patterns of coquimbite, ferricopiapite, and rhomboclase confirm this assumption. The small amounts of halotrichite and epsomite reveal local environments of relatively low humidity and pore waters with low activity of aluminum. As some XRD patterns of gypsum, along with the presence of pickeringite, show, there are indications of an evolution of weathering processes towards a natural neutralization of the acid leachates (stage III of Velasco et al., 2005).

The weathering of sericite, chlorite, and Na-feldspars from schists leads to a clay fraction, as X-ray patterns of illite show; though discrete, patterns of chlorite-vermiculite interlayered term were identified as well. The acid solutions of AMD processes act on chlorite and release Mg responsible for the formation of Mg sulfates (pickeringite, magnesiocopiapite, and hexahydrite). The dissolution of both K- and Na-feldspars from schists, which is highly effective in low pH environments, can produce – beyond clay mineral associations – amorphous Al hydroxides and/or Si-rich amorphous materials.

Chemical data on efflorescent materials confirm the mineralogical composition determined through XRD, showing large amounts of  $\text{SO}_3$ ,  $\text{Fe}_2\text{O}_3$  (as  $\text{FeO}+\text{Fe}_2\text{O}_3$ ),  $\text{Al}_2\text{O}_3$ , and, to some extent,  $\text{MgO}$ ; ratios between the contents of these oxides discriminate needle-like mineral grains, probably formed from  $\text{SO}_3$ -richer solutions, from the tabular-like minerals which display genetic conditions controlled by higher amounts of  $\text{Fe}_2\text{O}_3$ .

## References

- Cánovas C.R., Olías M., Nieto J.M., Galván L. 2010. Wash-out processes of evaporitic sulfate salts in the Tinto river: Hydrogeochemical evolution and environmental impact. *Applied Geochemistry*, **25**, 288–301.
- Lefebvre R., Hockley D., Smolensky J., Gélinas P. 2001. Multiphase transfer processes in waste rock piles producing acid mine drainage 1: Conceptual model and system characterization. *Journal of Contaminant Hydrology*, **52**, 137–164.
- Sracek O., Choquette M., Gélinas P., Lefebvre R., Nicholson R.V. 2004. Geochemical characterization of acid mine drainage from a waste rock pile, Mine Doyon, Québec, Canada. *Journal of Contaminant Hydrology*, **69**, 45–71.

- Velasco F., Alvaro A., Suarez S., Herrero J.-M., Yusta I. 2005. Mapping Fe-bearing hydrated sulphate minerals with short wave infrared (SWIR) spectral analysis at San Miguel mine environment, Iberian Pyrite Belt (SW Spain). *Journal of Geochemical Exploration*, **87**, 45–72.
- Mârza, I., 1985. Genesis of ore deposits of magmatic origin, vol. 2. Publishing House Dacia, Cluj-Napoca, 331p. (In Romanian).

## THE CLAY FRACTION FROM THE SOLID PRODUCTS OF ACID MINE DRAINAGE. A MINERALOGICAL APPROACH

DAN STUMBEA<sup>1</sup>

<sup>1</sup> „Al. I. Cuza” University of Iași, Department of Geology, 20A Carol I Blv., 700505 Iași, Romania; e-mail: dan.stumbea@uaic.ro

**Keywords:** acid mine drainage, clay fraction, acidity, XRD.

The acid mine drainage (AMD) is an important risk factor in the pollution of both active and abandoned mining areas; its either solid or liquid products have a long-term impact on the environment. The solid AMD products appear as efflorescent aggregates of yellow-brown or blue-green color, developed on the surface of fragments of sulfide-rocks, scattered in the open pits, quarries and mine wastes; mineralogically, the solid products display intergrowths of hydrated sulfates, hydrated carbonates and oxides, and clay minerals (Jambor et al., 2000). The liquid AMD products consist of acidic, heavy metal-rich leachates, emerging from the mine wastes which underwent weathering processes.

The present study is focused on the mineralogical characterization of the clay fraction formed as part of the efflorescent aggregates identified in the Wetter (Franz Johann) quarry, metalogenic district of Bălan (Romania). The solid products develop on the surfaces or along the fractures of fragments and blocks of pyrite±chalcopyrite-bearing schists (low-grade metamorphic schists of the Tulgheș Group, Bucovinian nappe – Berbeleac, 1988); the complex mineralogy of the efflorescent products may be explained by oxidation, hydration and even natural neutralization processes. Depending on factors such as temperature and rainfall regime, these processes occur successively.

XRD analyses carried out on efflorescent aggregates revealed three generations of minerals, as follows: (1) traces of remnant silicate minerals from the sulfide-bearing schists (i.e. chlorite), which may be considered primary minerals; (2) hydrated oxides (goethite, lepidocrocite) and carbonates (malachite, azurite) that belong to the oxidation zone developed at the upper part of the *in situ* sulfide ore deposit (secondary minerals); (3) intergrowths of hydrated sulfates and clay minerals, occurring through the weathering of the sulfide-bearing schist debris brought at the surface by the quarrying works (tertiary minerals).

In the attempt to understand the changes underwent by the primary minerals during AMD, XRD analyses on unaltered schists of the Tulgheș Group were performed as well. Macroscopical and microscopical identifications and XRD patterns indicate large

participations of quartz, sericite and feldspars; chlorite was also identified, while barite, tourmaline, hematite, rutile, graphite appear as accessory minerals.

In order to separate the clay fraction from the solid AMD products, the samples were ground until reaching a grain size of less than 0.4Mesh; afterwards, they were submitted to chemical procedures in order to remove chemical compounds such as carbonates, bivalent cations and Fe oxides. Each of the three samples used in the present study was split into four fractions that underwent XRD analyses: an untreated fraction, a fraction treated with ethylene glycol, and two fractions thermally treated by heating at 330 and 550°C.

The XRD data of the clay fraction indicate a simple mineralogy, consisting mostly of chlorite and illite; kaolinite appears as well, but only as an accessory mineral. As chlorite was also identified in the fresh schist samples, it is likely that this mineral is a remnant of the primary mineralogical associations of schists. By heating the samples at 550°C, some XRD peaks (i.e. 14.10Å, 7.05Å, and 3.53Å) underwent collapses and changes of intensity, revealing the presence of the interstratified terms chlorite-vermiculite and chlorite-kaolinite; the explanation may be found in the different degrees of chlorite alteration, during the weathering processes. Although no other remnants from the primary schists were identified, the presence of the clay mineral fraction suggests the weathering of feldspars and sericite from the schists. Previous studies on the impact of clay minerals on the pH of leachates emerged from the mining waste, carried out through AMD (Stumbea, 2010), showed the acidity they induce in the environment.

## References

- Berbeleac, I., 1988. Ore Deposits and Plate Tectonics (In Romanian). Technical Publishing House, Bucharest, Romania.
- Jambor, J.L., Nordstrom, D.K., Alpers, C.N., 2000. Metal-sulfide salts from sulfide mineral oxidation. *Reviews in Mineralogy and Geochemistry*, **40**, 305–340.
- Stumbea, D., 2010. Acid mine drainage-related products in Negoiiul Românesc quarrying waste deposits (Călimani Mts., Romania). *Carpathian Journal of Earth and Environmental Sciences*, **5**(2), 9–18.



# **Economic Geology**



## GEOLOGICAL FEATURES AND ORE DEPOSITS OF ALADAG (EZINE/CANAKKALE)

FETULLAH ARIK<sup>1</sup>, UMIT AYDIN<sup>2</sup>, YESIM BOZKIR OZEN<sup>1</sup>

<sup>1</sup> Selcuk University, Department of Geological Engineering, Konya, Turkey; e-mail: fetullah42@hotmail.com

<sup>2</sup> General Directorate of Mineral Research & Exploration, Ankara, Turkey; e-mail: umitaydin77@gmail.com

**Keywords:** skarn-type mineralization, geology, ore deposits, geochemistry, Aladag, Ezine.

The study area is located northwest of the Kazdağları, which is situated 8 km southwest of Ezine (Çanakkale-Turkey). Magmatic and metamorphic rocks of Permian-Miocene age crop out in the study area. The Middle-Late Permian Bozalan Formation consists of recrystallized limestones. The Denizgoren Ophiolites of Cretaceous age thrust over the Bozalan Formation and are generally observed as serpentinite in the study area. The Upper Oligocene-Lower Miocene Hallaçlar Volcanics are composed of altered andesite and rhyolite. On the other hand, the Kestanbol Pluton, of the same age as the Hallaçlar Volcanics, consists mainly of quartz-monzonite, monzonite, monzodiorite porphyry, syenite porphyry and quartz-syenite porphyry. The Ezine Volcanics, of Lower- Middle Miocene age, are composed of pyroxene-andesite and trachyte.

The Hallaçlar Volcanics and the Kestanbol Pluton were formed during the Late Oligocene-Early Miocene. After the Middle Miocene period, the collisional regime was followed by an extensional regime in the region; the Ezine Volcanics and the Bayramic Formation developed during this period.

In the study area, the Hallaçlar Volcanics and the Denizgoren Ophiolites were affected by alteration produced by the intrusion of the Kestanbol Pluton. A skarn-type mineralization developed north of Aladag, close to the contact points of the Kestanbol Pluton with the carbonaceous rocks of the Bozalan Formation and the Denizgoren Ophiolites. Pervasive clay alteration is observed near the contact of Hallaçlar Volcanics with the Kestanbol Pluton. As a result, Ca-silicates and some metallic enrichment, such as iron, copper, zinc and lead, developed in the skarn zone. Malachite fillings are noticed in the fractures of the pluton. Mainly garnet (grossular), tremolite/actinolite, epidote and zoisite/clinozoisite paragenesis was observed, while minor amounts of talc, wollastonite, augite, diopside were determined in thin section samples taken from the skarn mineralization which is located north of Aladag. In addition, main ore minerals are represented by magnetite, hematite, chalcopyrite, sphalerite, galenite, cerussite, covellite,

digenite, malachite and pyrite; they have been observed in the polished section of samples taken from the same location as the thin section samples.

### **References**

- Arik, F., Aydin, U., 2010. Geological Features and Ore Deposits of Kızıltepe (Ezine/Canakkale) Area, Selcuk University Scientific Research Projects Coordinatories, Project number 09201047, 97p.
- Aydin, U., 2010. Geological Features and Ore Deposits Of Kızıltepe (Ezine/Canakkale), MSc Thesis, Selcuk University, Konya, Turkey, 95p.

## NATIVE BISMUTH AND BISMUTH SULPHOSALTS IN CISMA POIANA BOTIZEI MINERALIZATIONS, BAI A MARE DISTRICT

GHEORGHE DAMIAN<sup>1</sup>, FLOAREA DAMIAN<sup>1</sup>, VLADIMIR A. KOVALENKER<sup>2</sup>,  
OLGA YU. PLOTINSKAYA<sup>2</sup>

<sup>1</sup> North University of Baia Mare, 62A Dr. Victor Babeş Street, 430083 Baia Mare,  
Romania; e-mail: gheorghe.damian@ubm.ro

<sup>2</sup> IGEM RAS, Moscow; e-mail: plotin@igem.ru

The metallogenetic activity in the Baia Mare district is associated to an intermediary calc-alkaline magmatism of Sarmatian – Pannonian age. The metallogenesis would correspond to a single stage for the entire district. Three phases of mineralization can be separated within this stage: copper, base-metal and gold-silver. These phases are clear within the polyascendent mineralizations and in the vein fields, where the zonality is well expressed.

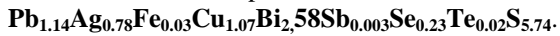
The mineralizations at Cisma are of the vein hydrothermal type, with a predominantly copper character, and would correspond to the copper stage. The mineralization can be found in paleogene sedimentary rocks, near the contact with intrusions of the microdioritic type. The sedimentary rocks are only partially affected by thermal transformations, being mainly affected by hydrothermal transformations, which do not exceed 2-3 m and consist of silicification, argilization and chloritization. The Cisma main vein has a length of over one km.

Pyrite and chalcopyrite are the dominant minerals, while galena and sphalerite appear especially in the upper and lateral parts of the veins. Rarely, the following also appear: stibnite, marcasite, arsenopyrite, oligist, magnetite, wolframite, tennantite-tetrahedrite, realgar, orpiment, bornite, covellite, cobaltite, pyrrhotite, together with some sulphosalts: semseyite, jamesonite, bournonite, boulangerite and native gold. Nonmetallic minerals are represented by quartz, amethyst, chalcedony, calcite, siderite, dolomite, barite, chlorite, and kaolinite. Native bismuth and bismuth sulphosalts have been emphasized through microscopical investigations and microprobe analyses (JCXA 8100 IGEM RAS, Moscow).

Native bismuth appears as *micronic* inclusions in lillianite – gustavite, associated with an intermediary component between galena and heyrovskite. The average composition of native bismuth for 4 analyses is as follows: Bi = 98.37%, Ag = 0.04%, Fe = 0.35%, Cu = 0.69%, Se = 0.02%, Te = 0.02%, Sb = 0.06%, As = 0.01%, S = 0.49%. What can be remarked is the high purity of native bismuth. The significant presence of copper and sulphur is attributed to the fact that native bismuth is included in chalcopyrite. Native bismuth is predominantly included in galenobismuthite, and to a lesser extent in lillianite –

gustavite. Native bismuth can be formed as a result of an exsolution, especially if we take into consideration the fact that the galenobismuthite has a bismuth shortage in its formula.

Bismuth sulphosalts are represented by lillianite – gustavite and an intermediary component between galena and heyrovskite. These appear as acicular inclusions in chalcopyrite, intimately overgrown between them, and they contain native bismuth inclusions. The empirical formula of lillianite – gustavite is the following:



The formula for the intermediary component galena – heyrovskite is the following:



Two metallogenetic models of epithermal Low sulphidation have been conceived for the Baia Mare district. These models do not contain the Cisma Poiana Botizei ore deposit. The latter would correspond to an epithermal model, intermediary between High sulphidation and Low sulphidation, due to the local context and to the mineralogical composition.

The bismuth sulphosalts are mentioned for the first time at Cisma Poiana Botizei and native bismuth is the first occurrence in the Baia Mare metallogenetic district.

## **USING THE HODOGRAM AS AN AVO ATTRIBUTE TO IDENTIFY ANOMALIES OF GAS**

MABROUK M. DJEDDI<sup>1</sup>, ABDELKADER A. KASSOURI<sup>1</sup>

<sup>1</sup> Université de Boumerdes, Faculté des Hydrocarbures et de la Chimie, Laboratoire de la Physique de la Terre (LABOPHYT)

In the present paper we study the causes of amplitude anomaly observed on true amplitude stacked seismic data in a southern Algerian gas field using AVO crossplot and hodogram analysis. We present an example associated with Carboniferous gas sandstones in the Sbaa basin.

The two factors that strongly determine the AVO behavior of sandstone reflections are the normal incidence reflection  $R(0)$ , called the intercept, and the relative change in amplitude with incidence angle and offset expressed by the gradient (G) that mostly depends on the contrast of Poisson's ratio at the reflector.

Traditional methods are based on the deviation of gas sands from the wet-sand/shale trend in an AVO crossplot, such as intercept and gradient. An inconvenience of this approach is that it neglects the seismic wavelet. When a wavelet is convolved with the reflection coefficients, each point on the AVO crossplot becomes a series of points, which typically spread across all four quadrants of the crossplot. This process gives an AVO hodogram in which the AVO particle motion is polarized along the background trend for nonanomalous events, and is polarized at angles different from the background trend for anomalous events. Consequently, it becomes apparent that the parameter defining an event in the hodogram is its polarization angle. This approach directly identifies class I-IV of AVO anomalies.

## ORGANIC GEOCHEMICAL CHARACTERISTICS OF HAFİK COAL DEPOSITS (SİVAS BASIN, TURKEY)

NAZAN YALÇIN ERIK<sup>1</sup>, SELİN SANCAR<sup>1</sup>

<sup>1</sup> Cumhuriyet University, Department of Geological Engineering, SİVAS, 58140, Turkey;  
e-mail: nyalcin@gmail.com

### Abstract

The present study provides organic geochemical data on Tertiary subbituminous coal of the Hafik area, the northwestern part of the Sivas Basin, Turkey. Rock-Eval analysis results show type II/III and III kerogens. The  $T_{\max}$  (°C) values range between 412 and 431 °C, with an average value of 422 °C, indicating that the samples are immature to early mature. The high proportions of long chain  $C_{27}$ - $C_{31}$  *n*-alkanes relative to the SOM contents of the *n*-alkanes are typical of higher terrestrial plants, while short chain *n*-alkanes (< $C_{20}$ ), detected in minor amounts, occur predominantly in algae and microorganisms. The organic geochemical data of the studied coaly and organic-matter-rich samples indicate the fact that the organic matter is present in sufficient amounts and that the samples are of the appropriate type, but that the rocks are characteristic of the early-mature and diagenetic stages.

**Key words:** Sivas Basin, Turkey, organic geochemistry, biomarker, Tertiary coals.

### Introduction

Limited, small-scale coal resources in Turkey have been mined by private companies but are insufficient to be exploited in an economic, industrial fashion. An ongoing increase in energy demand and costs requires that local sources be utilized much more efficiently, therefore geochemical studies aiming to determine hydrocarbon production capacities – especially from coals – have acquired great importance in Turkey (Yalçın et al., 2007).

The aims of the present study were to acquire detailed organic geochemical data (especially biomarker data) from borehole and surface samples, to perform a geochemical characterization of source-rock potential, and to determine the relationships between organic-geochemical and hydrocarbon data for the Hafik coal sequences.

### Geological Setting

The Sivas Basin, one of the largest basin in central Anatolia, is located within a collision zone; it developed mainly after the closure of the northern branch of Neotethys in the Early Tertiary (Görür et al., 1998). The Upper Paleocene-Lower Eocene Bahçecik conglomerate rests unconformably on the Upper Cretaceous Tekelidağı mélangé; these units are overlain by the Hafik Formation (Fig. 1). The studied coal seams are located at the base of the Bahçecik Formation. These are exposed in the Bahçecik village, northeast of the town of Hafik (Fig. 1). The coal resources of this area are exploited through open-cast mining.

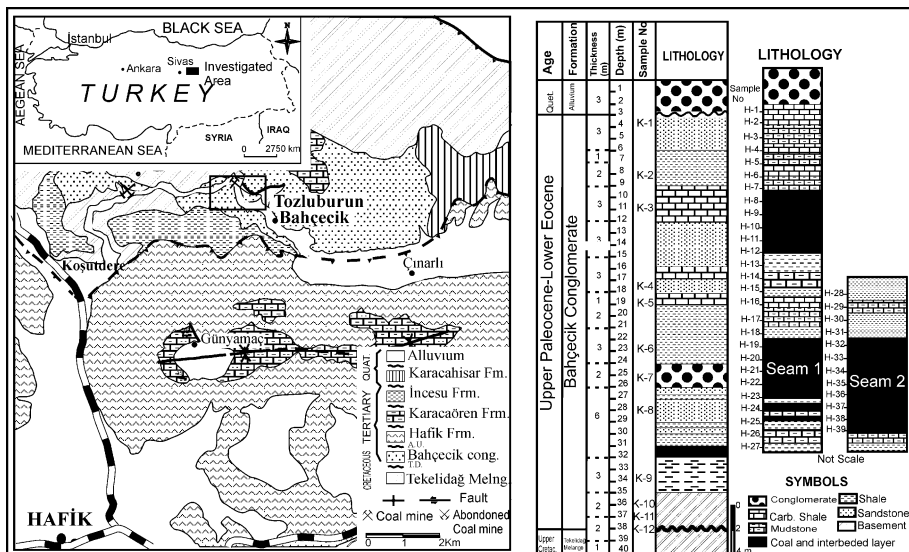


Fig.1 Generalized geological map and coal seams and drill section of investigated area (map modified Temiz, 1994)

### Sampling and Analytical Procedures

In order to define the organic geochemistry of the coals, TOC-Rock-Eval pyrolysis studies were performed on selected samples. For biomarker analyses, four representative coal samples were extracted for approximately 40 h using Dichloromethane in an ASE 300. Following extraction, the yields were analyzed through Agilent 6850 whole-extract gas chromatography (TPAO Research Group laboratories in Ankara, Turkey, according to ASTM D 5307-97, 2002). The saturate fractions were also analyzed using an Agilent 7890A/5975C GC-MS spectrometer.

## Results

### 1. Organic Geochemical Determinations

TOC contents vary from 0.32 to 72.45 wt.%, with an average TOC content of 28.32 wt.%. The total organic-carbon contents of the shale and carbonate intervals are between 0.32 and 16.11 wt.%, while those of the coaly levels are between 38.42 and 60.70 wt.% (Tab. 1).

### 2. Type of Organic Matter

Cross plots of hydrogen index and oxygen index on van Krevelen and HI vs  $T_{\max}$  diagrams (Fig. 2) prove that most of the samples are scattered in the type II - III mixed and type III areas (some marine/algal input). In particular, the coaly samples in Fig. 2 tend to be different from the samples rich in organic materials, and are thus distributed especially in the type III kerogen and immature fields. In gas chromatograms, there is no evidence of lower carbon *n*-alkane distribution and there are no *n*-alkanes of carbon number higher than  $C_{32}$  that would be indicative of both marine and terrestrial organic-matter input. Biomarker analysis data indicate that *n*-alkane distributions are dominated by the occurrence of high molecular-weight ( $C_{20+}$ ) *n*-alkanes and a distinct odd-even carbon number preference over the  $C_{25}$ - $C_{31}$  range typical of organic matter derived from higher terrestrial plants. Furthermore, the predominance of  $C_{29}$  sterane over  $C_{27}$  and  $C_{28}$  indicates a terrestrial source.

Tab. 1 Total Organic Carbon (TOC) and Rock - Eval pyrolysis results for the Hafik coal area

Sample	TOC	S1	S2	S2/S3	$T_{\max}$	HI	OI	PI	PY
H-1	16.11	0.32	46.97	4.7	430	292	62	0.01	47.29
H-3	26.31	0.56	68.20	4.65	430	259	56	0.01	68.76
H-5	8.03	0.20	30.98	7.83	431	386	49	0.01	31.18
H-9	10.26	0.77	10.67	3.95	423	104	26	0.07	11.44
H-10	43.59	1.13	50.54	5.68	417	116	20	0.02	51.67
H-16	0.75	0.03	0.75	1.15	426	100	87	0.04	0.78
H-19	40.58	0.93	54.68	6.82	418	135	20	0.02	55.61
H-22	70.49	1.07	108.54	8.85	412	154	17	0.01	109.61
H-25	60.57	1.45	78.30	5.48	418	129	24	0.02	79.75
H-29	23.75	1.18	95.49	19.5	426	402	21	0.01	96.67
H-31	14.18	0.54	62.73	18.24	429	442	24	0.01	63.27
H-34	63.76	0.81	69.25	4.7	424	109	23	0.01	70.06
H-37	57.25	1.20	97.66	8.3	419	171	20	0.01	98.86
H-39	72.45	1.15	125.85	10.5	417	174	16	0.01	127.0
K-6	0.32	0.01	0.07	0.13	418	22	172	0.15	0.08
K-8	0.51	0.02	0.21	0.48	426	41	86	0.08	0.23
K-10	0.48	0.03	0.08	0.11	416	17	152	0.31	0.11
K-12	0.41	0.02	0.09	0.1	418	22	210	0.02	0.36

### 3. Organic Maturity

The  $T_{\max}$  ( $^{\circ}\text{C}$ ) values range between 412 and 431  $^{\circ}\text{C}$ , with an average value of 422  $^{\circ}\text{C}$ , indicating that the samples are immature to early mature. On the HI vs  $T_{\max}$  diagram (Fig.

2), most of the samples plot in the early mature and immature zones. Moreover, the same samples have PI values < 0.10 and most of the samples suggest an immature-zone assignment.

$20(S)/(20S+20R)$ ,  $5\alpha$  (H),  $14\beta$  (H),  $17\beta$  (H)  $C_{29}$  sterane and  $5\alpha$  (H),  $14\alpha$  (H),  $17\alpha$  (H)  $C_{29}$  sterane ( $\alpha\beta\beta / \alpha\beta\beta + \alpha\alpha\alpha$ ), CPI ratios indicate immature zone, and that observation is in agreement with our  $T_{max}$  values.

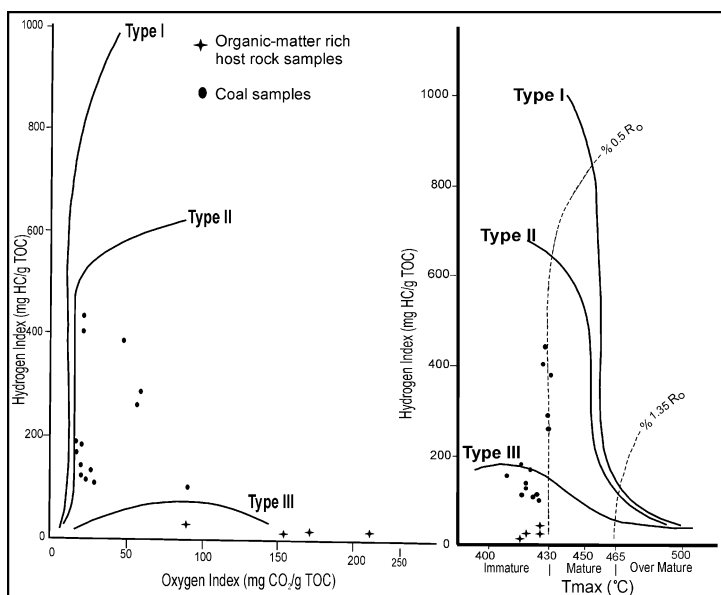


Fig. 2 Plots of Hydrogen Index vs Oxygen Index, b) Hydrogen Index vs. Tmax

#### 4. Hydrocarbon Generative Potential

Generally, the samples are characterized by lower S1 and S2 values, on the order of 50 mg HC/g rock of sample. Potential yield values range between 0.1 and 127 mg HC/g rock. S2/S3 values for five of the studied samples have values lower than 2, suggesting that the samples may have extremely limited gas-generation potentials (Tissot and Welte, 1984; Hunt, 1995). The S2/S3 values of the other samples are higher than 2 and their PI values < 0.1, indicating that the samples could produce liquid hydrocarbons, but that the  $T_{max}$  values indicate immaturity (Tab. 1).

#### 5. Molecular Composition of Coals

In order to determine the biomarker characteristics of the aliphatic fractions, GC and GC-MS analyses were performed on the studied samples. The relative proportions of the hydrocarbons in the SOM from the samples are low (77-5412 ppm), consistent with the low maturity of the organic matter. The SOM is mainly composed of resins and asphaltenes.

The *n*-alkanes for the studied samples range from C<sub>20</sub> to C<sub>32</sub>. In the present study, the high proportions of long chain C<sub>27</sub>-C<sub>31</sub> *n*-alkanes relative to the SOM of the *n*-alkanes are typical of higher terrestrial plants, while short chain *n*-alkanes (<C<sub>20</sub>), detected in low amounts, are predominantly found in algae and microorganisms. The studied samples are dominated by intermediate- and high-molecular weight *n*-alkanes (C<sub>21</sub>-<sub>25</sub>). These data indicate derivation from terrestrial and lagoonal organic matter. According to Bray and Evans (1961), our CPI values (C<sub>16</sub>-C<sub>26</sub>) range from 0.94 to 2.74.

### 6. Steroids, Hopanoids

The major biomarkers are C<sub>25</sub> (22S+22R) Tricycliterpane, C<sub>24</sub> Tetracycliterpane (seco), C<sub>26</sub> 22R Tricycliterpane and C<sub>28</sub> Tricycliterpane. The presence of these triterpanoids in these samples supports their higher plant origins, and the presence of gammacerane also indicates a hypersaline depositional environment. From the m/z 217 mass chromatograms of our samples, the relative abundances of the C<sub>27</sub>, C<sub>28</sub>, and C<sub>29</sub> steranes and their 20S and 20R epimers have been determined (Tab. 2) (Fig. 3).

Tab. 2 Biomarker parameters calculated from m/z 191 and m/z 217 mass chromatograms

Biomarker Parameters	Sample		
	H-22	H-32	H-39
Sterane/Hopane Ratio	0.14	1.72	0.71
C <sub>32</sub> 22S/(22S+22R) Ratio	0.36	0.21	0.26
Moretane/Hopane Ratio	0.37	0.47	0.30
C <sub>29</sub> /C <sub>30</sub> Hopane Ratio	0.58	0.67	0.59
Ts/(Ts+Tm) Ratio	0.65	0.34	-
C <sub>23</sub> /C <sub>24</sub> Ratio	0.94	1.68	1.26
Gammacerane Index	1.04	1.64	2.21
Diasterane/Sterane Index	4.20	2.89	3.62
C <sub>29</sub> 20S/(20S+20R) Ratio	0.29	0.44	0.27
% C <sub>27</sub>	43	40	48
% C <sub>28</sub>	14	14	20
% C <sub>29</sub>	44	46	32
C <sub>27</sub> /C <sub>29</sub>	0.98	0.86	1.5
C <sub>28</sub> /C <sub>29</sub> Sterane Ratio	2.41	0.30	2.78
C <sub>25</sub> /C <sub>26</sub> Tricyclic Terpane	1.11	1.07	0.9
αββ/(αββ+ααα) Sterane Ratio	0.11	0.13	0.11
CPI (Bray and Evans, 1961)	-	0.94	2.74
Total extract (ppm)	5412	3999	4214

C<sub>28</sub> steranes and C<sub>28</sub> diasteranes occur in very low quantities (C<sub>27</sub>>C<sub>29</sub>>C<sub>28</sub>). Algae have been proposed as the predominant primary producers of the C<sub>27</sub> sterols, while the C<sub>29</sub> sterols are more typically associated with land plants (Peters and Moldowan, 1993). Moreover, the richness in C<sub>27</sub> indicates a lagoonal environment and algal organic material in that environment. C<sub>30</sub> hopane is more abundant than C<sub>29</sub> norhopane. Oleanane was not detected, indicating that there was not a significant angiosperm contribution to the organic matter (Peters et al. 2004).

## Conclusions

Organic geochemical investigations of the Tertiary Hafik coals (Sivas Basin, Turkey) led to the conclusions that follow. High SOM contents were obtained from samples; the SOMs comprise mainly resins and asphaltenes. The *n*-alkanes are the dominant components of the saturated hydrocarbon fractions and range from C<sub>20</sub> to C<sub>32</sub>. The presence of C<sub>25</sub>, C<sub>24</sub>, C<sub>26</sub> and C<sub>28</sub> triterpanoids and the predominance of C<sub>29</sub> sterane over C<sub>27</sub> and C<sub>28</sub> indicate a terrestrial source. The studied samples are dominated by intermediate- and high-molecular weight *n*-alkanes (C<sub>21-25</sub>), and these data indicate a derivation from terrestrial and lagoonal organic matter. Based on these data, the studied coals are believed to have been deposited in a limnic environment which was periodically influenced by marine and fresh-water sources. The organic geochemical data of the studied coaly and organic-matter-rich samples indicate the fact that the organic matter is present in sufficient amounts and that the samples are of the appropriate type, but that the rocks are characteristic of the early-mature and diagenetic stages.

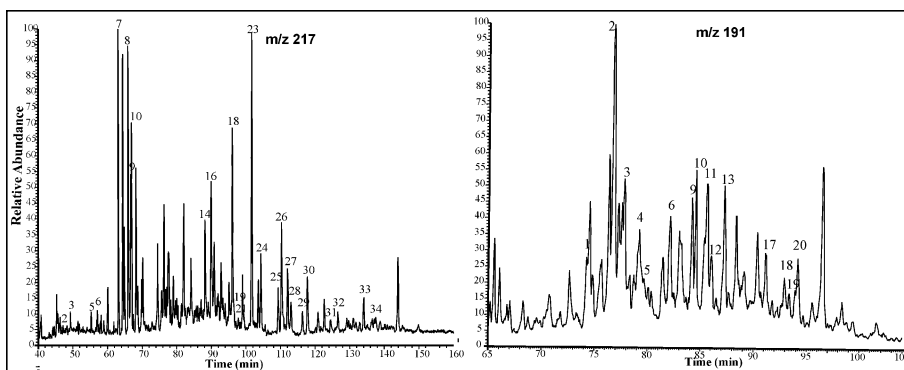


Fig. 3 m/z 217 and m/z 191 mass chromatograms of investigated coal samples

## Acknowledgments

The present work was financially supported by the Scientific Research Project Fund of Cumhuriyet University, Project Number M-319. The authors are grateful to Prof. Dr. M. Namık YALÇIN, Dr. Dursun Erik, Kayhan Pamuk and Dr. Steven Mittwede.

## References

American Society for Testing and Materials (ASTM) D5307-97, 2002. Standard Test Method for Determination of Boiling Range Distribution of Crude Petroleum by Gas Chromatography. In: 2004 Annual Book of ASTM Standards, Gaseous Fuels; Coal and Coke, vol. 05.06. ASTM, Philadelphia, PA, 245–247.

- Espitalié, J., Deroo, G., Marquis, F., 1985. La pyrolyse Rock-Eval et ses applications (deuxième partie). *Revue Institut Français du Pétrole* 40, 755–784.
- Görür, N., Tüysüz, O., Şengör, A.M.C., 1998. Tectonic evolution of the Central Anatolian basins. *International Geology Review* 40, 831–850.
- Hunt, J.M., 1995. *Petroleum Geochemistry and Geology*. W.H. Freeman & Company: New York, 743 p.
- Peters K.E., Moldowan, J.M., 1993. *The Biomarker Guide: Interpreting Molecular Fossils in Petroleum and Ancient Sediments*: Prentice-Hall, Englewood Cliffs, NJ. 363 p.
- Peters, K.E., Walters, C.C., Moldowan, J.M., 2004. *The Biomarker Guide - Volume 2: Biomarkers and Isotopes in Petroleum Exploration and Earth History* (2nd ed.). Cambridge University Press, 475–1155.
- Temiz, H., 1994. Tectonostratigraphy and tectonic deformation style in the Kemah-Erzincan and Hafik-Sivas areas of the Sivas Tertiary Basin. Unpublished doctoral dissertation, C.U. Sivas - Turkey, 239 p (in Turkish).
- Tissot, B.P., Welte, D.H., 1984. *Petroleum Formation and Occurrence*. Springer-Verlag: Berlin, 699 p.
- Yalçın, M.N., Schaefer, R.G., Mann, U., 2007. Methane generation from Miocene lacustrine coals and organic-rich sedimentary rocks containing different types of organic matter. *Fuel* 86 (4), 504–511.

## **HYDROGEOLOGICAL STUDY FOR THE SUPPLY WITH WATER OF THE GLĂVĂNEȘTI AND GĂICEANA LOCALITIES (BACĂU COUNTY)**

VIOREL IONESI<sup>1</sup>, MIHAELA CORINA MERFEA<sup>1</sup>, CIPRIAN APOPOEI<sup>1</sup>

<sup>1</sup> „Al. I. Cuza” University of Iași, Department of Geology, 20A Carol I Blv., 700505 Iași,  
Romania; e-mail: vion@uaic.ro

The present paper aims to identify and describe the sources of drinking water in the Găiceana and Glăvănești localities, located in the Bacău county. Therefore, a borehole was drilled and then investigated hydrodynamically in stationary and non-stationary flow of aquifer water. As a result of the research, the hydrogeologic parameters were estimated, in an attempt to avoid, through the “trial and error” method, any confusion that may occur in estimating the “K” filtration coefficient and the radius of influence in stationary flow. After the determination of the hydrological parameters, we proceeded to the estimation of the optimal drilling flow and, implicitly, of the optimal level oscillation. In the end, the areas of sanitary protection and the hydrogeological protection perimeter were established.

## THE PANXI REGION (SW CHINA) – STRUCTURE, MAGMATISM AND METALLOGENESIS

MARIAN MUNTEANU<sup>1,2</sup>, GORDON CHUNNETT<sup>2</sup>, YONG YAO<sup>3</sup>, ALLAN WILSON<sup>2</sup>,  
YAONAN LUO<sup>3</sup>

<sup>1</sup> Geological Institute of Romania, Bucharest, 012271, Romania; e-mail:  
munteanu.marian@igr.ro; marianmunteanu2000@yahoo.com

<sup>2</sup> University of the Witwatersrand, Johannesburg, Wits 2050, South Africa; e-mail:  
gchunnett@yahoo.com; allan.wilson@wits.ac.za

<sup>3</sup> Sichuan Bureau of Geology and Mineral Resources, Chengdu, 610081, China; e-mail:  
cdyongyao2007@yahoo.com

**Keywords:** Ni-Cu(PGE) deposits, Fe-Ti-V deposits, Permian, Yangtze craton, China.

### Introduction

The Panzhihua-Xichang (Panxi) region is a tectono-magmatic province located in the western part of the Yangtze craton (fig. 1). In its present-day configuration, the Panxi rift is elongated on the north-south direction, from the north-western part of the Sichuan Province to Vietnam. The interest for the Panxi region derives from its good potential for platinum group elements (PGE), which resulted from the combined effects of magmatism and tectonics.

### Structure

The Panxi region is defined by NS-striking faults (fig. 2) and is considered a continental rift (CGGCJ 1986; 1988; Zhang et al., 1990), with the major crustal extension taking place in the Permian. It is notable that the Panxi region is superimposed on a late Proterozoic back-arc extension. That older extension probably favoured the genesis of the Permian rift, creating the tectonic lineaments and thinner crust that determined its location and its geometry. After the Permian, the Panxi region was subjected to compression, which determined the uplift of its central and western parts. Its most uplifted zone is known as the Kangdian rise (fig. 2).

### Magmatism

The most widespread and best known magmatic rocks associated with the Panxi region are the Emeishan flood basalts, considered to make up a large igneous province. The Emeishan basalts (260 Ma old) are up to ca. 6000 m thick and extend across an area

considerably larger than the structural framework of the Panxi region (fig. 2). There are numerous intrusions associated with the Permian crustal extension in the Panxi region and with the Emeishan basalts. These Permian intrusions display varied petrography and chemical compositions: peridotite, pyroxenite, gabbro, syenite, alkaline granite.

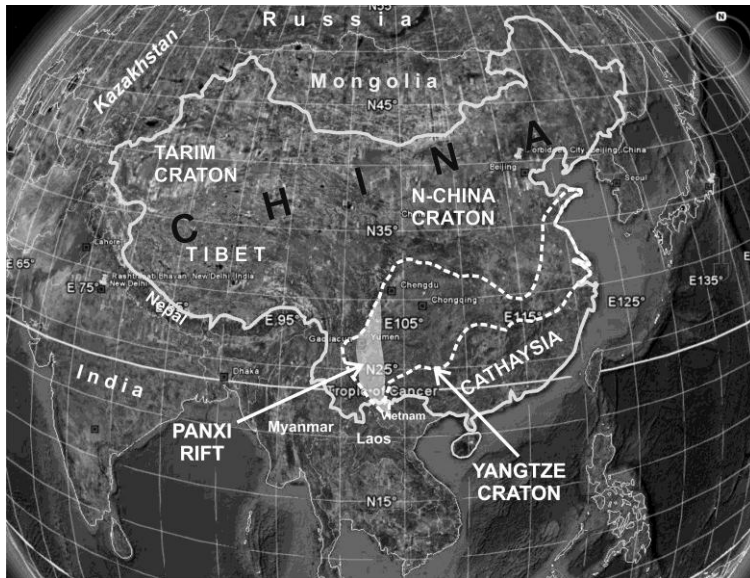


Fig. 1 Location of the Panxi region in China

## Mineralization

There are two types of magmatic deposits in the Panxi region: Fe-Ti-V oxide deposits and Ni-Cu(-PGE) sulfide deposits. The Fe-Ti-V deposits (Panzhihua, Baima and Taihe) are hosted in gabbroic intrusions. The Ni-Cu(-PGE) deposits (e.g. Yangliuping, Jinbaoshan, Baimazhai and Limahe) are hosted by ultramafic intrusions (pyroxenite and peridotite), sometimes with gabbro or diorite zones. There is evidence of the accumulation of the ultramafic rocks and Ni-Cu(-PGE) ore in magmatic conduits (Wang et al., 2005; 2006; Tao, 2007; Zhu et al., 2007). Two intrusions (Hongge and Xinjie) contain both ultramafic rocks with Ni-Cu-PGE sulfide ore, and gabbros with Fe-Ti-V accumulations.

## Spatial distribution and genesis of ore deposits

There is a spatial separation between the Fe-Ti-V oxide deposits and Ni-Cu(-PGE) sulfide deposits (fig. 2), which can be used to define an "iron zone" and a "base metal  $\pm$  PGE zone". It is notable that the Permian ore deposits occur within the structural limits of the Kangdian rise and west of it (fig. 2), with no deposit east of the Kangdian rise. Such a

distribution was induced by the tectonic uplift of the Kangdian rise and of the area west of it.

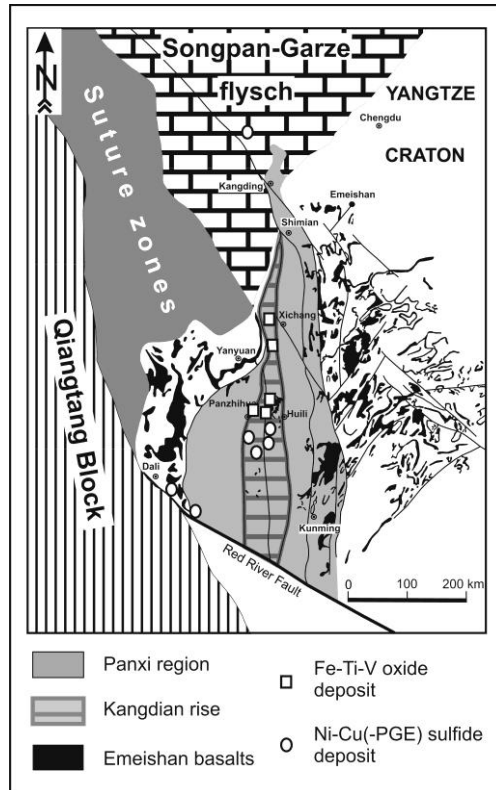


Fig. 2 The location of the Panxi region, Kangdian rise and main ore deposits related to the Permian magmatism. Background tectonic map of the western part of the Yangtze craton and adjacent areas after Zhang et al. (1990), with simplifications

The Kangdian rise contains both sulfide and oxide deposits, emplaced in Proterozoic country rocks; west of the Kangdian rise, only sulfide deposits occur, and these have Paleozoic country rocks. Therefore, the oxide deposits are restricted to Proterozoic country rocks, while the sulfide deposits are present both in Proterozoic and in Paleozoic rocks. This suggests that the location of the oxide deposits at stratigraphic levels is somehow lower than that of the sulfide deposits.

We infer that the oxide deposits were related to magmas that could not reach shallower levels and solidified within Proterozoic rocks. The sulfide deposits would have been formed

through the accumulation of mafic minerals and sulfide melt in wide zones of magmatic conduits. Ascending rapidly through magmatic conduits, the magmas parental to the sulfide deposits did not assimilate important volumes of crustal rocks deep within the crust, thus reaching sulfide saturation only at relatively shallow depths. This allowed the preservation of the initial PGE-undepleted character of the magmas and resulted in the numerous intrusions with PGE-rich mineralization relatively close to the surface.

## References

- CGGJC (Co-operative Geological Group of Japan and China in the Panxi Region), 1986. Geology of the Panxi region, Sichuan Province, southwest China. 340p. Yamaguchi University, Japan.
- CGGJC (Co-operative Geological Group of Japan and China in the Panxi Region), 1988. Petrotectonics of Panzihua-Xichang Region, Sichuan Province, China. 158p. China Ocean Press, Beijing.
- Tao, Y., Li, C., Hu, R., Ripley, E.M., Du, A., Zhong, H., 2007. Petrogenesis of the Pt–Pd mineralized Jinbaoshan ultramafic intrusion in the Permian Emeishan Large Igneous Province, SW China. *Contrib. Mineral. Petrol.* **153**, 321–337.
- Wang, C.Y., Zhou, M.-F., Zhao, D.G., 2005. Mineral chemistry of chromite from the Permian Jinbaoshan Pt–Pd-sulfide-bearing ultramafic intrusion in SW China with petrogenetic implications. *Lithos*, **83**, 47–66.
- Wang, C.Y., Zhou, M.-F., Keays, R.R., 2006. Geochemical constraints on the origin of the Permian Baimazhai mafic-ultramafic intrusion, SW China. *Contrib. Mineral. Petrol.*, **152**, 309–321.
- Zhang, Y., Luo, Y., Yang, C. (Eds), 1990. Panxi Rift and its geodynamics. Geological Publishing House, Beijing, 415p.
- Zhou, M.F., Arndt, N.T., Malpas, J., Wang, C.Y., Kennedy, A.K., 2008. Two magma series and associated ore deposit types in the Permian Emeishan large igneous province, SW China. *Lithos*, **103**, 352–368.
- Zhu, D., Xu, Y.G., Luo, T.Y., Song, X.Y., Tao, Y., Huang, Z.L., Zhu, C.M., Cai, E.Z., 2007. A conduit of the Emeishan basalts: the Zhubu mafic-ultramafic intrusion in the Yuanmou area of Yunnan Province, China. *Acta Mineralogica Sinica*, **27**, 3/4, 273–280. (In Chinese with English Abstract).

## HYDROGEOLOGICAL RESEARCH REGARDING THE BEȘTEPE-MAHMUDIA AREA, TULCEA COUNTY

TUDOR MUNTEANU<sup>1</sup>, EMILIA MUNTEANU<sup>2</sup>, MARIA CĂLIN<sup>1</sup>, DOINA DRĂGUȘIN<sup>1</sup>, RODICA MACALEȚ<sup>1</sup>, GEORGE DUMITRAȘCU<sup>1</sup>

<sup>1</sup> National Institute of Hydrology and Water Management, 97, București-Ploiești Road, 013686 Bucharest, Romania; e-mail: tudor.munteanu@hidro.ro; mimi.calin@yahoo.com; rmacalet@yahoo.fr; george.dumitrascu@hidro.ro

<sup>2</sup> National Agency for Mineral Resources, 36-38, Mendeleev Str., 010366 Bucharest, Romania; e-mail: emilia@namr.ro

**Keywords:** Beștepe-Mahmudia area, Paleozoic-Quaternary deposits, aquifers, water supply.

The Beștepe-Mahmudia area is located in the eastern part of Tulcea county. Geomorphologically, this area is situated at the boundary between the Tulcea Hills and the Danube Delta. Geologically, in the Beștepe-Mahmudia area, Late Paleozoic magmatic rocks, as well as Devonian, Triassic and Quaternary sedimentary deposits, crop out. Structurally, the study area pertains to the northeastern extremity of the Northern Dobrogea Orogen (the Tulcea Nappe subunit), in the proximity of its boundary with the Scythian Platform. Hydrogeologically, the field investigations and analyses of the wells drilled in the Beștepe-Mahmudia area have led to the identification of two formation types: aquiferous (interstitial and fissural), and impervious. Based on data resulted from the wells, a confined aquifer located in the Devonian and Triassic deposits, and a phreatic aquifer, hosted in the upper levels of the Triassic deposits, as well as in the Quaternary ones, have been revealed. The second aquifer displays a large surface, developing both in the hilly and in the meadow areas. Referring to the regional flow of the phreatic aquifer, the drainage process towards the Sfântu Gheorghe branch of the Danube river has been identified. Thus, the groundwaters flow locally from south to north, namely from the Beștepe hills to the Danube Delta, with a higher hydraulic gradient; the flow from northwest to southeast generally has a lower hydraulic gradient.

**THE GEOCHEMICAL RELATIONSHIP BETWEEN THE COPPER MINERALIZATIONS AND THEIR REE PATTERNS: AN EXAMPLE FROM LYCIAN ALLOCHTHON, ÇAVDIR (BURDUR), SW TURKEY**

ZEYNEP ORU<sup>1</sup>, HASAN EMRE<sup>1</sup>

<sup>1</sup> Istanbul University, Department of Geological Engineering, 34230 Istanbul, Turkey; e-mail: zynporu@istanbul.edu.tr

This paper presents the geochemical relationship between the alteration of copper mineralizations and their contents of rare earth elements. In the studied area, ophiolitic rocks of the Lycian Allochthon occur at the surface; however, the ophiolite sequence is inverted as the higher hills of the perimeter is surrounded by ultramafic rocks, while the lower slopes of the area are surrounded by a sheeted dyke complex, containing copper mineralizations. This geological environment and the products of alteration of the copper minerals (azurite, malachite) could imply a Cyprus-type copper deposit, even though pillow-lavas, known as host-rock of this ore-type, are absent in the area of study. This area gives important data regarding the lower parts of a Cyprus-type copper deposit.

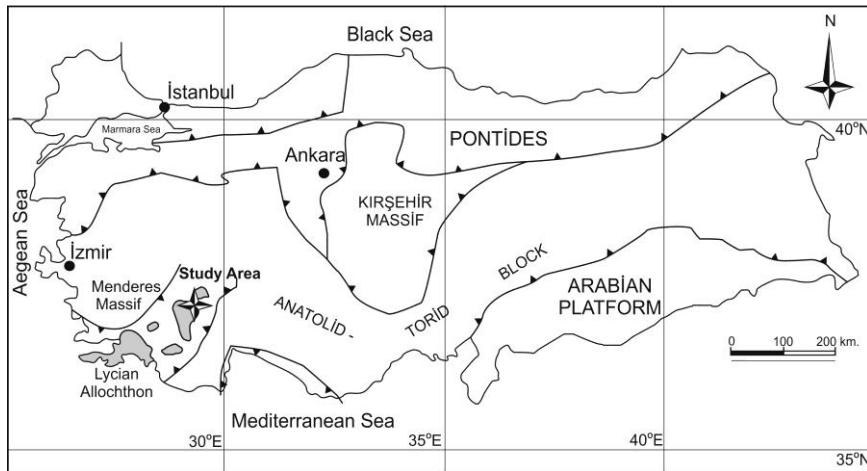


Fig. 1 Tectonic map of Turkey and the location of the studied area (modified from Okay and Tüysüz, 1999, and Akbulut and Pişkin, 2008)

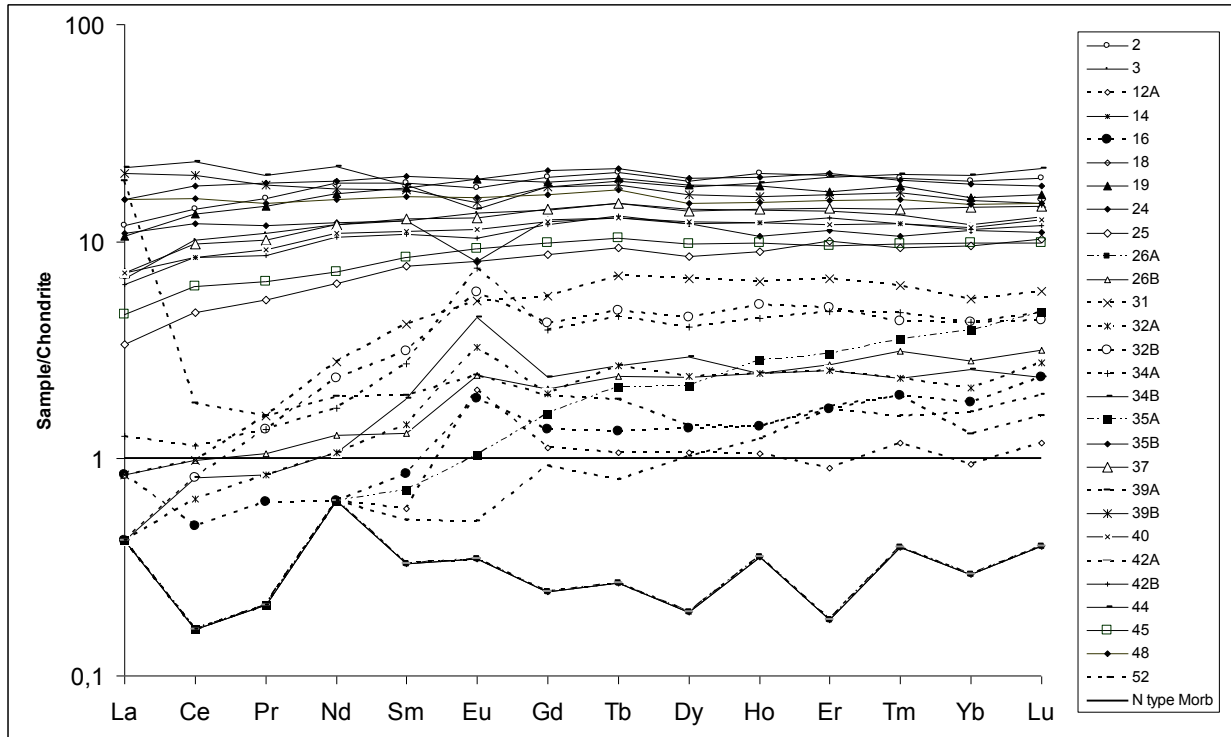


Fig. 2 Chondrite-normalized REE diagrams. Samples with amounts below the detection limit are accepted as having limit values. In the sample names, letter A symbolizes copper-rich rocks, and B symbolizes the host-rocks. Copper-rich samples are figured with dashed lines.

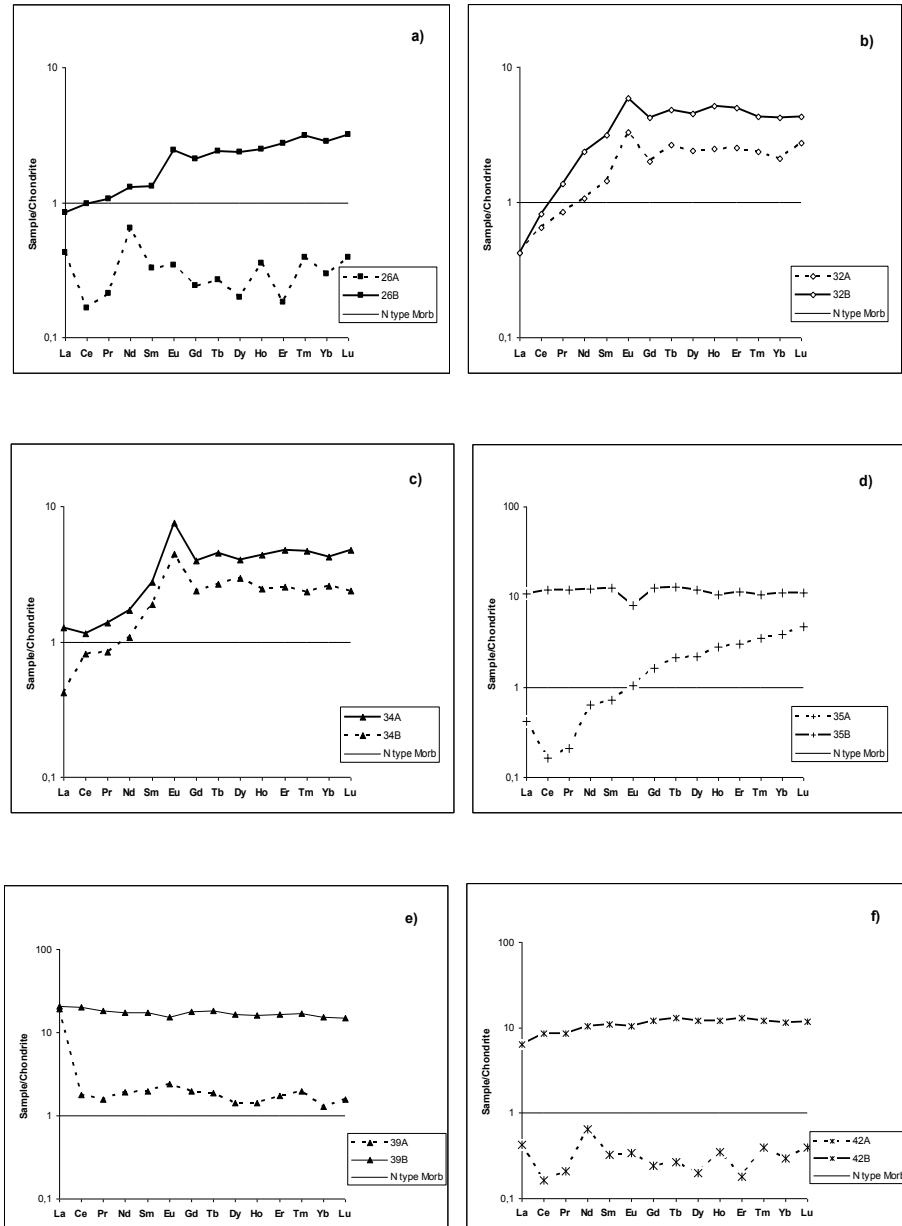


Fig. 3 Chondrite-normalized REE diagrams of the copper-rich and barren samples. In the sample name, A symbolizes the copper rich rocks, and B symbolizes the host rocks.

Ore-rich and barren host-rocks are compared according to their rare earth elements contents, and they showed different patterns. The data of non-altered host-rocks of the area occupy positions in the upper part of the REE diagrams, as they show relatively higher amounts of rare earth elements. These host-rocks have almost flat M-HREE patterns, with a slight L-REE depletion for most of them.

The most notable anomaly is that of Eu and it is generally associated with the crystallization of the plagioclase. The negative anomaly of Ce is notable for the copper-rich samples, fact that is associated by Rigby et al. (2002) with altered oceanic crust or oceanic sediments. The very high La content of sample 39A is associated with the talc mineral term, which was identified in the petrographical studies.

## References

- Akbulut, M., Pıksin, Ö., 2008. Preliminary investigations on a recently discovered copper mineralization in the Lycian Nappes, SW Turkey. *Ofioliti*, **33**/2, 87–93.
- Okay, A.I., Tüysüz, O., 1999. Tethyan sutures of northern Turkey. *The Mediterranean Basins: Tertiary extension within the Alpine orogen*. In: Durand, B., Jolivet, L., Horváth, F., Séranne M., (Eds.), Geological Society, London, Special Publication, **156**, 475–515.
- Rigby, S.J., Streck, M.J., Conrey, R.M., 2002. Origin of the Ce anomaly in a green ridge lava flow, Cascade range, Oregon. *GSA Abstracts with Programs*, **34**/5, A–28.
- Sun, S.S., McDonough, W.F., 1989. Chemical and isotopic systematics of oceanic basalts: implications for mantle composition and processes. In: Saunders, A.D., Norry, M.J., (Eds.), *Magmatism in Ocean Basins*. Geological Society of London, Special Publication, **42**, 313–345.

## REE CONTENTS AND BEHAVIORS OF PLACERS BELONGING TO THE BOZKIR OPHIOLITIC MELANGE IN BOZKIR COUNTY (KONYA-TURKEY)

ALICAN OZTURK<sup>1</sup>, FETULLAH ARIK<sup>1</sup>, M. MUZAFFER KARADAG<sup>1</sup>, YESIM BOZKIR OZEN<sup>1</sup>

<sup>1</sup> Selcuk University, Department of Geological Engineering, Konya, Turkey;  
e-mail: alicanozturktr@gmail.com; acan@selcuk.edu.tr

**Keywords:** Bozkir, Bozkir ophiolitic mélange, REE, placer.

The study area, located southeast of Konya City, Bozkir County, in Central Anatolia, covers a surface of approximately 250km<sup>2</sup>. In the region, the tectonostratigraphic sequence includes, from bottom to top, the Geyikdağı, Bozkır and Bolkardağ tectonic units. The lowermost unit is the autochthonous unit of Geyikdagi, consisting of the Seydisehir Formation (Upper Cambrian-Lower Ordovician), the Hacialabaz Formation (Upper Jurassic), the Cokelen diabases (Upper Cretaceous), and the Saytepe Formation (Upper Cretaceous). The Bolkardagi unit consists of the Hocalar Formation (Devonian-Lower-Middle Carboniferous), the Taskent Formation (Upper Permian), and the Sinatdagi formation (Jurassic-Upper Cretaceous); it rests allochthonously on the Geyikdagi unit. The Bozkir unit (the Bozkir mélange of ophiolite and various aged carbonate blocks) is also overthrust by the Bolkardagi unit.

The Bozkir unit crops out along a NE-SW direction in the area, and it consists of the Bozkir ophiolitic mélange (serpentinite, pyroxenite, gabbro, radiolarite, chert, limestone) and of the Boyalitepe group (limestones with different lithologies, facies and ages). The aim of the present study was the investigation of Rare Earth Elements (REE) in stream sediment samples of the Bozkır ophiolitic mélange; for this purpose, 62 placer samples were collected from the Bozkir ophiolitic mélange. During the sampling process, samples of approximately 10-20 kg were taken from the main streams and branches close to the main stream; a hand-type GPS was used as well.

After washing operations were performed on the samples, the latter were kept for 4 hours in an oven, at a temperature of 80°C. All samples were passed through a series of sieves, of 0.5 mm, 0.425 mm, and 0.106 mm, respectively. Chemical analyses were performed using the ICP-AES technique, at the ACME Analytical Laboratories of Vancouver (Canada).

According to these analyses, the most REE-rich samples were accumulated in the bottom pot (smaller than 0.106 mm); there were a total of 121.57ppm RRE (bottom pot), 117.37ppm RRE (0.106 mm sieve), and 116.64ppm RRE (0.425 mm sieve). In the bottom

pot, the amount of light REE ( $LREE_{La-Sm}$ : 105.49 ppm) is 6.65 times greater than the amount of heavy REE ( $HREE_{Eu-Lu}$ : 15.85 ppm). The average REE of the placers is higher than that of the standard reference rocks, such as peridotites, chondrites, primitive mantle, upper crust, basalts and MORB. In addition, the average REE amounts of placers are lower than those of NASC and PAAS. Some element ratios of placers were normalized with the same elements of the peridotites and chondrites:  $(La/Lu)_{N(peridotite)} = 6.05$ ;  $(Gd/Yb)_{N(peridotite)} = 1.19$ ;  $(Eu/Eu^*)_{N(peridotite)} = 0.71$ ;  $(Ce/Ce^*)_{N(peridotite)} = 0.93$ ;  $(La/Lu)_{N(chondrite)} = 5.44$ ;  $(Gd/Yb)_{N(chondrite)} = 1.22$ ;  $(Eu/Eu^*)_{N(chondrite)} = 0.78$ ;  $(Ce/Ce^*)_{N(chondrite)} = 0.96$ . The higher  $Eu^*$  and lower  $Ce^*$  anomalies suggest that the placers from the studied area were affected by surficial processes.

## References

- Ozturk, A., Karadag, M.M., Ayhan, A., Copuroglu, I., 2007. Investigation of heavy metals containing platinum in placers derived from ophiolitic rocks in around the Bozkır (Konya). *Geology Symposium of Kapadokya, Nigde*, p.193.
- Ozturk, A., 2008. Importance of Bozkır (Konya) in ore deposit. *Journal of Ipek Yolu*, **21**, 249, 38–3.
- Ozturk, A., Karadag, M.M., Deli. A., 2008. Stratigraphy of East and South of Bozkır (Konya) Region. *Journal of Enginnering and Architecture Faculty, Konya-Turkey*.
- Ozturk, A., Karadag, M.M., Ayhan, A., Arik, F., 2008. Geological setting and petrographical characteristics of the Bozkır ophiolitic melange, Bozkır (Konya -Turkiye). *Proceeding Volume 1 of 8th International Scientific Conference, SGEM 2008, Bulgary*, 81–82.
- Ozturk, A., Karadag, M.M., Arik, F., Ayhan, A., Bozkır, Y., 2008. Geostatistical and geochemical approach to Bozkır ophiolitic melange belonging to Bozkır Unit (Bozkır - Konya). *III. National Geochemistry Symposium, (TUBITAK - BUTAL), Bursa, Turkey*, 11–12.
- Ozturk, A., Karadag, M.M., Arik, F., 2009. Geochemical investigation of precious and heavy metals in the placers belonging to Bozkır Ophiolitic Melange (Bozkır-Konya-Turkey). *Mafic-ultramafic complexes of folded regions and related deposits. Institute of Geology and Geochemistry UB RAS*, **1**, Ekaterinburg, p. 28.

## THE ADVANTAGES OF USING THE MONTE CARLO SIMULATION METHOD IN ESTIMATING GEOLOGICAL GAS RESERVES

MIHAI REMUS ȘARAMET<sup>1</sup>, CONSTANTIN CĂTĂLIN CALU<sup>1</sup>, GABRIEL CHIRILĂ<sup>1</sup>

<sup>1</sup> „Al. I. Cuza” University of Iași, Department of Geology, 20A Carol I Blv., 700505 Iași, Romania; e-mail: gabiflogeoc@yahoo.com

**Keywords:** Monte Carlo method, Deleni, gas reserve.

The research documented in the present paper has highlighted the advantages of the proposed “Monte Carlo” simulation method in estimating geological gas reserves. A geological gas reserve can be considered proven only if it is estimated using the mass balance method. However, the mass balance method cannot be applied at the beginning of the exploiting process. This requires an analysis of the exploitation period of 5 ÷ 10 years, during which the necessary data is recorded to subsequently estimate the geological reserve. In this case, the uncertainty of the geological reserves at the beginning of the operation may lead to erroneous decisions in the allocation of funds necessary to exploit the gas reserves. In order to solve this problem, we have used the “Monte Carlo” simulation method, which allows, at the time of the reservoir opening, the assessment with certain probability (or risk) of the value closest to the real value of the hydrocarbon reservoir called “the proven reserve.”

In this context, we have tried to calculate the probability for which the value of free gas reserve estimated through the “Monte Carlo” method is the same with the proven reserve, determined through mass balance.

In order to illustrate the calculation procedure adopted, we have chosen the Deleni gas reservoir as case study. This structure is located in the center of the Transylvanian Basin, namely the Târnavelor Depression. From an administrative point of view, the Deleni gas reservoir is located in the Mures county, approx. 8 km SSE of the city of Târnaveni and approx. 12 km NNW of Medias. The proven reserve for the Buglovian VII (Delenii-Hărânglab) gas accumulation, determined through the mass balance method, is  $G_0 = 6.861 \cdot 10^6$  mil.  $m^3$ . By incorporating the results and using the “Monte Carlo” method, a reserve of  $7.782 \cdot 10^6$  mil.  $m^3$  was estimated, corresponding to a probability of 85%.

## ON THE ESTIMATION OF THE HYDROGEOLOGICAL PARAMETERS IN THE CASE OF THE STATIONARY FLOW OF UNDERGROUND WATER

MIHAI REMUS ȘARAMET<sup>1</sup>, RĂZVAN RĂDUCANU<sup>1</sup>, IULIAN DIACONU<sup>1</sup>,  
IULIA ZAHARIA<sup>1</sup>

<sup>1</sup> „Al. I. Cuza” University of Iași, Department of Geology, 20A Carol I Blv., 700505 Iași, Romania; e-mail: saramet@uaic.ro

In order to reach the best results for the characterization of underground bodies of water, one should use experimental pumping in the desired wells. Although pumping could be executed in both stationary and non-stationary flow regimes, still, currently, they are executed only in the stationary regime, in three or four steps of constant flow capacity. This way, the values of the transmissivity of the acvifers (**T**) and the filtration coefficients (**K**) are obtained.

Stationary pumping does not allow, however, the estimation of the storage and diffusion coefficients. In order to find out what these quantities are, one should execute pumping in non-stationary regimes, which implies additional expenses. In order to avoid the latter, the present paper proposes a new method for the computing of the storage coefficients (**S**) and diffusion coefficients (**a**), without using the non-stationary pumping results.

In order to apply and validate the proposed method we study the case of the hydrogeological drilling in Roșiori, Bacău county, Romania.

## THE DISTRIBUTION OF GOLD IN ROMANIA. ASSESSMENT OF ITS PRIMARY SOURCES

SORIN SILVIU UDUBASA<sup>1</sup>, GHEORGHE UDUBASA<sup>2</sup>

<sup>1</sup> Univeristy of Bucharest, Faculty of Geology and Geophysics, Bucharest, 010041,  
Romania; e-mail: sorin.udubasa@gmail.com

<sup>2</sup> Romanian Academy, 125, Calea Victoriei, sector 1, RO - 010071, Bucharest, Romania; e-  
mail: udubasa@geo.edu.ro

**Keywords:** hydrothermal gold, Metaliferi Mts., alluvial gold, metamorphic gold, South Carpathians.

Romania is a gold producing country, ranking 5 among the world gold producers before the closing of mines in 2005 (Tămaş-Bădescu, 2010). The richest and the most productive gold mines used to be those included in the Golden Quadrangle or Quadrilateral in the Metaliferi Mts., where gold was mined since the Roman times and, most likely, even before the Roman conquest of Dacia. In addition, gold as byproduct has been obtained from base metal ores in the Baia Mare area and the Banat region; locally, gold has been recovered from alluvial accumulations located on the southern slope of the South Carpathians and in the Apuseni Mts. Second order gold ores are represented by several shear-zone related gold occurrences, which did not, however, produce industrial gold, except for Valea lui Stan in the Căpăţâna Mts. Relatively important from this point of view was the Văliug occurrence in the Semenice Mts., with quite interesting reserves, but containing too high As contents to be economically recovered.

Looking at all the gold mines (including those with gold as a byproduct) and gold occurrences (alluvial ones included) over the territory of Romania, it appears that only the NW part of the country contains significant gold, either magmatic, shear-zone related or alluvial. The conclusion is that gold accumulated in certain magmatic rocks of  $K_3 - Pg_1$  in Banat or of Neogene age in the Metaliferi Mts., and in metamorphic rocks in the South Carpathians and the Apuseni Mts. The East Carpathians seem to be devoid of gold, as are the geologic formations of Dobrogea.

By mapping the distribution of gold occurrences in Romania (acc. to Borcoş et al., 1984; Tămaş-Bădescu, 2010) as a function of the above mentioned factors, a gold peak or gold spot in the Golden Quadrilateral can be delineated, followed by occurrences with less and less gold. Therefore, the metamorphic rocks in the East and South Carpathians are dissimilar as far as the presence of gold is concerned. Such a difference is also true for the

Neogene volcanics bearing associated gold ores in the Metaliferi Mts. and in the Baia Mare area, and practically lacking gold in the Călimani-Gurghiu-Harghita Mts.

### References

- Borcoş, M., Kräutner, H.G., Udubaşa, G., Săndulescu, M., Năstăseanu, S., Bişoiianu, Cornelia, 1984. Map of the mineral resources. 2<sup>nd</sup> edition. Explanatory note and representative areas. Publ. House Inst. Geology and Geophysics, Bucharest, Romania.
- Tămaş-Bădescu, S., 2010. Contribuţii privind geologia economică a aurului în România. (Contributions to the economic geology of gold in Romania). PhD Thesis, University of Bucharest, Romania.

# **Tectonics - Structural Geology**



## **GEOLOGY AND DEFORMATION HISTORY OF MARMARA ISLAND AT THE NORTHERN EDGE OF THE SAKARYA ZONE NORTHWESTERN TURKEY**

RAHMI AKSOY<sup>1</sup>

<sup>1</sup> Selcuk University, Faculty of Engineering and Architecture, Department of Geological Engineering, 42075 Konya, Turkey; e-mail: raksoy@selcuk.edu.tr

**Keywords:** geology, deformation history, metamorphism, Marmara Island, Turkey.

### **Abstract**

Detailed mapping of Marmara Island at the northern edge of the Sakarya Zone indicates that it consists of five lithodemic units. From south to north, these are the Permo-Triassic (?) Gündoğdu Metamorphics, the Erdek Complex, the Marmara Marble, the Saraylar Complex, and the Eocene İlyasdağı Metagranodiorite. The Gündoğdu Metamorphics is composed of pelitic and psammitic schists and marbles. This unit is tectonically overlain by the Erdek Complex. The Erdek Complex comprises metabasites, having intercalations of pelitic and psammitic schists and marble blocks. The Erdek Complex is unconformably overlain by a thick marble (the Marmara marble). The Marmara Marble is followed by the Saraylar Complex. It is composed of alternating beds of metapelite, metapsammite and metacarbonate, and exotic marble and metaultramafic blocks. In the central part of Marmara Island, the İlyasdağı Metagranodiorite is a SW-NE trending sill-like intrusion that cuts the basement rocks.

These rock units were metamorphosed to greenschist-amphibolite facies, and they deformed, generating four generations of structures. Index mineral assemblages of the metamorphic units show that the degree of metamorphism increases from north to south in the island. During its intrusion, the İlyasdağı Metagranodiorite gave rise to contact metamorphic effects, locally in the contact aureole with metacarbonates of the Erdek Complex and the Marmara Marble. This indicates that the imprint of the contact episode was not obliterated by the latter high-grade regional metamorphism.

The deformation phases are the following: (1) schistosity and foliation planes; (2) ENE-WSW trending folds, mineral and crenulation lineations, and mullion structures; (3) NNE-SSW trending folds, crenulation cleavages, mineral and crenulation lineations, and mullion structures; (4) WNW-ESE trending folds, crenulation cleavages and crenulation lineations. This last deformation affected the folds developed during previous phases and formed refolded-fold structures.

Marmara Island is surrounded by several complex tectonic terranes. Undated basement rocks make it difficult to determine to which terrane the rock units belong. Therefore, in the present study, the timing of deformation and the tectonic history of the island remain unanswered.

### Location

Marmara Island is located in the southern part of the Marmara region, in northwestern Turkey (fig. 1). It is an elevated metamorphic basement situated in the Marmara Sea. The island is surrounded by different tectonic units.



Fig. 1 Tectonic map of western Turkey showing the location of the study area (modified after Okay et al., 1996).

### Geological Setting

The geology of Marmara Island and the surrounding areas records a complex history, dominated by sedimentary, volcanic, plutonic and metamorphic effects (Aksoy, 1995). Rock units found in the island include metasedimentary, metavolcanic and metamagmatic rocks (fig. 2). The Gündoğdu Metamorphics deposited on a continental margin constitute the oldest unit in the island. This unit is composed of micaschists, calcschists and marbles. The pelitic schists have a mineral assemblage consisting of quartz + muscovite + biotite + plagioclase + staurolite + kyanite + granat, which represent the minerals of amphibolite facies. The unit is tectonically overlain by the Erdek Complex, consisting of volcano-sediments, mixed with basic and ultrabasic rocks. This lithological features suggest that the Erdek Complex was an ophiolitic mélange before metamorphism. Pelitic and psammitic schists of this unit have the same mineral

assemblages as the pelitic schists of the Gündoğdu Metamorphics. The Marmara Marble, deposited on a quiet shelf environment, unconformably overlies the Erdek Complex. It is followed by the flyschoid Saraylar Complex, formed in a fore-arc or back-arc basin. It consists of metapelitic and metapsammitic schists, metacarbonate and metachert intercalations, originally having turbidite texture, exotic marble blocks and interbedded basic and ultrabasic metavolcanics. The psammitic and pelitic schists have mineral assemblages that consist of quartz + plagioclase + muscovite + biotite. Epidote + chlorite + actinolite + tremolite + talc are the main mineral assemblages found in the metabasic rocks. Both mineral assemblages suggest greenschist facies metamorphic conditions. All these units were intruded, before the metamorphic events, by the calc-alkaline and metaluminous İlyasdağı Metagranodiorite (Karacık et al., 2008). It includes numerous meta-aplitic, meta-pegmatitic, meta-quartz and metagranitoid veins and dykes. Published data regarding the K/Ar and U-Pb radiometric age of the metagranodiorite suggest the Eocene (Karacık et al., 2008; Ustaomer et al., 2009). The most common mineral assemblages in the intrusion are

quartz + feldspar + hornblende + epidote + biotite + muscovite + garnet. Typical mineralogical changes of the metamorphic rocks determined in the island indicate that the degree of metamorphism increases from north to south. Based on these mineralogical changes, three metamorphic facies zones were distinguished. These are greenschist, epidote-amphibolite and amphibolite facies. These facies zones generally run parallel to the trend of the  $F_2$ -fold axis, in the ENE-WSW direction.

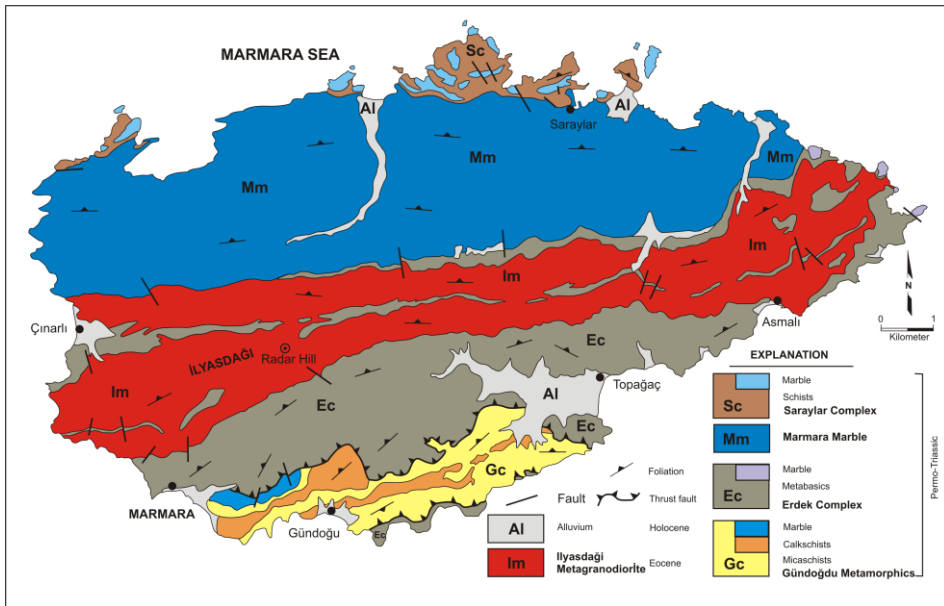


Fig. 2 Geologic map of Marmara Island

During its intrusion, the İlyasdağı Metagranodiorite gave rise to contact metamorphic effects in the contact aureole with the Erdek Complex and the Marmara Marble. Here, the metamorphism in the aureole was found to be in the pyroxene-hornfels facies (quartz + feldspar + scapolite + diopside + idocrase + epidote + garnet).

### Structural Geology

Mesoscopic structures observed and measured in the field include foliations, fold axis, fold axial surface and lineations. Structural features within the metamorphic rocks show four generations of structural elements. The first phase of deformation ( $F_1$ ) was the most intensive. It obliterated the primary bedding planes ( $S_0$ ) and generated the schistosity and foliation planes ( $S_1$ ), which are the most penetrative structural element. The  $S_1$  trends indicate continuity across the boundary of rock units. This continuity, along with the harmonious relationship of the schistosity and foliation planes, indicates that all the units

were metamorphosed and deformed during the same stage. The second phase of deformation ( $F_2$ ) is represented by: close to isoclinal, and gently to steeply inclined folds ( $B_1$ ), with fold axis plunging sub-horizontally to the northeast, mineral and crenulation lineations, and mullion structures. The third phase of deformation ( $F_3$ ) formed isoclinal to tight, and moderately to steeply inclined folds. Gentle, parallel and moderately to steeply inclined folds and crenulation lineations characterize the fourth phase of deformation ( $F_4$ ). This deformation affected the folds developed during previous phases and formed type-1, type-2 and type-3 (Ramsay, 1967) refolded-fold structures.

### Conclusions

The detailed mapping of Marmara Island indicates that it is composed of five lithodemic units. They are mainly made up of metapelitic and metapsammitic, metabasic, metacarbonatic and metamagmatic rocks. The Gündoğdu Metamorphics consist of continental-margin sediments and structurally form the base of the units. The Erdek Complex represents an ophiolitic mélangé and tectonically overlies the Gündoğdu Metamorphics before metamorphic events. All the lithodemic units were metamorphosed to the greenschist-amphibolite facies and deformed by four generations of structures. The foliation and mineral lineations of the İlyasdağı Metagranodiorite run parallel to adjacent metamorphic units. The harmonious fabric relationship of these units indicates that all the rock units were deformed and metamorphosed together, during the same stage.

### References

- Aksoy, R., 1995. Stratigraphy of the Marmara Island and the Kapıdağı Peninsula (In Turkish). TAPG (Turkish Association of Petroleum Geologist) Bulletin, *7/1*, 33–49.
- Karacık, Z., Yılmaz, Y., Pearce, J.A., Ece, Ö.I., 2008. Petrochemistry of the south Marmara granitoids northwest Anatolia, Turkey. *Int J. Earth Science (Geol Rundsch)*, *97*, 1181–1200.
- Okay, A.I., Satir, M., Maluski, H., Siyako, M., Monie, P., Metzger, R., Akyüz, S., 1996. Paleo- and Neo-Tethyan events in northwestern Turkey: Geologic and geochronologic constraints. In Yin, A., Harrison, M., (Eds.), *Tectonics of Asia*, Cambridge University Press, 420–441.
- Ramsay, J.G., 1967. *Folding and Fracturing of Rocks*. New York, McGraw Hill Book Company, 568p.
- Ustaömer, P.A., Ustaömer, T., Collins, A.S., Reischpeitsch, J., 2009. Lutetian arc-type magmatism along the southern Eurasian margin: New U-Pb LA-ICPMS and whole-rock geochemical data from Marmara Island, NW Turkey. *Miner Petrol*, *96*, 177–196.

## **THE APENNINIC-MAGHREBIAN OROGEN IN THE CENTRAL MEDITERRANEAN REGION: A REVIEW**

SERAFINA CARBONE<sup>1</sup>

<sup>1</sup> University of Catania, Department of Geological Sciences, Corso Italia 57, I95129 Catania, Italy; e-mail: carbone@unict.it

**Keywords:** Central Mediterranean Region, Apenninic-Maghrebian orogen, palaeogeography, orogenic stages, geodynamic evolution.

The present-day physiographic-tectonic features of the Central Mediterranean region are the product of the geodynamic evolution in which a fundamental role is played by the distribution of crustal components (Finetti et al., 1996) (fig. 1). The orogenic belt is located between an old oceanic crust, the Ionian basin, which has been partially consumed, and a new oceanic crust, the abyssal plane of the Tyrrhenian basin. Moreover, the CROP-Mare project (Finetti Ed., 2005) recognized a continental crust in the circum-Tyrrhenian margins associated with migrated tectonic stacks that were colliding with the continental blocks of the Africa and Adria plates.

### **Structural domains in the central Mediterranean**

In the Central Mediterranean region, the orogenic belt originated during the Tertiary through the convergence between the European margin and the Africa-Adria plates. The recognizable structural domains are the following: the Foreland Domain, the Orogenic Domain and the Hinterland Domain (Ben Avraham et al., 1990; Lentini et al., 1994, 2006, and references therein) (fig. 2).

The Foreland Domain includes the still undeformed continental areas of Africa, represented by the Pelagian Block, and that of the Adriatic microplate, consisting of the Apulian Block, which is separated since the Mesozoic from the main Africa Foreland by the oceanic crust of the Ionian Basin.

The Orogenic Domain is composed of three main tectonic belts, the External Thrust System (ETS), the Apenninic-Maghrebian Chain (AMC) and the Kabilo-Calabride Chain (KCC), generated by the detachment of the internal sedimentary cover of the flexured sector of the continental foreland, by the imbrication of the sedimentary sequences belonging both to the oceanic crust-type sectors (Tethys and Ionian basins) and to the continental crust-type ones (inner carbonatic platform), and by the delamination of the European margin, respectively.

The Hinterland Domain is represented by the Sardinia Block and the Tyrrhenian Basin. This latter is characterised by an oceanic crust, and its opening started in the Middle Miocene (Lentini et al., 1995, 2002).

In the south Tyrrhenian area, the features of the Apenninic-Maghrebian Orogen are controlled by the thickness of the crust of the Foreland Domain. The oceanic crust of the Ionian Basin is located between the continental crust of the Apulian Block to the north and the Pelagian Block to the south-west. This morpho-tectonic shape influences the evolution of the whole Calabrian Arc.

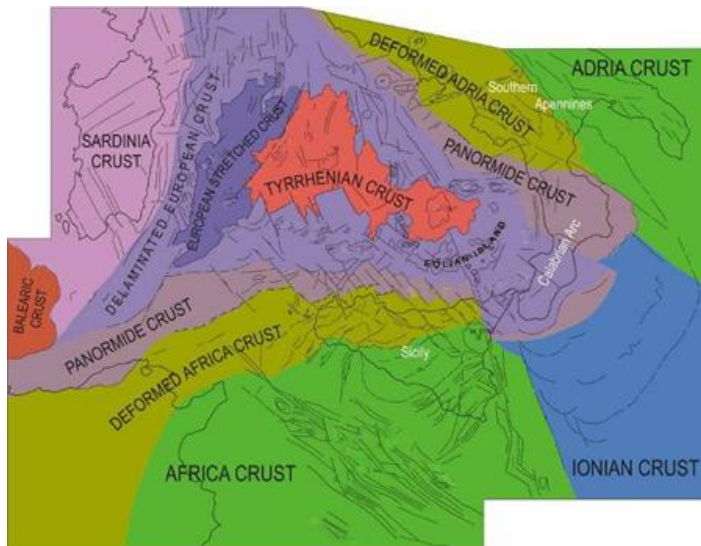


Fig. 1 Schematic representation of crustal domains in the central Mediterranean. The foreland domains are characterized by the Adria and the Africa continental crust separated by the old crust of the Ionian Sea. At the present time, the subduction of the Ionian crust is active only beneath the southern Calabrian Arc. Remains of parts of the Paleo-Ionian slab are seismically recognizable between the deformed margins of the continental blocks and a collisional crust (the Panormide crust). The Tyrrhenian Sea is constituted mostly of an oceanic crust placed on a delaminated European crust, and the Panormide crust before the forearc basin developed (after Lentini and Carbone, 2010)

The interpretation of regional profiles in Sicily and the Southern Apennines, based on the crustal sections of the CROP-Mare project (fig. 3), show that both foreland blocks are in collision with a continental crust, named the “Panormide crust”, recognised in the Tyrrhenian offshore of the northern coast of Sicily and of the Southern Apennines. This crust has been interpreted as the original basement of the carbonate platforms (Panormide and Apenninic Platform Units) (Lentini et al., 2006, 2009). The Meso-Cenozoic sedimentary covers originally located on the oceanic area have been interpreted as a

prosecution of the modern Ionian Basin involved in orogenesis. They are completely detached and tectonically rest on the ETS. These covers, named the Lagonegro and Imerese Units in the Southern Apennines and in Sicily, respectively, are grouped into the Ionide Units (Finetti et al., 2005a, 2005b).

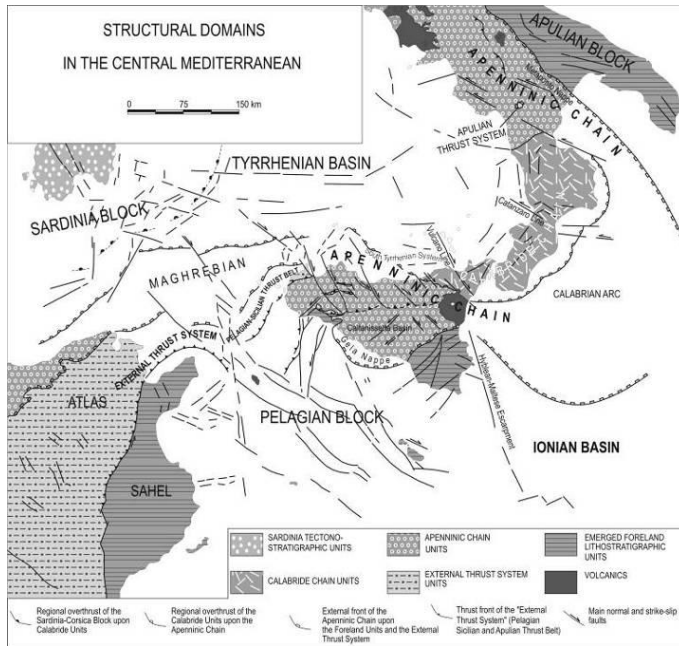


Fig. 2 Structural domains of the central Mediterranean. The Foreland domain consists of the Apulian Block (Adria crust) and the Pelagian Block (Africa crust), separated by the oceanic crust of the Ionian basin. The lowermost structural level of the orogen is an External Thrust System: Atlas in North Africa, the Pelagian-Sicilian Thrust Belt in Sicily and the Apulian Thrust System in the Southern Apennines. These are overlain by the Apenninic-Maghrebian Chain, a roof thrust system generated by post-Oligocene thin-skinned tectonics, underthrust an edifice composed of basement nappes derived through the Eocene-Oligocene delamination of the margin of the Europe Plate, the Kabilo-Calabride Chain (after Lentini et al., 2006)

The peculiarity of the orogenic belt in the Southern Apennines, as well as in Sicily, mainly lies in a general duplex geometry (fig. 3). The roof thrust system, several thousand meters thick, is made up of the allochthonous units of the AMC, while the floor thrust is represented by the ETS. This latter corresponds to the Apulian Thrust System in the Southern Apennines, and to the Pelagian-Sicilian Thrust Belt in Sicily, and is composed of more or less rooted carbonate units derived from the internal edge of the Adria and of the Africa plates, respectively (Finetti et al., 2005a, 2005b).



In the crustal profiles of figure 3, the continental crust of the Adria and Africa plates extends beneath the orogenic belt, which characterizes the on-shore areas to the Tyrrhenian shoreline. The Afro-Adriatic crusts show a progressive thinning and laterally grade into an old Ionian slab, completely subducted. The Panormide crust is currently colliding with the Adria and Africa crusts, in the Southern Apennines and Sicily, respectively. The geological evidences of this collisional setting are the NW-SE oriented transcurrent faults, sinistral in the Southern Apennines and dextral in Sicily. This latter constitutes the South Tyrrhenian System (STS) (Finetti et al., 1996), which affects both off-shore and on-shore areas of Sicily. Of the South Tyrrhenian faults, the most relevant is the NNW-SSE oriented Vulcano Line (fig. 2), that represents a boundary between the collisional setting to the west and the still subducting Ionian slab.

### **Palaeogeographic and geodynamic evolution**

The Ionian basin opened since the Permian-Triassic inside the Adria Plate, separating the Apulian Block from the “Apenninic” Block. Northward along the Apennines, the Ionides, represented by the Lagonegro basal sequences, progressively disappear. That indicates that the Ionian crust was narrowing and both continental blocks, the Apulian Block and the “Apenninic” one, were joined in a unique continental plate: the Adria Plate. Similarly, there is no continuity of the Ionides toward western Sicily, and this may indicate the progressive closure of the oceanic crust and the direct connection of both Apenninic continental crusts: the Africa one and the Panormide one. An Alpine Tethys basin was located between the Europa Plate and the Adria-Africa Plates.

The geodynamic evolution of the convergent system can be summarized into three orogenic stages:

**Eo-Alpine stage:** this stage occurred during Late Cretaceous-Eocene times. Africa-Ionian-Adria, as unique block, and the Eurasian plate converged. Poor evidences of an eo-alpine stage can be observed in western Calabria, in the Tyrrhenian basin and in the Alpine Corsica. A tectonic wedge, made up mainly by Ligurides and by ophiolites-bearing sequences, is characterized by a Europa vergence. In the Calabria-Lucania boundary, Jurassic-Cretaceous ophiolites and low metamorphic rocks, belonging to the Ligurides, are sealed by the Oligo-Miocene foredeep deposit. At the present time, they are completely detached onto the Apenninic Platform or directly overlying the Ionides tectonically, and display an Apulian vergence originated during the following stages.

**Balearic stage:** This stage (Oligocene-Early Miocene) produced an orogenic belt with opposite vergence, toward the Adria-Africa Block. In NE Corsica, the W-verging thrust systems, which originated during the Eo-Alpine stage, have been successively affected by Adria-verging low-angle thrust faults of the Balearic stage. Pre-rift, syn-rift and post-rift sequences are seismically well defined. This stage allowed a further consumption of the remnant of the Alpine Tethys oceanic crust and to the collision of the European Plate with the Panormide crust. The consumption of the Tethys crust was contemporaneous with the emplacement of extensive frontal nappes, with the opening of the Balearic back-arc basin, and the counter-clockwise rotation of the Corsica-Sardinia Block, which ended at the Burdigalian-Langhian boundary. The flysch-type successions of Late Oligocene to Early Miocene age, characterized by tuffitic sandstones, indicate the presence of a volcanic arc,

which belongs to the Alpine Tethys subduction complex. Contemporaneously, in the areas of the Ionian Foreland and partly on the carbonate platform itself, a pelitic-quartzarenitic sequence of Numidian flysch and “epicontinental” glauconitic calcarenites and marls were deposited.

**Tyrrhenian Stage:** Since the Burdigalian-Langhian boundary, the Apenninic-Panormide Platforms were stripped off from their basement and were thrust over the Ionides. Later, the latter suffered a general décollement and overrode the External Thrust System, with the consumption of the Palaeo-Ionian crust originally interposed between the continental crusts. In the Calabrian Arc, where the foreland is represented by the Ionian oceanic crust, the Ionian pelagic sequence was stripped off from their subducting oceanic basement and was transported eastward, forming most of the external wedge of the Calabrian Arc. In the Southern Apennines, the Late Miocene external flysch deposited in a basinal area, the Irpinian Basin, inherited by the Ionides (Lagonegro sequence). At that time, this basin represented the Ionian foredeep, with an inner tectonic wedge in which the topmost Tortonian levels of flysch-type deposits are tectonically overlain by a further nappe of Tethydes that indicates the involvement of the foredeep successions in the Ionian subduction. This marked the consumption of the oceanic crust of a part of the Ionian Paleobasin and, thus, the beginning of the phase that led to the opening of the Tyrrhenian backarc basin and the emplacement of the Aeolian volcanic island arc.

On the African foreland, the crustal lineaments inherited from the Mesozoic palaeogeography show an oblique direction with respect to that of the deformation front of the chain, conditioning its advance and causing a diachronous collision from west to east. This is expressed in the indentation of the continental margin and the formation of a transcurrent junction oriented about NW-SE, which has been active since Early Pleistocene times and indicates the cessation of the subduction process at this time in the Southern Apennines and in Central-Western Sicily.

## References

- Ben-Avraham, Z., Boccaletti, M., Cello, G., Grasso, M., Lentini, F., Torelli, L., Tortorici, L., 1990. Principali domini strutturali originatisi dalla collisione nogenico-quadernaria nel Mediterraneo centrale. *Memorie della Società Geologica Italiana*, **45**, 453–462.
- Finetti, I. R. (Editor), 2005. CROP Project, Deep Seismic Exploration of the Central Mediterranean and Italy. Book and Maps, Elsevier, 779p.
- Finetti, I., Lentini, F., Carbone, S., Catalano, S., Del Ben, A., 1996. Il sistema Appennino meridionale- Arco Calabro-Sicilia nel Mediterraneo centrale: studio geologico-geofisico. *Bollettino della Società Geologica Italiana*, **115**, 529–559.
- Finetti, I., Lentini, F., Carbone, S., Del Ben, A., Di Stefano, A., Forlin, E., Guarnieri, P., Pipan, Prizzon, A., 2005a. Geological Outline of Sicily and Lithospheric tectono-dynamics of its Tyrrhenian margin from new CROP seismic data. In: Finetti, I. R., (Ed.), CROP, Deep Seismic Exploration of the Mediterranean region. Spec. vol. Elsevier, chapter 15, 319–376.
- Finetti, I., Lentini, F., Carbone, S., Del Ben, A., Di Stefano, A., Guarnieri, P., Pipan, Prizzon, A., 2005b. Crustal tectonostratigraphy and geodynamics of the southern Apennines from CROP and other integrating geophysicalgeological data. In: Finetti, I. R. (Ed), CROP, Deep Seismic Exploration of the Mediterranean region. Spec. vol. Elsevier, chapter 12, 225–262.
- Lentini, F., Carbone, S., Catalano, S., 1994. Main structural domains of the central Mediterranean region and their Neogene tectonic evolution. *Bollettino di Geofisica Teorica e Applicata*, **36**, 103–125.

- Lentini, F., Carbone, S., Catalano, S., Di Stefano, A., Gargano, C., Romeo, M., Strazzulla, S., Vinci, G., 1995. Sedimentary evolution of basins in mobile belts: examples from tertiary terrigenous sequences of the Peloritani Mts (NE Sicily). *Terra Nova*, **7**, 161–170.
- Lentini, F., Catalano, S., Carbone, S., 1996. The External Thrust System in Southern Italy: a target for petroleum exploration. *Petroleum Geoscience*, **2**, 333–342.
- Lentini, F., Carbone, S., Di Stefano, A., Guarnieri, P., 2002. Stratigraphical and structural constraints in the Lucanian Apennines (southern Italy): tools for reconstructing the geological evolution. *Journal of Geodynamics*, **34**, 141–158.
- Lentini, F., Carbone, S., Guarnieri, P., 2006. Collisional and post-collisional tectonics of the Apenninic-Maghrebian Orogen (Southern Italy). In: Dilek, Y., Pavlides, S. (Eds.), *Post-collisional Tectonics and Magmatism in the Eastern Mediterranean Region*. Geological Society of America, Special Paper, **409**, 57–81, Boulder, Colorado (USA).
- Lentini, F., Carbone, S., Barreca, G., 2009. A Regional 1:250.000 scale Geological Map of Sicily as a tool for a Neotectonic Model of Central Mediterranean. 6<sup>th</sup> EUREGEO (European Congress on Regional Geoscientific Cartography), Munich, June 9-12, 2009. *Proceedings*, I, 77–79.
- Lentini, F., Carbone, S., 2010. Geological Map of Sicily, scale 1:250.000. S.EL.CA., Firenze, in press.

## **SEDIMENTOLOGIC CHARACTERISTICS OF THE PLIOCENE-QUATERNARY ALLUVIAL FAN DEVELOPED SOUTHEAST OF SIZMA (KONYA-TURKEY)**

FUAT ÇÖMLEKCİLER<sup>1</sup>, HÜKMÜ ORHAN<sup>1</sup>

<sup>1</sup> Selcuk University, Engineering and Architecture Faculty, Department of Geological Engineering, 42075Konya, Turkey; e-mail: fuatcomlekci@selcuk.edu.tr; horhan@selcuk.edu.tr

**Keywords:** alluvial fan, facies analysis, Konya fault zone, Konya, Turkey.

The sedimentological characteristics of the Pliocene-Quaternary alluvial fan deposits developed at southeast of Sızma, approximately 20km NW of Konya, Turkey, were examined by measuring six sedimentological successions.

In the alluvial fan deposits, six different lithofacies were described and interpreted; these are: the well cemented massive clasts of the conglomerate facies (Facies Gccu); the massive matrix of the conglomerate facies (Facies Gmu); the gray mud facies, bearing lenticular sand horizons (Facies Fms); the massive mud facies, bearing red-brown carbonate nodules (Facies Fm); the massive clasts of the conglomerate facies (Facies Gcu); and the intermediate- to coarse-grained massive sand-gravel facies (Facies Gu). These lithofacies were grouped into three facies associations: the proximal fan facies association, which is represented by Facies Gccu, Facies Gcu, and Facies Gmu; the mid-fan facies association of the Facies Gu; and the distal fan facies association, represented by Facies Fm and Facies Fms.

The development of these facies was mainly controlled by the subordinate faults of the Konya fault zone (KFZ). Repetitive conglomerate facies are thought to be the result of an uplift of the source area, following the fault reactivation.

## SYNSEDIMENTARY STRUCTURES IN JURASSIC ROCKS FOUND SOUTH-WEST OF ANKARA (TURKEY)

ARIF DELİ<sup>1</sup>, HÜKMÜ ORHAN<sup>1</sup>

<sup>1</sup> Selcuk Universty, 42031 Konya, Turkey; e-mail: adeli@selcuk.edu.tr;  
horhan@selcuk.edu.tr

**Keywords:** Ankara, Ammonitico Rosso, Neptunian dykes, slump folding, Pelagic Carbonate Platform (PCP), Jurassic.

There are several synsedimentary structures in Jurassic sedimentary rocks resting with angular unconformity on the low metamorphic rocks (Upper Triassic Karakaya Complex) in the Ankara region (Turkey), offering clues regarding the development of the basin. These are tectonic fractures, karstic dissolution voids, sediment types and filling styles in these structures, slumps and paleofaults. Having very limited detrital facies at the basal part of the Jurassic carbonates in the area and, the development of microbial facies (Sinemurian Uzundere member), starting within the tectonic fractures in the basement rocks, indicates that the base of the basin deepened rapidly under tectonic control.

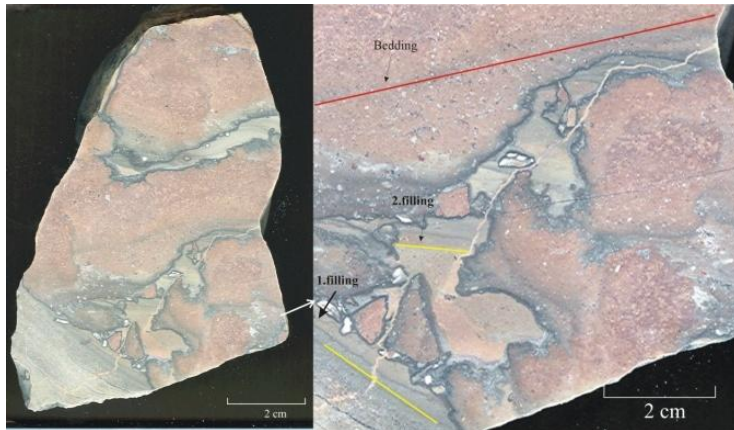


Fig. 1 Dissolution voids filled with laminated pelloidal sediments in microbialitic limestone at the Kudret Pınarı area, and the relationships between laminae

The karstic dissolution voids were formed in the intertidal zone, during the Early Jurassic (Deli and Orhan, 2007), when the sea floor was under subaerial conditions. The karstic voids were filled with peloidal materials when they were inundated by the sea. Laminae with differing dipping found in these fillings show the instability of the sea floor. These microstructures can easily be determined on polished rocks and acetate peels (fig. 1).

During the non-seismic periods, due to stable conditions and the low sedimentation rate, sediments were densely bioturbated, and ferriferous stromatoliths formed red-colored hardground (fig. 2). The development of Neptunian dykes in Late Sinemurian microbial carbonates, along with their coarse detritic fillings, point out the recurrence of the extensional regime in the study area.

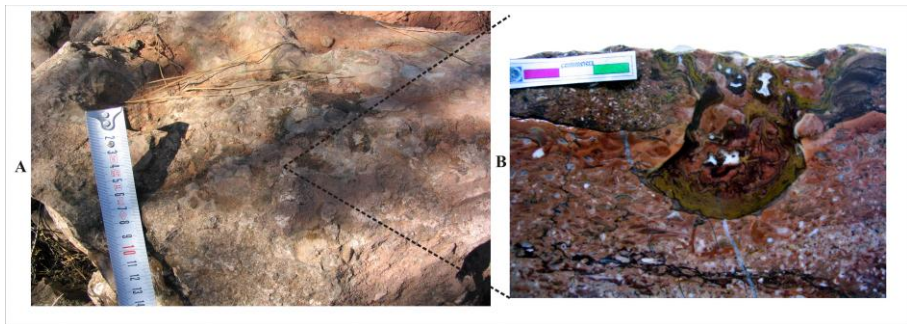


Fig. 2 A cutting of microbialitic limestone from Uzundere. **A:** The outcrop appearance of the hardground surface **B:** The appearance of the hardground level in a hand sample cut perpendicularly to the bedding and microbial mat in the voids.

There are large and deep Neptunian dykes cross-cutting bioclastic carbonates (Pliensbachian Şeyhlertepe member), indicating intense seismic activity during the Late Pliensbachian-Early Toarcian. The tectonic fractures developed in the shallow bioclastic carbonates were filled with pelagic mudstone. This indicates that the depositional environment deepened rapidly. The presence of turbiditic sandstone and large and angular blocks of shallow-water bioclastic carbonates in ammonitico rosso facies (Toarcian Beytepe member) indicate the development, through faulting, of pelagic carbonate platforms (Deli and Orhan, 2009). Turbiditic rocks (Upper Toarcian-Callovian Turnaçşme member) derived from basement rocks cover the post-Toarcian pelagic/hemipelagic carbonates. After a tectonic quiescence period, synsedimentary faults and slump structures were developed in mudstone and marl in relation to increasing seismic activity in the Callovian (fig. 3). Shallow pelagic carbonate platforms (PCP; Santantonio, 1993) were developed following the reshaping of the sea floor. On these uplifted surfaces, the ammonitico rosso facies (Callovian-Oxfordian Çakırlardere formation) were deposited, generally conformably, on the detritic facies. In some places, however, they developed unconformably, directly on basement rocks. The Ammonitico rosso-type facies were drawn by pelagic carbonates as a result of continuous deepening during the late Jurassic. The

presence of slump structures at the lower part of pelagic carbonates shows the recurrence of the seismic activity (fig. 4).

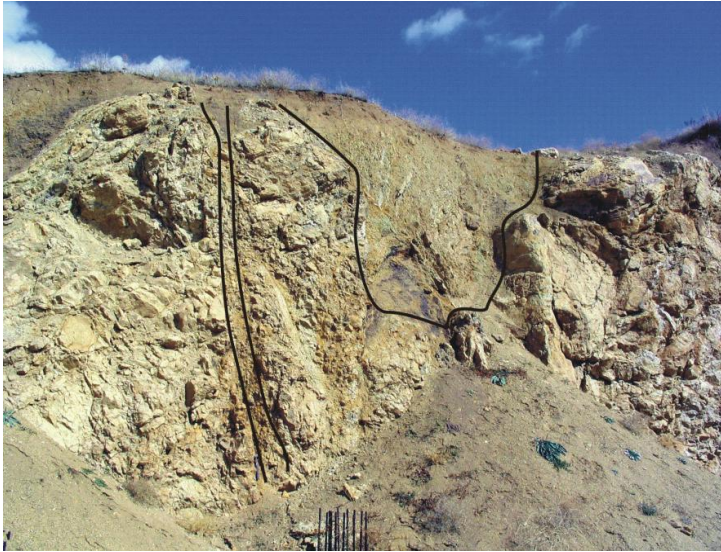


Fig. 3 Large Neptunian dykes in the Şeyhlertepe member in the Angora evleri area, which filled with red mud.



Fig. 4 Slump folding from the Çakırlardere formation at Başağaçtepe, in Ankara

## References

- Deli, A., Orhan, H., 2007. Geological importance of paleokarsts and neptunian dykes in the Lower Jurassic rocks at the Beytepe village - Çayyolu area (South west Ankara, Turkey). *Geochimica et Cosmochimica Acta*, **71**/15, Suppl. 1, p. A215.
- Deli, A., Orhan, H., 2009. Sedimentological Characteristics of Jurassic Pelagic Carbonate Platforms Around Beytepe-Umitkoy (SW Ankara, Turkey). 27th IAS Meeting Of Sedimentology, Alghero, Italy, Abstracts, p. 132.
- Santantonio, M., 1993. Facies associations and evolution of pelagic carbonate platform/basin systems: examples from the Italian Jurassic. *Sedimentology*, **40**, 1039–1067.

## EARLY CRETACEOUS FLYSCH OF THE TETHYS REALM AND ITS EO- TO MESO-ALPINE DIACHRONOUS DEFORMATIONS

DIEGO PUGLISI<sup>1</sup>

<sup>1</sup> University of Catania, Dipartimento di Scienze Geologiche, 55 Corso Italia, Catania, 95129, Italy; e-mail: dpuglisi@unict.it

### Abstract

The present paper emphasizes the presence of Early Cretaceous flysch in all the sectors of the Alpine Tethys, from the Gibraltar Arc to the Balkans, showing the same geological setting and analogies of sedimentary provenance.

These deposits and their tectonic framework indicate a common geological evolution in all the oceans of the Alpine Tethys, also including the Maghrebian Tethys. The latter, in particular, was affected by Meso-Alpine tectonic events, slightly diachronous with respect to the oldest ones characterizing the easternmost and central oceanic areas of the Alpine Tethys.

**Keywords:** Early Cretaceous flysch, sedimentary provenance, Maghrebian Chain, Europe Alpine Chains, Cretaceous tectonics.

### Introduction and objectives

Early Cretaceous flysch forms a distinct turbidite clan, which marks the boundary between the internal and external areas for more than 7,000 km, from the Betic-Rifian Chain to the Balkans (Fig. 1).

The deposition of these turbidite sequences, Middle Jurassic-Early Paleocene in age, occurred in sedimentary basins (oceanic or not) connected with the break-up of Pangaea and successively affected by a Late Cretaceous-Early Tertiary convergence (Stampfli, 2000).

Thus, because of this middle-Late Cretaceous plate tectonic re-organization, which involved almost all of the oceanic basins of the Alpine Tethys s.s. and of its easternmost sectors (e.g. the present Carpathian-Balkan orogenic system), the Early Cretaceous flysch was deformed.

In fact, the different areas of the Alpine Tethys include the following:

- the Ligurian-Piedmont and the Valais Oceans (or simply the Ligurian Ocean, Fig. 2; Plašienka, 2003; Schmid et al., 2008),

- the Magura Ocean and other minor basins (the Severin-Ceahlău Ocean and the “Nish-Troyan flysch trough” in the Carpathians and Balkans, respectively), located in its easternmost sectors (Oszyzko, 1992; 1999; 2006; Săndulescu, 1994),
- collateral branches of the main Tethyan Basin, such as the Vardar and Pindos Oceans, which were also sedimentary basins of Early Cretaceous flysch (Boeothian and Bosnian Flysch in the Hellenides and Dinarides, respectively).

Nevertheless, the westernmost segment of the Alpine Tethys (the Maghrebain Basin, Fig. 2) seems to have not been involved in Middle-Late Cretaceous tectonics or, on the contrary, similar events have not yet been recognized or, again, they have often been neglected and/or not sufficiently emphasized (Puglisi, 2009).

The aim of the present paper is to check the tectonic framework of all the Early Cretaceous flysch of the Maghrebain Chain and to compare it with other coeval turbidite deposits from the central Europe Alpine Chains, in order to emphasize the existence of the same tectonic evolutionary scheme.

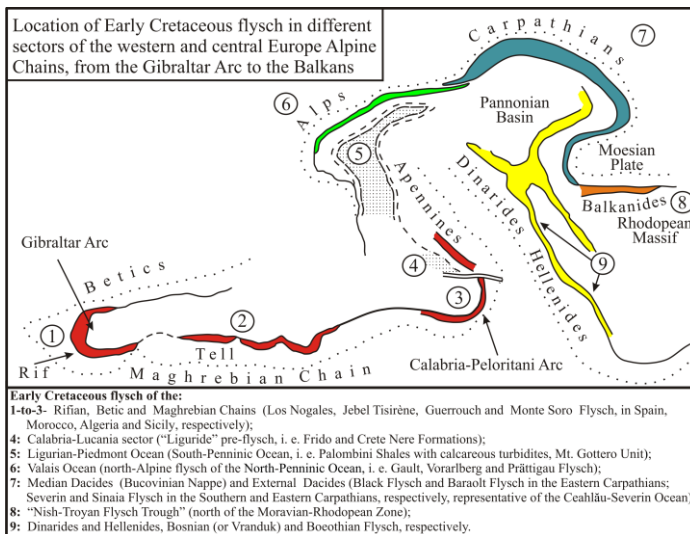


Fig. 1 Early Cretaceous flysch in the western-central Europe Alpine Chains (from Puglisi, 2009; modified after Durand-Delga, 1980)

### Early Cretaceous flysch of the Betic-Maghrebain Chain

The east-west-trending Betic-Maghrebain Chain extends along the North African coast from the Gibraltar Arc to the Calabria-Peloritani Arc (southern Italy, Fig. 3). This chain is formed by the superimposition of several nappes related to Internal, External and Flysch Domains, the latter located in an intermediate position.

The flysch successions (Early Cretaceous to Early Miocene) form a tectonic edifice, piled up and overthrust onto the external deposits, made up of different tectonic units usually re-grouped into two clans (Bouillin et al., 1970): *Maurétanien* and *Massylien* flysch, of internal and external provenance, respectively.

The *Maurétanien* deposits comprise Cretaceous Variegated Clays evolving to Oligocene turbidites, tectonically overlain by Early Cretaceous flysch [Los Nogaes Flysch in the Betic Cordillera (Puglisi and Coccioni, 1987), Jebel Tisirène Flysch in the Rif (Durand-Delga et al., 1999), Guerrouch Flysch in Algeria (Raoult et al., 1982) and Monte Soro Flysch in the Sicilian Maghrebian Chain (Puglisi, 1981)].

This Early Cretaceous flysch is tectonically overlain by Hercynian crystalline units [i.e. the Internal Zones of the Betic-Maghrebian Chain, known as the Betic-Rif-Alboran Realm, the Kabylidic and Calabria-Peloritani landmass (Mauffret et al., 2007) or as the AlKaPeCa Block (Alboran, Kabylides and Peloritani + Calabria terranes, Bouillin et al., 1986)], belonging to the southern Iberian palaeomargin (Stampfli et al., 1998; Sanz de Galdeano et al., 1993; Rosenbaum et al., 2002; Schettino and Turco, 2006).

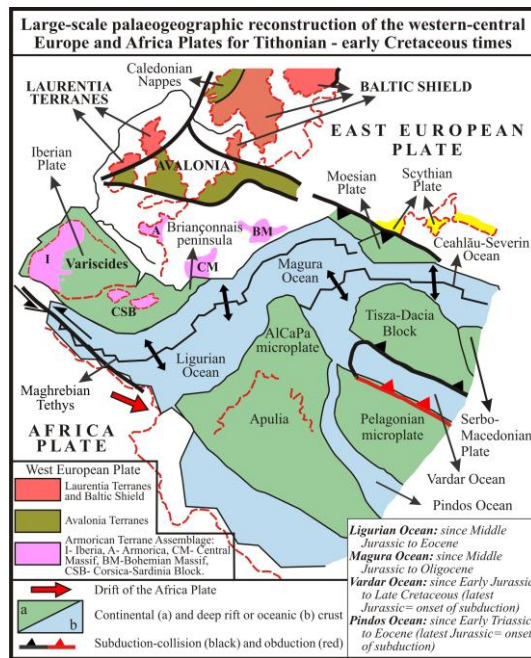


Fig. 2 Late Jurassic-Early Cretaceous palaeogeography (from Puglisi et al., 2010, modified by Channell and Kozur, 1997; Csontos and Vörös, 2004)

Finally, the following results represent the main conclusions regarding the Early Cretaceous flysch of the Maghrebian Chain:

- its provenance is linked to the erosion of the Hercynian crystalline basement and its Early Mesozoic carbonate cover (Puglisi, 1981; Raoult et al., 1982; Cassola et al., 1990),
- the absence of a Tertiary cover (locally, small and thin Paleocene-Eocene remnants) suggests the deformation of the Early Cretaceous Maurétanien flysch and their local underthrusting beneath the internal Hercynian crystalline units of the southern paleomargin of the AlKaPeCa Block in Sicily [“mesoalpine” event by Cassola et al. (1992) and Puglisi (1992)], as well as in Algeria [“Late Lutetian phase” by Raoult (1975) and Vila (1980)].

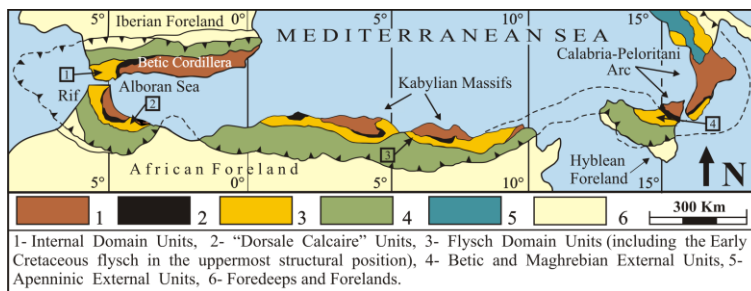


Fig. 3 Location of the Early Cretaceous flysch in the Maghrebian Chain (1, Los Nogales Flysch; 2, Jebel Tisirène Flysch; 3, Guerrouch Flysch; 4, Monte Soro Flysch)

### The Ligurian Tethys and the Western Alps

A first oceanic branch of the Alpine Tethys (the Ligurian-Piedmont or South-Penninic Ocean) is related to the pre-Jurassic rifting and Late Jurassic spreading, occurred in the central Atlantic as a consequence of the passive extension of the Europe-Adria (Africa) continental lithosphere (Dal Piaz, 2001; Dal Piaz et al., 2003). A Cretaceous plate convergence regime led to the subduction of the oceanic crust under the Adriatic margin and dismembered the oceanic lithosphere to form ophiolitic bodies within the orogenic system of the Western-Central Alps, the Northern Apennines and the Alpine Corsica (Dal Piaz et al., 2003).

The Jurassic ophiolitic and cherty-calcareous stratigraphic succession of the internal sector of this basin grades upwards to Late Cretaceous-Early Paleocene siliciclastic turbidites (Gottero Sandstones, Auct.).

The second oceanic branch of the Alpine Tethys (the Valais or North-Penninic Ocean) opened during the Early Cretaceous times, cutting off the Briançonnais microcontinent from South-Western Europe. Its detrital sedimentation continued until the Middle Eocene (the Rhenodanubian Flysch group, such as Gault, Voralberg and Prättigau Flysch), while the former one was completely closed in the Early Tertiary.

## **Dinarides and Hellenides**

The Boeothian and Bosnian Flysch of the Hellenide and Dinaride Chains, respectively, have recently been referred to the clan of the Early Cretaceous flysch of the Tethys Realm, deposited on the Pindos Ocean and on the western Vardar Ocean, respectively, and connected to the Cretaceous tectonics of their internal domain (Puglisi et al., 2009; 2010; Kyriakopoulos et al., 2010).

The provenance of both these types of flysch, in fact, derives from the dismantling of the Hercynian Pelagonian and/or Serbo-Macedonian terranes and their Mesozoic carbonate platforms, and from ophiolitic complexes, obducted since Late Jurassic from the western margin of the adjacent Vardar Ocean (Fig. 2).

## **Carpathians and Balkans**

The Magura and Ceahlău-Severin Oceans, opened during Early-Middle Jurassic times as an eastern prolongation of the Ligurian Ocean (Csontos and Vörös, 2004; Oszczytko, 2006), are located in the northern side of the Tisza-Dacia Blok (Fig. 2), already separated from the AlCaPa microplate (Schmid et al., 2008).

Cretaceous compressive events, probably connected with the movement of the Moesian microplate, led to a considerable crustal shortening in the Carpathian area.

Mid- and Late-Cretaceous deformations, in fact, affected the Median and External Dacides (Eastern Carpathians), both are also characterized by Early Cretaceous flysch, as well as the Severin Nappe (Southern Carpathians), whose deposits are considered to be equivalent to the former ones (Săndulescu, 1994).

Analogously, intense Mid- and Late-Cretaceous deformations, connected with an extensive northeast-vergency thrusting of the Serbo-Macedonian massif over the Rhodopean region (north-east of the Vardar Ocean, Balkan area; Zagorchev, 2001), caused closure of the “Nish-Troyan flysch trough”, located between the Rhodopean Massif and the Moesian Plate (Minkovska et al., 2002 and references therein).

## **Conclusions**

The present paper emphasizes the significant palaeogeographic continuity between the Maghrebian Basin and other oceanic areas of the Alpine Tethys during Mesozoic times, and the occurrence of an Early Cretaceous flysch family showing a very similar structural setting and provenance linked to the dismantling of internal areas. Thus, it is possible to consider only one sedimentary basin (Alpine Tethys s.s.), subdivided into minor oceanic areas, with a similar geological history.

Late Cretaceous or slightly more recent deformations, in fact, diachronously affected the Maghrebian Basin (“Mesoalpine” stage) during its progressive closure, and the Cretaceous plate tectonics triggered one (or more) tectonic phases, well recorded in all the sectors of the Alpine Tethys (“Eoalpine” stage).

In conclusion, it is possible to emphasize that the Maghrebian Tethys did not escape similar tectonic events, as suggested during the ‘70s (Raoult, 1975; Vila, 1980) and confirmed at the beginning of the ‘90s (Cassola et al., 1992; Puglisi, 1992), but, unfortunately, neglected in many recent geological studies.

## References

- Bouillin, J.P., Durand-Delga, M., Gelard, J.P., Leikine, M., Raoult, J.F., Raymond, D., Tefiani, M., Vila, J.M., 1970. Définition d'un flysch massylien et d'un flysch maurétanien au sein des flyschs allochtones de l'Algérie. *C. R. Acad. Sc. Paris*, **270**, 2249–2252.
- Bouillin, J.P., Durand-Delga, M., Olivier, Ph., 1986. Betic-Rifain and Tyrrhenian Arcs: distinctive features, genesis and development stages. In: Wezel, F.C. (Ed.), *The Origin of Arcs*. Elsevier, Amsterdam, 281–304.
- Cassola, P., Giammarino, S., Puglisi, D., 1990. Il Flysch di M. Soro: caratteri e significato geodinamico di un flysch cretacico ad affinità "maurétanien" nel segmento siculo della Catena Maghrebide. *Bollettino dell'Accademia Gioenia di Scienze Naturali di Catania*, **23/336**, 93–117.
- Cassola, P., Costa, E., Loiacono, F., Moretti, E., Morlotti, E., Puglisi, D., Villa, G., 1992. New sedimentologic, petrographic, biostratigraphic and structural data on some "late-orogenic" sequences of Maghrebian Chain North-eastern Sicily. *Riv. Ital. Paleontologia e Stratigrafia*, **98/2**, 205–228.
- Channell, J.E.T., Kozur, H.W., 1997. How many oceans? Meliata, Vardar, and Pindos oceans in Mesozoic Alpine paleogeography. *Geology*, **25**, 183–186.
- Csontos, L., Vörös, A., 2004. Mesozoic plate tectonic reconstruction of the Carpathian region. *Palaeogeography, Palaeoclimatology, Palaeoecology*, **210**, 1–56.
- Dal Piaz, G.V., 2001. History of tectonic interpretations of the Alps. *Journal of Geodynamics*, **32**, 99–114.
- Dal Piaz, G.V., Bistacchi, A., Massironi, M., 2003. Geological outline of the Alps. *Episodes*, **26**, 175–180.
- Durand-Delga, M., 1980. Considérations sur les flyschs du Crétacé inférieur dans les chaînes alpines d'Europe. *Bull. Soc. Géol. France*, **32/1**, 15–30.
- Durand-Delga, M., Gardin, S., Olivier, Ph., 1999. Datation des Flysch éocrétaqués maurétaniens des Maghrébides: la Formation du Jbel Tisirène (Rif, Maroc). *C. R. Acad. Sc. Paris*, **328**, 701–709.
- Kyriakopoulos, K., Karakitsios, V., Tsioura-Vlachou, M., Barbera, G., Mazzoleni, P., Puglisi, D., 2010. Petrological characters of the Early Cretaceous Boeothian Flysch (Central Greece). *Bull. Geol. Soc. Greece*, 2010 Proceedings of the 12<sup>th</sup> International Congress, Patras, May, 2010.
- Mauffret, A., Ammar, A., Gorini, C., Jabour, H., 2007. The Alboran Sea (Western Mediterranean) revisited with a view from the Moroccan Margin. *Terra Nova*, **19**, 195–203.
- Minkovska, V., Peyberné, B., Nikolov, T., 2002. Palaeogeography and geodynamic evolution of the Balkanides and Moesian 'microplate' (Bulgaria) during the earliest Cretaceous. *Research*, **23**, 37–48.
- Oszczypko, N., 1992. Late Cretaceous through Paleogene evolution of Magura Basin. *Geologica Carpathica*, **43/6**, 333–338.
- Oszczypko, N., 1999. From remnant oceanic basin to collision related foreland basin - a tentative history of the Outer Western Carpathians. *Geologica Carpathica*, **50**, 161–163.
- Oszczypko, N., 2006. Late Jurassic-Miocene evolution of the Outer Carpathian fold-and-thrust belt and its foredeep basin (Western Carpathians, Poland). *Geological Quarterly*, **50/1**, 169–194.
- Plašienka, D., 2003. Dynamics of Mesozoic pre-orogenic rifting in the Western Carpathians. *Mitteilungen der Österreichischen Geologischen Gesellschaft*, **94**, 79–98.
- Puglisi, D., 1981. Studio geologico-petrografico del Flysch di M. Soro nei Peloritani occidentali (Sicilia). *Mineralogica et Petrographica Acta*, **25**, 103–115.
- Puglisi, D., 1992. Le successioni torbiditiche "tardorogene" della Sicilia orientale. *Giornale di Geologia*, **54/1**, 181–194.
- Puglisi, D., 2009. Early Cretaceous flysch from Betic-Maghrebian and Europe Alpine Chains (Gibraltar Strait to Balkans): comparison and palaeotectonic implications. *Geologica Balcanica*, **37/3-4**, 13–20.
- Puglisi, D., Coccioni, R., 1987. Il Flysch di Los Nogales (Cretacico, Catena Betica): studio compositivo e confronti con il Flysch di Monte Soro della Catena Maghrebide siciliana. *Memorie della Società Geologica Italiana*, **38**, 577–591.
- Puglisi, D., Kyriakopoulos, K., Karakitsios, V., Tsioura-Vlachou, M., Barbera, G., Mazzoleni, P., 2010. Petrographic features of the Early Cretaceous Boeothian Flysch (External Hellenides, Central Greece); provenance and palaeogeographic implications. *Proc. XIX CBGA Congress*, in press.
- Raoult, J.F., 1975. Évolution paléogéographique et structurale de la chaîne alpine entre le golfe de Skikda et Constantine (Algérie orientale). *Bull. Soc. Géol. France*, **XVII**, 391–409.
- Raoult, J.F., Renard, M., Melieres, F., 1982. Le flysch maurétanien de Guerrouch: structure, données sédimentologiques et géochimiques (Petite Kabylie, Algérie). *Bull. Soc. Géol. France*, **24/3**, 611–626.

- Rosenbaum, G., Lister, G.S., Duboz, C., 2002. Reconstruction of the tectonic evolution of the western Mediterranean since the Oligocene. In: Rosenbaum G. & Lister G.S. (Eds.): Reconstruction of the evolution of the Alpine-Himalayan Orogen. *Jour. Virtual Explorer*, **8**, 107–126.
- Săndulescu, M., 1994. Overview on Romanian geology. ALCAPA II, Field Guidebook, 3–15.
- Sanz de Galdeano, C., Serrano, F., López Garrido, A.C., Martín Pérez, J.A., 1993. Palaeogeography of the Late Aquitanian-Early Burdigalian Basin in the Western Betic Internal Zone. *Geobios*, **26**/1, 43–55.
- Schettino, A., Turco, E., 2006. Plate kinematics of the Western Mediterranean region during the Oligocene and Early Miocene. *Geophys. J. Int.*, **166**, 1398–1423.
- Schmid, S.M., Bernoulli, D., Fügenschuh, B., Matenco, L., Schefer, S., Schuster, R., Tischler, M., Ustaszewski, K., 2008. The Alpine-Carpathian-Dinaridic orogenic system: correlation and evolution of tectonic units. *Swiss Journal of Geosciences*, **101**/1, 139–183.
- Stampfli, G.M., Mosar, J., Marquer, D., Marchant, R., Baudin, T., Borel, G., 1998. Subduction and obduction processes in the Swiss Alps. *Tectonophysics*, **296**, 159–204.
- Stampfli, G., 2000. Tethyan oceans. In: Bozkurt, E., Winchester, J.A., Piper, J.D.A. (Eds.), *Tectonics Magmatism in Turkey and surrounding area*. Geological Society, London, Sp. Publication, **173**, 1–23.
- Vila, J.M., 1980. La chaîne alpine d'Algérie et des confins algéro-tunisiens. Thèse, Paris, 3 vol., 661p.
- Zagorchev, I., 2001. Introduction to the geology of SW Bulgaria. *Geologica Balcanica Special Issue "Geodynamic hazards (earthquakes, landslides), Late Alpine tectonics and neotectonics in the Rhodope Region"*, **31**/1-2, 3–52.

## **WEBGIS – A FRAMEWORK FOR THE WEB PRESENTATION OF THE 1:1 MILLION SCALE GEOLOGICAL MAP**

GEORGE TUDOR<sup>1</sup>

<sup>1</sup> Geological Institute of Romania, 1, Caransebes Street, 012271, Bucharest, Romania; e-mail: george.tudor@igr.ro

**Keywords:** GIS, webGIS, geological map, MapServer, PostgreSQL, PostGIS.

The GIS technology, meant to create a database of geological maps, associated with information displayed on Internet technologies, has resulted in a webGIS application able to display and query the information contained in the geological map. The server side contains a PostgreSQL / PostGIS database, Mapserver, an Apache web server and a GUI application, written using PHP programming language associated with PHPMapScript functions. Thus, the client may view and query geological map using a web browser. Currently, the geological map of Romania at the 1:1 million scale was used, but information from maps at various scales may also be included.

## THE TROVANTS OF THE CRETACEOUS AND NEOZOIC DEPOSITS IN THE CARPATHIAN AREA (ROMANIA)

MIRCEA ȚICLEANU<sup>1</sup>, RADU NICOLESCU<sup>1</sup>, ADRIANA ION<sup>1</sup>, ROXANA CIUREAN<sup>1</sup>,  
RODICA TIȚĂ<sup>1</sup>, ȘTEFAN GRIGORIU<sup>2</sup>

<sup>1</sup> Geological Institute of Romania-Bucharest, 1, Caransebeș Street, 012271 Bucharest,  
Romania; e-mail: mircea.ticleanu@yahoo.com

<sup>2</sup> Independent researcher

**Keywords:** “sandstone concretions”, sand deposits, paleodynamic textures, paleoearthquakes, soft trovants, trovant-like forms.

### Introduction

In order to support the theory of the paleoseismic origin of the trovants that we have advanced (Țicleanu et al., 2008), a deeper analytical study was required. In the Carpathian area, we have examined trovants bearing levels ranging from the Upper Cretaceous to the Pleistocene. This fact determined us to consider that the phenomena leading to the appearance of the trovants, as well as the conditions necessary for their formation, were repeated more often than we can now imagine. Currently, we can review, from old to new, the stratigraphic levels containing trovants: Cenomanian, Lower Eocene, Oligocene (Rupelian), Oligocene – the Fusaru Sandstone, Upper Oligocene - the Kliwa Sandstone, Lower and Upper Burdigalian, Upper Badenian, Lower Sarmatian, Upper Sarmatian, Meotian, Pontian (Middle and Upper), Lower and Upper Dacian, Lower Romanian, Lower and Upper Pleistocene. The study of the ellipsoidal "concretions" that can be found in the Badenian tuff in the Iza Basin, corroborated with the documentation on these "concretions" found at this stratigraphic level (the Dej Tuff), suggests that the dynamic conditions requested for the building of proper trovants (the spherical sandstone "concretions" in sand deposits) can also produce similar effects in very different natural deposits.

### The description of the trovants found in the Carpathian area

The following description orders the trovants chronologically (from old to new) and stratigraphically.

**The Vraconian-Cenomanian trovants** are known at the stratigraphic level of the Valea lui Paul Beds (Ampoi Basin). These beds contain compact, coarse or fine friable sandstones, including clay and micro-conglomerates lenses. The sandstone levels may contain trovants. A very good outcrop can be seen on the left side of the Ampoi valley, across the church in the Galați village. In this place, the sandstones are poorly consolidated

and contain, along the stratification lines, many big trovants. On the left bank of the Ampoi, along the Feneş creek, spherical trovants can be found here and there, in the floodplain. The presence of these Cretaceous trovants was reported by Lupu et al. (1967) in the notes accompanying the Turda map.

**The Eocene trovants.** They are known in the deposits known as the Tarcău Sandstone, especially in the central part of the Eastern Carpathians (at the border of the Comăneşti Basin). Such trovants have also been reported in the Ursei area (along the Cricovul Dulce).

**The Eocene trovants in the Tarcău Sandstone.** In the Eocene sandstone deposits of the Comăneşti Basin area, the trovants have a simple, quasi-spherical shape and large diameters. We observed these trovants right in their place along the Păcurii valley. What must be remarked is that these trovants could be taken over in newer deposits, such as in the Sarmatian conglomerates found in the southern part of the Comăneşti Basin (Doftăneasa valley).

**The Eocene trovants of the Cricovul Dulce Basin.** These trovants are connected with the Eocene deposits exposed over a restricted surface along the upper course of the Cricovul Dulce. They were reported by Popp (1939), near Ursei. These trovants are also big, simply-shaped, quasi-spherical. Their material is micaceous sandstone, which is often fine, rarely coarse.

**The Eocene trovants in the Bran area.** From the lithological point of view, north of Bran the exposed Eocene deposits vary very much. The trovant-bearing sandstones have medium granularity, which is finer or coarser here and there, and they are yellow or yellowish in colour. The trovants are often ellipsoidal, and they may be brittle or very hard, well cemented. On the Braşov map, the Eocene deposits north of Bran are considered Lutetian-Priabonian. If we take into consideration the Tarcău Sandstone age (Paleocene-Lutetian), we could admit the Lutetian age of the trovants from Bran.

**The Oligocene trovants.** In the sandstone-sandy banks of the Pucioasa-Fusaru facies, more precisely in Fusaru Sandstone facies, there are trovants with various shapes and sizes. This situation can be found between the Ialomiţa and Cricovul Dulce valleys. Better known are the trovants at Bela and Miculeşti (north Pucioasa), the trovants on the Valea Rea, and those at Vişineşti. They are placed in fine or coarse, grey and yellowish sands. Generally, these trovants are large: their diameter is often over 1 m. In many cases, the concentric internal structure is obvious. Oligocene quasi-spherical trovants can also be found in the Cetate Beds (Rupelian) around Treznea (Sălaj district). Oligocene trovants made of fine, grey-white sandstones are driven by the water along the Sibiciu valley (Buzău district), which goes through a region with exposed Oligocene deposits. These trovants are large and spherical. It is more than likely that these trovants are connected with the Kliwa Sandstone facies of the external margin of the Tarcău Unit, more precisely with the Upper Kliwa Sandstone horizon, in some cases poorly cemented or even sandy. Near Colţii de Jos village, to the east, the whitish sandstone banks contain trovant-like forms or even trovants having great sizes.

**The Lower Burdigalian trovants.** On the surface covered by the Cluj map (Dumitrescu, 1968), east of the Cliţ village, there are Chattian-Burdigalian deposits (excluding the old "Helvetian" deposits), including the Buzaş Beds and the Chechiş Beds. The Buzaş Beds are comprised of a sandstone and sand complex with marl intercalations in

its lower part, and sandstones with "ellipsoidal concretions" in its upper part. Above all these, there are the Chechiş Marls, considered „Helvetian”. If we include the ex-"Helvetian" deposits, in the actual Burdigalian stage we can appreciate the "ellipsoidal concretions" as Lower Burdigalian. The Chattian-Burdigalian deposits of the Transylvanian slope of the Hudin and Țibleş Mountains are made of an alternation of sandstones and marls containing, at different levels, "spherical sandstone concretions". In the Lăpuş valley basin, the Chattian-Burdigalian deposits are represented by an alternation of fine or coarse sandstone with numerous "concretionary and trovant-like forms". As a result, during the lower part of the Burdigalian stage, it seems that there are a few levels with trovants or with trovant-like "concretions". Thus, we could speak about Lower Burdigalian trovants. The same age can be attributed to the trovant-like forms and to the trovants of the Corbi Sandstone, exposed at Corbii de Piatră, on the Doamnei River.

**The Upper Burdigalian trovants.** Across the surface covered by the Bacău map, at the level of the ex-Helvetian stage, there are sands with "sandstone concretions". This upper horizon of the "Helvetian" is also known as the "upper variegated sandy series" (Mirăuță, 1969). The upper part of this "horizon" is a sandy complex well developed in the Poduri-west Berzunț and Ardeoani-Tărița-Pirjol-Cîmpeni sectors. This is made of sands (with "sandstone concretions"), gypsum, calcareous schists, tuffs and marls. As a result, we could speak about trovants which could be Upper Burdigalian. At the same level of the ex-Helvetian stage, some marl levels with "sandstone concretions" were also reported, such as north Olteni (Olt valley) and, to the east, north Godeni. The "Helvetian" series starts with conglomerates, fine gravels, sandstone sands and argillaceous marls. This series ends with sandstone sands, gravels and marl levels with "sandstone concretions".

**The Upper Badenian trovants.** In the south-western part of the Odorhei map, in the Transylvanian Depression, in the upper part of the ex-"Tortonian" deposits, there are "sands with trovants". Here, above the Salt Formation, there are argillaceous marls, sands with trovants, sandstones and marlaceous clays. In the Ciocadia-Pițicu area, there are clays with concretions (presumably trovants) and marly limestone with sandstone lenses. Above these deposits, there are marls and marly limestone with Spiratela, which in turn are covered by Sarmatian marls.

**The Sarmatian trovants.** In the Orman valley area (west Gherla), east of Ocna Dejului, and in the Cojocna area, there are deposits considered to belong to the past Upper Buglovian. These deposits are placed between the Iclod Tuff, at the bottom, and the Ghiriş Tuff. The lithology consists in a series of marls with sandy intercalations containing concretions. We could consider these trovants "Buglovian", in order to distinguish between them and the newer Volhinian trovants. At this level, we can mention the sandstone concretions described by Larisa Ungureanu (fide Vancea, 1960) in the Cenade-Soroștin-Șeica Mare area. Here, under the Ghiriş Tuff, there are three whitish, fine sand intercalations with concretions. Under these deposits, in another marl series, three yellow sand intercalations contain "big sandstone concretions". In the same area, L. Ungureanu reported that, above the Ghiriş Tuff, a 35m-thick lithologic complex contains "big shapeless concretions". Sandstone concretions were reported by L. Ungureanu in the Veseud, Agnita and Dealu Frumos areas. Near Dealu Frumos (not far from Agnita), a little sand quarry exposed a lot of big well-individualized trovants. With the same age (Volhinian), there are

trovants in the small sand quarries near Cașolț and Cornățel. In the quarry near Cașolț, along ~8m, a succession of sand and gravels contain trovants with diameters generally under 1 m. In this outcrop, there are also "soft trovants" made of local accumulations of manganese and iron oxides, some of them with a ferruginous, limonite shell. Near Cornățel, a smaller sand quarry contains big spherical trovants and trovant-like forms. In this quarry, there are also some big "soft trovants" whose colour is different, compared with the surrounding sand. In the north of the Transylvanian Basin, above the Ghiriș Tuff, Vancea (1960) reported "spherical concretions" in an alternation of marls and sands. In this area, we can mention the outcrop with trovants north of Domnești. Here the sands and sandstones contain levels with single or twinned trovants with very complicated shapes. The trovant-like forms are rounded at the lower part. In the western part of the Transylvanian Basin, Ilie M. D. (quoted by Vancea, 1960) reported the existence of "sands with concretions" in the Sarmatian deposits around Aiud, Cojocna and Turda. Very well known Sarmatian trovants deposits are placed in the area of Feleacu, near Cluj. These trovants were described as far back as in 1898 and 1900 by A. Koch. Moreover, he mentioned the sandstone concretions near Aiudul de Sus, Gîrbova de Jos, Teiuș, Stremț and Galda de Jos. Koch quoted other authors on the "big concretions of sandstone spheres" in the area of Daia Săsească and Cornățel. In the area of Feleacu, the best-known trovants are to be found along the Căprioara valley, in few cases in their original places. Their dimensions vary very much and they are often perfectly spherical. In many places, they can be found as various twinned or mameloned masses. The trovants are made up of fine or medium grey sand, but there are also levels of small gravels caught in their mass. They are contained in a marl-sandy series with sandstones and tuff intercalations, placed above the Ghiriș Tuff. Ciupagea et al. (1970) mentioned the presence of the "spherical concretions" in the sand deposits of the Transylvania Basin as an "extremely interesting and frequent peculiarity".

In Mountenia, Sarmatian trovants are described as well: along the Lupa valley (near Cămpina), and along the Gresarea creek (a tributary of Luncavăț), at Oteșani. The trovants of the Lupa valley are often spherical, with small to a-few-decimeter diameters, but trovants with complicated forms can also be found here. Along the Gresarea valley, the trovants are made of a grey, well-cemented sandstone. Huică and Dicea (1964) noted that the Lower and the Middle Sarmatian in an area between the Buzău and Zîmbroaia valleys would be characterized by the presence of trovants. These authors also mentioned a paper by Saulea (1956), who recorded the presence of trovants in the lower part of the Sarmatian deposits in the Odăile synclinal. Large trovants and trovant-like sandstone blocks can be seen south of Bozioru, on the way to Cozieni. Between the Dîmbovița and Ialomița valleys, in an alternation of Sarmatian sands, sandstones and grey marls, Patrușiu et al. (1968) noted the presence of "spherical concretions". In the Trotuș-Năruja area, Băncilă (1958) recorded "concretionary forms (trovants)" in calcareous, oölitic or conglomerate-like sandstones. For the Platform area, trovants and trovant-like sandstone forms were reported as far back as the XIX<sup>th</sup> century. In 1883, G. Cobălcescu described sandstone concretions in the Lower Sarmatian deposits of Moldavia. In 1894, Sabba Ștefănescu reported the presence of "concrétions de grès" in the bulk of the Sarmatian sands at Lespezi (by Siret) and at Hălărești, Mircești and Florești. Chintăoan (2004) wrote about "sandstone fossiliferous concretions" in the Sarmatian deposits at Izvoarele (Dobrogea). At Andreiașu de Jos, in

yellowish or grey fine Sarmatian sands, there are small, spherical or ellipsoidal trovants. Upper Sarmatian trovants can be seen on the right side of the Silei valley, north of Pânățau.

**The Meotian trovants.** The well-known trovants of this age are those at Costești (Oltenia). One of the features of those trovants is the presence of numerous spherical tubercles on the surface of the great trovants. Apart from the big trovants, there are numerous smaller, imperfect ones, but with a clear tendency toward sphericity. All these trovants are placed in yellow fine, medium or coarse sands also containing fine gravel levels. West of the Olt river, the trovants can be found in the upper horizon of the Meotian. To the east, over the surface covered by the Țirgoviște map, there are exposed Upper Meotian deposits formed of sandstones with spherical concretions, sands with marl intercalations, and grey marls. In the Drajna synclinal axis, exposed Meotian deposits formed by sandstones with trovants appear here and there. In the Mio-Pliocene area outside the Carpathians, and in the Platform area, over the surface covered by the Bacău map, in the upper part of the Meotian deposits, there are sandstones with frequent "spherical concretions".

**The Pontian trovants.** In the drainage area of the Doftăneț and Mislea valleys, in the Middle Pontian sand banks, there are trovants with different sizes and shapes. The sand levels contain quasi-spherical trovants with small diameters. In the Mislea valley, there are several distinct trovant-bearing levels. These Pontian concretions are big and flattened, made mostly of marl with sandstone content; generally, only the sandstone concretions are spherical. Some trovants contain *Congeria* shells indicating the Portaferrian. Small trovants are to be found in a quarry near Cohani (SW Marghita). In our opinion, the deposits here are newer than Pannonian s. str., consequently they could be Pontian. The Pontian-Dacian deposits in the Bîrlad Depression are made up of three distinct horizons. The middle, sandy horizon contains Pontian trovants. The best outcrop in this area is located between Căbești and Ivești.

**The Lower Dacian (Getian) trovants.** In the upper part of the Lazu Sands (near Bistrița), we could find small trovants with a diameter of 7-8cm, seldom 20cm. They can be found in a grey, yellowish-grey or white fine, medium or, rarely, coarse sand. Similar Getian trovants were recorded north of this perimeter or south, at Hinova. In the Slănic valley (tributary of Buzău), there are ellipsoidal sandstone forms in the lower part of the sand banks placed under thick marl layers.

**The Upper Dacian trovants.** On the left bank of the Milcov, between Mera and Sîndrilarii de Jos, there are exposed banks of yellowish sandstone with trovant-like forms and big trovants. The stratigraphic position of this outcrop is not quite certain, but for the time being we appreciate it as Upper Dacian.

**The Romanian trovants.** In the western part of Oltenia, at the base level of the Lower Romanian deposits on the left side of the Blahnița valley, there are small (1-2cm) quasi-spherical trovants. From the sand deposits of the same age, in the Husnicioara quarry, several agglomerations of different-size trovants have been collected and can be seen at the Iron Gates Museum in Tr. Severin (Diaconu, 2001). The conservation of the lamination in these trovants is obvious, in spite of their trovant-like development. In the area covered by the Bîrlad map, the upper part of the Pliocene (classic acceptance) contains a fine or coarse sand horizon with "sandstone concretions".

**The Lower Pleistocene trovants.** Near Matca, on the Corozel valley, east of Tecuci, under the Upper Pleistocene loess deposits, there is a 15-18m sand level with cross-bedding. These sands are synchronous with the "Villafranchian" (Lower Pleistocene) sands described north-east of Matca, between Corod and Blinzi. In the sand, there are small ellipsoidal trovants (1.5-4cm). The trovants generally preserve inside the lamination of the surrounding sands. Only in the case of the imperfectly spherical trovants is the lamination blurred. The bigger (5-8cm) trovants are rare.

**The Upper Pleistocene trovants.** In the bulk of the Mostiștea Sands placed under the Upper Pleistocene loess beds, small trovants formed in the grey or yellowish sand can be found (the youngest trovants of the entire Carpathians area). The trovants appear as simple individuals or as aggregates, never complicated.

### Conclusions

From the present study have resulted the following clarifications: (1) The stratigraphic intervals with trovants are much more numerous than it was previously thought; (2) Most of them are connected with the Eocene-Pleistocene interval; (3) This high frequency proves that the dynamical conditions requested for the genesis of the trovants are pretty common in the geodynamic evolution of the Earth; (4) This point of view is sustained by the existence, in other parts of the world, of other deposits with trovants, older than the Upper Cretaceous; (5) Numerous outcrops of different ages contain the trovants in their original place and, as a result, their study is much facilitated; (6) These exposures show all phases between clear bedding and its complete blurring, with the apparition of trovants with concentric structures; (7) The presence of certain-age trovants on vast areas excludes the idea of local causes; (8) The thickness of the deposits with trovants may reach tens of meters, and this indicates that thick layers of sediments may support the same diagenetic factors simultaneously (strong paleoseisms); (9) In many outcrops, the trovants are associated with levels of sandstone containing trovant-like forms, with "soft trovants" and with different types of spherical and ellipsoidal concretions, and this leads us to the conclusion of a common origin; (10) The extension of our study to other texture forms with sphericity tendencies found in a variety of rock types (limestone, tuffs) suggests that the trovants could be nothing more than a particular case; (11) For the future, the detailed study of the "concretions" in tuff or in limestone becomes imperative.

### References

- Băncilă, I., 1958. Geology of the Eastern Carpathians (In Romanian). Ed. Științifică, București, 367p.
- Chintăuan, I., 2004. Les concrétions gréseuses fossilifères en Sarmatien de Izvoarele (Dobrogea de Sud-Ouest). St. Cerc. Geol.-Geogr., **9**, 47–60.
- Ciupagea, D., Paucă, M., Ichim, Tr., 1970. The geology of the Transylvanian Depression (In Romanian). Editura Academiei R.S.R., București, 256p.
- Cobălcescu, Gr., 1883. Geological and paleontological studies on certain Tertiary lands in some parts of Romania (In Romanian), București.
- Diaconu, F., 2001. The "sculptural" forms and the Dacian trovants of the Husnicioara quarry (The Dunare-Motru area) (In Romanian). Geoforum, **1**, Craiova.

- Dumitrescu, I., 1968. Explanatory notes for the Cluj geological map, scale 1:200,000 (In Romanian). Comitetul de Stat al Geologiei, București, 43p.
- Huică, I., Dicea, O., 1964. The geology of the area between the Buzau and Zimbroaia valleys, emphasizing the age of the salt deposits (the Soimari-Calvini cuvette) (In Romanian). D. S. Com. Geol., **XL**, București.
- Koch, A., 1900. Der Tertiärbildungen des Beckens der siebenbürgischen Landesteile. II Neogene Abteilung Herausgegeben von d. ungar. geol. Gesellsch., Budapesta.
- Lupu, M., Borcoș, M., Dimitrescu, R., 1967. Turda geological map, scale 1:200.000 (In Romanian). Comitetul de Stat al geologiei, București, 42p.
- Mirăuță, O., 1969. Stratigraphy and structure of the Miocene Subcarpathians in the Moinesti-Tazlau area (In Romanian). D. S. Com. Geol., **LIV/3**, București.
- Patrulus, D., Ghenea, C., Ghenea, A., Gherasi, N., 1968. Explanatory notes for the Targoviste geological map, scale 1:200.000. Comitetul de Stat al Geologiei, București, 54p.
- Popp, N.M., 1939. The Subcarpathians between the Dimbovita and Prahova Valleys (In Romanian). St. Cerc. Geogr., București.
- Ștefănescu, S., 1894. L'extension des couches sarmatiques en Valachie et en Moldavie (Roumanie). Bulletin de la Société Géologique de France, 3<sup>e</sup> serie, **XXII**.
- Țicleanu, M., Pantea, A., Constantin, A., Țicleanu, N., Nicolescu, R., 2008. Hypothesis on the paleodynamic (paleoseismic) origin of the trovants („Sandsteinkonkretionen”). 33<sup>rd</sup> IGC, Abstracts, Oslo.
- Vancea, A. 1960. The Neogene of the Transylvanian Basin (In Romanian). Ed. Acad. R.P.R., București.

## INDEX OF AUTHORS

AKSOY Rahmi	217	KAVAK Orhan	64, 228, 229
ALTAYLI Cemal	57	KAYANI Saheeb Ahmed	71
ALTUNCU Sinan	57	KOCAK Kerim	14
ANASTASE Șerban	60	KOŠUTH Marián	43, 74
APOPEI Andrei Ionut	13	KOVALENKER Vladimir A.	189
APOPOEI Ciprian	199	KUŞCU Mustafa	83
APOSTOAE Laviniu	153	LAMOLDA Marcos-Antonio	117
ARIK Fetullah	80, 187, 209	LAZĂR Iuliana	144
AȘTEFANEI Dan	49	LUO Yaonan	200
AYDIN Umit	187	MACALEȚ Rodica	168, 204
AYHAN Ahmet	80	MARCINČÁKOVÁ Zdenka	43, 74
BACIU Dorin Sorin	87	MELINTE Mihaela C.	117, 141
BALABAN Sorin-Ionuț	157	MERFEA Mihaela Corina	199
BALINT Ramona	159	MINCIUNA Marian	168
BEJAN Daniel	109	MIURA Yasunori	16, 21, 26, 76
BEJLERI Ariana	93	MOLDOVEANU Simona	30
BRÂNZILĂ Mihai	110	MUNTEANU Emilia	204
BRICEAG Andrei	141	MUNTEANU Marian	200
BRUSTUR Titus	141	MUNTEANU Tudor	168, 204
BULGARIU Dumitru	47, 49, 157	NICOLESCU Radu	241
BULGARIU Laura	47	OLARU Leonard	120
BUTNAR Cosmin	144	ORHAN Hükümü	228, 229
BUZATU Andrei	13	ORU Zeynep	205
BUZGAR Nicolae	13, 47, 49, 51, 178	OZEN Yesim Bozkir	80, 187, 209
CALU Constantin Cătălin	211	ÖZTÜRK Hüseyin	57
CARBONE Serafina	221	OZTURK Alican	80, 209
CĂLIN Maria	204	PARLAK Osman	35
CHIHAIIA Marina	120	PARLAR Seyda	82, 128
CHIRILĂ Gabriel	94, 100, 110, 211	PASCARIU Florentina	115
CHUNNETT Gordon	200	PAZOKI Amir	38
CIOACĂ Ionuț V.	104	PLOTINSKAYA Olga Yu.	189
CIUREAN Roxana	241	PRELA Mensi	93, 129, 131, 133
CODREA Vlad	109	PRIVITERA Sandro	173

ÇÖMLEKCİLER Fuat	228	PRUNDEANU Ionuț Mihai	178
COTIUGA Vasile	13	PUGLISI Diego	233
DAMIAN Floarea	189	RĂDUCANU Răzvan	212
DAMIAN Gheorghe	30, 189	REZAEI Peiman	38
DELİ Arif	229	RIZAOĞLU Tamer	35
DIACONU Iulian	212	SAHAMIEH Reza Zarei	38
DJEDDI Mabrouk M.	191	SAKET Ali	38
DOBNIKAR Meta	51	SANCAR Selin	192
DRĂGUȘIN Doina	204	SEGHEDI Ioan	39
DUMITRAȘCU George	204	STUMBEA Dan	179, 182
EMRE Hasan	205	SZOBOTKA Stefan-Andrei	141
ERIK Nazan Yalçın	192	ŞARAMET Mihai Remus	211, 212
FILIPOV Feodor	47	TANOSAKI Takao	16, 21
GORMUS Muhittin	82, 128	TATU Mihai	39
GRIGORAȘ Valentin	51	TIȚĂ Rodica	241
GRIGORE Dan	104, 144	TOPOLEANU Florin	13
GRIGORIU Ștefan	241	TUDOR George	240
HAFIZI Flutura	93	TURCULEȚ Ilie	135
HANİLÇİ Nurullah	57	ȚABĂRĂ Daniel	94, 100, 110, 120
HOECK Volker	35	ȚIBULEAC Paul	135
HORAICU Corneliu	165	ȚICLEANU Mircea	241
IAMANDEI Eugenia	110, 113	UDUBAȘA Gheorghe	213
IAMANDEI Stănilă	110, 113	UDUBAȘA Sorin Silviu	213
IANCU Ovidiu Gabriel	21, 30, 51, 157	URSACHI Laurențiu	109
ICHIM Mihael-Cristin	51	VĂRZARU Camelia	141
ION Adriana	60, 241	WILSON Allan	200
IONESI Viorel	115, 199	YAO Yong	200
İŞLER Fikret	35	YILMAZ Asuman	83
KARADAG M. Muzaffer	209	ZAHARIA Iulia	212
KASPER Haino Uwe	30	ZEDEF Veysel	14
KASSOURI Abdelkader A.	191		